



**HAL**  
open science

# Inverse problems in fluid mechanics solved by game strategies

Marwa Ouni

► **To cite this version:**

Marwa Ouni. Inverse problems in fluid mechanics solved by game strategies. Fluid mechanics [physics.class-ph]. Université Côte d'Azur; Université de Tunis El Manar, 2021. English. NNT : 2021COAZ4021 . tel-03482834v2

**HAL Id: tel-03482834**

**<https://inria.hal.science/tel-03482834v2>**

Submitted on 1 Feb 2022

**HAL** is a multi-disciplinary open access archive for the deposit and dissemination of scientific research documents, whether they are published or not. The documents may come from teaching and research institutions in France or abroad, or from public or private research centers.

L'archive ouverte pluridisciplinaire **HAL**, est destinée au dépôt et à la diffusion de documents scientifiques de niveau recherche, publiés ou non, émanant des établissements d'enseignement et de recherche français ou étrangers, des laboratoires publics ou privés.



$$\rho \left( \frac{\partial v}{\partial t} + v \cdot \nabla v \right) = -\nabla p + \nabla \cdot T + f$$

$$e^{i\pi} + 1 = 0$$

# THÈSE DE DOCTORAT

Problèmes inverses en mécanique des fluides résolus par des stratégies de jeux

**Marwa OUNI**

LJAD & LAMSIN

**Présentée en vue de l'obtention du grade de docteur en Mathématiques** de l'Université Côte d'Azur et de l'Université de Tunis El Manar.

**Dirigée par :** Abderrahmane HABBAL / Moez KALLEL.

**Soutenue le :** 25 Mars 2021.

**Devant le jury, composé de :**

Mourad Bellassoued, Professeur, Université Tunis El Manar.

Faker Ben Belgacem, Professeur, Université de Technologie de Compiègne.

Abderrahmane Habbal, MCF HDR, Université Côte d'Azur.

Moez Kallel, MCF HDR, Université Tunis El Manar.

Salwa Mani Aouadi, Professeur, Université Tunis El Manar.

Olivier Pantz, Professeur, Université Côte d'Azur.

# **Problèmes inverses en mécanique des fluides résolus par des stratégies de jeux**

## **Jury**

### **Président du jury**

Mourad Bellassoued, Professeur, Ecole Nationale des Ingénieurs de Tunis,  
Université Tunis El Manar, Tunisie.

### **Rapporteurs**

Faker Ben Belgacem, Professeur, Laboratoire de Mathématiques Appliquées de  
Compiègne, Université de Technologie de Compiègne, France.

Salwa Mani Aouadi, Professeur, Département de Mathématiques, Université  
Tunis El Manar, Tunisie.

### **Examineur**

Olivier Pantz, Professeur, Laboratoire de Mathématiques, Université Côte  
d'Azur, Nice.

### **Directeurs de Thèse**

Abderrahmane Habbal, MCF HDR, EPC ACUMES, Université Côte d'Azur,  
Nice.

Moez Kallel, MCF HDR, Ecole Nationale des Ingénieurs de Tunis, Université  
Tunis El Manar, Tunisie.

# Acknowledgements

*First and foremost, I am incredibly grateful to my research supervisors, Professor Abderrahmane HABBAL and Professor Moez KALLEL, for their invaluable advice, continuous support, and patience during my Ph.D study. Their immense knowledge and ample experience have encouraged me in my academic research and daily life. They introduced me to exciting and challenging problems and motivated me in my creative thinking. Without their guidance and constant feedback, this Ph.D would not have been achievable.*

*I would also like to express my sincere gratitude to my defense committee members : Professor Mourad BELLASSOUED, Professor Faker BEN BELGACEM, Professor Salwa MANI AOUADI, and Professor Olivier PANTZ. Thank you for accepting my Ph.D thesis evaluation, for your fruitful discussion, and your valuable comments and suggestions.*

*I take this opportunity to express gratitude to all my colleagues and Professors from the LAMSIN laboratory and all my teachers who taught me during all these years of studies. I will remember every beautiful memory of the time spent during these academic years.*

*I would also like to thank the Jean Alexandre Dieudonné laboratory, the ACUMES team, and INRIA Sophia Antipolis for welcoming me to its premises and provide access to its resources.*

*To conclude, I cannot forget to thank my family and friends for all the unconditional support, incredible patience, for always believing in me and encouraging me to follow my dreams.*



# Résumé

Dans cette thèse, on s'intéresse à étudier la capacité de l'approche de la théorie des jeux à traiter certains problèmes inverses 'mal posé', gouvernés par les équations de Stokes ou quasi-Stokes. La première partie concerne la détection d'un ou plusieurs objets (Chapitre 2), et l'identification de sources ponctuelles dans un écoulement (Chapitre 3), en utilisant des données du type Cauchy qui seront ainsi fournies seulement sur une partie frontière de l'écoulement. Ce type de problème est mal posé au sens d'Hadamard du fait de l'absence de solution si les données ne sont pas compatibles mais surtout du fait de son extrême sensibilité aux données bruitées, dans le sens où une légère perturbation des données entraîne une grande perturbation de la solution. Cette difficulté de stabilité fournit aux chercheurs un défi intéressant pour la mise au point de méthodes numériques permettant d'approcher de la solution du problème inverse original. L'approche développée ici est différente de celles existantes, elle a traité simultanément la question de la reconstruction des données manquantes avec celle de l'identification des inclusions ou de sources ponctuelles dans un fluide visqueux, incompressible et stationnaire. En considérant une méthode de type minimisation de critères, la solution est réinterprétée en termes d'équilibre de Nash entre les deux problèmes complétion/identification. Des nouveaux algorithmes originaux dédiés au calcul d'équilibre de Nash sont présentés et implémentés avec FreeFem ++. Une extension pour le problème d'identification de petits objets de l'approche proposée de jeu de Nash a été réalisée (Chapitre 4). La deuxième partie est consacrée à la résolution des problèmes inverses non linéaires dans le cadre des écoulements de fluide quasi-newtonien (Chapitre 5). La viscosité est supposée une fonction non linéaire, varie en fonction du tenseur des déformations. Un problème inverse non linéaire du type Cauchy est reformulé comme un problème de contrôle optimal, puis comme un jeu de Nash à deux joueurs. Deux algorithmes ont été utilisés et comparés afin de résoudre les problèmes aux limites non linéaires : un algorithme classique de point fixe et un nouveau schéma proposé 'one-shots'. Enfin, on applique la théorie des jeux pour la résolution du problème de couplage de complétion des données et identification des inclusions pour le modèle de quasi-Stokes.

**Mots-clés :** Complétion des données, système de Stokes, méthode level-set, détection des sources, calcul des variations, sensibilité topologique, Jeux de Nash, problème inverse géométrique, écoulements quasi-Newtoniens.

# Abstract

This thesis aims to study the ability of theoretic game approaches to deal with ill-posed problems. The first part of the thesis is dedicated to the Stokes system's linear problem, with the goal of detecting unknown geometric inclusions or pointwise sources in a stationary viscous fluid, using a single compatible pair of Dirichlet and Neumann data, available only on a partially accessible part of the boundary. Inverse geometric-or-source identification for the Cauchy-Stokes problem is severely ill-posed (in the sense of Hadamard) for both the inclusions or sources and the missing data reconstructions, and designing stable and efficient algorithms is challenging. To solve the joint completion/detection problem, we reformulate it as a three players Nash game. The two first players aim at recovering the missing data (Dirichlet and Neumann conditions prescribed over the inaccessible boundary), while the third player seeks to identify the shape and locations of the inclusions (in Chapter 2) or determine the source term (in Chapter 3). We then introduce new algorithms dedicated to the Nash equilibria, which is expected to approximate the original coupled problems' solutions. We present different numerical experiments to illustrate the efficiency and robustness of our 3-player Nash game strategy. The extension of this work to another situation, such as identifying small objects, has been carried out (in Chapter 4). The second purpose of this thesis is to extend those results to the case of quasi-Newtonian fluid flow whose viscosity is assumed to be a nonlinear function that varies upon the imposed rate of deformation. The considered problem then is a nonlinear Cauchy type because of the non-linearity of the viscosity function. Two different iterative procedures, control-type and Nash game algorithms, are considered to solve it. From a computational point of view, the non-linearity needs some particular algorithms. We propose a novel one-shot algorithm to solve the nonlinear state equations during a recovery process, representing a different idea to treat the nonlinear Cauchy problems. Some numerical experiments are provided to demonstrate our algorithm's efficiency in the noise-free and noisy data cases. A comparison between the one-shot scheme and the fixed-point method was performed. Finally, we introduce an algorithm to jointly recover the missing boundary data and the location and shape of the inclusions for nonlinear Stokes models based on the Game-Theoretic approach.

**Keywords :** Data completion, Cauchy-Stokes problem, level-set method, point-force detection, calculus of variations, topological sensitivity, Nash game, shape identification, quasi-Newtonian Stokes flows.

# Table of Contents

<b>Acknowledgements</b>	<b>iii</b>
<b>Abstract</b>	<b>v</b>
<b>1 Introduction</b>	<b>6</b>
1.1 Cauchy-Stokes problem . . . . .	8
1.1.1 The model problem . . . . .	9
1.1.2 Instability in the Cauchy problem for the Stokes equations . . . . .	10
1.1.3 An optimal control formulation . . . . .	12
1.2 Game Theory . . . . .	13
1.2.1 Game . . . . .	13
1.2.2 Some Applications of Game Theory . . . . .	14
1.3 Geometric inverse problem . . . . .	17
1.3.1 Level set approach . . . . .	17
1.3.2 Shape optimization method . . . . .	18
1.3.3 Topological gradient method . . . . .	19
1.4 Quasi-Newtonian Fluids . . . . .	20
<b>2 Nash strategies for the inverse inclusion Cauchy-Stokes problem</b>	<b>23</b>
2.1 Introduction . . . . .	25
2.2 Data completion for the Stokes problem . . . . .	28
2.3 An identifiability result for the inverse inclusion Cauchy-Stokes problem . . . . .	32
2.4 Coupled data completion and geometry identification for the Stokes problem . . . . .	34
2.4.1 A level-set formulation . . . . .	35
2.4.2 Level-set sensitivity and optimality condition . . . . .	36
2.4.3 The three-player Nash algorithm . . . . .	39
2.5 Numerical experiments . . . . .	40
2.6 Conclusion . . . . .	45
<b>3 A Three-player Nash game for point-wise source identification in Cauchy-Stokes problems</b>	<b>59</b>
3.1 Introduction . . . . .	61
3.2 An identifiability result for the inverse point-forces Cauchy-Stokes problem . . . . .	63
3.3 A game formulation of the coupled data completion and point-forces identification problems . . . . .	65
3.3.1 Relaxation step . . . . .	66
3.3.2 Localization of the source position. . . . .	68
3.3.3 Identification of the source intensity. . . . .	73

---

3.3.4	The three-player Nash algorithm . . . . .	74
3.4	Numerical experiments . . . . .	77
3.5	Conclusion . . . . .	81
<b>4</b>	<b>A Nash-game approach to joint data completion and location of small inclusions in Stokes flow</b>	<b>90</b>
4.1	Introduction and motivation . . . . .	92
4.2	Data completion and localization of small objects . . . . .	93
4.2.1	The topological gradient method . . . . .	95
4.2.2	Application to the model problem . . . . .	96
4.3	Numerical simulations. . . . .	102
4.4	Conclusion . . . . .	104
<b>5</b>	<b>A Nash game strategy to model the nonlinear Cauchy-Stokes problems : Quasi-Newtonian flow</b>	<b>107</b>
5.1	Introduction . . . . .	109
5.2	Data completion problem for the quasi-Newtonian flow . . . . .	110
5.2.1	The direct Problem . . . . .	111
5.2.2	Existence of the Cauchy-Stokes solution . . . . .	115
5.2.3	A control-type method for solving the nonlinear Cauchy-Stokes problem . . . . .	116
5.2.4	A Nash game formulation of the nonlinear Cauchy-Stokes problem	119
5.2.5	A one-shot algorithm to deal with nonlinear Cauchy problems :	122
5.3	Extension for a nonlinear coupled problem : Data completion and Geometry identification . . . . .	124
5.4	Numerical results . . . . .	128
5.4.1	Data completion problem. . . . .	128
5.4.2	Application to coupled problem : Data completion and geometry identification . . . . .	131
5.5	Conclusion . . . . .	133
	<b>Conclusion and perspectives</b>	<b>146</b>
	<b>Bibliography</b>	<b>148</b>



# List of Tables

2.1	Test-case A. $L^2$ relative errors on missing data on $\Gamma_i$ (on Dirichlet and Neumann data), and the error between the reconstructed and the real shape of the inclusion for various noise levels. . . . .	42
2.2	Test-case C. $L^2$ -errors on missing data over $\Gamma_i$ (on Dirichlet and Neumann data), and the error between the reconstructed and the real shape for various noise levels. . . . .	43
2.3	Relative errors on the reconstructed missing data and inclusion shape for the Stokes problem (with noise free measurements), compared for a classical Nash algorithm and Algorithm 2.4.1 : (left) test-case A (right) test-case C. . . . .	43
3.1	Test-case A. $L^2$ relative errors on missing data on $\Gamma_i$ (on Dirichlet and Neumann data), and the relative errors on the identified source position and on the identified source intensity for various noise levels. . . . .	78
3.2	Test-case C. $L^2$ relative errors on missing data on $\Gamma_i$ (on Dirichlet and Neumann data), and the relative errors on the identified source position and on the identified source intensity for various noise levels. . . . .	80
3.3	$L^2$ relative errors of reconstructed solution in the whole domain and missing data on $\Gamma_i$ (on Dirichlet and Neumann data), and the relative errors on the identified source position and on the identified source intensity for noise-free, where $err_{u_i} = \ u_{i,\epsilon} - u\ _{0,\Omega}/\ u\ _{0,\Omega}$ , for $i = 1, 2$ . . . . .	81
3.4	Test-case A. Identified source position and their intensity for various noise levels. . . . .	84
3.5	Test-case B. $L^2$ relative errors on missing data on $\Gamma_i$ (on Dirichlet and Neumann data), and the relative errors on the identified source position and on the identified source intensity for various noise levels. . . . .	86
3.6	Test-case C. Identified source position and their intensity for various noise levels. . . . .	89
5.1	Test-case D. $L^2$ -errors on missing data over $\Gamma_i$ , and the error between the reconstructed and the real shape of the inclusion for various noise levels.	132
5.2	Control type (classic) compared to Nash (game) algorithms. Relative $L^2$ -errors on missing data on $\Gamma_i$ (on Dirichlet and Neumann data) are shown for various noise levels (w.r.t a uniform noise). . . . .	133
5.3	Test case A. A CPU time performance's comparison, between the fixed-point algorithm and the new scheme, through CPUs' results (w.r.t a uniform noise). . . . .	134

---

5.4	Test case-A "Control type (classic) compared to Nash (game) algorithms". Relative L2-errors on missing data on $I_i$ (on Dirichlet and Neumann data) are shown for various noise levels (w.r.t a Gaussian noise). . . . .	135
5.5	Test case-A. A CPU time performance's comparison, between the fixed-point algorithm and the new scheme, through CPUs' results (w.r.t a Gaussian noise). . . . .	136
5.6	Test case B "The mesh refinement effect". Relative L2-errors on missing data on $I_i$ (on Dirichlet and Neumann data) with noise free Dirichlet data over $I_c$ , for various $M = \{100, 150, 200\}$ . . . . .	137

# List of Figures

1	Configuration géométrique du notre problème. . . . .	2
1.1	Example in a two-dimensional geometry : An annular domain represents a region between two concentric circles. . . . .	9
1.2	Exponential explosion for high frequencies. . . . .	11
1.3	The 2D model of a circular tumor with a vascular network : strategies converging to a Nash equilibrium [54]. . . . .	15
1.4	Top row : noisy image with Gaussian noise and initial contour, evolution by iterations. Bottom row : segmentation and restoration of image by the Nash game algorithm [65]. . . . .	16
1.5	Reconstructed nonradial Dirichlet ( $\tau_N$ , left) and Neumann ( $\eta_N$ , right) data over $I_i$ . The profiles are presented at convergence and for a noise level $\sigma = 5\%$ [56]. . . . .	17
1.6	Perturbed domain. . . . .	19
2.1	An example of the geometric configuration of the problem : the whole domain including cavities is denoted by $\Omega$ . It contains an inclusion $\omega^*$ . The boundary of $\Omega$ is composed of $I_c$ , an accessible part where over-specified data are available, and an inaccessible part $I_i$ where the data are missing. . . . .	25
2.2	Different situations . . . . .	32
2.3	Test case A. (Left) sensitivity of the reconstruction w.r.t. the mesh size (on abscissae : the number of F.E. nodes on the boundary $\partial\Omega$ ). (Right) sensitivity of the reconstruction w.r.t. the distance to the inaccessible boundary $I_i$ (on abscissae : the distance of the center of the circular inclusion from $I_i$ ). . . . .	44
2.4	Test case C. (Left) Mesh used for solving the direct problem with the P1bubble-P1 finite element, in order to construct the synthetic data. (Right) Mesh used for solving the coupled inverse problem with P2-P1 finite element, using the P1 bubble-P1 synthetic data. . . . .	44
2.5	Test case A. Reconstruction of the inclusion shape and missing boundary data with noise free Dirichlet data over $I_c$ . (a) initial contour is $\phi_1^{(0)}$ (b) exact inclusion shape -green line- and computed one - blue dashed- (c) exact -line- and computed -dashed line- first component of the velocity over $I_i$ (d) exact -line- and computed -dashed line- second component of the velocity over $I_i$ (e) exact -line- and computed -dashed line- first component of the normal stress over $I_i$ (f) exact -line- and computed -dashed line- second component of the normal stress over $I_i$ . . . . .	46

2.6	Test case A. Reconstruction of the inclusion shape and missing boundary data with noise free Dirichlet data over $\Gamma_c$ . <b>(a)</b> initial contour is $\phi_2^{(0)}$ <b>(b)</b> exact inclusion shape -green line- and computed one - blue dashed- <b>(c)</b> exact -line- and computed -dashed line- first component of the velocity over $\Gamma_i$ <b>(d)</b> exact -line- and computed -dashed line- second component of the velocity over $\Gamma_i$ <b>(e)</b> exact -line- and computed -dashed line- first component of the normal stress over $\Gamma_i$ <b>(f)</b> exact -line- and computed -dashed line- second component of the normal stress over $\Gamma_i$ . . . . .	47
2.7	Test case A. Reconstruction of the inclusion shape and missing boundary data with noisy Dirichlet data over $\Gamma_c$ with noise levels $\sigma = \{1\%, 3\%, 5\%\}$ . <b>(a)</b> initial contour is $\phi_2^{(0)}$ <b>(b)</b> exact inclusion shape -green line- and computed ones for different noise levels <b>(c)</b> exact and computed first components of the velocity over $\Gamma_i$ <b>(d)</b> exact and computed second components of the velocity over $\Gamma_i$ <b>(e)</b> exact and computed first components of the normal stress over $\Gamma_i$ <b>(f)</b> exact and computed second components of the normal stress over $\Gamma_i$ . . . . .	48
2.8	Test case B. Reconstruction of the inclusion shape and missing boundary data with noise free Dirichlet data over $\Gamma_c$ . <b>(a)</b> initial contour is $\phi_2^{(0)}$ <b>(b)</b> exact inclusion shape -green line- and computed one - blue dashed- <b>(c)</b> exact -line- and computed -dashed line- first component of the velocity over $\Gamma_i$ <b>(d)</b> exact -line- and computed -dashed line- second component of the velocity over $\Gamma_i$ <b>(e)</b> exact -line- and computed -dashed line- first component of the normal stress over $\Gamma_i$ <b>(f)</b> exact -line- and computed -dashed line- second component of the normal stress over $\Gamma_i$ . . . . .	49
2.9	Test case B. Reconstruction of the inclusion shape and missing boundary data with noisy Dirichlet data over $\Gamma_c$ with levels $\sigma = \{1\%, 3\%, 5\%\}$ . <b>(a)</b> initial contour is $\phi_2^{(0)}$ <b>(b)</b> exact inclusion shape -green line- and computed ones for different noise levels <b>(c)</b> exact and computed first components of the velocity over $\Gamma_i$ <b>(d)</b> exact and computed second components of the velocity over $\Gamma_i$ <b>(e)</b> exact and computed first components of the normal stress over $\Gamma_i$ <b>(f)</b> exact and computed second components of the normal stress over $\Gamma_i$ . . . . .	50
2.10	Test case C. Reconstruction of the inclusion shape and missing boundary data with noise free Dirichlet data over $\Gamma_c$ . <b>(a)</b> initial contour is $\phi_2^{(0)}$ <b>(b)</b> exact inclusion shape -green line- and computed one - blue dashed- <b>(c)</b> exact -line- and computed -dashed line- first component of the velocity over $\Gamma_i$ <b>(d)</b> exact -line- and computed -dashed line- second component of the velocity over $\Gamma_i$ <b>(e)</b> exact -line- and computed -dashed line- first component of the normal stress over $\Gamma_i$ <b>(f)</b> exact -line- and computed -dashed line- second component of the normal stress over $\Gamma_i$ . . . . .	51
2.11	Test case C. Reconstruction of the inclusion shape and missing boundary data with noisy Dirichlet data over $\Gamma_c$ with levels $\sigma = \{1\%, 3\%, 5\%\}$ . <b>(a)</b> initial contour is $\phi_2^{(0)}$ <b>(b)</b> exact inclusion shape -green line- and computed ones for different noise levels <b>(c)</b> exact and computed first components of the velocity over $\Gamma_i$ <b>(d)</b> exact and computed second components of the velocity over $\Gamma_i$ <b>(e)</b> exact and computed first components of the normal stress over $\Gamma_i$ <b>(f)</b> exact and computed second components of the normal stress over $\Gamma_i$ . . . . .	52

2.12	Assessing Inverse-Crime-Free reconstruction. Test case C. Top : initial and optimal contour. Middle : the two components of the velocity on $\Gamma_i$ . Bottom : the two components of the normal stress on $\Gamma_i$ ( $err_D = 0.0615048$ , $err_N = 0.124296$ , and $err_O = 0.113156$ ). . . . .	53
3.1	Relaxation step . . . . .	66
3.2	Test case B. (Left) Mesh used for solving the direct problem, in order to construct the synthetic data. (Right) Mesh used for solving the coupled inverse problem, with P2-P1 finite element. . . . .	79
3.3	Test case C. Sensitivity of the reconstruction w.r.t. the distance to the inaccessible boundary $\Gamma_i$ , the distance of the center of $\mathcal{S}_{P,\epsilon}$ from $\Gamma_i$ , for $y = -0.25$ . . . . .	80
3.4	The iso-values of the topological gradient at convergence, $P_{op} = (0.2, 0.2, 0.2)$ and $\Lambda_{op} = (0.233, 0.204, 0.005)$ . Exact values : $P_{ex} = (0.25, 0.25, 0.25)$ and $\Lambda_{ex} = (0.25, 0.2, 0)$ . . . . .	81
3.5	Test case A. Reconstruction of the point-forces and missing boundary data with noise free Dirichlet data over $\Gamma_c$ . <b>(a)</b> the iso-values of the topological gradient at convergence. <b>(b)</b> exact elements defining the source-term -red vector- and computed one -blue vector- <b>(c)</b> exact -line- and computed -dashed line- first component of the velocity over $\Gamma_i$ . <b>(d)</b> exact -line- and computed -dashed line- second component of the velocity over $\Gamma_i$ . <b>(e)</b> exact -line- and computed -dashed line- first component of the normal stress over $\Gamma_i$ <b>(f)</b> exact -line- and computed -dashed line- second component of the normal stress over $\Gamma_i$ . . . . .	83
3.6	Test case A. Reconstruction of the missing boundary data with noisy Dirichlet data over $\Gamma_c$ with noise levels $\sigma = \{1\%, 3\%\}$ . <b>(a)</b> exact and computed first components of the velocity over $\Gamma_i$ <b>(b)</b> exact and computed second components of the velocity over $\Gamma_i$ <b>(c)</b> exact and computed first components of the normal stress over $\Gamma_i$ <b>(d)</b> exact and computed second components of the normal stress over $\Gamma_i$ . . . . .	84
3.7	Test case B. Reconstruction of the point-forces and missing boundary data with noise free Dirichlet data over $\Gamma_c$ . <b>(a)</b> the iso-values of the topological gradient at convergence. <b>(b)</b> exact elements defining the source-term -red vector- and computed one -blue vector- <b>(c)</b> exact -line- and computed -dashed line- first component of the velocity over $\Gamma_i$ . <b>(d)</b> exact -line- and computed -dashed line- second component of the velocity over $\Gamma_i$ . <b>(e)</b> exact -line- and computed -dashed line- first component of the normal stress over $\Gamma_i$ <b>(f)</b> exact -line- and computed -dashed line- second component of the normal stress over $\Gamma_i$ . . . . .	85
3.8	Test case B. Reconstruction of the missing boundary data with noisy Dirichlet data over $\Gamma_c$ with noise levels $\sigma = \{1\%, 3\%\}$ . <b>(a)</b> exact and computed first components of the velocity over $\Gamma_i$ <b>(b)</b> exact and computed second components of the velocity over $\Gamma_i$ <b>(c)</b> exact and computed first components of the normal stress over $\Gamma_i$ <b>(d)</b> exact and computed second components of the normal stress over $\Gamma_i$ . . . . .	86

3.9	Test case B : Assessing Inverse-Crime-Free reconstruction. Test case B. Top : the iso-values of the topological gradient at convergence, and the exact and optimal elements defining the source-term. Middle : the two components of the velocity on $\Gamma_i$ . Bottom : the two components of the normal stress on $\Gamma_i$ ( $err_\tau = 0.00768152$ , $err_\eta = 0.0713575$ , $err_P = 0.0105486$ , and $err_\Lambda = 0.0560551$ ).	87
3.10	Test case C. Reconstruction of the point-forces and missing boundary data with noise free Dirichlet data over $\Gamma_c$ . (a) the iso-values of the topological gradient at convergence. (b) exact elements defining the source-term -red vector- and computed one -blue vector- (c) exact -line- and computed -dashed line- first component of the velocity over $\Gamma_i$ . (d) exact -line- and computed -dashed line- second component of the velocity over $\Gamma_i$ . (e) exact -line- and computed -dashed line- first component of the normal stress over $\Gamma_i$ (f) exact -line- and computed -dashed line- second component of the normal stress over $\Gamma_i$ .	88
3.11	Test case C. Reconstruction of the missing boundary data with noisy Dirichlet data over $\Gamma_c$ with noise levels $\sigma = \{1\%, 3\%\}$ . (a) exact and computed first components of the velocity over $\Gamma_i$ (b) exact and computed second components of the velocity over $\Gamma_i$ (c) exact and computed first components of the normal stress over $\Gamma_i$ (d) exact and computed second components of the normal stress over $\Gamma_i$ .	89
4.1	An example of the geometric configuration of the problem : The whole domain $\Omega$ , the inclusions $\mathcal{O}_\epsilon^*$ , and two parts of the boundary $\Gamma_c$ and $\Gamma_i$ .	93
4.2	Case A- . Plots of the three costs $\mathcal{J}_1$ , $\mathcal{J}_2$ and $\mathcal{J}_3$ as functions of overall Nash iterations	103
4.3	Case A- Detection of a single object (for unnoisy data). (a) the iso-values of the topological gradient at convergence (b) the approximate location $z_{opt}$ is equal to $(-0.294, -0.174)$ , while the exact one $z_{ex}$ is equal to $(-0.3, -0.15)$ .	104
4.4	Case A- Reconstruction of the missing boundary data (for unnoisy data). (a) exact -line- and computed -dashed line- first component of the velocity over $\Gamma_i$ (b) exact -line- and computed -dashed line- second component of the velocity over $\Gamma_i$ (c) exact -line- and computed -dashed line- first component of the normal stress over $\Gamma_i$ (d) exact -line- and computed -dashed line- second component of the normal stress over $\Gamma_i$ .	105
4.5	Case B- Detection of two objects (for unnoisy data). (a) the iso-values of the topological gradient at convergence (b) the approximate locations are equal to $z_{opt}^1 = (-0.422006, -0.160662)$ and $z_{opt}^2 = (-0.416224, 0.159772)$ , while the exact ones are equal to $z_{ex}^1 = (-0.4, -0.15)$ and $z_{ex}^2 = (-0.4, 0.15)$ .	106
4.6	Case B- Reconstruction of the missing boundary data (for unnoisy data). (a) exact -line- and computed -dashed line- first component of the velocity over $\Gamma_i$ (b) exact -line- and computed -dashed line- second component of the velocity over $\Gamma_i$ (c) exact -line- and computed -dashed line- first component of the normal stress over $\Gamma_i$ (d) exact -line- and computed -dashed line- second component of the normal stress over $\Gamma_i$ .	106
5.1	Test case A. Iso-values of the velocity (left) and pressure (right) fields.	129

5.2	Test case C. (Left) Mesh used for solving the coupled inverse problem. (Right) Iso-values of the velocity field. . . . .	131
5.3	Test case D. Plots of the three costs $\mathcal{J}_1$ , $\mathcal{J}_2$ and $\tilde{\mathcal{J}}_3$ as functions of overall Nash iterations. . . . .	132
5.4	Test case-A "Classic Method". Reconstruction of the missing boundary data from unnoisy data. <b>(a)</b> exact and computed first components of the velocity over $I_i$ <b>(b)</b> exact and computed second components of the velocity over $I_i$ <b>(c)</b> exact and computed first components of the normal stress over $I_i$ <b>(d)</b> exact and computed second components of the normal stress over $I_i$ . . . . .	134
5.5	Test case-A "Classic Method". Reconstruction of the missing boundary data with noisy Dirichlet data over $I_c$ with noise levels $\sigma = \{3\%, 5\%, 10\%, 15\%\}$ . <b>(a)</b> exact and computed first components of the velocity over $I_i$ <b>(b)</b> exact and computed second components of the velocity over $I_i$ <b>(c)</b> exact and computed first components of the normal stress over $I_i$ <b>(d)</b> exact and computed second components of the normal stress over $I_i$ (w.r.t a uniform noise). . . . .	135
5.6	Test case-A "NGM-FPA". Reconstruction of the missing boundary data with noisy Dirichlet data over $I_c$ with noise levels $\sigma = \{3\%, 5\%, 10\%, 15\%\}$ . <b>(a)</b> exact and computed first components of the velocity over $I_i$ <b>(b)</b> exact and computed second components of the velocity over $I_i$ <b>(c)</b> exact and computed first components of the normal stress over $I_i$ <b>(d)</b> exact and computed second components of the normal stress over $I_i$ (w.r.t a uniform noise). . . . .	136
5.7	Test case-A "NGM-NS". Reconstruction of the missing boundary data with noisy Dirichlet data over $I_c$ with noise levels $\sigma = \{3\%, 5\%, 10\%, 15\%\}$ . <b>(a)</b> exact and computed first components of the velocity over $I_i$ <b>(b)</b> exact and computed second components of the velocity over $I_i$ <b>(c)</b> exact and computed first components of the normal stress over $I_i$ <b>(d)</b> exact and computed second components of the normal stress over $I_i$ (w.r.t a uniform noise). . . . .	137
5.8	Test case-A "Classic Method". Reconstruction of the missing boundary data with noisy Dirichlet data over $I_c$ with noise levels $\sigma = \{1\%, 3\%, 5\%, 8\%\}$ . <b>(a)</b> exact and computed first components of the velocity over $I_i$ <b>(b)</b> exact and computed second components of the velocity over $I_i$ <b>(c)</b> exact and computed first components of the normal stress over $I_i$ <b>(d)</b> exact and computed second components of the normal stress over $I_i$ (w.r.t a Gaussian noise). . . . .	138
5.9	Test case A "NGM-FPA". Reconstruction of the missing boundary data with noisy Dirichlet data over $I_c$ with noise levels $\sigma = \{1\%, 3\%, 5\%, 8\%\}$ . <b>(a)</b> exact and computed first components of the velocity over $I_i$ <b>(b)</b> exact and computed second components of the velocity over $I_i$ <b>(c)</b> exact and computed first components of the normal stress over $I_i$ <b>(d)</b> exact and computed second components of the normal stress over $I_i$ (w.r.t a Gaussian noise). . . . .	139

5.10	Test case-A "NGM-NS". Reconstruction of the missing boundary data with noisy Dirichlet data over $\Gamma_c$ with noise levels $\sigma = \{1\%, 3\%, 5\%, 8\%\}$ . <b>(a)</b> exact and computed first components of the velocity over $\Gamma_i$ <b>(b)</b> exact and computed second components of the velocity over $\Gamma_i$ <b>(c)</b> exact and computed first components of the normal stress over $\Gamma_i$ <b>(d)</b> exact and computed second components of the normal stress over $\Gamma_i$ (w.r.t a Gaussian noise). . . . .	140
5.11	Test case B "Classic Method". Reconstruction of the missing boundary data with noise free Dirichlet data over $\Gamma_c$ . <b>(a)</b> exact -line- and computed -dashed line- first component of the velocity over $\Gamma_i$ <b>(b)</b> exact -line- and computed -dashed line- second component of the velocity over $\Gamma_i$ <b>(c)</b> exact -line- and computed -dashed line- first component of the normal stress over $\Gamma_i$ <b>(d)</b> exact -line- and computed -dashed line- second component of the normal stress over $\Gamma_i$ . . . . .	141
5.12	Test case B "NGM-NS". Reconstruction of the missing boundary data with noise free Dirichlet data over $\Gamma_c$ . <b>(a)</b> exact -line- and computed -dashed line- first component of the velocity over $\Gamma_i$ <b>(b)</b> exact -line- and computed -dashed line- second component of the velocity over $\Gamma_i$ <b>(c)</b> exact -line- and computed -dashed line- first component of the normal stress over $\Gamma_i$ <b>(d)</b> exact -line- and computed -dashed line- second component of the normal stress over $\Gamma_i$ . . . . .	142
5.13	Test case-C. Reconstruction of the missing boundary data from unnoisy data using Nash game algorithm. The exact and computed first component of the velocity and the normal stress, respectively : (Top) over $\Gamma_{i_1}$ , (Middle) over $\Gamma_{i_2}$ and (Bottom) over $\Gamma_{i_3}$ . . . . .	143
5.14	Test case D. Reconstruction of the inclusion shape and missing boundary data with noisy Dirichlet data over $\Gamma_c$ with noise levels $\sigma = \{1\%, 3\%, 5\%, 8\%\}$ . <b>(a)</b> initial contour is $\phi^{(0)}$ <b>(b)</b> exact inclusion shape -green line- and computed ones for different noise levels <b>(c)</b> exact and computed first components of the velocity over $\Gamma_i$ <b>(d)</b> exact and computed second components of the velocity over $\Gamma_i$ <b>(e)</b> exact and computed first components of the normal stress over $\Gamma_i$ <b>(f)</b> exact and computed second components of the normal stress over $\Gamma_i$ . . . . .	144
5.15	Test case E. Reconstruction of the inclusion shape and missing boundary data with noisy Dirichlet data over $\Gamma_c$ with noise levels $\sigma = \{1\%, 3\%, 5\%, 8\%\}$ . <b>(a)</b> initial contour is $\phi^{(0)}$ <b>(b)</b> exact inclusion shape -green line- and computed ones for different noise levels <b>(c)</b> exact and computed first components of the velocity over $\Gamma_i$ <b>(d)</b> exact and computed second components of the velocity over $\Gamma_i$ <b>(e)</b> exact and computed first components of the normal stress over $\Gamma_i$ <b>(f)</b> exact and computed second components of the normal stress over $\Gamma_i$ . . . . .	145



# Introduction générale

La théorie des jeux définit un cadre pour traiter les problèmes d'optimisation multi-critère et multidisciplinaire. Dans ce contexte, la notion d'optimum se remplace par la notion de concepts de solution ou équilibre, qui est un concept fondamental dans la théorie des jeux. Il existe de nombreuses définitions d'équilibres de jeu, qui dépend généralement du type de jeu considéré. Le plus célèbre entre eux est l'équilibre de Nash dans les jeux non-coopératifs. La théorie des jeux a été commencée en économie, elle se propose d'étudier des situations (jeux) dans lesquelles les décideurs (joueurs) interagissent dans un environnement d'interdépendance stratégique. Elle a été ensuite largement étudiée et appliquée à un large éventail de disciplines, où les décideurs (joueurs) traitent des systèmes régis par les équations aux dérivées partielles (EDP). De nouvelles applications liées à la conception de la topologie de systèmes couplés physiques ou biologiques sont présentées dans [53, 54, 58]. D'une façon générale, un jeu non-coopératif est défini par l'ensemble des joueurs  $N = \{1, \dots, n\}$  et l'ensemble des stratégies possibles pour chacun d'eux. Chaque joueur  $i$  choisit une stratégie  $s_i$  au sein de l'espace de ses stratégies possibles  $S_i$  et cherche à améliorer son propre critère  $\mathfrak{J}_i : S_1 \times \dots \times S_n \rightarrow \mathbb{R}$  simultanément et indépendamment des autres. L'état d'équilibre est atteint lorsque aucun joueur ne peut améliorer son propre critère unilatéralement, c'est la notion de l'équilibre de Nash (EN) :

*Un équilibre de Nash est un profil  $s^* = \{s_1^*, \dots, s_n^*\} \in S_1 \times \dots \times S_n$ , tel que la stratégie du joueur  $i$  est une meilleure réponse :*

$$B_i(s_{-i}^*) = \left\{ \begin{array}{l} \forall i \in N, s_i^* \in B_i(s_{-i}^*), \\ s_i \in S_i / \mathfrak{J}_i(s_i, s_{-i}^*) \leq \mathfrak{J}_i(s_i', s_{-i}^*), \forall s_i' \in S_i \end{array} \right\} \quad (1)$$

*avec  $s_{-i}$  est le profil  $s$  des stratégies autres que celles du joueur  $i$  :  $s_{-i} = \{s_1, \dots, s_{i-1}, s_{i+1}, \dots, s_n\}$ .*

Dans cette thèse, on s'intéresse essentiellement à exploiter l'approche de la théorie des jeux pour traiter certains problèmes inverses gouvernés par les équations de Stokes. L'un des objectifs de cette thèse est de montrer l'intérêt et l'utilité de l'approche introduite par la théorie des jeux dans des applications issues de la mécanique des fluides. Le problème inverse que nous traiterons par la suite va transformer en  $N$  sous-problèmes d'optimisation, qui vont considérer comme des joueurs. Chacun contrôle seulement sa propre variable stratégie et tente de minimiser simultanément son propre coût en cherchant à converger vers un équilibre qui représente un compromis entre eux, et qui devrait être la solution approchée du problème inverse initial.

La première partie de la thèse se décompose en trois chapitres. Le premier chapitre est dédié à la résolution du problème de détection des inclusions dans un écoulement, lorsque le mouvement de fluide est régi par les équations de Stokes : On

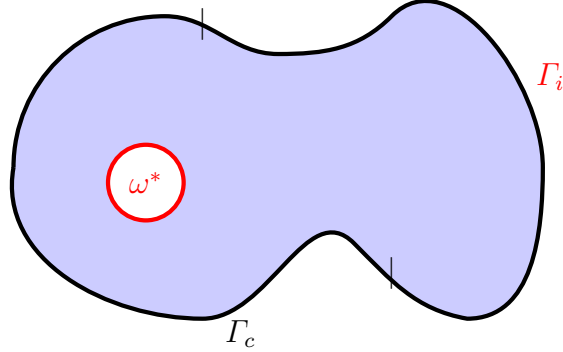


FIGURE 1 – Configuration géométrique du notre problème.

considère un écoulement de fluide visqueux et incompressible dans un domaine borné  $\Omega$  de  $\mathbb{R}^d$  (avec  $d=2$  ou  $d=3$ ). Soit  $\omega^* \subset \Omega$  un objet inconnu immergé dans le domaine  $\Omega$  rempli d'un fluide (voir la figure 1). On s'intéresse alors à identifier  $\omega^*$ , à partir de mesure sur  $\Gamma_c$  de la vitesse  $f$  et de la contrainte normale  $\Phi$ , où  $\Gamma_c$  est une partie de la frontière  $\partial\Omega$ , tel que la vitesse du fluide  $u = (u_1, \dots, u_d)$  et la pression correspondante  $p$  dans  $\Omega$  satisfont le problème de Stokes suivant :

$$\left\{ \begin{array}{ll} -\operatorname{div}(\sigma(u, p)) = 0 & \text{dans } \Omega \setminus \overline{\omega^*}, \\ \operatorname{div} u = 0 & \text{dans } \Omega \setminus \overline{\omega^*}, \\ \sigma(u, p)n = 0 & \text{sur } \partial\omega^*, \\ u = f & \text{sur } \Gamma_c, \\ \sigma(u, p)n = \Phi & \text{sur } \Gamma_c, \end{array} \right. \quad (2)$$

avec  $\sigma$  est le tenseur des contraintes défini par  $\sigma(u, p) := -pI_d + (\nabla u + \nabla u^T)$ , où  $I_d$  est la matrice identité. Le problème (2) est du type Cauchy, qui est considéré comme un problème inverse mal posé au sens d'Hadamard [59], du fait de l'absence de solution si les données  $f$  et  $\Phi$  ne sont pas compatibles mais surtout du fait de son extrême sensibilité aux données bruitées, dans le sens où une légère perturbation des données entraîne une grande perturbation de la solution. Nous visons alors à traiter simultanément la question de l'identification d'un ou plusieurs objets  $\omega^*$  immergés dans un fluide avec celle de la reconstruction des données manquantes sur une partie du bord du domaine  $\Gamma_i = \partial\Omega \setminus \Gamma_c$  à partir des données surabondantes  $(f, \Phi)$ . Afin de modéliser notre problème inverse couplé, on utilise la classe des jeux statiques avec des information complètes. Cette approche est une extension de celles publiées par Habbal et Kallel [55, 56] sur la résolution du problème de Cauchy pour un opérateur elliptique de type divergence. Il s'agit alors de considérer une formulation de jeu de Nash entre trois joueurs : les deux premiers sont consacrés à contrôler les données de Neumann et Dirichlet sur la partie du bord inaccessible  $\Gamma_i$ , tandis que le troisième joueur contrôle la position et la forme des objets. Pour une représentation implicite de bord de l'objet  $\partial\omega^*$ , nous avons adopté la méthode de courbes de niveau où

l'idée est de considérer le bord  $\partial\omega^*$  comme une courbe de niveau zéro d'une fonction lipschitzienne  $\phi : \Omega \rightarrow \mathbb{R}$ . Après la réécriture de nos problèmes directs et nos critères en fonction de courbes de niveau, on présente notre nouvel algorithme de jeux. La classe d'algorithmes que nous proposons s'applique à un large éventail de problèmes inverses mal posés, les techniques de calcul étant plutôt classiques : L'utilisation de la méthode de descente de gradient pour la résolution de trois problèmes de minimisations partielles, l'utilisation de la méthode de l'état adjoint pour calculer les sensibilités, et l'utilisation de la méthode des éléments finis pour la résolution numérique d'équations aux dérivées partielles, ainsi que pour mettre à jour les fonctions de courbes de niveau. Notre code est implémenté avec FreeFem++. Une étude numérique a été développée dans un domaine de deux dimensions, où nous avons réalisé trois tests numériques. Dans le deuxième chapitre, on résout le problème du couplage entre la complétion des données et l'identification des sources : on considère un écoulement de fluide visqueux et incompressible sous l'action d'un nombre fini des particules. On suppose que chaque particule n'est pas plus qu'un seul point et que ce point exercera une force sur le fluide, qui exprime mathématiquement en termes de distribution de Dirac  $\lambda_k \delta_{P_k}$ , où  $P_k$  représente l'emplacement des particules et  $\lambda_k$  est l'intensité de la force. Dans ce cadre, la vitesse du fluide  $u$  et la pression  $p$  satisfont le système suivant :

$$\left\{ \begin{array}{ll} -\operatorname{div}(\sigma(u, p)) = \sum_{k=1}^m \lambda_k \delta_{P_k} & \text{dans } \Omega, \\ \operatorname{div} u = 0 & \text{dans } \Omega, \\ u = G & \text{sur } \Gamma_c, \\ \sigma(u, p)n = \Phi & \text{sur } \Gamma_c, \end{array} \right. \quad (3)$$

avec  $G$  et  $\Phi$  sont deux fonctions connues. L'idée essentielle de notre analyse consiste à reconstruire deux problèmes aux limites bien posés. Chacun utilise l'une ou l'autre des données surabondantes. Ensuite, on utilise une technique de relaxation afin de construire un nouvel algorithme de minimisation. Cette étape consiste à considérer une approximation classique d'une fonction de Dirac au point  $P_k$  par une fonction caractéristique d'une petite boule de centre  $P_k$  et de rayon  $\epsilon$  divisé par son volume. Le problème (3) est reformulé comme un jeu de Nash à trois joueurs. Les deux premiers résolvent le problème de reconstruction des données manquantes sur  $\Gamma_i = \partial\Omega \setminus \Gamma_c$ , tandis que le troisième joueur minimise une fonctionnelle du type Kohn-Vogelius afin de déterminer le nombre de points sources  $m$ , leur emplacement relatif  $P_k$  et leurs intensités approximatives  $\lambda_k$ . La notion de gradient topologique a été utilisée pour la localisation des centres de source présents dans l'écoulement. Trois tests numériques ont été effectués afin d'étudier la robustesse de l'algorithme proposé vis-à-vis des données bruitées en bidimensionnel (2D) et en tridimensionnel (3D). Tous les codes de résolution ont été implémentés avec FreeFem++ MPI, et le besoin de plus d'espace mémoire pour les simulations (3D) nous a conduits à utiliser ffddm. Le troisième chapitre est consacré à la détection de petits objets immergés dans un fluide à partir des mesures effectuées sur une partie du bord extérieur. L'approche introduite par la théorie des jeux s'applique pour ce problème couplé, où le troisième joueur ici utilise la méthode du gradient topologique pour identifier le nombre d'objets et leur emplacement approximatif.

La deuxième partie de cette thèse concerne la résolution des problèmes inverse non linéaire. On considère un écoulement de fluide incompressible et quasi-Newtonien

---

dont la viscosité obéit à la loi de carreau. On présente deux formulations de problème de Cauchy pour le système de Stokes non linéaire, une basée sur une approche de contrôle optimal et l'autre basée sur une stratégie de jeux de Nash. Le traitement numérique de la non linéarité de la fonction de viscosité nécessite des algorithmes spécifiques pour la résolution des problèmes aux limites non linéaires. Parmi eux, on présente l'algorithme de point fixe et on propose un nouveau schème, qui montre une autre façon de traiter les problèmes de Cauchy non linéaire avec un coût très avantageux comparé avec une résolution classique des problèmes non-linéaires. Les résultats numériques obtenus sont satisfaisants et ont montré la performance de notre nouveau schème par rapport à l'algorithme de point fixe. Les deux méthodes proposées sont efficaces et robustes, puisqu'il est capable de débruiter les données et de fournir des reconstructions satisfaisantes. Enfin, on étend l'approche de jeux de Nash pour le problème du couplage non linéaire entre la reconstruction des données manquantes et la détection des inclusions.

# Scientific production

## Publications

1. A. Habbal, M. Kallel, and M. Ouni. Nash strategies for the inverse inclusion Cauchy-stokes problem. *Inverse problems and imaging*, 13 :827–862, 2019.
2. A. Habbal, M. Kallel, and M. Ouni. A Nash-game approach to joint data completion and location of small inclusions in Stokes flow. Accepted for publication in the *ARIMA* journal in December 2020.
3. A. Habbal, M. Kallel, and M. Ouni. A Three-player Nash game for point-wise source identification in Cauchy-Stokes problems. Submitted.
4. A. Habbal, M. Kallel, and M. Ouni. A Nash game strategy to model the nonlinear Cauchy-Stokes problems : Quasi-Newtonian flow. In preparation.

## Conferences

1. 6th International Conference on Engineering Optimization, EngOpt2018, Lisbonne, Portugal.
2. African Conference on Research in Computer Science and Applied Mathematics, CARI'2020, Thiès, Senegal.

# Introduction

*“Satisfaction lies in the effort,  
not in the attainment, full effort  
is full victory.”*

---

Mahatma Gandhi

An inverse problem in science is determining the causal factors that produced them from a collection of observations. It is called an inverse problem because it begins with the effects and calculates the causes. It amounts to reconstructing the past state of a physical system knowing its current state, unlike the direct problem, which predicts the future knowing its current state. Inverse problems are some of the majority significant mathematical problems in science because they inform us of necessary parameters that we cannot directly follow. There are many types of inverse problems, and their applications are found in numerous fields such as hydrogeology, geophysics, acoustics, signal processing, medical imaging, and many other fields. The intensive study of inverse problems is dictated by the subjects' richness from the theoretical and numerical viewpoints. Any direct problem generates a local variety of inverse problems, which gives rise to theoretical questions and numerical challenges. In particular, the inverse problems in fluid mechanics governed by Stokes equations can be properly classified into three possible types : reconstruction of the missing boundary data, geometric/source inverse problem, and parameter (viscosity of the fluid) identification. Inverse problems are well known to be severely ill-posed, and such algorithms require supplementary prior information on the geometries or parameters to be recovery. Various algorithms have been developed, and their abilities to recover their aims have been confirmed. All of the proposed algorithms still require a complete set of data, demanding to carry out measurements on the whole boundary, which is unrealistic in practical situations because parts of the boundary may be inaccessible. In this thesis, we investigate game theory to deal with such problems. We will show that the game's formulation could effectively deal with these problems, and treat even those previously inaccessible, coupling ill-posedness. We will overview the most common approaches for reconstructing the missing data and the identification problem and highlighting their advantages and challenges in the following.

---

## Contents

---

<b>1.1</b>	<b>Cauchy-Stokes problem</b> . . . . .	<b>8</b>
1.1.1	The model problem . . . . .	9
1.1.2	Instability in the Cauchy problem for the Stokes equations . .	10
1.1.3	An optimal control formulation . . . . .	12
<b>1.2</b>	<b>Game Theory</b> . . . . .	<b>13</b>
1.2.1	Game . . . . .	13
1.2.2	Some Applications of Game Theory . . . . .	14
<b>1.3</b>	<b>Geometric inverse problem</b> . . . . .	<b>17</b>
1.3.1	Level set approach . . . . .	17
1.3.2	Shape optimization method . . . . .	18
1.3.3	Topological gradient method . . . . .	19
<b>1.4</b>	<b>Quasi-Newtonian Fluids</b> . . . . .	<b>20</b>

---

---

## 1.1 Cauchy-Stokes problem

Cauchy's problem involves solving a partial differential equation PDE on a domain for which overdetermined boundary conditions are given only on the part of its boundary. The Cauchy problem, also known as a data completion problem, consists of recovering the missing data on the boundary's remaining part. It is a prototype of inverse boundary value problems (IBVP), suitable for many industrial and biomedical applications. Among the different applications already achieved : medical imaging and thermal inspection, such as reconstructing the temperature on the inside wall of a pipeline. Medical imaging provides a large number of inverse problems, we can cite Electrocardiography, Electroencephalography [23, 32, 50, 80, 89, 98]... For instance, Electrocardiography (ECG) is a medical test measuring cardiac activity's electrical potential, using electrodes placed on the patient's chest. However, this tool does not allow to know the potential values on the surface of the heart. But, if we consider the domain delimited by the thorax, such that the overspecified boundary data are the obtained measurements by the electrocardiogram on the thorax surface, and the values of the potentials are the missing data on the surface of the heart. Thus, the numerical resolution of the Cauchy problem, in this case, allows the reconstruction of the electrical potential on the surface of the heart.

The Cauchy problem is known to be severely ill-posed and computationally challenging. The mathematical term well-posed problem was basically introduced by Jacques Hadamard [59] in 1923. He believed that mathematical models of physical problems must have the properties of uniqueness, existence, and stability of the solution. If at least one of these properties is not satisfied, the problem is ill-posed. Inverse problems are often ill-posed. In particular, the Cauchy problem's ill-posedness is mostly related to the solution's instability, even it exists, for a small perturbation of the Cauchy data. Various regularization approaches have been used in the literature to solve certain inverse problems, particularly the ill-posed Cauchy problem. Regularization's method principle consists of substituting the ill-posed problem with a sequence of well-posed problems whose approximate solutions converge to the original inverse problem's exact solution.

One of the most popular methods for ill-posed problems governed by partial differential equations is the Tikhonov method [96, 97], which was introduced by the Russian mathematician Andrey Nikolayevich Tikhonov. The general regularization concept can be found in many papers and books on inverse theory [69]. Tikhonov's regularization method involves solving the inverse problem in the least-squares sense by adding a stabilizing term. The additional term is the norm of solution or its gradient. Cimetièrè et al. [38] proposed to solve the Cauchy problem using an iterative Tikhonov regularization method, and the regularizing term is the distance between two successive iterated solutions. Ben Belgacem and El Fekih [27] treated the Cauchy problem for Laplace's equation interpreted by solving an interface problem by introducing the Steklov Poincaré operator. With Azaiez [15], they are interested in the construction of a stable solution of the Steklov-Poincaré problem using the Tikhonov method.

Lattès and Lion [74] proposed the quasi-reversibility method of changing an ill-posed problem into a well-posed one by introducing a parameter. The convergence



to the original problem is achieved when the parameter tends to zero. Several authors then took up this method to solve certain elliptic inverse problems, Klibanov and Santosa [87], Bourgeois [28].

The iterative method used by Kozlov et al. [71, 72] was extended in [22] for the stationary Stokes system. This method is an altering iterative one, where successive solutions of well-posed mixed boundary value problems for the original equation are computed. This method has been interpreted in terms of an interfacial operator in [10, 24]. Three iterative procedures have been developed by Johansson and Lesnic [63, 62, 64] for obtaining a stable solution to the Cauchy problem for the generalized Stokes system. The first paper proposed an algorithm based on the Landweber-Fridman method, an iteration scheme based on solving a series of mixed well-posed boundary value problems for the generalized Stokes system and its adjoint. A variational conjugate gradient iterative procedure has been proposed in the second one. These two latter algorithms are compared in the third paper with another iterative method, namely, the minimal error method. Notice that in all these mentioned works, the regularizing procedure lies in selecting an appropriate stopping criterion. Other contributions are focused on carefully developing a control type method, which is graciously allowed to approximate the Cauchy problem's solution. Andrieux et al. [85] proposed a new procedure for linear elliptic Cauchy problem based on minimizing energy like error functional. This method has been studied and adapted in different frameworks : elasticity equations [19], Stokes system [24]. A conjugate gradient type optimization procedure used in the works of Aboulaich et al. [1, 2]. A regularization technique has achieved the stabilization of the proposed algorithm. In [55, 56], the authors used a Nash game approach to solve the Cauchy-Laplace problem. Moreover, they compare the Nash game algorithm to a control type method and show its efficiency.

### 1.1.1 The model problem

The considered Cauchy-Stokes problem is given in the following framework : Let  $\Omega$  be a bounded open domain in  $\mathbb{R}^d$  ( $d=2,3$ ), which is filled with a viscous incompressible fluid flowing at low Reynolds numbers governed by the Stokes equations. Its boundary is sufficiently smooth and composed of two parts  $\Gamma_i$  and  $\Gamma_c$ .

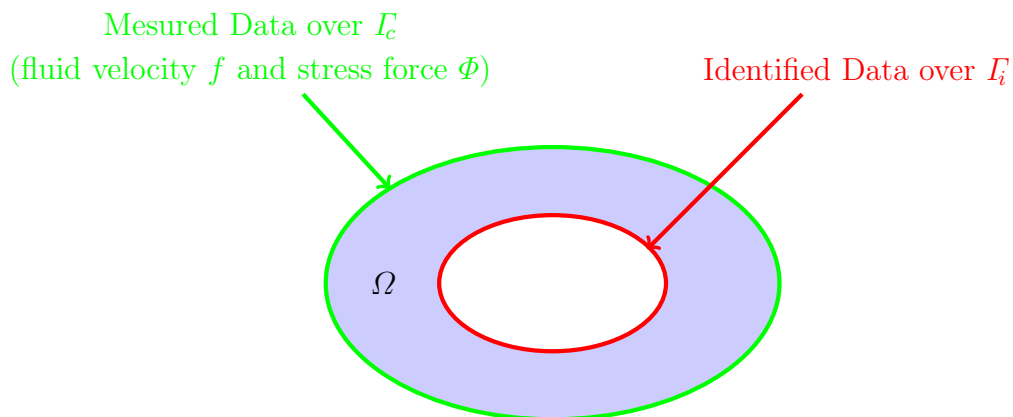


FIGURE 1.1 – Example in a two-dimensional geometry : An annular domain represents a region between two concentric circles.

---

Our Cauchy problem here consists to find  $(u, p) \in H^1(\Omega)^d \times L^2(\Omega)$  such that :

$$(CS) \begin{cases} -\operatorname{div}(\sigma(u, p)) = 0 & \text{in } \Omega, \\ \operatorname{div} u = 0 & \text{in } \Omega, \\ u = f & \text{on } \Gamma_c, \\ \sigma(u, p)n = \Phi & \text{on } \Gamma_c, \end{cases}$$

where  $f \in H^{\frac{1}{2}}(\Gamma_c)^d$  and  $\Phi \in (H_{00}^{\frac{1}{2}}(\Gamma_c)^d)'$  are given functions, and  $\sigma$  being the stress tensor satisfying the following constitutive law

$$\sigma(u, p) = -pI_d + 2\nu D(u),$$

with  $I_d$  is the identity matrix, the coefficient  $\nu > 0$  denotes the kinematic viscosity and  $D(u) = (\nabla u + \nabla u^T)/2$  represents the deformation tensor. The Dirichlet data  $f$  and the Neumann data  $\Phi$  are the so-called Cauchy data, which are known on the accessible part  $\Gamma_c$  of the boundary  $\partial\Omega$ . The problem under study  $(CS)$  is known as a data completion problem, which consists to find the fluid velocity and the normal stress on the inaccessible part of the boundary  $\Gamma_i$ .

The above Cauchy-Stokes problem does not always admit a solution for any given data  $(f, \Phi)$ , but when a solution exists, it is necessarily unique graciously according to the unique continuation property for the Stokes system (see [47]). Therefore, if the Cauchy problem  $(CS)$  has a solution, the Cauchy data are justly said to be compatible.

### 1.1.2 Instability in the Cauchy problem for the Stokes equations

In 1923 (*Lectures on Cauchy's Problem in Linear PDEs* (New York, 1953)) [59], J. Hadamard has been provided precisely a fundamental example to elucidate the ill-posedness of a Cauchy problem for Laplace's equation. He showed that the solution does not depend continuously on the given boundary data.

In our case, we will properly build an analytical example for the stokes system by naturally inspiring from the classic example of J. Hadamard. This example is as follows :

Consider the solution  $(u, p) = ((u_1, u_2), p)$  to the Cauchy-Stokes problem in the upper half plane,

$$\begin{cases} -\operatorname{div}(\sigma(u, p)(x, y)) = 0 & \text{in } \Omega, \\ \operatorname{div} u(x, y) = 0 & \text{in } \Omega, \\ u(x, 0) = f & \text{for every } x \in \mathbb{R}, \\ \sigma(u, p)(x, 0)n = \Phi & \text{for every } x \in \mathbb{R}, \end{cases} \quad (1.1)$$

where  $\Omega = \{(x, y) \in \mathbb{R}^2 | y > 0\}$ . In particular, when the Cauchy data  $(f, \Phi)$  are equal to zero, we have the following solution

$$(u(x, y), p(x, y)) = (0, 0),$$

( $p=cte$  is also a solution, and to have a uniqueness we can choose  $p$  such that its average is zero). For  $n > 0$ , we introduce the pair  $(f^n, \Phi^n)$ , the perturbation of the data  $(f, \Phi)$ , given by

$$\begin{cases} f^n &= (0, -\frac{1}{n^2}\cos(nx)) \\ \Phi^n &= (\frac{1}{n}\sin(nx), 0). \end{cases}$$

Then, the perturbed solution of the Cauchy-Stokes problem (1.1) becomes,

$$\begin{cases} u_1^n(x, y) &= \frac{1}{n^2}\sin(nx)\sinh(ny), \\ u_2^n(x, y) &= -\frac{1}{n^2}\cos(nx)\cosh(ny), \\ p^n(x, y) &= 0. \end{cases}$$

One can remark that if  $n \rightarrow \infty$ , then we have  $(\Phi^n - \Phi)$  and  $(f^n - f)$  tend to zero, while the perturbation  $(u^n(x, y) - u(x, y))$  takes high values for any  $y > 0$ . Therefore, to sufficiently illustrate this example we have plotted the two components of  $(u^n(x, y) - u(x, y))$ , for  $n = 10000$  with different values of  $y$ , see Figure 1.2.

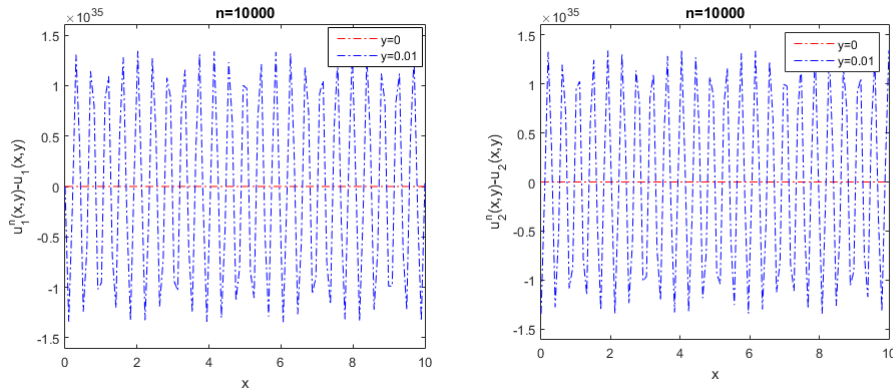


FIGURE 1.2 – Exponential explosion for high frequencies.

This problem's ill-posed character makes its mathematical resolution delicate enough and cannot directly consider due to the risk of having unstable solutions. A large number of approaches can be found in the literature for solving the Cauchy-Laplace problem. In the following subsection, we will present an extension for the Stokes system by two control-type approaches introduced in [2, 24]. The main idea of those approaches was borrowed liberally from the domain decomposition. It consists of reconstructing two well-posed problems. The solution to the Cauchy problem breaks down into a couple of functions.

In consequence, the Cauchy-Stokes problem can be split into two well-posed sub-problems with mixed boundary conditions as follows :

$$\begin{cases} (P_1) \left\{ \begin{array}{l} \text{Find } (u_1, p_1) \in H^1(\Omega)^d \times L^2(\Omega) \text{ such that :} \\ -\text{div}(\sigma(u_1, p_1)) = 0 \quad \text{in } \Omega, \\ \text{div} u_1 = 0 \quad \text{in } \Omega, \\ u_1 = f \quad \text{on } \Gamma_c, \\ \sigma(u_1, p_1)n + \alpha u_1 = \eta + \alpha \tau \quad \text{on } \Gamma_i, \end{array} \right. \\ (P_2) \left\{ \begin{array}{l} \text{Find } (u_2, p_2) \in H^1(\Omega)^d \times L^2(\Omega) \text{ such that :} \\ -\text{div}(\sigma(u_2, p_2)) = 0 \quad \text{in } \Omega, \\ \text{div} u_2 = 0 \quad \text{in } \Omega, \\ \sigma(u_2, p_2)n = \Phi \quad \text{on } \Gamma_c, \\ \sigma(u_2, p_2)n + \beta u_2 = \eta + \beta \tau \quad \text{on } \Gamma_i, \end{array} \right. \end{cases}$$

---

where  $\eta \in (H_{00}^{\frac{1}{2}}(\Gamma_i^d))'$ ,  $\tau \in H^{\frac{1}{2}}(\Gamma_i^d)$  are given functions,  $\alpha$  and  $\beta$  are real parameters, that makes it possible to specify the different types of boundary conditions on  $\Gamma_i$  :

- The Neumann-Dirichlet case corresponds to  $\alpha = 0$  and  $\beta = +\infty$  (i.e. a Neumann boundary condition over  $\Gamma_i$  and a Dirichlet boundary condition over  $\Gamma_i$  respectively in  $(P_1)$  and  $(P_2)$  ).
- The Dirichlet-Dirichlet case corresponds to  $\alpha = \beta = +\infty$ .
- The Neumann-Neumann case corresponds to  $\alpha = \beta = 0$ .

In general, these two problems are distinct for any values of  $\eta$  and  $\tau$ . Although when they coincide, the Cauchy problem is solved efficiently. The researchers carefully have introduced methods that minimize the gap between the two sub-problems' two solutions to solve the initial inverse problem.

### 1.1.3 An optimal control formulation

**Minimization of an energy-like error functional :** In this paragraph, we present an approach developed in [24] to solve the Cauchy-Stokes problem (Laplace equation in [10]), where this latter is converted into an optimization one, and an energy-like functional is introduced. Then, the authors proposed an optimal control formulation given by :

$$\left\{ \begin{array}{l} \text{Minimize } \mathfrak{E}_{\alpha,\beta}(\eta, \tau), \text{ for all } (\eta, \tau) \in (H_{00}^{\frac{1}{2}}(\Gamma_i^d))' \times H^{\frac{1}{2}}(\Gamma_i^d), \\ \text{where } \mathfrak{E}_{\alpha,\beta}(\eta, \tau) = \frac{1}{2} \int_{\Omega} \sigma(u_1 - u_2, p_1 - p_2) : \nabla(u_1 - u_2) dx, \\ \text{such that } (u_1, p_1) \text{ and } (u_2, p_2) \text{ are the solutions of the respective BVP}(P_1) \text{ and } (P_2). \end{array} \right.$$

The authors used an iterative process based on the preconditioned gradient algorithm. To show the efficiency of the proposed method, they make a comparison with the Kozlov–Maz'ya–Fomin's algorithm [72], which is an alternative method introduced for solving the ill-posed problem. The basic idea of KMF's method is to reduce the ill-posed problem to a sequence of well-posed mixed boundary value problems, and it describes in the following steps for the Neumann-Dirichlet case :

- Step I : Choose an initial guess  $\eta_0 \in (H_{00}^{\frac{1}{2}}(\Gamma_i^d))'$ , and solve the problem  $(\mathcal{P}_1)$  with  $\eta = \eta_0$ .
- Step II : For  $j \geq 1$ , a sequence of well-posed mixed BVP  $(u^j, p^j)$  is generated as follows :
- 1-  $(u^{2j+1}, p^{2j+1})$  solve the well-posed mixed BVP  $(P_2)$  with  $\tau = u^{2j}$  on  $\Gamma_i$ .
  - 2-  $(u^{2j+2}, p^{2j+2})$  solve the well-posed mixed BVP  $(P_1)$  with  $\eta = \sigma(u^{2j+1}, p^{2j+1})_n$  on  $\Gamma_i$ .
  - 3- Repeat step 1 until a prescribed stopping criterion is satisfied.

The KMF's algorithm can be properly characterized as an alternating-direction minimization method for the energy-like error functional  $\mathfrak{E}$ .

**A control-type regularized data recovering process :** A control-type method for solving the Cauchy problem was presented in the work of Aboulaich et al. [1, 2]. The overall idea of this approach is to convert the problem into an optimization one.

---

A regularization technique is developed here in order to properly handle the instability of the solution of the ill-posed problem. For the Neumann-Dirichlet case, the authors exploit the problems  $(P_1)$  and  $(P_2)$ , to solve the following minimization problem :

$$\left\{ \begin{array}{l} \text{Find } (\eta^*, \tau^*) \in (H_{00}^{\frac{1}{2}}(I_i)^d)' \times H^{\frac{1}{2}}(I_i)^d \text{ such that :} \\ (\eta^*, \tau^*) = \arg \min_{\eta, \tau} \mathfrak{J}(\eta, \tau), \\ \text{where } \mathfrak{J}(\eta, \tau) = \frac{1}{2} \|\sigma(u_1(\eta), p_1(\eta))n - \Phi\|_{(H_{00}^{\frac{1}{2}}(I_c)^d)'}^2 + \frac{1}{2} \|u_1(\eta) - u_2(\tau)\|_{H^{\frac{1}{2}}(I_i)^d}^2. \end{array} \right.$$

The functional  $\mathfrak{J}$  splits into a classical least square term on  $I_c$  and a regularizing one on  $I_i$ , where the data is to be completed. The authors showed that this function is twice Fréchet differentiable and strictly convex, and they used the Lagrangian method, which makes it possible to evaluate the gradient components. Then, they used a conjugate gradient algorithm to minimize the above function  $\mathfrak{J}$ .

## 1.2 Game Theory

Game theory is the study of mathematical models. It allows a formal analysis of conflicts posed by agents' strategic interaction (are called -players), pursuing their own goals. A formal theory of games was suggested by the mathematician John Von Neumann and economist Oskar Morgenstern in a "*Theory of Games and Economic Behavior*" in 1944 [81]. Mathematician John Nash is considered by many as contributing the first significant extension of Neumann and Morgenstern's work. He introduced what has now been named the *Nash equilibrium* of a strategic game in the 1950s.

### 1.2.1 Game

The game is the object of studying game theory. All games are described as a set of circumstances that depend on all decision-makers' actions (players). It is defined as a formal description of a strategic situation. It has three essential elements :

- A (finite) number of players  $N = \{1, \dots, n\}$ .
- Each player  $i$  has a strategy set  $S_i$ .
- Each player  $i$  has a cost functional  $F_i : S_1 \times S_2 \times \dots \times S_n \rightarrow \mathbb{R}$ .

Different categories of games can distinguish in game-theory according to three main criteria :

- (i) the ability of players to formally commit to their future decisions,
- (ii) the complete or incomplete nature of the information,
- (iii) the static or dynamic nature of the game.

This classification is necessary because we do not use the same tools to solve any game type. Roughly speaking, the first criterion refers to the two main approaches, *cooperative vs non-cooperative*, around which game theory has historically been built. *Cooperative* games in which players are allowed to cooperate on a joint strategy. For *non-cooperative* is the basic assumption that players cannot cooperate; they are completely free to decide when making their choices. Games with complete information, meaning that all players know each others' strategy spaces and cost functionals. The failure of this assumption is termed as a game with incomplete information. Thus,

---

a game will be dynamic if the game's progress provides information to at least one player; otherwise, it is static.

In a game, an equilibrium is when the players have made their decisions, and an outcome is reached. John Nash proved that every finite n-player non-cooperative game has what is now known as a Nash equilibrium :

*A Nash equilibrium is a strategy profile  $s^* = \{s_1^*, \dots, s_n^*\} \in \prod_{i=1}^n S_i$ , such that the strategy of player  $i$  is a better answer :*

$$B_i(s_{-i}^*) = \left\{ s_i \in S_i / F_i(s_i, s_{-i}^*) \leq F_i(s'_i, s_{-i}^*), \forall s'_i \in S_i \right\} \quad (1.2)$$

where  $s_{-i}$  is the profile  $s$  of strategies other than those of player  $i$  :  $s_{-i} = \{s_1, \dots, s_{i-1}, s_{i+1}, \dots, s_n\}$ .

Game theory's object is to formalize the interactions to predict the possible outcome and help the player or players choose the best strategy.

## 1.2.2 Some Applications of Game Theory

In the present section, we overview some applications in applied mathematics and in biology carefully studied by using the game-theoretic approach.

**Tumoral angiogenesis as a Nash game :** In [53, 54], an original approach based on game theory frameworks proposed to model pro- and antiangiogenesis. Angiogenesis is a blood network created by cancer cells, and this network allows both to feed the tumor and disperse the cancer cells via the blood networks. Indeed, this network is produced thanks to activators' action, which naturally induces the migration of endothelial cells from a nearby vessel toward the tumor and the destruction of the tissues in their direct path to making easy the construction of new capillary and vascular networks.

Angiogenesis can be described as a competition between a density of activators, which act to provide the tumor with an optimum blood network, and a density of inhibitors which act to reduce the tissue degradation. These densities act in a context described by a fluid-structure coupling model, which means a porous media model, representing the fluid needs of the tumor, and a linear elasticity model, representing the need for good structural behavior of the host tissue.

For that, the authors considered a two-player zero-sum game. The two players are activator and inhibitor, where activators aim to maximize the tumor drainage while the inhibitors play with exactly the opposite objective. The combined action of activators and inhibitors leads to creating a blood network, whose shape is obtained using topological optimization. Figure 1.3 illustrates the porosity distribution at convergence, obtained by Habbal et al. [54].

**Game-theoretic approach to joint image restoration and segmentation :** Kallel et al. [65] proposed a game-theoretic approach to solving the problem of image restoration and segmentation jointly. The authors considered a two-player static of complete information game where the first player is restoration, and the second is

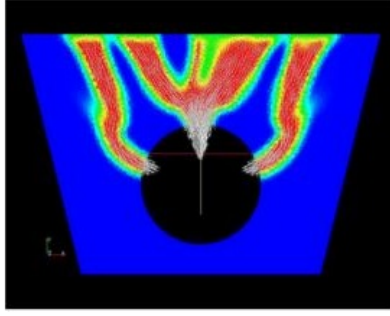


FIGURE 1.3 – The 2D model of a circular tumor with a vascular network : strategies converging to a Nash equilibrium [54].

segmentation. The restoration player's goal is to minimize, with an image intensity  $I$  as a strategy variable, the functional :

$$\mathfrak{J}_1(I, C) = \int_{\Omega} (I - I_0)^2 dx + \mu \int_{\Omega \setminus C} |\nabla I|^2 dx,$$

while the segmentation player aims at minimizing the following functional with the discontinuity set  $C$  -contours- as strategy variable,

$$\mathfrak{J}_2(I, C) = \sum_{i=1}^k \int_{\Omega_i} (I_0 - I_i)^2 dx + \nu |C|, \text{ where } I_i = \frac{1}{|\Omega_i|} \int_{\Omega_i} I(x) dx.$$

Since both objectives depend on both strategies, then, solving the game amounts to finding a Nash equilibrium, defined as a possible of strategies  $(I^*, C^*)$  such that the following holds

$$\begin{aligned} (I^*, C^*) &= \arg \min_I \mathfrak{J}_1(I, C^*), \\ &= \arg \min_C \mathfrak{J}_2(I^*, C), \end{aligned}$$

with  $I^*$  is sought in the Sobolev space  $H^1(\Omega \setminus C^*)$ , and  $C^*$  is sought the set of the union of curves made of a finite set of  $C^{1,1}$ -arcs. In order to compute this equilibrium, the authors used a classical iterative method with relaxation. Figure 1.4 present a numerical result using a level set approach, obtained by the authors of article [65].

**A Nash game formulation of the Cauchy problem :** Habbal and Kallel [55, 56] introduced a game theory-based algorithm for solving the Cauchy problem for an elliptic operator, which consists of recovering the Dirichlet and Neumann missing data over  $I_i$ . Then, in order to solve this inverse problem, the authors proposed to formulate it as a two-player Nash game, and introduced the two following cost functional : for  $\eta \in H^{-\frac{1}{2}}(I_i)$  and  $\tau \in H^{\frac{1}{2}}(I_i)$ ,

$$\begin{aligned} \mathcal{J}_1(\eta, \tau) &= \frac{1}{2} \|k \nabla u_1 \cdot \nu - \Phi\|_{H^{-\frac{1}{2}}(I_c)}^2 + \frac{1}{2} \|k \nabla u_1 \cdot \nu - k \nabla u_2 \cdot \nu\|_{H^{-\frac{1}{2}}(I_i)}^2, \\ \mathcal{J}_2(\eta, \tau) &= \frac{1}{2} \|u_2 - f\|_{H^{\frac{1}{2}}(I_c)}^2 + \frac{1}{2} \|k \nabla u_1 \cdot \nu - k \nabla u_2 \cdot \nu\|_{H^{-\frac{1}{2}}(I_i)}^2, \end{aligned}$$

where the fields  $u_1(\eta)$  and  $u_2(\tau)$  are the unique solutions to the respective BVP,

$$(SP_1) \begin{cases} \nabla \cdot (k \nabla u_1) = 0 & \text{in } \Omega, \\ u_1 = f & \text{on } I_c, \\ k \nabla u_1 \cdot \nu = \eta & \text{on } I_i. \end{cases} \quad (SP_2) \begin{cases} \nabla \cdot (k \nabla u_2) = 0 & \text{in } \Omega, \\ u_2 = \tau & \text{on } I_i, \\ k \nabla u_2 \cdot \nu = \Phi & \text{on } I_c. \end{cases}$$

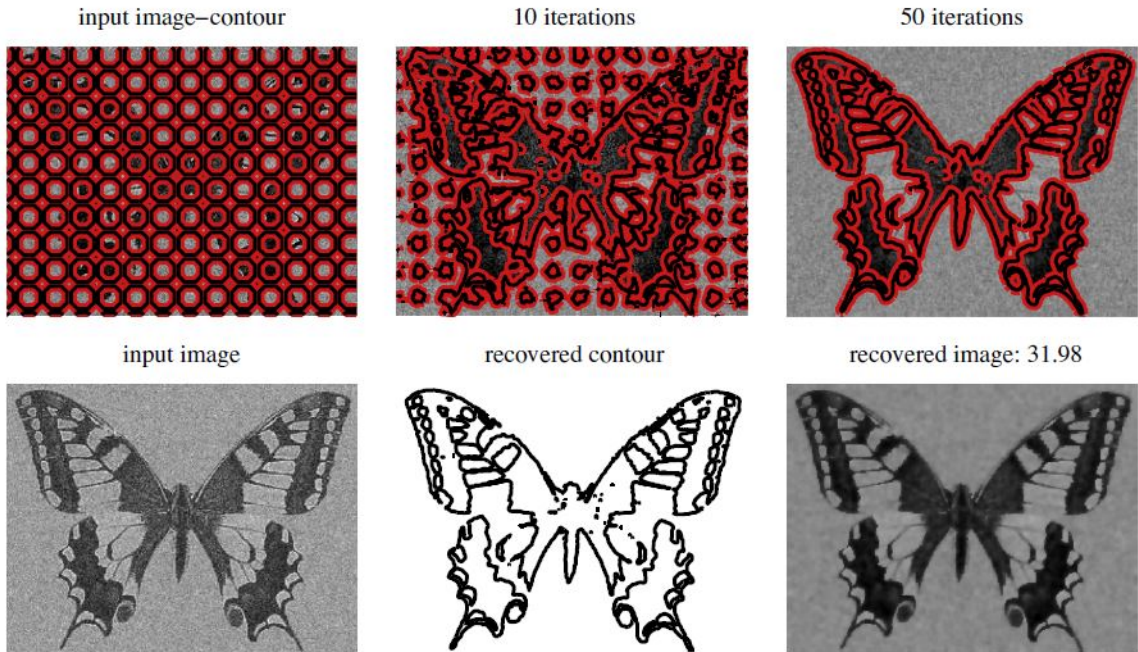


FIGURE 1.4 – Top row : noisy image with Gaussian noise and initial contour, evolution by iterations. Bottom row : segmentation and restoration of image by the Nash game algorithm [65].

In a few words, the first player controls the strategy variable  $\eta$ , which belongs to the space strategy  $H^{-\frac{1}{2}}(I_i)$ , and the second player controls the strategy variable  $\tau$ , which belongs to the space strategy  $H^{\frac{1}{2}}(I_i)$ . Each of the two players tries to minimize its own cost, namely,  $\mathcal{J}_1$  for the first player and  $\mathcal{J}_2$  for player the second one. Clearly each player's cost depends on other strategy. Then, the Neumann and Dirichlet controls  $\eta$  and  $\tau$  do cooperate to minimize either  $\mathcal{J}_1$  or  $\mathcal{J}_2$ . A pair of strategies  $(\eta^*, \tau^*)$  is a Nash equilibrium if

$$\begin{aligned} (\eta^*, \tau^*) &= \arg \min_{\eta} \mathcal{J}_1(\eta, \tau^*), \\ &= \arg \min_{\tau} \mathcal{J}_2(\eta^*, \tau). \end{aligned}$$

The authors proved that there always exists a unique Nash equilibrium, which is exactly the missing data when the Cauchy problem has a solution. The game separable structure is crucial for the proof, by the fact that the Neumann gap in  $\mathcal{J}_1$  depending only on  $\eta$  and the Dirichlet gap in  $\mathcal{J}_2$  depending only on  $\tau$ . According to the Nash theorem [56], the existence of a Nash equilibrium has been proved by using the partial ellipticity of  $\mathcal{J}_1$  and  $\mathcal{J}_2$  with respect to  $\eta$  and  $\tau$ , respectively. This property allows us to restrict the search for Nash equilibria to bounded subsets of the strategy spaces, which remains consistent with the classical results of the conditional stability of the Cauchy problem [3]. They also proved that the completion process by the Nash-game approach is stable with respect to noisy data. The nonradial missing data, obtained by Habbal and Kallel [56], are presented in Figure 1.5, with noisy Cauchy data over  $I_c$ .

Many other investigations are focusing on the game theory framework. For instance, in electrocardiography imaging [36], the authors have introduced a Nash game algorithm to simultaneously recover the value of different tissues' conductivity and the potential



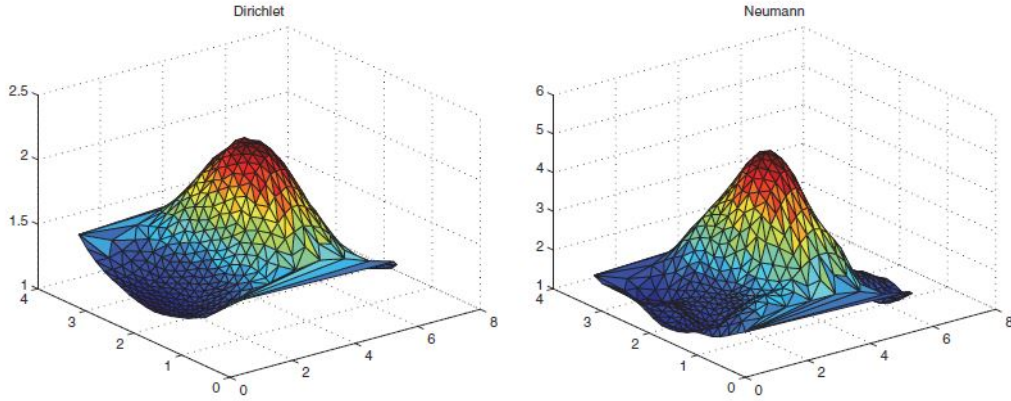


FIGURE 1.5 – Reconstructed nonradial Dirichlet ( $\tau_N$ , left) and Neumann ( $\eta_N$ , right) data over  $\Gamma_i$ . The profiles are presented at convergence and for a noise level  $\sigma = 5\%$  [56].

and flux on the heart’s surface from available measurements on the thorax’s surface. An application related to the topology design of coupled heat transfer-thermoelastic system is presented in [58]. The authors formulated the problem as a 2-players Nash game, where the structure and the temperature distribution in the structure are considered as strategies to respectively the first and second players. In [66], the authors studied the image inpainting problem, where the data are not available on a part of the damaged region’s boundary. They used a Nash game approach after reformulating the inpainting image problem as a Cauchy one.

### 1.3 Geometric inverse problem

The geometric inverse problem, i.e., a problem where the unknown is a geometric shape, has been studied theoretically and numerically. It consists precisely of finding the optimal geometry of an object with respect to certain criteria. Generally, this problem can be modeled as follows :

$$\min_{\Omega \in E} \mathcal{J}(\Omega, u_\Omega) \quad (1.3)$$

where  $E$  is a given set of admissible geometries,  $u_\Omega$  is a solution to a given partial differential equation PDE defined in  $\Omega$ . Various mathematical approaches in different frameworks are available to solve this type of problem(1.3) : Level-set approach, topological sensitivity analysis method, shape gradient approach, and homogenization theory.

#### 1.3.1 Level set approach

The level-set method was proposed first by the mathematicians Stanley Osher and James Sethian [83]. It has become popular in many disciplines, such as computational fluid dynamics, optimization, and image processing [13, 65, 82]. This approach supplies an efficient way of describing time-evolving curves and surfaces that may undergo a topological change; with this approach, one can perform numerical computations on a fixed grid without parameterizing the unknown objects included in the domain.

---

In a few words, the level set method is used to describe interfaces that evolve along a given velocity field implicitly, as zero level sets of an evolving scalar function  $\phi = \phi(x, t)$ . This function  $\phi$  attains positive values in one subdomain and negative values in the other, while the material interface is given by the zero level set of the function  $\phi$ . Therefore, the level set function  $\phi$  here represents the shape's boundary to be identified during the optimization process. The Hamilton–Jacobi equation governs the change of the level set function  $\phi$  as follows :

$$\frac{\partial}{\partial t}\phi + V \cdot \nabla \phi = 0,$$

where  $t$  is a pseudo-time parameter and  $V$  is the desired normal velocity on the boundary. In a conventional level set method, it is crucial to keep the level set function as a distance function during the evolution procedure because steep or flat slopes can develop in the evolution of  $\phi$  through the Hamilton–Jacobi equation. It is well known that a signed distance function must satisfy the property  $|\nabla \phi| = 1$ . This initialization, which does not affect the zero level set's computation, increases the computation accuracy and has been extensively used as a remedial measure.

### 1.3.2 Shape optimization method

Advanced shape optimization techniques have become a potent tool in the design and construction of industrial structures. The shape optimization problem is formulated as the minimization of a given shape functional (1.3), which consists of finding the unknown shape of domain or subdomain of  $\mathbb{R}^n$ , whose topology is given. The sensitivity analysis has been rigorously investigated in several published works [60].

There is either nonparametric (free form) or parametric shape optimization. In parametric shape optimization, the shape of a body is varied by parameters, typically assuming the role of dimensions or orientations of this body to build the optimal shape. Thus, when a spline curve or surface describes a shape, the shape sensitivities may also be related to the control points' position meanings this curve or surface. On the other hand, the nonparametric shape optimization is excessively linked to the body's general geometry. A shape functional's sensitivity concerning a smooth arbitrary perturbation of these shapes is called the shape derivative. The last method is based on the accurate computation of the shape derivative of the functional  $\mathcal{J}$  :

$$d\mathcal{J}(\Omega; V) = \lim_{t \rightarrow \infty} \frac{\mathcal{J}(\Omega_t) - \mathcal{J}(\Omega)}{t}, \quad (1.4)$$

where  $\Omega_t = T_t(\Omega)$  denotes the transformed domain under the flow  $T_t(V)$  generated by a smooth vector field  $V$ .

There exists a certain number of methods available to compute the shape derivative above (1.4) the direct method based on calculating the material derivative of a solution of a partial differential equation PDE [99], and the Lagrangian method developed by J. C ea [33].

If in addition the derivative is linear with respect to  $V$ , then, one can be written it as follows :

$$d\mathcal{J}(\Omega; V) = \int_{\partial\Omega} g V \cdot n \, ds,$$

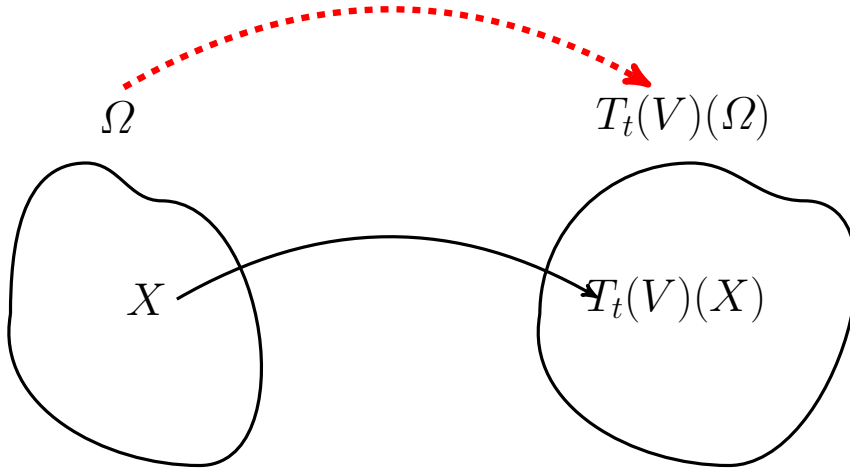


FIGURE 1.6 – Perturbed domain.

where  $g \in L^2(\partial\Omega)$ . This gives a natural idea of gradient descent, where the boundary  $\partial\Omega$  is evolved in the direction of negative shape gradient in order to reduce the value of the cost functional.

As soon as a descent direction  $V$  is obtained, it advects the shape in the direction of  $V$ . There are, respectively, two different processes to describe a shape, explicitly and implicitly. If the interface is given explicitly, e.g., by a spline, then the procedure consists of simply moving the interface a certain distance into the direction given by  $V$  and looking at the impact of these variations on the objective function. One of the difficulties of this method is the remeshing. Indeed, so that the computation by finite elements is reliable, the mesh must respect certain criteria. If the form varies a lot, that imposes to remesh the domain. However, the software generally uses the number of the elements to define the boundary conditions or the extraction of the results, and a remeshing necessarily implies a renumbering. Another way is possible, where the shape can be represented in an implicit mode, employing a level set function where the Hamilton-Jacobi equation describes its evolution.

### 1.3.3 Topological gradient method

To present the basic idea, let  $\Omega$  be a bounded domain of  $\mathbb{R}^d$  ( $d = 2, 3$ ), and  $j(\Omega) = \mathcal{J}(\Omega, u_\Omega)$ . For  $\epsilon > 0$ , let  $\Omega_\epsilon = \Omega \setminus \overline{(x_0 + \epsilon B)}$  be the domain obtained by removing a small part  $(x_0 + \epsilon B)$  from  $\Omega$ , at a location  $x_0 \in \Omega$ , and  $B$  is a fixed bounded domain containing the origin. Then, the asymptotic expansion of the cost function  $j$  with respect to  $\epsilon$ , takes the form

$$j(\Omega \setminus \overline{(x_0 + \epsilon B)}) - j(\Omega) = \rho(\epsilon)g(x_0) + o(\rho(\epsilon)).$$

In this expansion,  $\rho(\epsilon)$  denotes an explicit positive function going to zero with  $\rho$  and  $g(x_0)$  is called the topological gradient or topological derivative. Therefore, to minimize the cost functional  $j$ , one has to create holes at some points  $x$  where the topological gradient  $g(x)$  is the most negative. It is usually simple to compute using direct and adjoint problems defined in the initial domain. Various kinds of topology optimization problems

---

have been solved efficiently by using the topological gradient method : the elasticity case [52], Laplace equation [9], Navier-Stokes equations [8] and Maxwell equations [79]...

In [25], a numerical process based on the topological gradient method is applied to solve the inverse problem of detecting of small flaws' locations from boundary measurements. The topological sensitivity analysis is given for the Stokes system with respect to the insertion of a small hole (gas bubble)  $\mathcal{B}_\epsilon$  in the domain  $\Omega$ , with a homogeneous Neumann condition is prescribed on the boundary  $\partial\mathcal{B}_\epsilon$ . In [35], Caubet et al. used the notion of a topological gradient in combination with the shape derivative of a Kohn-Vogelius functional to find the number, the location, and the shape of the obstacle, which are immersed in a fluid, for the two-dimensional case via the measurement of the velocity of the fluid and the Cauchy forces on the outer boundary. They considered the homogeneous Dirichlet boundary conditions on the obstacles. Ben Ameer et al. [26] studied the geometric inverse problem in linear elasticity. This problem consists of identifying an unknown interface or inclusion from a single boundary measurement. A regularization approach was used to compute stable approximations of the solutions by adding multiple perimeters as a penalty to the least-square functional. The authors employed the level-set approach with the shape gradient method for the reconstruction problem's numerical solution.

The topological gradient method has also been greatly used to identify the source location. In [49], Ferchichi et al. investigated a Dirac–Stokes problem under the action point-forces located inside the domain. In order to solve this problem, they have properly used relaxation techniques and have formulated the relaxed problem as a topological optimization one.

## 1.4 Quasi-Newtonian Fluids

Experimental observations show that, for some fluids as water, the viscosity is constant. These precious fluids are called Newtonian. However, considered experiments show that the viscosity, for several other fluids such as biological or polymer fluids, is no more constant, called non-Newtonian or complex fluids. The latter sufficiently showed that the fluid viscosity might typically vary depending on gradient tensor or temperature or else time... Governed by the classical Stokes or Navier–Stokes equations, the Newtonian fluid flows are a well-reasoned estimation of the more realistic non-Newtonian fluids. In this work, we will be interested in the quasi-Newtonian fluid flow models, which could be considered a first step into the world of complex fluids. The most applied formulations of the viscosity, in this case, are based on the deformation tensor [18, 20, 21, 88].

The model that we work is as follows : consider the motion of incompressible fluids in a bounded open domain  $\Omega \in \mathbb{R}^d$  ( $d=2,3$ ), described by the fluid velocity  $u$  and the pressure  $p$  such that

$$(QNS) \begin{cases} -\operatorname{div}(\sigma(u, p)) = f & \text{in } \Omega, \\ \operatorname{div} u = 0 & \text{in } \Omega, \end{cases}$$

---

where  $f$  is a given source term, and the stress tensor  $\sigma$  expresses as follows :

$$\sigma(u, p) = -pI_d + 2\nu(|D(u)|^2)D(u),$$

with  $\nu : \mathbb{R}_+ \rightarrow \mathbb{R}_+$  is a viscosity function. There are two prevalent classical models : Carreau's law and the power law. The boundary Dirichlet condition allows us to close simply the equation's system ( $QNS$ ) and write their weak formulation. There are other boundary conditions gently leading to a closed system of equations, i.e., capable of admitting a unique solution [18, 21, 39]. Existence and uniqueness results are given in the previous references, for the system ( $QNS$ ) with homogeneous Dirichlet boundary data. Specific techniques developed in these investigations allow the correct handling of non-linearity. To the best of our knowledge, there is no work devoted to the case where a single pair of Dirichlet and Neumann data are available only on the part of the boundary, that is, the case of the Cauchy problem for nonlinear Stokes system. But, there are a few works that were concerned with nonlinear elliptic Cauchy problems ; we can cite the work of Avdonin et al. [14] which used an iterative method for solving a nonlinear elliptic Cauchy problem in glaciology. In [66], the authors used a game strategy to solve the image inpainting problem as a nonlinear Cauchy problem. In [73], the authors proposed two iterative methods based on the segmenting Mann iteration applied to fixed point equations. The first approach consists of transforming the nonlinear Cauchy problem into a linear Cauchy problem and analyzing a linear fixed point equation. A nonlinear fixed point equation is considered on the second approach, and a thoroughly nonlinear iterative method is investigated. An approach is based on a Tikhonov regularization method in [42].

## Organization of the Thesis

This thesis is organized into five chapters and a conclusion.

**Chapter 1** gives an overview of the most common approaches used to solve parameter or geometric identification problems highlight their advantages and challenges. **Chapter 2** takes the form of an article published in *Inverse problems and imaging* [57]. It is dedicated to solving the inverse inclusion Cauchy-Stokes problem. This problem involves detecting one or more inclusions immersed in a stationary viscous fluid, using only a single pair of Dirichlet and Neumann boundary measurements. We use the simplest class of games in order to model our coupled inverse problem, specifically, the class of static games with complete information.

In **Chapter 3**, we present an approach to recover jointly the location, magnitude of a finite but unknown number of point-wise sources, and missing boundary data using an original Nash game strategy. This approach studies the strategic interactions between players, where the optimal point-force location is characterized as the solution to the topological optimization problem.

**Chapter 4** is based on the work presented in [57]. We consider the topological gradient method to determine some small objects' best locations, using incomplete measurements, which was the subject of a paper that has been accepted for publication in the ARIMA journal.

---

**Chapter 5** aims to treat nonlinear Stokes models arising in quasi-Newtonian fluids and the Cauchy type problem framework. Thus, we consider two well-posed mixed BVPs, and we propose a new one-shot scheme to solve the nonlinear Cauchy problem. Two iterative procedures were developed to reconstruct the solution of our inverse problem numerically. A comparison of the one-shot scheme with a fixed-point method to solve the nonlinear BVPs is performed. This comparison shows our novel scheme's excellent performance from a data completion viewpoint for noise-free and noisy cases.

# Nash strategies for the inverse inclusion Cauchy-Stokes problem

*“But in my opinion, all things in nature occur mathematically.”*

---

René Descartes

**Abstract.** We introduce a new algorithm to solve the problem of detecting unknown cavities immersed in a stationary viscous fluid, using partial boundary measurements. The considered fluid obeys a steady Stokes regime, the cavities are inclusions and the boundary measurements are a single compatible pair of Dirichlet and Neumann data, available only on a partial accessible part of the whole boundary. This inverse inclusion Cauchy-Stokes problem is ill-posed for both the cavities and missing data reconstructions, and designing stable and efficient algorithms is not straightforward. We reformulate the problem as a three-player Nash game. Thanks to an identifiability result derived for the Cauchy-Stokes inclusion problem, it is enough to set up two Stokes boundary value problems, then use them as state equations. The Nash game is then set between 3 players, the two first targeting the data completion while the third one targets the inclusion detection. We used a level-set approach to get rid of the tricky control dependence of functional spaces, and we provided the third player with the level-set function as strategy, with a cost functional of Kohn-Vogelius type. We propose an original algorithm, which we implemented using Freefem++. We present 2D numerical experiments for three different test-cases. The obtained results corroborate the efficiency of our 3-player Nash game approach to solve parameter or shape identification for Cauchy problems.

**keywords :** Data completion, Cauchy-Stokes problem, shape identification, Nash games.

This chapter takes the form of a published article :  
 A. Habbal, M. Kallel, and M. Ouni. Nash strategies for the inverse inclusion Cauchy-stokes problem. *Inverse problems and imaging*, 13 :827–862, 2019.

---

## Contents

---

<b>2.1</b>	<b>Introduction</b>	<b>25</b>
<b>2.2</b>	<b>Data completion for the Stokes problem</b>	<b>28</b>
<b>2.3</b>	<b>An identifiability result for the inverse inclusion Cauchy-Stokes problem</b>	<b>32</b>
<b>2.4</b>	<b>Coupled data completion and geometry identification for the Stokes problem</b>	<b>34</b>
2.4.1	A level-set formulation	35
2.4.2	Level-set sensitivity and optimality condition	36
2.4.3	The three-player Nash algorithm	39
<b>2.5</b>	<b>Numerical experiments</b>	<b>40</b>
<b>2.6</b>	<b>Conclusion</b>	<b>45</b>

---



---

## 2.1 Introduction

Fluid dynamics are central in many industrial, biological and biomedical processes. The good functioning of the involved systems could be dramatically damaged in the presence of undesired small obstacles (impurities) or inclusions (cavitation). For example, polymer material degradation is related to the formation of inclusions during polymer extrusion [92]; as well, the mechanism of joint cracking is related to cavity formation [68].

A large spectrum of the processes above can be considered as Stokes flows, though they should be taken unsteady and anisotropic to render satisfactorily the complex phenomenon of the formation of cavities [93]. The shape and location of the inclusions is generally out of reach for direct observation, hence the need for effective nondestructive monitoring solutions, known as geometric inverse problems when mathematics and algorithms are involved. Popular mathematical models build on the assumption that some specific measurements are available over the whole boundary of the structure under investigation, dealing with partial differential equations of boundary value -BVP- type. However, it should be noticed that from a technological point of view, when industrial devices are involved, the assumption above is in general impossible to fulfill, either because it is too expensive, or simply because part of the boundary is not accessible to probing, think of a heart valve [76]. Such restrictions lead to develop complex protocols like for the detection of flaws in metal melts in foundry industry [67]. Industrial solutions use in general protocols where emission and reception of the probing signals are set on the same location of the boundary. From a mathematical point of view, we have access to over specified boundary data (e.g. temperature and thermal flux) on the probing location, and no data elsewhere. Thus, we deal with partial differential equations, having access to over specified boundary data, and missing data to recover as well as unknown inclusions to detect. We are then in the framework of geometric inverse problems for the so called Cauchy-Stokes system. We shall restrict ourselves to the case of steady and Newtonian Stokes flows.

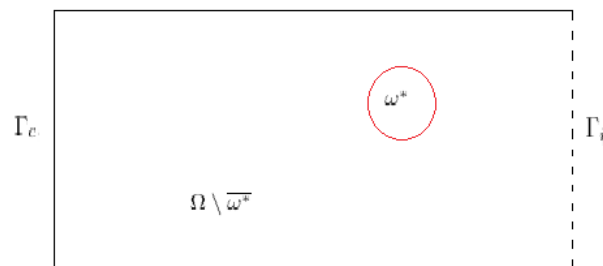


FIGURE 2.1 – An example of the geometric configuration of the problem : the whole domain including cavities is denoted by  $\Omega$ . It contains an inclusion  $\omega^*$ . The boundary of  $\Omega$  is composed of  $\Gamma_c$ , an accessible part where over-specified data are available, and an inaccessible part  $\Gamma_i$  where the data are missing.

Let us introduce a preliminary mathematical description of the problem. Consider a bounded open domain  $\Omega \subset \mathbb{R}^d$  ( $d=2, 3$ ) occupied by an incompressible viscous fluid, see Figure-2.1. We assume that the outer boundary of  $\Omega$  is sufficiently smooth and composed of two parts  $\Gamma_c$  and  $\Gamma_i$ . Let  $\omega^* \subset\subset \Omega$  be an unknown inclusion immersed in

$\Omega$ . The Cauchy-Stokes geometric inverse problem considered here consists, then, from given velocity  $f$  and fluid stress forces  $\Phi$  prescribed only on the accessible part  $\Gamma_c$  of the boundary, to identify  $\omega^* \in \mathcal{D}_{\text{ad}}$  (a set of admissible shapes defined later) such that the fluid velocity  $u$  and the pressure  $p$  are solution of the following Stokes problem :

$$\left\{ \begin{array}{ll} \nu \Delta u - \nabla p = 0 & \text{in } \Omega \setminus \overline{\omega^*}, \\ \operatorname{div} u = 0 & \text{in } \Omega \setminus \overline{\omega^*}, \\ \sigma(u, p)n = 0 & \text{on } \partial\omega^*, \\ u = f & \text{on } \Gamma_c, \\ \sigma(u, p)n = \Phi & \text{on } \Gamma_c, \end{array} \right. \quad (2.1)$$

where  $n$  is the unit outward normal vector on the boundary, and  $\sigma(u, p)$  the fluid stress tensor defined as follows :

$$\sigma(u, p) = -pI_d + 2\nu D(u)$$

with  $D(u) = \frac{1}{2}(\nabla u + \nabla u^T)$  being the linear strain tensor and  $I_d$  denotes the  $d \times d$  identity matrix. For the sake of simplicity, from now on, the viscosity  $\nu$  of the fluid is set to  $\nu = 1$ .

Additionally to the geometric identification problem (i.e. detect the inclusions  $\omega^*$ ) one has to complete the boundary data, that is to recover the missing traces of the velocity  $u$  and of the normal stress  $\sigma(u, p).n$  over  $\Gamma_i$  the inaccessible part of the boundary. Remark that the difference between obstacles and inclusions amounts to which boundary condition is used : homogeneous Dirichlet one for the obstacles and homogeneous Neumann condition for the inclusions (considered as free surfaces).

Even when restricted to elliptic equations, mostly Laplace and Stokes systems, there exists a prolific literature dedicated to each of these two problems separately, and because of their well known ill-posedness (in the sense of Hadamard) [59], most of the literature addresses as well (if not exclusively) the ensuing stability and other computational issues. For the Cauchy problem, far from being exhaustive, an excerpt of popular approaches are the least-square penalty techniques used in [48] and in the earlier paper [50], Tikhonov regularization methods [38], quasi reversibility methods [28], alternating iterative methods [72, 62] and control type methods [10, 2]. Recently, an approach based on game theory, using decentralized strategies, was proposed in [56]. This work has been extended in [66], in the image inpainting problem for a nonlinear Cauchy problem and in [36] for the solution of coupled conductivity identification and data completion in cardiac electrophysiology.

Let us mention that many of the papers dedicated to data completion or to obstacle detection and based on control or optimization approaches, minimize a so-called Kohn-Vogelius type functional, an energy error function introduced in the framework of parameter identification in [70].

Regarding the obstacle identification problem, a more challenging geometric inverse problem, and again with a very partial on the existing literature, the authors in [5] address the obstacle detection problem for unsteady Stokes and Navier-Stokes flows, quasi reversibility coupled to a level set approach is used in [29] for the Laplace equation, shape optimization [16] and topological gradient [46] are used for the Stokes system, and in [17] stability issues are addressed for the inverse obstacle problem in a Stokes flow.

In contrast, rather a few papers address the joint geometric and data completion inverse problems, at least regarding its computational aspects. Close to our present

---

work, the inverse obstacle problem for the Cauchy-Laplace equation is studied in [35] where a control-type approach is used and applied to a Kohn-Vogelius functional. In [30] the authors use quasi reversibility coupled to a level set approach to solve the inverse obstacle problem for the Cauchy-Stokes equations. A formulation based on nonlinear integral equations arising from the reciprocity gap [11] principle is used in [6].

Presently, we consider the inverse inclusion problem for the Cauchy-Stokes system. In order to solve the joint completion/detection problem, we reformulate it as a three players Nash game, following the ideas introduced earlier in [56] to solve the Cauchy-Laplace (completion) problem.

The game is defined as follows : first, the Cauchy-Stokes problem is formulated as two boundary value problems (BVP). The first BVP defines the first player, it inherits the available Dirichlet data  $f$  specified on the boundary  $\Gamma_c$ , and has control on a Neumann data set over the inaccessible boundary  $\Gamma_i$ , the latter control being the first player's strategy aimed at minimizing the gap over  $\Gamma_c$  between first player's normal stress and the prescribed normal stress  $\Phi$ . The second BVP defines the second player, as it inherits the available normal stress data  $\Phi$  set over  $\Gamma_c$ , and uses Dirichlet data set over the inaccessible boundary  $\Gamma_i$  as strategy variables. The second player's Dirichlet strategy is aimed at minimizing the gap over  $\Gamma_c$  between second player's and the prescribed Dirichlet data  $f$ . The fading and regularizing difference between the solutions to these two BVPs is shared by the two players. The third player has no own BVP, but has access to the two previous ones, and uses as control variable the shape of the inclusion(s). The third player's criteria to minimize is a Kohn-Vogelius type functional. The three players play a static Nash game with complete information, whose relevant solution concept is the so-called Nash equilibrium (NE).

We shall present and prove some theoretical results for the Cauchy-Stokes problem, precisely that a Nash equilibrium exists and is unique, and coincides with the missing data as soon as the Cauchy problem has a solution (that is, when the over specified data are compatible). Then, we propose a new algorithm dedicated to the joint computation of the missing data and the obstacle shapes. In this algorithm, a Nash subgame is played by the completion first and second players in order to precondition the Cauchy problem and tackle its ill-posedness. A level set approach is used for the latter geometric identification problem. We lead a sensitivity analysis, and present several numerical experiments that corroborate the efficiency of our approach and its nice stability with respect to noisy data.

The paper is organized as follows. In Section 2.2, we extend our previous [56] Nash game approach to the data completion for the steady Stokes flows. In view of the formulation of the geometric inverse problem, we first recall in Section 2.3 a now classical identifiability proof [5] usually established for obstacles, so with homogeneous Dirichlet boundary condition, with a minor adaption to fit the case of inclusions, whose boundary conditions are of homogeneous Neumann type. Then, we formulate in Section 2.4 the Nash game approach to tackle the joint completion and geometric identification problem. We detail our algorithm, and some numerical aspects of the level set method, used to capture the inclusion boundary. Section 2.5 is devoted to the presentation of three numerical 2D test cases which assess the ability of our algorithm to jointly recover the missing boundary data and the location and shape of the inclusions as well. We finally draw some concluding remarks in Section 2.6.

## 2.2 Data completion for the Stokes problem

We consider in the present section the case where possible obstacles or inclusions are known, which amounts to simply not consider them, focusing solely on the data completion problem. In the following, we apply the Nash game formulation of [56] to the Stokes problem. Results and proofs in the cited reference extend easily to the present case.

With the previous notations, let be  $f \in H^{\frac{3}{2}}(\Gamma_c)^d$  and  $\Phi \in H^{\frac{1}{2}}(\Gamma_c)^d$  given Cauchy data. The Cauchy-Stokes problem is stated as follows : find  $u \in H^1(\Omega)^d$  and  $p \in L^2(\Omega)$  such that

$$\begin{cases} \Delta u - \nabla p = 0 & \text{in } \Omega, \\ \operatorname{div} u = 0 & \text{in } \Omega, \\ u = f & \text{on } \Gamma_c, \\ \sigma(u, p)n = \Phi & \text{on } \Gamma_c. \end{cases}$$

The data completion problem, which is simply a reformulation of the Cauchy-Stokes one, amounts to find  $\tau^* \in H^{\frac{3}{2}}(\Gamma_i)^d$  and  $\eta^* \in H^{\frac{1}{2}}(\Gamma_i)^d$  such that  $u = \tau^*$  and  $\sigma(u, p)n = \eta^*$  over  $\Gamma_i$ .

For any given  $\eta \in H^{\frac{1}{2}}(\Gamma_i)^d$  and  $\tau \in H^{\frac{3}{2}}(\Gamma_i)^d$ , we define the states  $(u_1(\eta), p_1(\eta)) \in H^1(\Omega)^d \times L^2(\Omega)$  and  $(u_2(\tau), p_2(\tau)) \in H^1(\Omega)^d \times L^2(\Omega)$  as the unique weak solutions of the following Stokes mixed boundary value problems  $(SP_1)$  and  $(SP_2)$  :

$$(SP_1) \begin{cases} \Delta u_1 - \nabla p_1 = 0 & \text{in } \Omega, \\ \operatorname{div} u_1 = 0 & \text{in } \Omega, \\ u_1 = f & \text{on } \Gamma_c, \\ \sigma(u_1, p_1)n = \eta & \text{on } \Gamma_i, \end{cases} \quad (SP_2) \begin{cases} \Delta u_2 - \nabla p_2 = 0 & \text{in } \Omega, \\ \operatorname{div} u_2 = 0 & \text{in } \Omega, \\ u_2 = \tau & \text{on } \Gamma_i, \\ \sigma(u_2, p_2)n = \Phi & \text{on } \Gamma_c. \end{cases}$$

The existence and uniqueness of solutions to  $(SP_1)$  and  $(SP_2)$  can be derived from the general theory on existence of solutions to the incompressible steady state Stokes equations, which can be found e.g. in [40, 95]. See also [34] annex A.1 which is suitable to the Cauchy-Stokes framework of the present paper. Notice that, thanks to the assumption on Cauchy data, we have  $(u_1(\eta), p_1(\eta)) \in H^2(\Omega)^d \times H^1(\Omega)^d$ .

We then define the following cost functionals :

$$\mathcal{J}_1(\eta, \tau) = \frac{1}{2} \|\sigma(u_1(\eta), p_1(\eta))n - \Phi\|_{H^{\frac{1}{2}}(\Gamma_c)^d}^2 + \frac{1}{2} \|u_1(\eta) - u_2(\tau)\|_{H^{\frac{3}{2}}(\Gamma_i)^d}^2 \quad (2.2)$$

$$\mathcal{J}_2(\eta, \tau) = \frac{1}{2} \|u_2(\tau) - f\|_{H^{\frac{3}{2}}(\Gamma_c)^d}^2 + \frac{1}{2} \|u_1(\eta) - u_2(\tau)\|_{H^{\frac{3}{2}}(\Gamma_i)^d}^2 \quad (2.3)$$

We are now in a position to formulate the two-player Nash game. The first player is defined by its strategy  $\eta \in H^{\frac{1}{2}}(\Gamma_i)^d$  and cost  $\mathcal{J}_1$ , while the second one has control on  $\tau \in H^{\frac{3}{2}}(\Gamma_i)^d$  and aims at minimizing the cost  $\mathcal{J}_2$ . The two players play a static Nash game with complete information. The most popular solution concept for such games is the one of a Nash equilibrium (NE) given by the

**Definition 2.2.1** *A strategy pair  $(\eta_N, \tau_N) \in H^{\frac{1}{2}}(\Gamma_i)^d \times H^{\frac{3}{2}}(\Gamma_i)^d$  is a Nash equilibrium if the following holds :*

$$\begin{cases} \mathcal{J}_1(\eta_N, \tau_N) \leq \mathcal{J}_1(\eta, \tau_N), & \forall \eta \in H^{\frac{1}{2}}(\Gamma_i)^d, \\ \mathcal{J}_2(\eta_N, \tau_N) \leq \mathcal{J}_2(\eta_N, \tau), & \forall \tau \in H^{\frac{3}{2}}(\Gamma_i)^d. \end{cases} \quad (2.4)$$

Recall that, similarly as [56], this two players solve in parallel the associated BVP's (SP1) and (SP2). Their respective objectives involve the gap between the non used Neumann/Dirichlet known data and the traces of the BVP's solutions over the accessible boundary  $\Gamma_c$ , plus a common coupling term  $\frac{1}{2}\|u_1(\eta) - u_2(\tau)\|_{H^{\frac{3}{2}}(\Gamma_i)^d}^2$ . This term depends on both  $\eta$  and  $\tau$ , has a regularizing effect in partial minimization,  $u_1$  (resp.  $u_2$ ) is fixed in the partial minimization process of  $\mathcal{J}_2$  (resp.  $\mathcal{J}_1$ ). Furthermore, the partial mapping  $\eta \mapsto \mathcal{J}_1(\eta, \tau)$  (resp.  $\tau \mapsto \mathcal{J}_2(\eta, \tau)$ ) is a quadratic strongly convex functional over  $H^{\frac{1}{2}}(\Gamma_i)^d$  (resp.  $H^{\frac{3}{2}}(\Gamma_i)^d$ ). This partial ellipticity property of  $J_1$  holds uniformly w.r.t.  $\tau$ , and conversely for  $J_2$ . It allows to restrict the search for Nash equilibrium in data completion to a bounded subsets of the strategy spaces, which remains consistent with the classical results of conditional stability of Cauchy problem (see e.g. [3]).

The recourse to a game formulation and to a NE solution finds its justification in the following result :

**Proposition 2.2.1** *Consider the Nash game defined above, with costs given by (2.2) and (2.3).*

(i) *There always exists a unique Nash equilibrium  $(\eta_N, \tau_N) \in H^{\frac{1}{2}}(\Gamma_i)^d \times H^{\frac{3}{2}}(\Gamma_i)^d$ , which is also the minimum of the potential*

$$L(\eta, \tau) = \frac{1}{2}\|\sigma(u_1(\eta), p_1(\eta))n - \Phi\|_{H^{\frac{1}{2}}(\Gamma_c)^d}^2 + \frac{1}{2}\|u_2(\tau) - f\|_{H^{\frac{1}{2}}(\Gamma_c)^d}^2 + \frac{1}{2}\|u_1(\eta) - \tau\|_{H^{\frac{3}{2}}(\Gamma_i)^d}^2.$$

(ii) *If the Cauchy problem has a solution  $(u, p)$ , then  $(u_1(\eta_N), p_1(\eta_N)) = (u_2(\tau_N), p_2(\tau_N)) = (u, p)$  and  $(\eta_N, \tau_N)$  are the missing data, i.e.  $\eta_N = \sigma(u, p)n|_{\Gamma_i}$  and  $\tau_N = u|_{\Gamma_i}$ .*

**Proof 2.2.1** (i). *We first prove the uniqueness of a NE. It is easy to check that the potential  $L$  is strictly convex by computing its second order differential with respect to  $(\eta, \tau)$ , see [2]. Thus,  $L$  has at most a one minimum. Moreover, if it exists, the minimum of  $L$  is a Nash equilibrium, and conversely. Indeed, let be  $(\eta_0, \tau_0)$  the minimum of  $L$ , then, we have*

$$\begin{cases} L(\eta_0, \tau_0) \leq L(\eta, \tau_0), & \forall \eta \in H^{\frac{1}{2}}(\Gamma_i)^d, \\ L(\eta_0, \tau_0) \leq L(\eta_0, \tau), & \forall \tau \in H^{\frac{3}{2}}(\Gamma_i)^d. \end{cases}$$

*Thanks to the specific structure of  $L$ , this is equivalent to write*

$$\begin{cases} \mathcal{J}_1(\eta_0, \tau_0) \leq \mathcal{J}_1(\eta, \tau_0), & \forall \eta \in H^{\frac{1}{2}}(\Gamma_i)^d, \\ \mathcal{J}_2(\eta_0, \tau_0) \leq \mathcal{J}_2(\eta_0, \tau), & \forall \tau \in H^{\frac{3}{2}}(\Gamma_i)^d. \end{cases}$$

*That is,  $(\eta_0, \tau_0)$  is a Nash equilibrium. Conversely, if  $(\eta_0, \tau_0)$  is a Nash equilibrium then,*

$$\begin{cases} \mathcal{J}_1(\eta_0, \tau_0) \leq \mathcal{J}_1(\eta, \tau_0), & \forall \eta \in H^{\frac{1}{2}}(\Gamma_i)^d, \\ \mathcal{J}_2(\eta_0, \tau_0) \leq \mathcal{J}_2(\eta_0, \tau), & \forall \tau \in H^{\frac{3}{2}}(\Gamma_i)^d. \end{cases}$$

*Adding the term  $\frac{1}{2}\|u_2(\tau) - f\|_{H^{\frac{3}{2}}(\Gamma_c)^d}^2$  in the first inequality and the term  $\frac{1}{2}\|\sigma(u_1, p_1)n - \Phi\|_{H^{\frac{1}{2}}(\Gamma_c)^d}^2$  in the second one, we get,*

$$\begin{cases} L(\eta_0, \tau_0) \leq L(\eta, \tau_0), & \forall \eta \in H^{\frac{1}{2}}(\Gamma_i)^d, \\ L(\eta_0, \tau_0) \leq L(\eta_0, \tau), & \forall \tau \in H^{\frac{3}{2}}(\Gamma_i)^d. \end{cases}$$

---

By the optimality conditions, we have

$$\begin{cases} \frac{\partial L}{\partial \eta}(\eta_0, \tau_0) = 0, \\ \frac{\partial L}{\partial \tau}(\eta_0, \tau_0) = 0, \end{cases}$$

thus,  $(\eta_0, \tau_0)$  is the minimum of  $L$ , the uniqueness of which implies that of the Nash equilibrium.

The proof of existence follows the same lines as in [56], the main ingredient being the uniform ellipticity of the convex partial maps  $\eta \rightarrow \mathcal{J}_1(\eta, \tau)$  and of  $\tau \rightarrow \mathcal{J}_2(\eta, \tau)$  which allows for a direct application of the Nash Theorem, see *ibidem* references to the Nash games and theorem.

(ii). If we assume that the Cauchy-Stokes problem has a solution  $(u, p)$ , which is then unique by the unique continuation property, proved by Fabre and Lebeau in [47], then let us define the following  $\eta_C = \sigma(u, p)n|_{\Gamma_i}$  and  $\tau_C = u|_{\Gamma_i}$ . It is then straightforward to check that the solutions  $(u_1(\eta_C), p_1(\eta_C))$  to  $(SP_1)$  and  $(u_2(\tau_C), p_2(\tau_C))$  to  $(SP_2)$  coincide with the Cauchy solution  $(u, p)$ , thanks to the uniqueness of the solution of the boundary value Stokes problem. Thus,  $L(\eta_C, \tau_C) = 0$  so that  $(\eta_C, \tau_C)$  is a minimum of  $L \geq 0$ . Thanks to the uniqueness result above,  $(\eta_N, \tau_N) = (\eta_C, \tau_C)$ .

For the computation of the NE for the Cauchy-Stokes problem, we used a popular algorithm [12] which amounts basically to solve iteratively the following coupled problem, using gradient descent methods,

$$\begin{aligned} (\eta_N, \tau_N) &= \operatorname{argmin}_{\eta} \mathcal{J}_1(\eta, \tau_N), \\ (\eta_N, \tau_N) &= \operatorname{argmin}_{\tau} \mathcal{J}_2(\eta_N, \tau). \end{aligned}$$

We describe in Algorithm 2.2.1 below the main steps of the method, with a version where the Cauchy data of the Dirichlet type  $f$  are possibly perturbed by a noise with some magnitude  $\sigma$ , yielding for the Cauchy problem a noisy Dirichlet data  $f^\sigma$  :

---

**Algorithm 2.2.1:** Computation of a Cauchy-Stokes Nash equilibrium

---

Given :  $\varepsilon > 0$  a convergence tolerance,  $K_{max}$  a computational budget,  $\sigma$  a noise level and  $\rho(\sigma)$  a -tuned- function which depends on the noise.

Choose an initial guess  $S^{(0)} = (\eta^{(0)}, \tau^{(0)}) \in H^{\frac{1}{2}}(\Gamma_i)^d \times H^{\frac{3}{2}}(\Gamma_i)^d$ . Set  $k = 1$ .

- Step 1 : Compute  $\bar{\eta}^{(k)}$  solution of  $\min_{\eta} \mathcal{J}_1(\eta, \tau^{(k-1)})$   
and determine  $\eta^{(k)} = t\eta^{(k-1)} + (1-t)\bar{\eta}^{(k)}$  with  $0 \leq t < 1$ .
- Step 2 : Compute  $\bar{\tau}^{(k)}$  solution of  $\min_{\tau} \mathcal{J}_2(\eta^{(k-1)}, \tau)$   
and determine  $\tau^{(k)} = t\tau^{(k-1)} + (1-t)\bar{\tau}^{(k)}$  with  $0 \leq t < 1$ .
- Step 3 : Compute  $s_k = \|u_2^{(k)} - f^\sigma\|_{L^2(\Gamma_c)}$ , where  $(u_2^{(k)}, p_2^{(k)})$  is the solution of the following direct problem

$$\begin{cases} \Delta u_2^{(k)} - \nabla p_2^{(k)} = 0 & \text{in } \Omega, \\ \operatorname{div} u_2^{(k)} = 0 & \text{in } \Omega, \\ u_2^{(k)} = \tau^{(k)} & \text{on } \Gamma_i, \\ \sigma(u_2^{(k)}, p_2^{(k)})n = \Phi & \text{on } \Gamma_c. \end{cases}$$

While  $s_k \geq \rho(\sigma)\varepsilon$  and  $k < K_{max}$  set  $k = k + 1$ , return back to step 1.

---

The gradient descent methods used to solve steps 1 and 2 in the algorithm above do require the computation of the gradients of the costs  $\mathcal{J}_1$  and  $\mathcal{J}_2$ , with respect to their respective strategies. The fast computation of the latter is classical, and led by means of an adjoint state method, as shown by the Proposition 2.2.2 below.

We shall use the following classical notation :

$$H_{\Gamma}^1(\Omega) = \{\varphi \in H^1(\Omega)^d \quad / \varphi|_{\Gamma} = 0\} \quad \text{and} \quad H_{\Gamma}^2(\Omega) = \{\varphi \in H^2(\Omega)^d \quad / \varphi|_{\Gamma} = 0\}$$

whenever  $\Gamma$  is a non empty subset of the boundary of  $\Omega$ .

**Proposition 2.2.2** *We have the following two partial derivatives :*

$$(AP_1) \left\{ \begin{array}{l} \frac{\partial \mathcal{J}_1}{\partial \eta} \psi = - \int_{\Gamma_i} \psi \lambda_1 ds, \quad \forall \psi \in H^{\frac{1}{2}}(\Gamma_i)^d, \\ \text{with } (\lambda_1, \kappa_1) \in H_{\Gamma_c}^1(\Omega) \times L^2(\Omega) \quad \text{solution of the adjoint problem :} \\ \left\{ \begin{array}{l} \int_{\Gamma_c} (\sigma(u_1, p_1)n - \Phi)((\nabla \gamma + \nabla \gamma^T)n) ds + \int_{\Gamma_i} (u_1 - \tau) \gamma ds \\ \quad + \int_{\Omega} (\nabla \gamma + \nabla \gamma^T) : \nabla \lambda_1 dx - \int_{\Omega} \kappa_1 \operatorname{div} \gamma dx = 0, \quad \forall \gamma \in H_{\Gamma_c}^1(\Omega). \\ - \int_{\Gamma_c} (\sigma(u_1, p_1)n - \Phi) \delta n ds - \int_{\Omega} \delta \operatorname{div} \lambda_1 dx = 0, \quad \forall \delta \in H^1(\Omega)^d, \end{array} \right. \end{array} \right.$$

$$(AP_2) \left\{ \begin{array}{l} \frac{\partial \mathcal{J}_2}{\partial \tau} \mu = \int_{\Gamma_i} (\sigma(\lambda_2, \kappa_2)n - (u_1(\eta) - u_2(\tau))) \mu ds, \quad \forall \mu \in H^{\frac{3}{2}}(\Gamma_i)^d, \\ \text{with } (\lambda_2, \kappa_2) \in H^1(\Omega)^d \times L^2(\Omega) \quad \text{solution of the adjoint problem :} \\ \left\{ \begin{array}{l} \int_{\Omega} (\nabla \lambda_2 + \nabla \lambda_2^T) : \nabla \varphi dx - \int_{\Omega} \kappa_2 \operatorname{div} \varphi dx = \int_{\Gamma_c} (f - u_2(\tau)) \varphi ds, \\ \quad \forall \varphi \in H_{\Gamma_i}^1(\Omega), \\ \int_{\Omega} \xi \operatorname{div} \lambda_2 dx = 0, \quad \forall \xi \in L^2(\Omega), \end{array} \right. \end{array} \right.$$

where, by a classical convention,  $\nabla u : \nabla v = \operatorname{Tr}(\nabla u \nabla v^T) = \sum_{i,j} \frac{\partial u_i}{\partial x_j} \frac{\partial v_i}{\partial x_j}$ .

**Remark 2.2.1** *The existence and uniqueness of the solutions to the problems  $(AP_1)$  and  $(AP_2)$ , namely the adjoint states  $(\lambda_1, \kappa_1) \in H_{\Gamma_c}^1(\Omega) \times L^2(\Omega)$  and  $(\lambda_2, \kappa_2) \in H^1(\Omega)^d \times L^2(\Omega)$  is straightforward, thanks to the regularity assumption on the Cauchy data  $(f, \Phi) \in H^{\frac{3}{2}}(\Gamma_c)^d \times H^{\frac{1}{2}}(\Gamma_c)^d$  and to the regularity  $H^2(\Omega)^d \times H^1(\Omega)^d$  results on the solutions to the Stokes problems  $(SP_1)$  and  $(SP_2)$ , see e.g. [51] (or [22] Theorem 5.2).*

Later on, Algorithm 2.2.1 described above will be embedded into an overall algorithm with the specific task of processing the data recovery problem. We shall then use the partial derivatives given by Proposition 2.2.2. The overall algorithm stems from the Nash game played by the data recovery problem against the inclusion inverse problem. Next section is then devoted to a mandatory preamble for geometric inverse problems, that is the identifiability question.

## 2.3 An identifiability result for the inverse inclusion Cauchy-Stokes problem

In the present section, we adapt an identifiability result in [5], established for the case of obstacles, that is with a homogeneous Dirichlet condition, to the case of inclusions defined by Neumann (or free surface) boundary conditions.

The set of admissible inclusions is defined by :

$$\mathcal{D}_{\text{ad}} = \{\omega \subset\subset \Omega \text{ is a } \mathcal{C}^{1,1} \text{ open set and } \Omega \setminus \bar{\omega} \text{ is connected}\}.$$

We follow *grosso modo* the same proof technique of [5], noticing that, differently from the obstacle (Dirichlet) case, inclusions are not identifiable in case of over specified data  $f$  of affine free divergence form. Consequently, even if the over specified fluid stress  $\Phi$  is identically zero, it is enough for the identifiability to hold, that the velocity data  $f$  be non affine.

**Theorem 2.3.1** *Let be  $\Omega \subset \mathbb{R}^2$  an open bounded Lipschitz domain and  $\Gamma_c$  a non-empty open subset of the boundary  $\partial\Omega$ . Assume there exists a pair of compatible data  $(f, \Phi) \in H^{\frac{3}{2}}(\Gamma_c)^d \times H^{\frac{1}{2}}(\Gamma_c)^d$  for the Cauchy-Stokes problem, such that either  $\Phi \not\equiv 0$  or  $f(x) \not\equiv Ax + b$  where  $A$  is a constant matrix with null diagonal. Consider two admissible open sets  $\omega_1$  and  $\omega_2$  in  $\mathcal{D}_{\text{ad}}$ . For  $i = 1, 2$ , let be  $(u_i, p_i)$  the solutions to the following Cauchy-Stokes inclusion problem :*

$$\begin{cases} \Delta u_i - \nabla p_i = 0 & \text{in } \Omega \setminus \bar{\omega}_i, \\ \operatorname{div} u_i = 0 & \text{in } \Omega \setminus \bar{\omega}_i, \\ \sigma(u_i, p_i)n = 0 & \text{on } \partial\omega_i, \\ u_i = f & \text{on } \Gamma_c, \\ \sigma(u_i, p_i)n = \Phi & \text{on } \Gamma_c. \end{cases} \quad (2.5)$$

Then  $\omega_1 = \omega_2$ .

**Proof 2.3.1** *Denote by  $\omega = \omega_1 \cup \omega_2$  and define, over the set  $\Omega \setminus \bar{\omega}$ ,  $v = u_1 - u_2$  and  $q = p_1 - p_2$ , where  $(u_1, p_1)$  and  $(u_2, p_2)$  are the solutions to the system (2.5).*

One sees that  $(v, q)$  satisfies

$$\begin{cases} \Delta v - \nabla q = 0 & \text{in } \Omega \setminus \bar{\omega}, \\ \operatorname{div} v = 0 & \text{in } \Omega \setminus \bar{\omega}, \\ v = 0 & \text{on } \Gamma_c, \\ \sigma(v, q)n = 0 & \text{on } \Gamma_c. \end{cases}$$

Thus, thanks to the unique continuation property for the Stokes system (see [47] or [5] Corollary 2.2), we have  $v = 0$  in  $\Omega \setminus \bar{\omega}$  and then  $u_1 = u_2$  in  $\Omega \setminus \bar{\omega}$ .

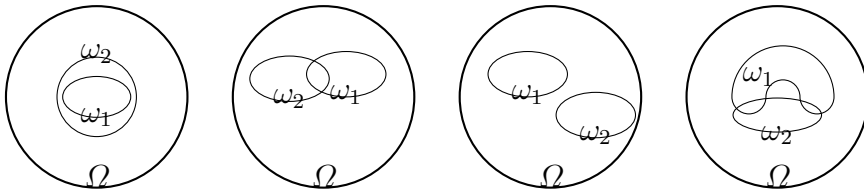


FIGURE 2.2 – Different situations



Let us suppose that  $\omega_1 \neq \omega_2$ , and assume then (up to a swap in subscripts) that  $\omega_1 \setminus \overline{\omega_2}$  is an open non-empty subset of  $\Omega$ . We know from system (2.5) that :  $\Delta u_2 - \nabla p_2 = 0$  in  $\omega_1 \setminus \overline{\omega_2}$ .

First, let us consider the case where  $\omega_1 \setminus \overline{\omega_2}$  is Lipschitz. Then, we multiply the equation above by  $u_2$  and take the integral over  $\omega_1 \setminus \overline{\omega_2}$ . Observe then that, thanks to  $\operatorname{div} u_2 = 0$  in  $\omega_1 \setminus \overline{\omega_2}$ , one has  $\Delta u_2 = 2\operatorname{div}(D(u_2))$  where we recall that  $D(u_2) = 1/2(\nabla u_2 + \nabla u_2^T)$ . By use of the Green formula, we obtain

$$\int_{\omega_1 \setminus \overline{\omega_2}} D(u_2) : \nabla u_2 dx - \int_{\omega_1 \setminus \overline{\omega_2}} p_2 \operatorname{div} u_2 dx = \int_{\partial(\omega_1 \setminus \overline{\omega_2})} (-p_2 I_d + D(u_2)) n u_2 ds,$$

which can be rewritten as follows :

$$\frac{1}{2} \int_{\omega_1 \setminus \overline{\omega_2}} |D(u_2)|^2 dx = \int_{\partial(\omega_1 \setminus \overline{\omega_2})} \sigma(u_2, p_2) n u_2 ds.$$

Now, since  $\sigma(v, q)$  vanishes in  $\Omega \setminus \overline{\omega}$ , and thanks to the continuity of the involved - normal- traces, one has  $\sigma(v, q)n = 0$  on  $\partial\omega$ . From other part, one has  $\sigma(u_1, p_1)n = 0$  on  $\partial\omega_1$  thanks to equations (2.5). We then have  $\sigma(u_2, p_2)n = 0$  on  $\partial\omega_1 \setminus \partial(\omega_1 \cap \omega_2)$ . Now, since we know that  $\sigma(u_2, p_2)n = 0$  on  $\partial\omega_2$  thanks to equations (2.5), we obtain

$$\int_{\partial(\omega_1 \setminus \overline{\omega_2})} \sigma(u_2, p_2) n u_2 ds = 0,$$

that is,

$$\frac{1}{2} \int_{\omega_1 \setminus \overline{\omega_2}} |D(u_2)|^2 dx = 0.$$

Since  $\|D(u_2)\|_{L^2(\omega_1 \setminus \overline{\omega_2})}^2 = 0$ , the components of the matrix of  $D(u_2)$  are a.e. zero. Consequently, the velocity field  $u_2$  has an affine form in  $\omega_1 \setminus \overline{\omega_2}$ , shortly given by  $u_2(x) = Ax + b$  where  $A$  is a constant matrix with null diagonal.

We know from above and from equations (2.5) that  $(u_2, p_2)$  satisfies the following system,

$$\begin{cases} \Delta u_2 - \nabla p_2 = 0 & \text{in } \omega_1 \setminus \overline{\omega_2}, \\ \operatorname{div} u_2 = 0 & \text{in } \omega_1 \setminus \overline{\omega_2}, \\ \sigma(u_2, p_2)n = 0 & \text{on } \partial(\omega_1 \setminus \overline{\omega_2}). \end{cases} \quad (2.6)$$

Thus, by application to  $u_2(x) - (Ax + b)$  which fulfills the system (2.6) above, of the unique continuation theorem for the steady Stokes equation established in [47], we conclude that  $u_2(x) = Ax + b$  and  $p_2 = 0$  in the whole domain  $\Omega \setminus \overline{\omega_2}$ . Finally, reasoning with the traces on the boundary of the domain  $\partial\Omega$ , we observe that  $u_2(x) = Ax + b$  and  $p_2 = 0$  in  $\Omega \setminus \overline{\omega_2}$  yields  $\sigma(u_2, p_2)n = \Phi = 0$  and  $u_2(x) = f(x) = Ax + b$  over  $\Gamma_c$ , which, by assumption, is impossible. We conclude that  $\omega_1 \setminus \overline{\omega_2} = \emptyset$ , and so  $\omega_1 = \omega_2$ .

Now, when  $\omega_1 \setminus \overline{\omega_2}$  is not Lipschitz, then the use the Green formula is not justified. We recall and follow here the solution given by [34] : the author in the cited reference introduces an additional regularity assumption on  $\omega_1$  and  $\omega_2$ , assuming that they have  $\mathcal{C}^{1,1}$  boundary. We assumed more regularity on the Cauchy data in order to have more regularity for the solution  $(u_2, p_2)$ , that is  $u_2 \in H^2(\Omega \setminus \overline{\omega_2})^d$  and  $p_2 \in H^1(\Omega \setminus \overline{\omega_2})$ . Then, consider two Lipschitz open sets  $\mathcal{O}_1, \mathcal{O}_2 \in \Omega \setminus \overline{\omega_2}$ , such that  $\mathcal{O}_1 \subset \Omega \setminus \overline{\omega_1}$ ,  $\partial\mathcal{O}_1 \setminus (\partial\omega_1 \cup \partial\omega_2) = \partial\mathcal{O}_2 \setminus (\partial\omega_1 \cup \partial\omega_2)$  and  $\partial\omega_2 \cap \omega_1 \subset \partial\mathcal{O}_1$ .

Next, by use the Green formula on  $\mathcal{O}_1$  and  $\mathcal{O}_2$ , we obtain

$$\frac{1}{2} \int_{\mathcal{O}_1} |D(u_2)|^2 dx = \int_{\partial\mathcal{O}_1} \sigma(u_2, p_2) n u_2 ds \quad \text{and} \quad \frac{1}{2} \int_{\mathcal{O}_2} |D(u_2)|^2 dx = \int_{\partial\mathcal{O}_2} \sigma(u_2, p_2) n u_2 ds.$$

---

Subtracting these two equalities, we get

$$\frac{1}{2} \int_{\omega_1 \setminus \overline{\omega_2}} |D(u_2)|^2 dx = 0.$$

Hence, we conclude as previously. Finally, for the case where the domain  $\Omega \setminus \overline{\omega_1 \cup \omega_2}$  is not connected (fourth case in figure 2.2), we refer the reader to the same cited above [34] where this case is successfully handled.

The identifiability result suggests that there is no need for a third party state equation, the two state equations ( $SP_1$ ) and ( $SP_2$ ) formulated with inclusions and dedicated to the completion problem should suffice. Only a third player's cost functional should be defined, playing with inclusions as strategies. Hence we enforced the data completion steps, by letting the first and second players lead a Nash subgame during the overall iterations, see next section. Numerical experiments show that this choice turned out to be efficient.

## 2.4 Coupled data completion and geometry identification for the Stokes problem

The aim of the present section is to introduce an algorithm dedicated to recover the missing boundary data while solving the inverse inclusion problem for steady Stokes flows. We extend the two-player Nash game set for the completion problem to a three-player Nash game, the third player being in charge of the inverse inclusion problem.

We recall that the inverse inclusion problem amounts to find  $\omega^* \in \mathcal{D}_{\text{ad}}$  such that the fluid velocity  $u$  and the pressure  $p$  are solution to the following Cauchy-Stokes problem :

$$\begin{cases} \Delta u - \nabla p = 0 & \text{in } \Omega \setminus \overline{\omega^*}, \\ \operatorname{div} u = 0 & \text{in } \Omega \setminus \overline{\omega^*}, \\ \sigma(u, p)n = 0 & \text{on } \partial\omega^*, \\ u = f & \text{on } \Gamma_c, \\ \sigma(u, p)n = \Phi & \text{on } \Gamma_c. \end{cases} \quad (2.7)$$

Thanks to the identifiability result stated in section 2.3, a single pair of -compatible- measurements  $(f, \Phi)$  is enough to recover the inclusion(s) as well as the missing data. Next, we shall set up a three-player Nash game following the same philosophy than in section 2.2 dedicated for the sole completion.

For  $\eta \in H^{\frac{1}{2}}(\Gamma_i)^d$ ,  $\tau \in H^{\frac{3}{2}}(\Gamma_i)^d$  and  $\omega \in \mathcal{D}_{\text{ad}}$ , let us define the following three cost functionals :

$$\mathcal{J}_1(\eta, \tau; \omega) = \frac{1}{2} \|\sigma(u_1^\omega(\eta), p_1^\omega(\eta))n - \Phi\|_{H^{\frac{1}{2}}(\Gamma_c)^d}^2 + \frac{1}{2} \|u_1^\omega(\eta) - u_2^\omega(\tau)\|_{H^{\frac{3}{2}}(\Gamma_i)^d}^2, \quad (2.8)$$

$$\mathcal{J}_2(\eta, \tau; \omega) = \frac{1}{2} \|u_2^\omega(\tau) - f\|_{H^{\frac{3}{2}}(\Gamma_c)^d}^2 + \frac{1}{2} \|u_1^\omega(\eta) - u_2^\omega(\tau)\|_{H^{\frac{3}{2}}(\Gamma_i)^d}^2, \quad (2.9)$$

$$\mathcal{J}_3(\eta, \tau; \omega) = \|\sigma(u_1^\omega(\eta), p_1^\omega(\eta)) - \sigma(u_2^\omega(\tau), p_2^\omega(\tau))\|_{L^2(\Omega \setminus \overline{\omega})^d}^2 + \mu |\partial\omega|, \quad (2.10)$$

where the parameter  $\mu > 0$  is a penalization of the perimeter  $|\partial\omega|$ , defined as the Hausdorff measure  $\mathcal{H}^1(\partial\omega)$ ,  $(u_1^\omega(\eta), p_1^\omega(\eta))$  and  $(u_2^\omega(\tau), p_2^\omega(\tau))$  are the solutions of the

respective BVP  $(\mathcal{P}_1)$  and  $(\mathcal{P}_2)$  :

$$(\mathcal{P}_1) \begin{cases} \Delta u_1^\omega - \nabla p_1^\omega = 0 & \text{in } \Omega \setminus \bar{\omega}, \\ \operatorname{div} u_1^\omega = 0 & \text{in } \Omega \setminus \bar{\omega}, \\ \sigma(u_1^\omega, p_1^\omega)n = 0 & \text{on } \partial\omega, \\ u_1^\omega = f & \text{on } \Gamma_c, \\ \sigma(u_1^\omega, p_1^\omega)n = \eta & \text{on } \Gamma_i, \end{cases} \quad (\mathcal{P}_2) \begin{cases} \Delta u_2^\omega - \nabla p_2^\omega = 0 & \text{in } \Omega \setminus \bar{\omega}, \\ \operatorname{div} u_2^\omega = 0 & \text{in } \Omega \setminus \bar{\omega}, \\ \sigma(u_2^\omega, p_2^\omega)n = 0 & \text{on } \partial\omega, \\ \sigma(u_2^\omega, p_2^\omega)n = \Phi & \text{on } \Gamma_c, \\ u_2^\omega = \tau & \text{on } \Gamma_i. \end{cases}$$

In a few words, there are three players : Player (1) controls the strategy variable  $\eta \in H^{\frac{1}{2}}(\Gamma_i)^d$  and aims at minimizing the cost  $\mathcal{J}_1$  and Player (2) controls the strategy variable  $\tau \in H^{\frac{3}{2}}(\Gamma_i)^d$  and aims at minimizing the cost  $\mathcal{J}_2$ . These two players may be interpreted exactly the same way than in the completion game stated section 2.2 : they are given Dirichlet (resp. Neumann) data and try to minimize the gap with the Neumann (resp. Dirichlet) remaining condition. The player (3) controls the strategy variable  $\omega \in \mathcal{D}_{\text{ad}}$  and aims at minimizing the Kohn-Vogelius type functional  $\mathcal{J}_3$ , to which we added the regularizing term  $\mu|\partial\omega|$  which prevents from obtaining too irregular contours, as classical from Mumford-Shah functionals, see e.g. [13].

Notice that the state variables  $(u_1^\omega(\eta), p_1^\omega(\eta))$  and  $(u_2^\omega(\tau), p_2^\omega(\tau))$  belong to the space  $(H^1(\Omega \setminus \bar{\omega}))^d \times L^2(\Omega \setminus \bar{\omega})$ , which obviously depends on  $\omega$ , a variable intended to be a control. In order to circumvent this tricky dependence, we recourse to a level-set formulation, before stating the actual three-player Nash game effectively implemented.

### 2.4.1 A level-set formulation

The level-set approach is a very convenient tool in shape identification, see [77] for a general introduction, or [86] where the approach is applied to detect obstacles in a Stokes flow. The boundary of the shape to be identified is postulated to be a zero level-set of a smooth enough (say Lipschitz) function  $\phi : \Omega \rightarrow \mathbb{R}$ . In other words, when  $\phi$  varies in some -admissible- functional space, admissible open subsets  $\omega \in \Omega$  are those defined by the following

$$\begin{cases} \phi(x) < 0 & \text{in } \omega, \\ \phi(x) > 0 & \text{in } \Omega \setminus \bar{\omega}, \\ \phi(x) = 0 & \text{on } \partial\omega. \end{cases}$$

The open set  $\Omega \setminus \bar{\omega}$  is then given in terms of the level-set function as follows :

$$\Omega \setminus \bar{\omega} = \{x \in \Omega \text{ such that } H(\phi(x)) = 1\}, \quad (2.11)$$

where  $H(\cdot)$  is the Heaviside function. The perimeter of  $\omega$  can then be formally given by

$$|\partial\omega| = \int_{\Omega} |\nabla H(\phi)| dx = \int_{\Omega} \delta(\phi) |\nabla \phi| dx,$$

where  $\delta$  is the Dirac distribution.

For regularity reasons, and for ensuring the well-posedness of the modified Stokes system as well, it is usual to use smoothed versions of the Heaviside and Dirac distributions. Given two small enough parameters  $\varepsilon > 0$  and  $\beta > 0$ , we used smoothed versions denoted respectively by  $H_{\varepsilon, \beta}(\cdot)$  and  $\delta_{\varepsilon, \beta}(\cdot)$ , expressed as follows, for  $s \in \mathbb{R}$ ,

$$H_{\varepsilon, \beta}(s) = \begin{cases} 1 & \text{if } s > \varepsilon, \\ \frac{1}{2} \left( 1 + \frac{2}{\pi} \arctan\left(\frac{s}{\varepsilon}\right) \right) & \text{if } |s| \leq \varepsilon, \\ \beta & \text{if } s < -\varepsilon, \end{cases}$$

$$\delta_{\varepsilon,\beta}(s) = \begin{cases} \frac{1}{\pi} \left( \frac{\varepsilon}{s^2 + \varepsilon^2} \right) & \text{if } |s| \leq \varepsilon, \\ \beta & \text{if } |s| > \varepsilon. \end{cases}$$

Let us define the -control free- Sobolev state spaces :

$$\text{Given } g \in H^{\frac{1}{2}}(\Gamma_c)^d, \psi \in H^{\frac{3}{2}}(\Gamma_i)^d, \quad V_g = \{v \in H^1(\Omega)^d / \text{div} v = 0; v|_{\Gamma_c} = g\}$$

$$\text{and } W_\psi = \{v \in H^1(\Omega)^d \quad / \text{div} v = 0 \quad v|_{\Gamma_i} = \psi\}.$$

Problems  $(\mathcal{P}_1)$  and  $(\mathcal{P}_2)$  are then rephrased in terms of the level-set, yielding the modified weak form :

$$(\mathcal{P}_{1_{\varepsilon,\beta}}) \left\{ \begin{array}{l} \text{Find } (u_1^\phi, p_1^\phi) \in V_f \times L^2(\Omega) \text{ such that} \\ \int_{\Omega} (\sigma(u_1^\phi, p_1^\phi) : \nabla v_1) H_{\varepsilon,\beta}(\phi) dx = \int_{\Gamma_i} \eta v_1 ds, \quad \forall v_1 \in H_{\Gamma_c}^1(\Omega), \end{array} \right.$$

$$(\mathcal{P}_{2_{\varepsilon,\beta}}) \left\{ \begin{array}{l} \text{Find } (u_2^\phi, p_2^\phi) \in W_\tau \times L^2(\Omega) \text{ such that} \\ \int_{\Omega} (\sigma(u_2^\phi, p_2^\phi) : \nabla v_2) H_{\varepsilon,\beta}(\phi) dx = \int_{\Gamma_c} \Phi v_2 ds, \quad \forall v_2 \in H_{\Gamma_i}^1(\Omega). \end{array} \right.$$

The existence and uniqueness of solutions to the problems  $(\mathcal{P}_{1_{\varepsilon,\beta}})$  and  $(\mathcal{P}_{2_{\varepsilon,\beta}})$  follows from the fact that  $H_{\varepsilon,\beta}(\phi) \geq \beta > 0$  is bounded, and thanks to the well-posedness of the Stokes system with mixed boundary conditions (see Remark 2.2.1).

It is not the scope of the present paper to discuss the dependence of the modified Stokes problems with respect to  $(\varepsilon, \beta)$ , which is known to behave consistently [41, 94], so we still refer to problems  $(\mathcal{P}_{1_{\varepsilon,\beta}})$  and  $(\mathcal{P}_{2_{\varepsilon,\beta}})$  as  $(\mathcal{P}_1)$  and  $(\mathcal{P}_2)$ , and we omit to underline the dependence of the state variables w.r.t.  $(\varepsilon, \beta)$  as well.

## 2.4.2 Level-set sensitivity and optimality condition

The player (3) in charge of the inverse inclusion problem has now control on the level-set function  $\phi$  instead of the open subset  $\omega \in \mathcal{D}_{\text{ad}}$ . The new form of the third player's cost functional is now as follows :

$$\mathcal{J}_3(\eta, \tau; \phi) = \int_{\Omega} |\sigma(u_2^\phi, p_2^\phi) - \sigma(u_1^\phi, p_1^\phi)|^2 H_{\varepsilon,\beta}(\phi) dx + \mu \int_{\Omega} \delta_{\varepsilon,\beta}(\phi) |\nabla \phi| dx$$

where  $(u_1^\phi, p_1^\phi)$  and  $(u_2^\phi, p_2^\phi)$  solve respectively problems  $(\mathcal{P}_{1_{\varepsilon,\beta}})$  and  $(\mathcal{P}_{2_{\varepsilon,\beta}})$ . We choose as convenient space for the level-set variables the Sobolev space  $\mathcal{S} = H^1(\Omega)$  though it is not optimal (in the sense that it may introduce too much regularity requirement, hampering the capture of non  $H^1$  inclusions).

In order to perform the partial optimization of  $\mathcal{J}_3(\eta, \tau; \phi)$  w.r.t.  $\phi$  for  $(\eta, \tau)$  given by players (1) and (2), one needs to compute the derivative of  $\mathcal{J}_3$  w.r.t.  $\phi$ . We have the following :

**Proposition 2.4.1** *Assume  $\phi \in \mathcal{S}$  satisfies  $\Delta \phi \in L^2(\Omega)$  and  $|\nabla \phi| \neq 0$  with the boundary condition  $\frac{\partial \phi}{\partial n} = 0$  over  $\partial \Omega$ . Then  $\mathcal{J}_3(\eta, \tau; \phi)$  is Fréchet-differentiable with respect to*

$\phi$ , and the partial derivative of  $\mathcal{J}_3(\eta, \tau; \phi)$  with respect to  $\phi$ , in any direction  $\psi \in \mathcal{S}$ , is given by

$$\begin{aligned} \left(\frac{\partial \mathcal{J}_3}{\partial \phi}(\eta, \tau; \phi), \psi\right) &= \int_{\Omega} \delta_{\varepsilon, \beta}(\phi) \left[ |\sigma(u_2^\phi, p_2^\phi) - \sigma(u_1^\phi, p_1^\phi)|^2 - \mu \operatorname{div} \left( \frac{\nabla \phi}{|\nabla \phi|} \right) \right. \\ &\quad \left. + \sigma(u_1^\phi, p_1^\phi) : \nabla \lambda_1 + \sigma(u_2^\phi, p_2^\phi) : \nabla \lambda_2 \right] \psi dx, \end{aligned}$$

where  $(\lambda_1, \pi_1) \in H_{\Gamma_c}^1(\Omega) \times L^2(\Omega)$  and  $(\lambda_2, \pi_2) \in H_{\Gamma_i}^1(\Omega) \times L^2(\Omega)$  are respective solutions of the adjoints problems,

$$\begin{cases} -2 \int_{\Omega} (\sigma(u_2^\phi, p_2^\phi) - \sigma(u_1^\phi, p_1^\phi)) : (\nabla h_1 + \nabla h_1^T) H_{\varepsilon, \beta}(\phi) dx - \int_{\Omega} \pi_1 \operatorname{div} h_1 H_{\varepsilon, \beta}(\phi) dx \\ \quad + \int_{\Omega} ((\nabla h_1 + \nabla h_1^T) : \nabla \lambda_1) H_{\varepsilon, \beta}(\phi) dx = 0, \quad \forall h_1 \in H_{\Gamma_c}^1(\Omega), \\ 2 \int_{\Omega} (\sigma(u_2^\phi, p_2^\phi) - \sigma(u_1^\phi, p_1^\phi)) : (k_1 I_d) H_{\varepsilon, \beta}(\phi) dx - \int_{\Omega} k_1 \operatorname{div} \lambda_1 H_{\varepsilon, \beta}(\phi) dx = 0, \\ \quad \forall k_1 \in L^2(\Omega), \end{cases} \quad (2.12)$$

$$\begin{cases} 2 \int_{\Omega} (\sigma(u_2^\phi, p_2^\phi) - \sigma(u_1^\phi, p_1^\phi)) : (\nabla h_2 + \nabla h_2^T) H_{\varepsilon, \beta}(\phi) dx - \int_{\Omega} \pi_2 \operatorname{div} h_2 H_{\varepsilon, \beta}(\phi) dx \\ \quad + \int_{\Omega} ((\nabla h_2 + \nabla h_2^T) : \nabla \lambda_2) H_{\varepsilon, \beta}(\phi) dx = 0, \quad \forall h_2 \in H_{\Gamma_i}^1(\Omega), \\ -2 \int_{\Omega} (\sigma(u_2^\phi, p_2^\phi) - \sigma(u_1^\phi, p_1^\phi)) : (k_2 I_d) H_{\varepsilon, \beta}(\phi) dx - \int_{\Omega} k_2 \operatorname{div} \lambda_2 H_{\varepsilon, \beta}(\phi) dx = 0, \\ \quad \forall k_2 \in L^2(\Omega), \end{cases} \quad (2.13)$$

and where  $(u_1^\phi, p_1^\phi)$  and  $(u_2^\phi, p_2^\phi)$  are the solutions to respectively  $(\mathcal{P}_{1, \varepsilon, \beta})$  and  $(\mathcal{P}_{2, \varepsilon, \beta})$ .

**Proof 2.4.1** To prove Proposition 2.4.1 above, let us first remark that we are in a classical elliptic case : the states  $(u_1^\phi, p_1^\phi)$  and  $(u_2^\phi, p_2^\phi)$  solve respectively problems  $(\mathcal{P}_{1, \varepsilon, \beta})$  and  $(\mathcal{P}_{2, \varepsilon, \beta})$  which are elliptic, and with a smooth dependence of energy functionals on  $\phi$ , namely on the regularized parameter  $H_{\varepsilon, \beta}(\phi)$ . It is then well known that the states  $(u_1^\phi, p_1^\phi)$  and  $(u_2^\phi, p_2^\phi)$  are Frechet-differentiable with respect to  $\phi$ , see [84] or [37] page 107, the assumptions made therein are straightforward in our case. From other part, the assumption  $|\nabla \phi| \neq 0$  is fulfilled by the reinitialisation step (2.17) which forces  $|\nabla \phi|$  to be close to 1. The cost function  $\mathcal{J}_3(\eta, \tau; \phi)$  is then partially Frechet-differentiable with respect to  $\phi$ , as it is partially with respect to a generic state  $(v_1, q_1)$  and  $(v_2, q_2)$  (dismissing the dependence of these w.r.t.  $\phi$ , the functional is quadratic w.r.t. the states  $(v_i, q_i), i = 1, 2$ ). The cited references state then that the reduced cost function (taking into account the implicit dependence of the states w.r.t. the control  $\phi$ ) is Frechet-differentiable with respect to  $\phi$ , and the derivative is computable by means of an adjoint state method, as stated in Proposition 2.4.1. The derivation of the adjoint state equations and of the formula for the derivative is given in Appendix A.2.

**Remark 2.4.1** The assumption that  $\phi$  satisfies  $\Delta \phi \in L^2(\Omega)$  is necessary for the existence of the Neumann trace of  $\phi$ . Indeed, from one part, stating regularity results for the nonlinear implicit equation (2.14) fulfilled by  $\phi$  below is not straightforward; and from other part, the discretized scheme (2.16) of the latter equation provides iterates  $\phi^{(n)}$  which are in  $H^2(\Omega)$ .

The necessary optimality condition for the minimization problem  $\min_{\phi \in \mathcal{S}} \mathcal{J}_3(\eta, \tau; \phi)$  is then formulated as the following Euler-Lagrange equation :

$$\begin{cases} \delta_{\varepsilon, \beta}(\phi) \left[ |\sigma(u_2^\phi, p_2^\phi) - \sigma(u_1^\phi, p_1^\phi)|^2 - \mu \operatorname{div}\left(\frac{\nabla \phi}{|\nabla \phi|}\right) \right. \\ \quad \left. + \sigma(u_1^\phi, p_1^\phi) : \nabla \lambda_1 + \sigma(u_2^\phi, p_2^\phi) : \nabla \lambda_2 \right] = 0, & \text{in } \Omega, \\ \frac{\partial \phi}{\partial n} = 0, & \text{on } \partial \Omega. \end{cases} \quad (2.14)$$

The strongly nonlinear equation above -with implicit terms- is solved iteratively as the stationary state of the following evolution equation

$$\begin{cases} \frac{\partial \phi}{\partial t} + \delta_{\varepsilon, \beta}(\phi) \left[ |\sigma(u_2^\phi, p_2^\phi) - \sigma(u_1^\phi, p_1^\phi)|^2 - \mu \operatorname{div}\left(\frac{\nabla \phi}{|\nabla \phi|}\right) \right. \\ \quad \left. + \sigma(u_1^\phi, p_1^\phi) : \nabla \lambda_1 + \sigma(u_2^\phi, p_2^\phi) : \nabla \lambda_2 \right] = 0, & \text{in } \mathbb{R}^+ \times \Omega, \\ \frac{\partial \phi}{\partial n} = 0, & \text{on } \mathbb{R}^+ \times \partial \Omega, \\ \phi(0, x) = \phi_0(x), & \text{in } \Omega, \end{cases} \quad (2.15)$$

where  $\phi_0 \in \mathcal{S}$  is a given initial condition.

The variational formulation associated to the problem (2.15) above reads

$$\begin{aligned} \int_{\Omega} \frac{\partial \phi}{\partial t} \psi dx &= - \int_{\Omega} \delta_{\varepsilon, \beta}(\phi) |\sigma(u_2^\phi, p_2^\phi) - \sigma(u_1^\phi, p_1^\phi)|^2 \psi dx + \mu \int_{\Omega} \delta_{\varepsilon, \beta}(\phi) \operatorname{div}\left(\frac{\nabla \phi}{|\nabla \phi|}\right) \psi dx \\ &\quad - \int_{\Omega} \delta_{\varepsilon, \beta}(\phi) \left[ \sigma(u_1^\phi, p_1^\phi) : \nabla \lambda_1 + \sigma(u_2^\phi, p_2^\phi) : \nabla \lambda_2 \right] \psi dx, \quad \forall \psi \in H^1(\Omega). \end{aligned}$$

But, since one has

$$\operatorname{div}\left(\delta_{\varepsilon, \beta}(\phi) \frac{\nabla \phi}{|\nabla \phi|}\right) = \delta'_{\varepsilon, \beta}(\phi) \nabla \phi \frac{\nabla \phi}{|\nabla \phi|} + \delta_{\varepsilon, \beta}(\phi) \operatorname{div}\left(\frac{\nabla \phi}{|\nabla \phi|}\right),$$

we get,

$$\begin{aligned} \int_{\Omega} \frac{\partial \phi}{\partial t} \psi dx &= - \int_{\Omega} \delta_{\varepsilon, \beta}(\phi) |\sigma(u_2^\phi, p_2^\phi) - \sigma(u_1^\phi, p_1^\phi)|^2 \psi dx - \mu \int_{\Omega} \frac{\delta_{\varepsilon, \beta}(\phi)}{|\nabla \phi|} \nabla \phi \nabla \psi dx \\ &\quad - \int_{\Omega} \delta_{\varepsilon, \beta}(\phi) \left[ \sigma(u_1^\phi, p_1^\phi) : \nabla \lambda_1 + \sigma(u_2^\phi, p_2^\phi) : \nabla \lambda_2 \right] \psi dx \\ &\quad - \mu \int_{\Omega} \delta'_{\varepsilon, \beta}(\phi) |\nabla \phi| \psi dx, \quad \forall \psi \in H^1(\Omega). \end{aligned}$$

The problem above is solved numerically by means of a semi-implicit Euler scheme with  $\frac{\partial \phi}{\partial t}$  approximated by  $\frac{\phi^{n+1} - \phi^n}{\delta t}$ , where  $\phi^n(\cdot) = \phi(t_n, \cdot)$  and  $t_n = n\delta t$ , with  $\delta t > 0$  a given time step.

We obtain the following iterative scheme :

$$\begin{cases} \text{Given } \phi^n, \text{ Find } \phi^{n+1} \in H^1(\Omega) \text{ such that :} \\ a(\phi^{n+1}, \psi) = l(\psi), \quad \forall \psi \in H^1(\Omega), \end{cases} \quad (2.16)$$

where

$$\begin{cases} a(\phi^{n+1}, \psi) = \int_{\Omega} \phi^{n+1} \psi dx + \mu \delta t \int_{\Omega} \frac{\delta_{\varepsilon, \beta}(\phi^n)}{|\nabla \phi^n|} \nabla \phi^{n+1} \nabla \psi dx, \\ l(\psi) = -\delta t \int_{\Omega} \delta_{\varepsilon, \beta}(\phi^n) |\sigma(u_2^n, p_2^n) - \sigma(u_1^n, p_1^n)|^2 \psi dx - \mu \delta t \int_{\Omega} \delta'_{\varepsilon, \beta}(\phi^n) |\nabla \phi^n| \psi dx \\ \quad + \int_{\Omega} \phi^n \psi dx - \delta t \int_{\Omega} \delta_{\varepsilon, \beta}(\phi^n) \left[ \sigma(u_1^n, p_1^n) : \nabla \lambda_1 + \sigma(u_2^n, p_2^n) : \nabla \lambda_2 \right] \psi dx, \end{cases}$$

with  $(u_1^n, p_1^n) = (u_1(\eta, \phi^n), p_1(\eta, \phi^n))$ ,  $(u_2^n, p_2^n) = (u_2(\tau, \phi^n), p_2(\tau, \phi^n))$  are solutions to  $(\mathcal{P}_{1_{\varepsilon, \beta}})$  and  $(\mathcal{P}_{2_{\varepsilon, \beta}})$  for a given  $\phi^n$ , and  $\lambda_{\{i=1,2\}}^n = \lambda_{\{i=1,2\}}(\phi^n)$  are the adjoint state solutions of the problems (2.12) and (2.13).

In order to prevent the level set iterates from being too flat or too steep, we trigger from time to time a regularization pass that reinitializes the level set to a signed distance (see e.g. [4]). This step is mandatory in order to keep the iterated level sets smooth enough, but is also necessary to have a non vanishing  $|\nabla\phi^n|$  that ensures the ellipticity of  $a(.,.)$  in (2.16). The update is performed by solving the following equation :

$$\begin{cases} \frac{\partial\psi}{\partial t} + \text{sign}(\phi^n)(|\nabla\psi| - 1) = 0 & \text{in } \mathbb{R}^+ \times \Omega, \\ \frac{\partial\psi}{\partial n} = 0 & \text{on } \mathbb{R}^+ \times \partial\Omega, \\ \psi(0, x) = \phi^n(x) & \text{in } \Omega. \end{cases} \quad (2.17)$$

In practice, equation (2.17) above is solved for a few time steps (typically 5 or 6) then one reassigns the last computed  $\psi$  to  $\phi^n(x)$ .

The six variational problems  $(\mathcal{P}_{1_{\varepsilon, \beta}})$ ,  $(\mathcal{P}_{2_{\varepsilon, \beta}})$ , (2.12), (2.13), (2.16) and (2.17) are solved by means of *ad hoc* Finite Element methods (see Section 2.5 below).

### 2.4.3 The three-player Nash algorithm

We are now ready to state the three-player identification/completion Nash game. As aforementioned in section 2.4, players (1) and (2) aim at solving the Cauchy problem, while player (3) is aimed at minimizing a Kohn-Vogelius type energy, intended to capture the shape of the inclusion. The game is of Nash type, which means that it is static with complete information [56] and hence its solution is a Nash equilibrium (NE), see Definition 2.4.

Given a triplet  $(\eta, \tau, \phi) \in H^{\frac{1}{2}}(\Gamma_i)^d \times H^{\frac{3}{2}}(\Gamma_i)^d \times \mathcal{S}$ , let  $(u_1^\phi(\eta), p_1^\phi(\eta))$  be the solution to the approximate Stokes problem  $(\mathcal{P}_{1_{\varepsilon, \beta}})$  and  $(u_2^\phi(\tau), p_2^\phi(\tau))$  the solution to the approximate Stokes problem  $(\mathcal{P}_{2_{\varepsilon, \beta}})$ , then the three players and their respective costs are defined as follows :

- Player (1) has control on the Neumann strategies  $\eta \in H^{\frac{1}{2}}(\Gamma_i)^d$ , and its cost functional is given by

$$\mathcal{J}_1(\eta, \tau, \phi) = \frac{1}{2} \|\sigma(u_1^\phi(\eta), p_1^\phi(\eta))n - \Phi\|_{H^{\frac{1}{2}}(\Gamma_c)^d}^2 + \frac{1}{2} \|u_1^\phi(\eta) - u_2^\phi(\tau)\|_{H^{\frac{3}{2}}(\Gamma_i)^d}^2 \quad (2.18)$$

- Player (2) has control on the Dirichlet strategies  $\tau \in H^{\frac{3}{2}}(\Gamma_i)^d$ , and its cost functional is given by

$$\mathcal{J}_2(\eta, \tau, \phi) = \frac{1}{2} \|u_2^\phi(\tau) - f\|_{H^{\frac{3}{2}}(\Gamma_c)^d}^2 + \frac{1}{2} \|u_1^\phi(\eta) - u_2^\phi(\tau)\|_{H^{\frac{3}{2}}(\Gamma_i)^d}^2 \quad (2.19)$$

- Player (3) has control on the inclusion level-set strategies  $\phi \in \mathcal{S}$ , and its cost functional is given by

$$\mathcal{J}_3(\eta, \tau; \phi) = \int_{\Omega} |\sigma(u_2^\phi(\tau), p_2^\phi(\tau)) - \sigma(u_1^\phi(\eta), p_1^\phi(\eta))|^2 H_{\varepsilon, \beta}(\phi) dx + \mu \int_{\Omega} \delta_{\varepsilon, \beta}(\phi) |\nabla\phi| dx \quad (2.20)$$

In Algorithm 2.4.1 below, we describe the main steps in computing the Nash equilibrium. This algorithm is unusual in the sense that, first, it introduces a completion-oriented Nash subgame, solved incompletely ( $K_{max}$  is small, around ten iterations), and second, it processes the third player's minimization step by iterating on the necessary optimality condition. Classical algorithms compute Nash equilibria with  $K_{max} = 1$ . It is easy to check (by writing down the stationarity equations) that when the two algorithms converge, they lead to the same limit point, which is a Nash equilibrium of the three-player's game defined above.

As we shall see in section 2.5 below, Algorithm 2.4.1 outperforms the classical one.

---

**Algorithm 2.4.1:** Computation of the coupled inclusion-completion Nash equilibrium

---

Given : convergence tolerances  $\varepsilon_N > 0$ ,  $\varepsilon_S > 0$ ,  $K_{max}$  a computational budget per Nash iteration,  $N_{max}$  a maximum Nash iterations,  $\sigma$  a noise level and  $\rho(\sigma)$  a -tuned- function which depends on the noise.

Set  $n = 0$ , choose an initial level-set  $\phi^{(0)} \in \mathcal{S}$ .

- Step I : (a completion Nash subgame) Set  $k = 1$ .  
Choose an initial guess  $S^{(k-1)} = (\eta^{(k-1)}, \tau^{(k-1)}) \in H^{\frac{1}{2}}(I_i)^d \times H^{\frac{3}{2}}(I_i)^d$ .
    - Step 1 : Compute  $\bar{\eta}^{(k)}$  solution of  $\min_{\eta} \mathcal{J}_1(\eta, \tau^{(k-1)}, \phi^{(n)})$   
and set  $\eta^{(k)} = \alpha \eta^{(k-1)} + (1 - \alpha) \bar{\eta}^{(k)}$  with  $0 \leq \alpha < 1$ .
    - Step 2 : Compute  $\bar{\tau}^{(k)}$  solution of  $\min_{\tau} \mathcal{J}_2(\eta^{(k-1)}, \tau, \phi^{(n)})$   
and set  $\tau^{(k)} = \alpha \tau^{(k-1)} + (1 - \alpha) \bar{\tau}^{(k)}$  with  $0 \leq \alpha < 1$ .
    - Step 3 : While  $\|S^{(k)} - S^{(k-1)}\| > \varepsilon_S$  and  $k < K_{max}$ , set  $k = k + 1$ ,  
return back to step 1.
  - Step II : Compute  $r_k = \|u_2^{(k)} - f^\sigma\|_{L^2(I_c)}$ , where  $(u_2^{(k)}, p_2^{(k)})$  is the solution of the problem  $(\mathcal{P}_{2\varepsilon, \beta})$  with the level-set  $\phi = \phi^{(n)}$  and with the Dirichlet condition  $u_2^{(k)} = \tau^{(k)}$  over  $I_i$ .
  - Step III : While  $r_k \geq \rho(\sigma)\varepsilon$  and  $n < N_{max}$  update the level-set : compute  $\phi^{(n+1)}$  solution to the variational problem (2.16) and set  $n = n + 1$ , go back to step I.
- 

## 2.5 Numerical experiments

In this section, we provide and discuss the numerical results of experiments led for three test cases, named A, B and C. These 3 test-cases share the following common settings :

**The domain**  $\Omega = ]-\frac{1}{2}, \frac{1}{2}[ \times ]-\frac{1}{2}, \frac{1}{2}[$

**The boundaries**  $I_i = \{\frac{1}{2}\} \times ]-\frac{1}{2}, \frac{1}{2}[$ ;  $I_c = \partial\Omega \setminus I_i$

**Normal stress**  $\Phi(x, y) = -2(y^2 - 1/4; 0)$  prescribed over  $\partial\Omega$

**Initial strategies** for Step I, we always used  $S^{(0)} = (\eta^{(0)}, \tau^{(0)}) = (0, 0)$  and took  $\alpha = 0.1$

**Parameters** for Step III : we took  $\delta t = 0.02$  for solving equation (2.16).



The test-cases differ in the shape and/or number of connexe components of the inclusions.

Given a known shape and location of the inclusion  $\omega^* \in \mathcal{D}_{\text{ad}}$ , we solve the following Stokes problem :

$$\begin{cases} \Delta u - \nabla p = 0 & \text{in } \Omega \setminus \overline{\omega^*}, \\ \operatorname{div} u = 0 & \text{in } \Omega \setminus \overline{\omega^*}, \\ \sigma(u, p)n = 0 & \text{on } \partial\omega^*, \\ \sigma(u, p)n = \Phi & \text{on } \partial\Omega, \end{cases}$$

where the (phantom) exact solution  $(u, p)$  is used to build the remaining Cauchy data  $f = u|_{\Gamma_c}$ , and the exact missing data  $u|_{\Gamma_i}$  and  $\sigma(u, p)n|_{\Gamma_i}$ . The two latter data together with the known inclusion shape  $\omega^*$  are used to compute the following relative errors :

$$\begin{aligned} \operatorname{err}_D &= \frac{\|\tau_N - u|_{\Gamma_i}\|_{L^2(\Gamma_i)}}{\|u|_{\Gamma_i}\|_{L^2(\Gamma_i)}}, & \operatorname{err}_N &= \frac{\|\eta_N - \sigma(u, p)n|_{\Gamma_i}\|_{L^2(\Gamma_i)}}{\|\sigma(u, p)n|_{\Gamma_i}\|_{L^2(\Gamma_i)}}, \\ \operatorname{err}_O &= \frac{\operatorname{mes}(\omega^* \cup \omega_N) - \operatorname{mes}(\omega^* \cap \omega_N)}{\operatorname{mes}(\omega^*)}, \end{aligned} \quad (2.21)$$

where  $(\eta_N, \tau_N, \phi_N)$  is the approximate Nash equilibrium output from Algorithm 2.4.1, and  $\omega_N = 1_{\{\phi_N < 0\}}$ . These metrics are used to assess the efficiency of our approach. The stability w.r.t. noise was stressed by solving the joint inverse inclusion/completion problem with noisy perturbations of the Dirichlet data  $f^\sigma = f + \sigma N$  with  $N$  being a Gaussian white noise.

Two different initial level-sets were used :  $\phi_1^{(0)}$  has as zero level-set the disk  $B(c_0, r_0)$  where  $c_0 = (0, 0)$  and  $r_0 = 0.3$ , and  $\phi_2^{(0)}$  is a periodic function with as zero level-set 30 small ellipsoids with uniformly distributed centers, see Figures 2.5(a) and 2.6(a).

The solvers for Stokes, equation (2.16) and adjoint systems, the sensitivity routines, and the minimization algorithms as well, were implemented using the Finite Element package FreeFem++ [61].

## Test-case A

The exact inclusion is a disk  $\omega^* = B(c, r)$  centered at  $c$  and with a radius  $r$  where  $c = (0, 0)$  and  $r = 0.1$ .

The FreeFem++ implementation of Algorithm 2.4.1 was ran for two different initial contours, leading to very close results, both of them in good accordance with the exact solutions (inclusion and missing data). It can be however observed from Figure 2.5(c)(e) and Figure 2.6(c)(e) that the initial contour  $\phi_2^{(0)}$  outperforms  $\phi_1^{(0)}$  as the computed first component of the fluid velocity and normal stress are more accurate with the initial contour  $\phi_2^{(0)}$ . Indeed, in all our subsequent numerical experiments, the initial contour  $\phi_2^{(0)}$  outperformed  $\phi_1^{(0)}$ , so we shall later on present only those results obtained with  $\phi_2^{(0)}$ .

For the case of noisy Dirichlet data  $f^\sigma$  given over  $\Gamma_c$ , it can be seen from the profiles presented in Figure 2.7 that the boundary data recovery is remarkably stable with respect to the noise magnitude, and even more striking is the stability of the detected inclusion.

The relative errors defined by formulas (2.21) are summarized in Table 2.1 for the test-case A.

---

Noise level	$\sigma = 0\%$	$\sigma = 1\%$	$\sigma = 3\%$	$\sigma = 5\%$
$err_D$	0.010	0.015	0.039	0.063
$err_N$	0.031	0.033	0.051	0.07
$err_O$	0.032	0.043	0.066	0.117

---

Table 2.1 – Test-case A.  $L^2$  relative errors on missing data on  $\Gamma_i$  (on Dirichlet and Neumann data), and the error between the reconstructed and the real shape of the inclusion for various noise levels.

## Test-case B

The exact inclusion  $\omega^*$  has a peanut-like shape, with a boundary parameterized as follows :

$$\partial\omega = \left\{ \begin{pmatrix} x_0 \\ y_0 \end{pmatrix} + r(\theta) \begin{pmatrix} a \sin \theta \\ b \cos \theta \end{pmatrix}; \quad \theta \in [0, 2\pi) \right\},$$

where  $r(\theta) = \sqrt{\sin^2 \theta + 0.25 \cos^2 \theta}$ ,  $(x_0, y_0) = (0, 0)$  and  $(a, b) = (0.15, 0.18)$ .

In this test-case, the shape of the inclusion is nonconvex. We observe from Figure 2.8(b) that while the computed zero level-set is in good accordance with the exact one, it is however unable to accurately capture the nonconvex features of the real inclusion. This is not very surprising in view of the different smoothed approximations used for the inclusion Stokes problems as well as for the level-set equation. The data completion results are however very satisfactory, as shown by the velocity and normal stress profiles in Figures 2.8(c)-(e). There is also a remarkable stability with respect to noisy data of both the inclusion detected and the recovered boundary data, see Figure 2.9.

## Test-case C

The inclusion to be detected is the union of two separate disks  $\omega_1^* = B(c_1, r_1)$  centered at  $c_1 = (0.2, 0.2)$  and with a radius  $r_1 = 0.10$  and  $\omega_2^* = B(c_2, r_2)$  centered at  $c_2 = (-0.2, -0.2)$  and with a radius  $r_2 = 0.12$ .

This third and last test-case was set up to assess the ability of our algorithm to identify inclusions with several components. One observes from Figure 2.10(b) that the locations and the shapes of the two components of the inclusion are well detected, as well as the recovered data Figure 2.10(c)-(f). The recovery of missing boundary data is stable with respect to noisy Dirichlet measurements while there is a barely slight shift in the location of the detected approximation of  $\omega_1^*$  for the noise levels 3% and 5%, as shown Figure 2.11.

The relative errors presented in Table 2.2 corroborate the stability of the detected contours and missing data with respect to noisy Dirichlet measurements.

Noise level	$\sigma = 0\%$	$\sigma = 1\%$	$\sigma = 3\%$	$\sigma = 5\%$
$err_D$	0.042	0.044	0.046	0.08
$err_N$	0.095	0.1	0.13	0.16
$err_O$	0.099	0.11	0.13	0.15

Table 2.2 – Test-case C.  $L^2$ -errors on missing data over  $I_i$  (on Dirichlet and Neumann data), and the error between the reconstructed and the real shape for various noise levels.

### Algorithm 2.4.1 vs classical.

In a classical algorithm [75] dedicated to the computation of a Nash equilibrium, there would be no inner do loop as performed during step I in Algorithm 2.4.1, or in other words,  $K_{max} = 1$ . We have compared these two approaches, for two noise free test-cases. We used the same number of total calls (400) to the Stokes Finite Element solvers. We see from Table 2.3 that, for both test-cases, Algorithm 2.4.1 outperforms the classical one. Iterations in step I compute a two-player Nash equilibrium for a *fixed level-set*. This step, which we call a preconditioning Nash subgame, is dedicated to enforce the data completion part does indeed enforce the identifiability property as well, since from the result established in Proposition 2.3, it is enough for a candidate velocity  $u(\omega)$ , for some inclusion  $\omega$ , to be a Cauchy solution for the pair of boundary measurements  $(f, \Phi)$ , to ensure that  $\omega = \omega^*$ , the real inclusion.

Case A	Classical algorithm	Algorithm 2.4.1
$err_D$	0.058	0.033
$err_N$	0.106	0.032
$err_O$	0.358	0.140
Case C	Classical algorithm	Algorithm 2.4.1
$err_D$	0.067	0.058
$err_N$	0.208	0.122
$err_O$	0.566	0.167

Table 2.3 – Relative errors on the reconstructed missing data and inclusion shape for the Stokes problem (with noise free measurements), compared for a classical Nash algorithm and Algorithm 2.4.1 : (left) test-case A (right) test-case C.

### Sensitivity to the mesh size, to closeness to the inaccessible boundary and inverse crime.

The coupled completion/detection problem for the Cauchy-Stokes system involves many numerical tricks of more or less severity. In the lack of theoretical convergence results, which are not easy to establish in the present framework, we led three kinds of numerical experiments.

The first one is related to the behaviour of the overall coupled algorithm with respect to finite element discretization of the domain  $\Omega$ . The second one is related to the study of the efficiency of the algorithm in detecting obstacles located near the inaccessible

boundary  $\Gamma_i$ . Figure-2.3 shows that the relative errors decrease w.r.t. the mesh size, with different convergence rates; it also shows that the errors increase dramatically when the inclusion becomes too close to the inaccessible boundary  $\Gamma_i$ .

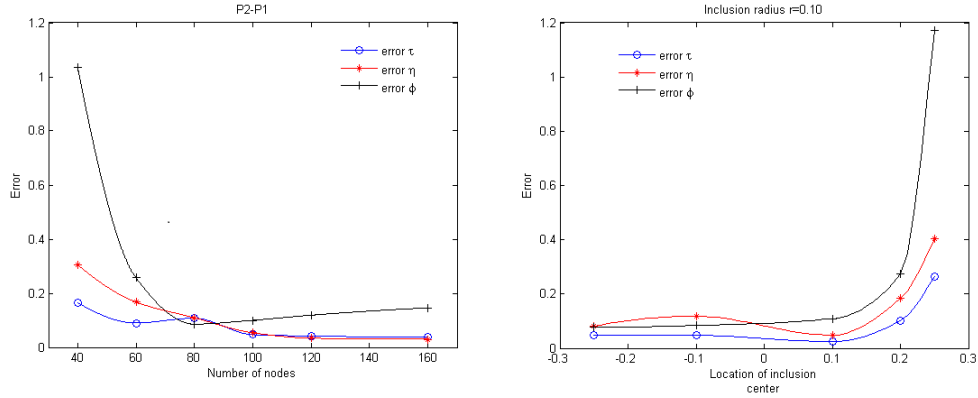


FIGURE 2.3 – Test case A. (Left) sensitivity of the reconstruction w.r.t. the mesh size (on abscissae : the number of F.E. nodes on the boundary  $\partial\Omega$ ). (Right) sensitivity of the reconstruction w.r.t. the distance to the inaccessible boundary  $\Gamma_i$  (on abscissae : the distance of the center of the circular inclusion from  $\Gamma_i$ ).

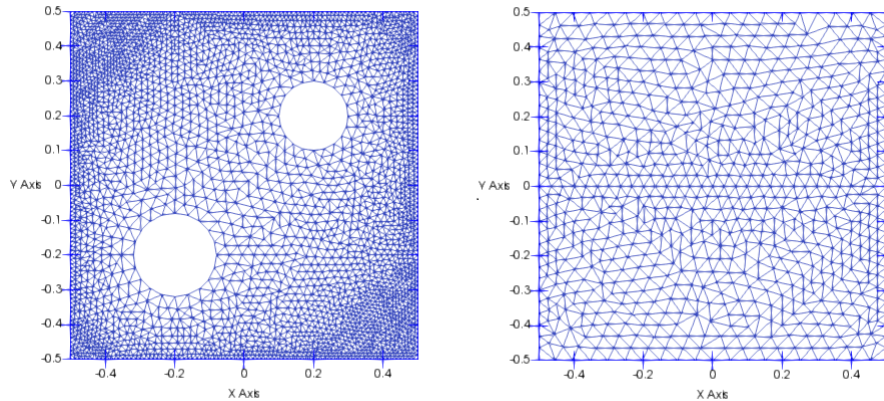


FIGURE 2.4 – Test case C. (Left) Mesh used for solving the direct problem with the P1bubble-P1 finite element, in order to construct the synthetic data. (Right) Mesh used for solving the coupled inverse problem with P2-P1 finite element, using the P1 bubble-P1 synthetic data.

The third set of experiments was led to assess our algorithm and results against the so-called inverse crime, that arises when the same model is used to synthesize Cauchy data and to solve the corresponding inverse problem, resulting in possible artificial outperformance. To prevent such a bias, we synthesized Cauchy data using different meshes, and solving the direct problem with the well known P1 bubble - P1 finite element, see one example figure 2.4. All our numerical experiments produced results, in data completion as well as in obstacle detection, of the same good quality than the results presented in figures 2.5–2.11, see figure 2.12.

---

## 2.6 Conclusion

We addressed in the present paper the delicate problem of detecting unknown cavities immersed in a stationary viscous fluid, using partial boundary measurements. The considered fluid obeys a Stokes regime, the cavities are inclusions and the boundary measurements are a single compatible pair of Dirichlet and Neumann data, available only on a partial accessible part of the whole boundary. This inverse inclusion Cauchy-Stokes problem is ill-posed for both the cavities and missing data reconstructions, and designing stable and efficient algorithms, which is the main goal of our work, is not straightforward.

The ill-posedness is tackled by decentralization : we reformulate it as a three players Nash game, following the ideas introduced earlier in [56] to solve the Cauchy-Laplace (completion) problem. Thanks to a simple yet strong identifiability result for the Cauchy-Stokes system, it is enough to set up two Stokes BVP, then use them as state equations. The Nash game is then set between 3 players, the two first targeting the data completion while the third one targets the inclusion detection. The latter problem is formulated using a level-set approach, and we provided the third player with the level-set function as strategy, while its cost functional is of Kohn-Vogelius type.

The class of algorithms we propose are summarized in Algorithm 2.4.1, the involved computational apparatus being rather classical : use of descent algorithms for the different minimizations, use of adjoint state method to compute the sensitivities, and use of Finite Element methods to solve the state and adjoint state equations, as well as to update the level-sets. We used Freefem++ to implement these routines.

We led 2D numerical experiments for three different test-cases. For noise free, as well as for noisy -Cauchy data- Dirichlet measurements, we obtained satisfactory results, exhibiting very stable behaviour with respect to the noise level (1%, 3%, 5%). The obtained results favor our 3-player Nash game approach to solve parameter or shape identification for Cauchy problems. Finally, our approach rises difficult theoretical questions that we did not address here, such as the existence, uniqueness and convergence issues for the level-set solution to the implicit optimality condition (2.14) and, related to the game-theoretic approach, the existence and convergence issues for the 3-player Nash equilibrium.

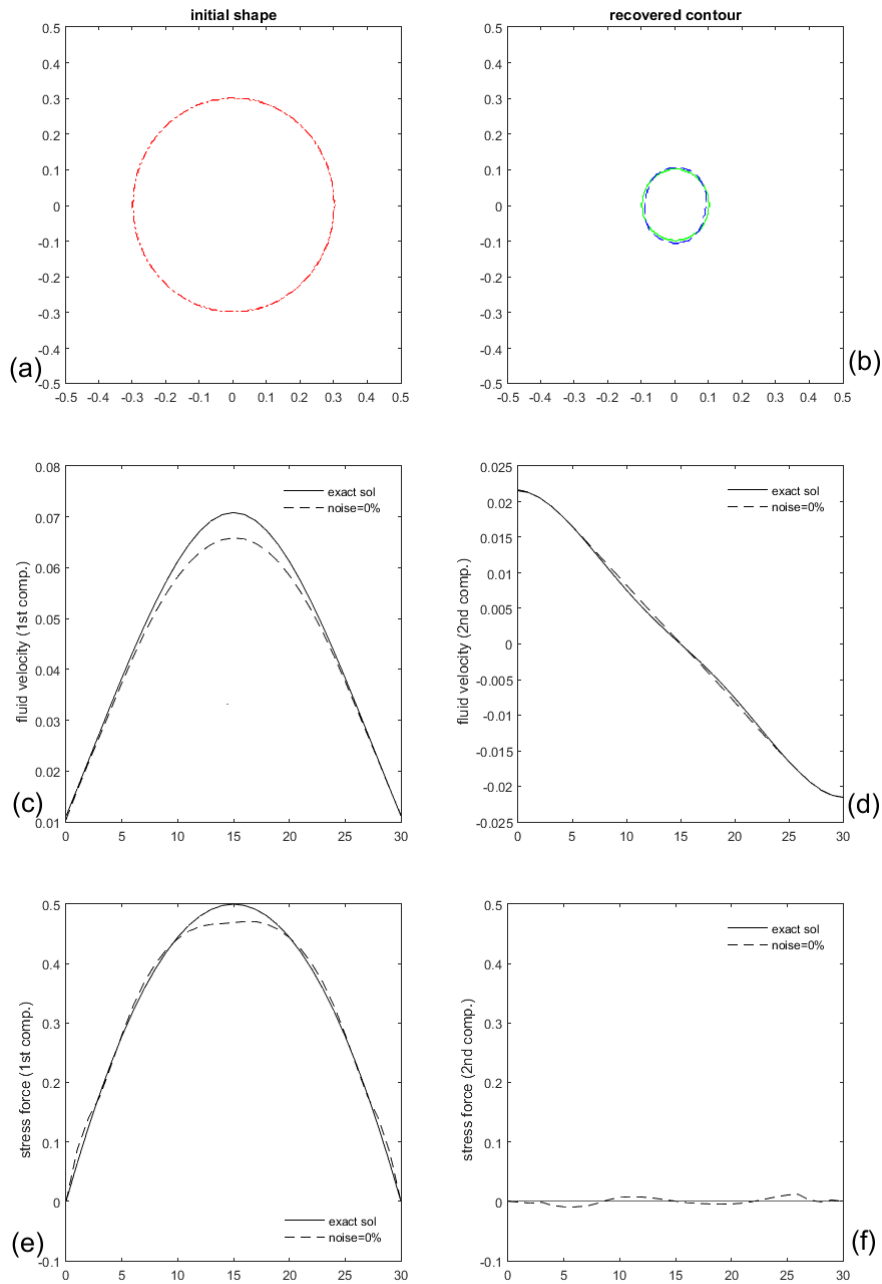


FIGURE 2.5 – Test case A. Reconstruction of the inclusion shape and missing boundary data with noise free Dirichlet data over  $I_c$ . **(a)** initial contour is  $\phi_1^{(0)}$  **(b)** exact inclusion shape -green line- and computed one - blue dashed- **(c)** exact -line- and computed -dashed line- first component of the velocity over  $I_i$  **(d)** exact -line- and computed -dashed line- second component of the velocity over  $I_i$  **(e)** exact -line- and computed -dashed line- first component of the normal stress over  $I_i$  **(f)** exact -line- and computed -dashed line- second component of the normal stress over  $I_i$ .

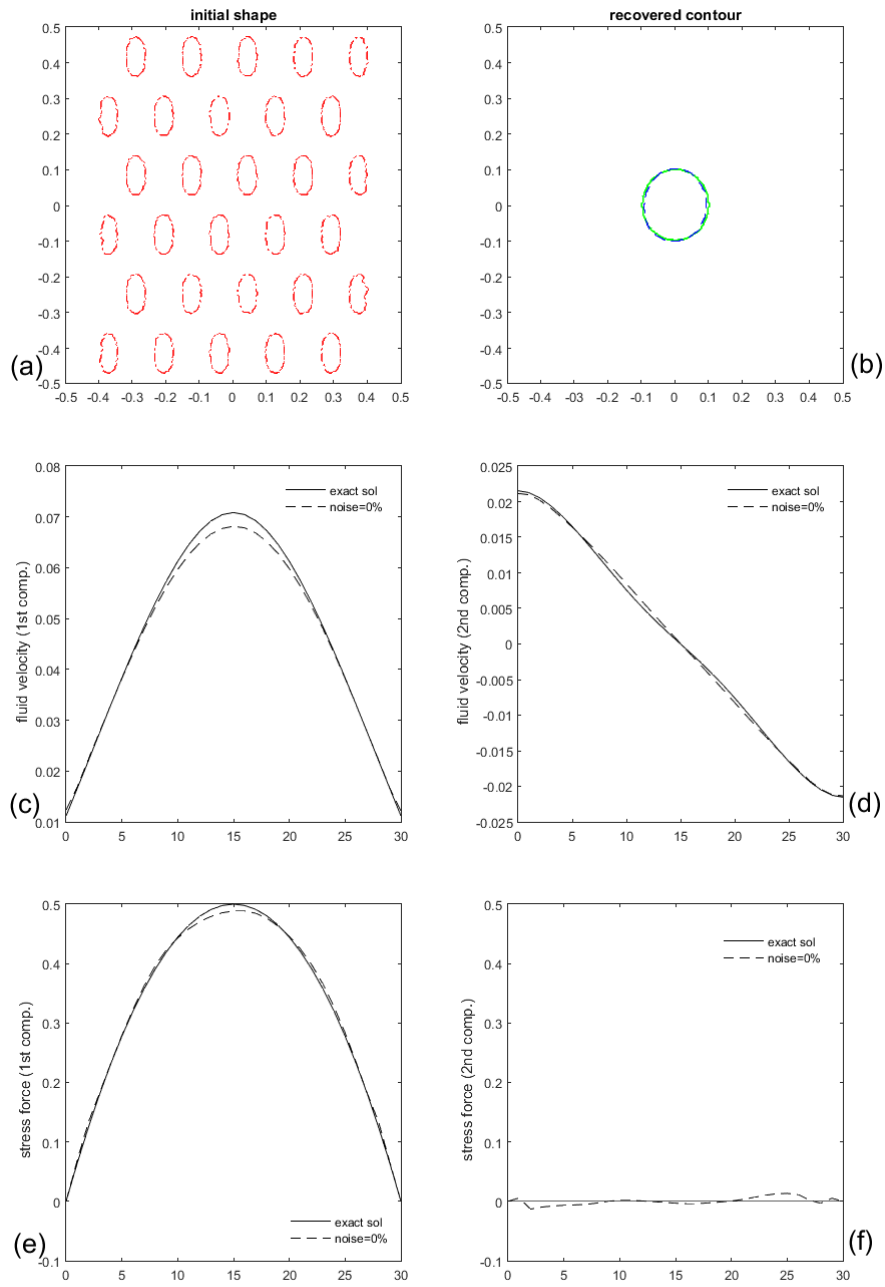


FIGURE 2.6 – Test case A. Reconstruction of the inclusion shape and missing boundary data with noise free Dirichlet data over  $I_c$ . (a) initial contour is  $\phi_2^{(0)}$  (b) exact inclusion shape - green line- and computed one - blue dashed- (c) exact -line- and computed -dashed line- first component of the velocity over  $I_i$  (d) exact -line- and computed -dashed line- second component of the velocity over  $I_i$  (e) exact -line- and computed -dashed line- first component of the normal stress over  $I_i$  (f) exact -line- and computed -dashed line- second component of the normal stress over  $I_i$ .

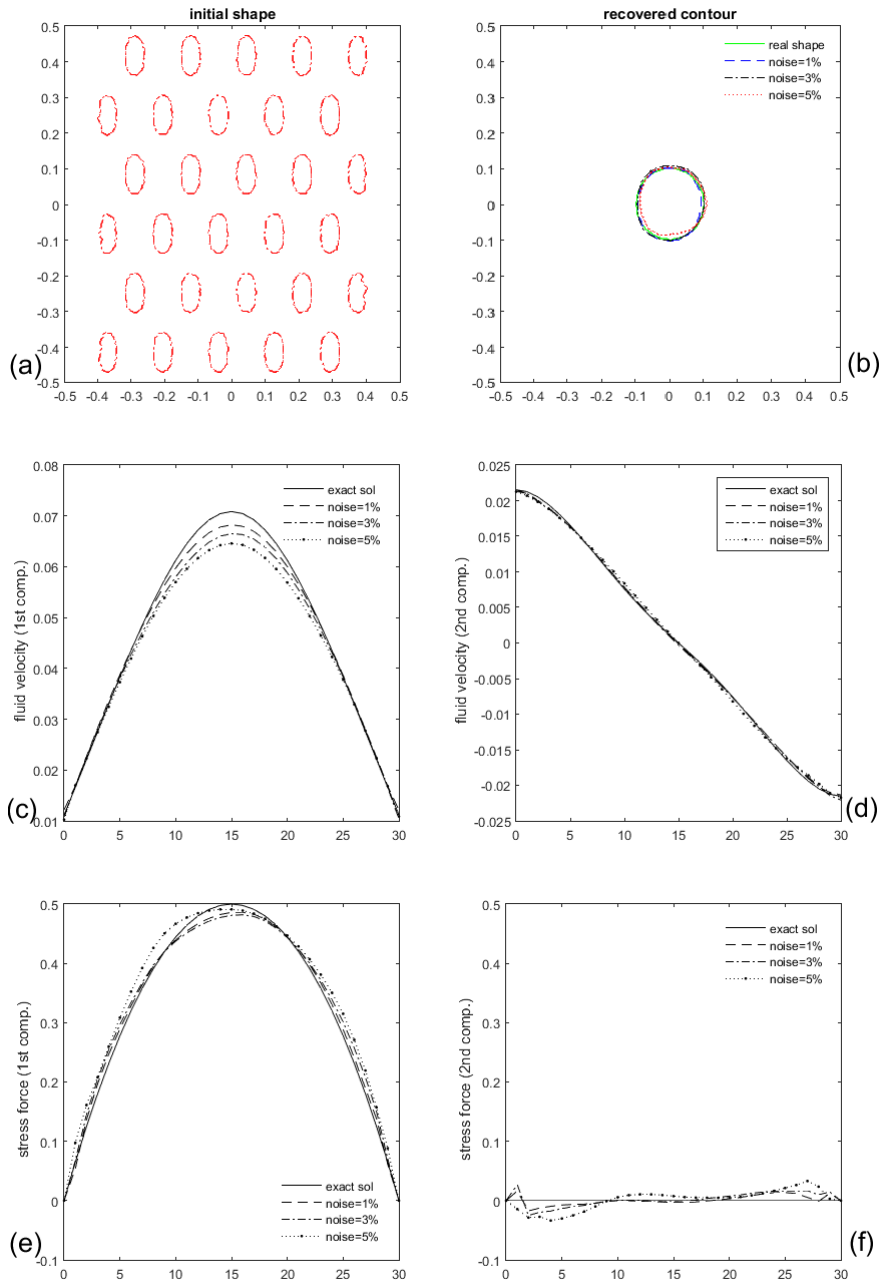


FIGURE 2.7 – Test case A. Reconstruction of the inclusion shape and missing boundary data with noisy Dirichlet data over  $I_C$  with noise levels  $\sigma = \{1\%, 3\%, 5\%\}$ . **(a)** initial contour is  $\phi_2^{(0)}$  **(b)** exact inclusion shape -green line- and computed ones for different noise levels **(c)** exact and computed first components of the velocity over  $I_i$  **(d)** exact and computed second components of the velocity over  $I_i$  **(e)** exact and computed first components of the normal stress over  $I_i$  **(f)** exact and computed second components of the normal stress over  $I_i$ .



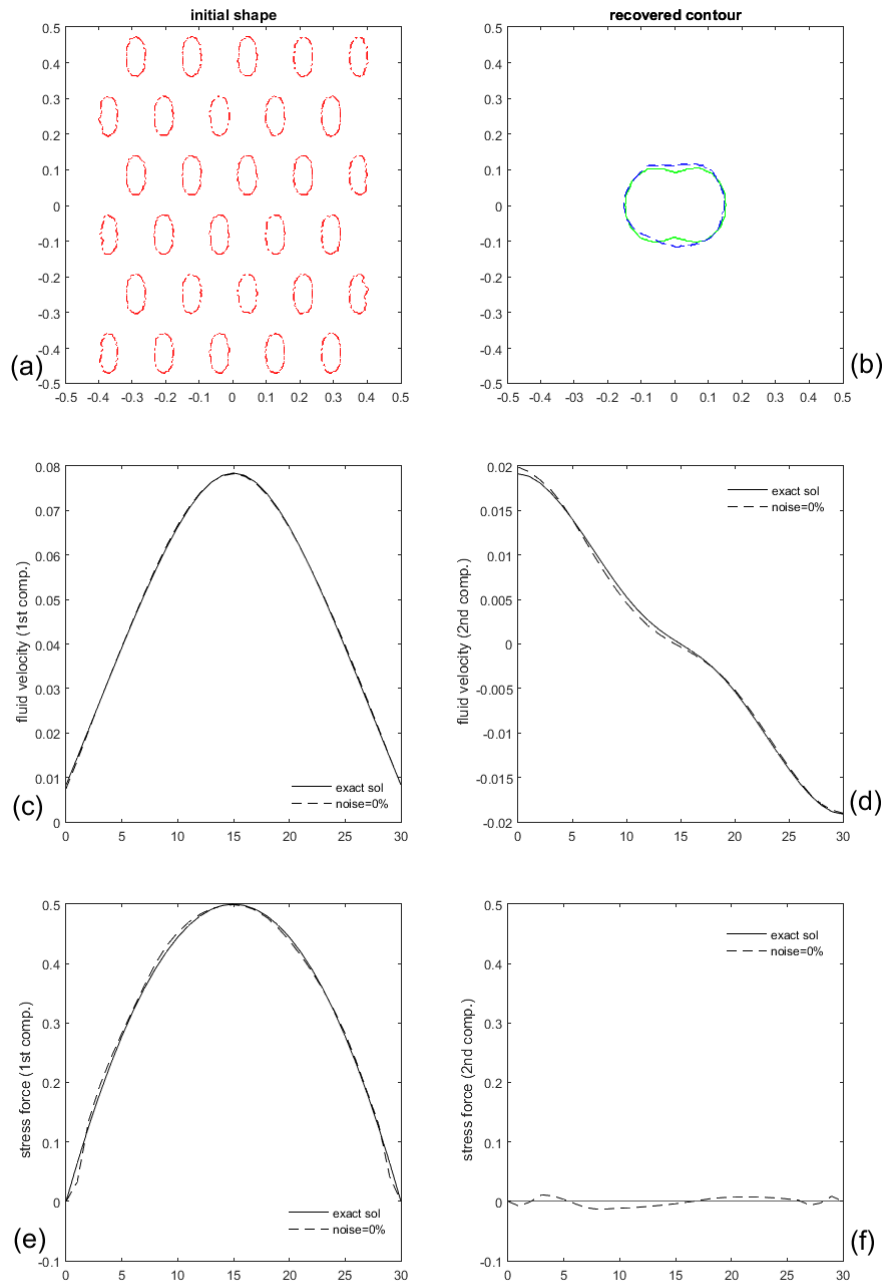


FIGURE 2.8 – Test case B. Reconstruction of the inclusion shape and missing boundary data with noise free Dirichlet data over  $I_c$ . (a) initial contour is  $\phi_2^{(0)}$  (b) exact inclusion shape -green line- and computed one - blue dashed- (c) exact -line- and computed -dashed line- first component of the velocity over  $I_i$  (d) exact -line- and computed -dashed line- second component of the velocity over  $I_i$  (e) exact -line- and computed -dashed line- first component of the normal stress over  $I_i$  (f) exact -line- and computed -dashed line- second component of the normal stress over  $I_i$ .

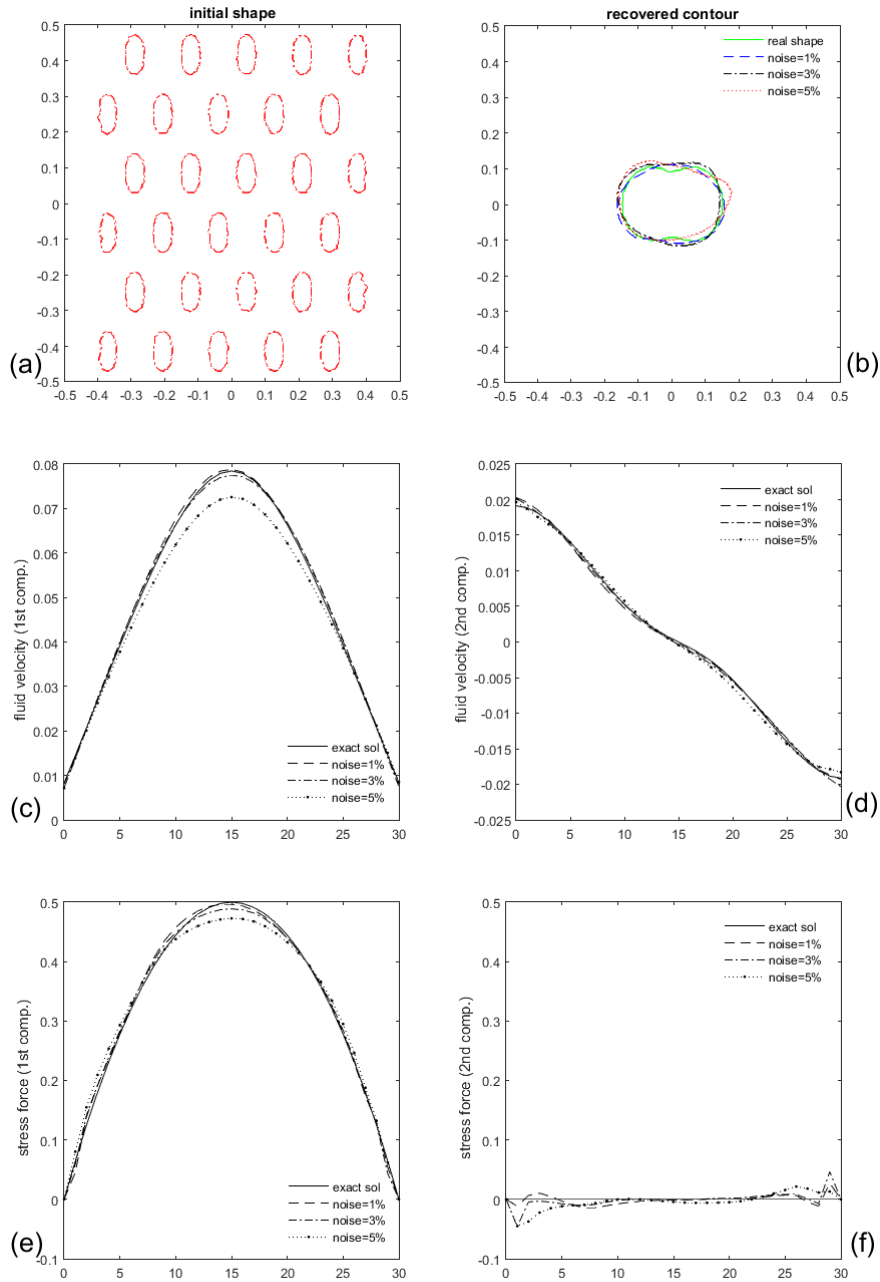


FIGURE 2.9 – Test case B. Reconstruction of the inclusion shape and missing boundary data with noisy Dirichlet data over  $I_c$  with levels  $\sigma = \{1\%, 3\%, 5\%\}$ . (a) initial contour is  $\phi_2^{(0)}$  (b) exact inclusion shape -green line- and computed ones for different noise levels (c) exact and computed first components of the velocity over  $I_i$  (d) exact and computed second components of the velocity over  $I_i$  (e) exact and computed first components of the normal stress over  $I_i$  (f) exact and computed second components of the normal stress over  $I_i$ .

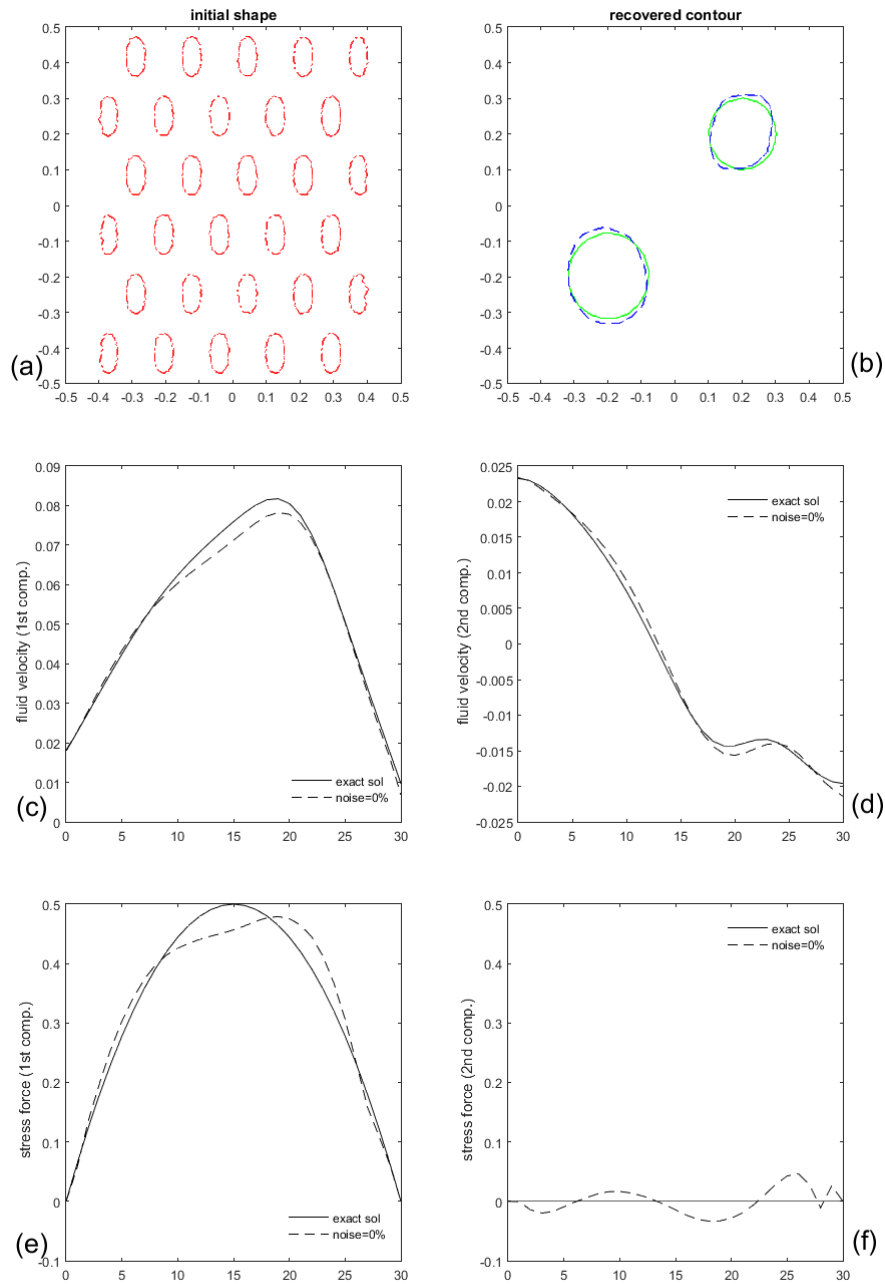


FIGURE 2.10 – Test case C. Reconstruction of the inclusion shape and missing boundary data with noise free Dirichlet data over  $I_c$ . **(a)** initial contour is  $\phi_2^{(0)}$  **(b)** exact inclusion shape -green line- and computed one - blue dashed- **(c)** exact -line- and computed -dashed line- first component of the velocity over  $I_i$  **(d)** exact -line- and computed -dashed line- second component of the velocity over  $I_i$  **(e)** exact -line- and computed -dashed line- first component of the normal stress over  $I_i$  **(f)** exact -line- and computed -dashed line- second component of the normal stress over  $I_i$ .

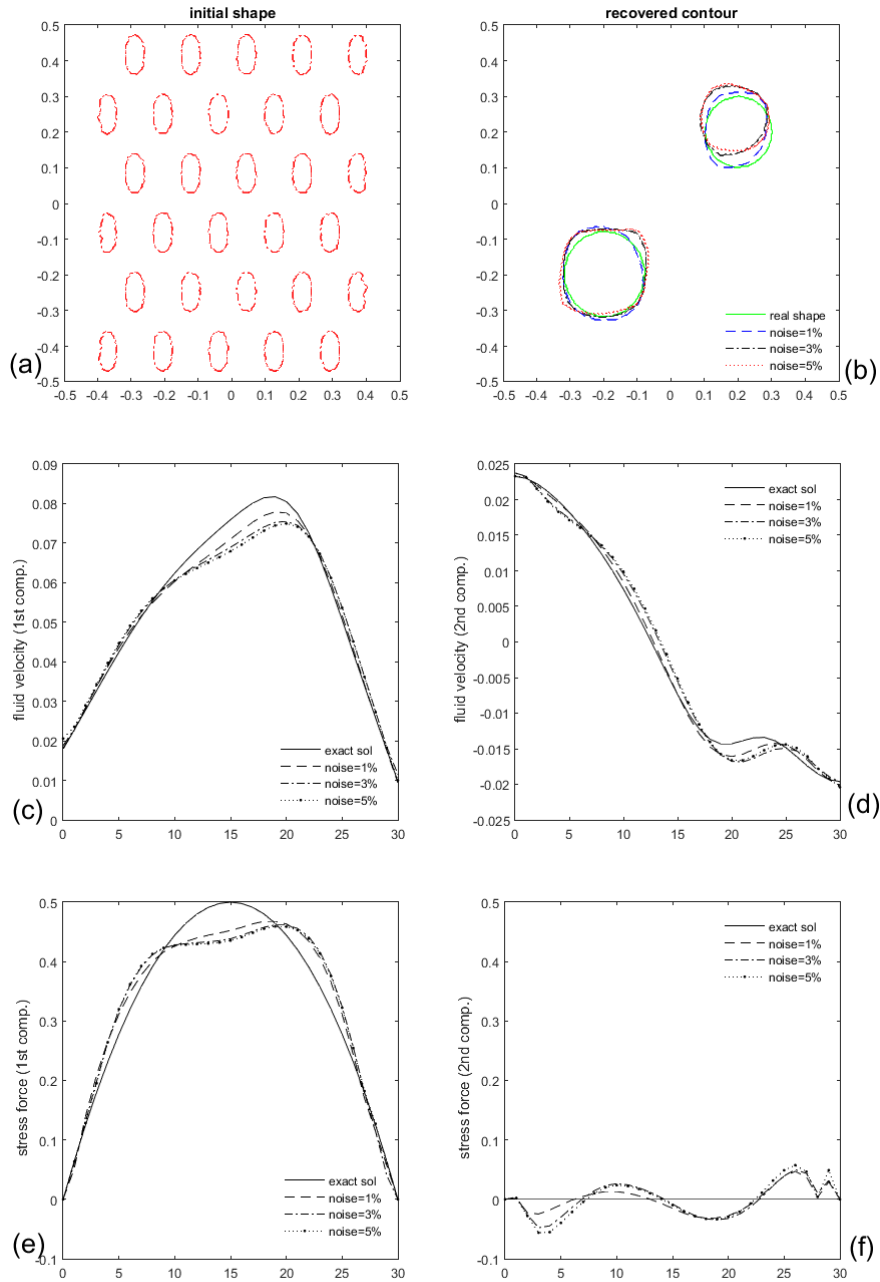


FIGURE 2.11 – Test case C. Reconstruction of the inclusion shape and missing boundary data with noisy Dirichlet data over  $I_c$  with levels  $\sigma = \{1\%, 3\%, 5\%\}$ . (a) initial contour is  $\phi_2^{(0)}$  (b) exact inclusion shape -green line- and computed ones for different noise levels (c) exact and computed first components of the velocity over  $I_i$  (d) exact and computed second components of the velocity over  $I_i$  (e) exact and computed first components of the normal stress over  $I_i$  (f) exact and computed second components of the normal stress over  $I_i$ .

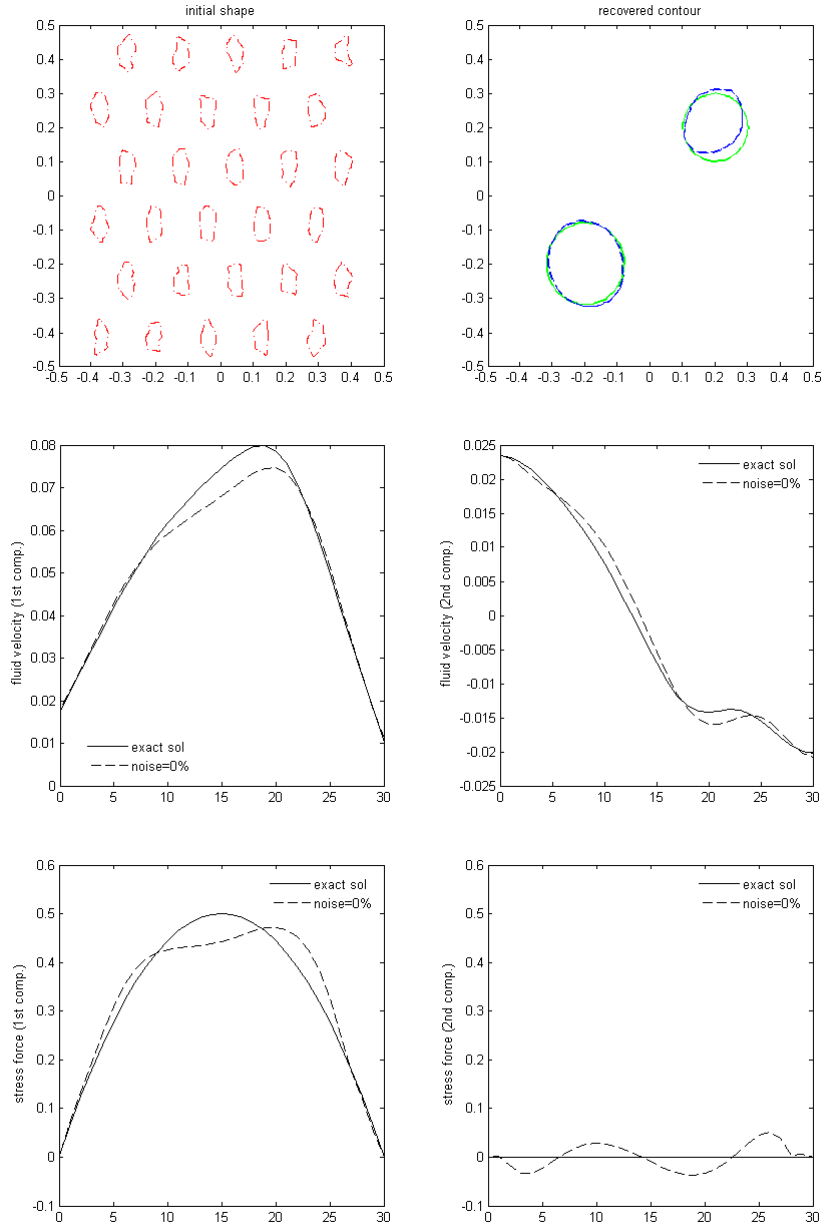


FIGURE 2.12 – Assessing Inverse-Crime-Free reconstruction. Test case C. Top : initial and optimal contour. Middle : the two components of the velocity on  $\Gamma_i$ . Bottom : the two components of the normal stress on  $\Gamma_i$  ( $err_D = 0.0615048$ ,  $err_N = 0.124296$ , and  $err_O = 0.113156$ ).

# Appendix A

## A.1 Proof of proposition 2.2.2.

The Lagrange function  $\mathcal{L}$  is defined as follows :

$$\begin{aligned} \mathcal{L}(\eta, \tau, u_1, p_1, u_2, p_2, v_1, q_1, v_2, q_2, \pi) &= \frac{1}{2} \|u_1 - \tau\|_{H^{\frac{3}{2}}(\Gamma_i)^d}^2 + \frac{1}{2} \|u_2 - f\|_{H^{\frac{3}{2}}(\Gamma_c)^d}^2 \\ &+ \frac{1}{2} \|\sigma(u_1, p_1)n - \Phi\|_{H^{\frac{1}{2}}(\Gamma_c)^d}^2 + \int_{\Omega} \sigma(u_1, p_1) : \nabla v_1 dx - \int_{\Gamma_i} \eta v_1 ds \\ &- \int_{\Omega} q_1 \operatorname{div} u_1 dx + \int_{\Omega} \sigma(u_2, p_2) : \nabla v_2 dx - \int_{\Gamma_c} \Phi v_2 ds - \int_{\Omega} q_2 \operatorname{div} u_2 dx \\ &- \int_{\Gamma_i} \sigma(u_2, p_2) n v_2 ds - \int_{\Gamma_i} \pi (u_2 - \tau) ds \end{aligned}$$

for every  $(\eta, \tau) \in H^{\frac{1}{2}}(\Gamma_i)^d \times H^{\frac{3}{2}}(\Gamma_i)^d$ ,  $(u_1, u_2, v_1, v_2) \in H^2(\Omega)^d \times H^1(\Omega)^d \times H_{\Gamma_c}^1(\Omega) \times H^1(\Omega)^d$ ,  $\pi \in H^{\frac{1}{2}}(\Gamma_i)^d$  and  $(p_1, p_2, q_1, q_2) \in H^1(\Omega)^d \times L^2(\Omega)^3$ .

First, we compute the derivative of  $J_1$  with respect to  $\eta$  in some direction  $\psi \in H^{\frac{1}{2}}(\Gamma_i)^d$ , we have then

$$\frac{\partial J_1}{\partial \eta}(\eta, \tau) \cdot \psi = \int_{\Gamma_c} (\sigma(u_1, p_1)n - \Phi) \sigma(u'_1, p'_1) n ds + \int_{\Gamma_i} (u_1 - \tau) u'_1 ds,$$

where  $u'_1 = \frac{\partial u_1}{\partial \eta} \cdot \psi$  and  $p'_1 = \frac{\partial p_1}{\partial \eta} \cdot \psi$ . We now derive the Lagrangian with respect to  $u_1$  and w.r.t.  $p_1$ , we obtain

$$\begin{aligned} \frac{\partial \mathcal{L}}{\partial u_1} \cdot \gamma &= \int_{\Gamma_c} (\sigma(u_1, p_1)n - \Phi) (\nabla \gamma + \nabla \gamma^T) n ds + \int_{\Gamma_i} (u_1 - \tau) \gamma ds \\ &+ \int_{\Omega} (\nabla \gamma + \nabla \gamma^T) : \nabla v_1 dx - \int_{\Omega} q_1 \operatorname{div} \gamma dx = 0, \quad \forall \gamma \in H_{\Gamma_c}^1(\Omega), \end{aligned} \quad (2.22)$$

$$\frac{\partial \mathcal{L}}{\partial p_1} \cdot \delta = - \int_{\Gamma_c} (\sigma(u_1, p_1)n - \Phi) \delta n ds - \int_{\Omega} \delta \operatorname{div} v_1 dx = 0, \quad \forall \delta \in H^1(\Omega)^d. \quad (2.23)$$

By replacing  $(\gamma, \delta)$  with  $(u'_1, p'_1)$  in (2.22) and (2.23), then by summing them, we get

$$\begin{aligned} &\int_{\Gamma_c} (\sigma(u_1, p_1)n - \Phi) \sigma(u'_1, p'_1) n ds + \int_{\Gamma_i} (u_1 - \tau) u'_1 ds \\ &+ \int_{\Omega} \sigma(u'_1, p'_1) : \nabla v_1 dx - \int_{\Omega} q_1 \operatorname{div} u'_1 dx = 0, \end{aligned}$$

which is equivalent to,

$$\begin{aligned} \int_{\Omega} \sigma(u'_1, p'_1) : \nabla v_1 dx &= - \int_{\Gamma_c} (\sigma(u_1, p_1)n - \Phi) \sigma(u'_1, p'_1) n ds \\ &- \int_{\Gamma_i} (u_1 - \tau) u'_1 ds + \int_{\Omega} q_1 \operatorname{div} u'_1 dx, \end{aligned} \quad (2.24)$$

with  $(u'_1, p'_1)$  solves the following problem

$$\begin{cases} \Delta u'_1 - \nabla p'_1 = 0 & \text{in } \Omega, \\ \operatorname{div} u'_1 = 0 & \text{in } \Omega, \\ u'_1 = 0 & \text{on } \Gamma_c, \\ \sigma(u'_1, p'_1)n = \psi & \text{on } \Gamma_i. \end{cases}$$

The weak formulation associated to this problem is

$$\int_{\Omega} \sigma(u'_1, p'_1) : \nabla \varphi dx = \int_{\Gamma_i} \psi \varphi ds + \int_{\Gamma_c} \sigma(u'_1, p'_1) n \varphi ds, \quad \forall \varphi \in H^1(\Omega)^d,$$

in particular for  $\varphi = v_1$ , we have

$$\int_{\Omega} \sigma(u'_1, p'_1) : \nabla v_1 dx = \int_{\Gamma_i} \psi v_1 ds, \quad \text{because } v_1 \in H^1_{\Gamma_c}(\Omega). \quad (2.25)$$

Now since  $\text{div} u'_1 = 0$  in  $\Omega$ , using (2.24) and (2.25), we find

$$-\int_{\Gamma_c} (\sigma(u_1, p_1) n - \Phi) \sigma(u'_1, p'_1) n ds - \int_{\Gamma_i} (u_1 - \tau) u'_1 ds = \int_{\Gamma_i} \psi v_1 ds,$$

then, we deduce that

$$\frac{\partial J_1}{\partial \eta}(\eta, \tau) \cdot \psi = - \int_{\Gamma_i} \psi v_1 ds,$$

with  $(v_1, q_1)$  solves the adjoint problem

$$\begin{cases} \int_{\Gamma_c} (\sigma(u_1, p_1) n - \Phi) (\nabla \gamma + \nabla \gamma^T) n ds + \int_{\Gamma_i} (u_1 - \tau) \gamma ds \\ \quad + \int_{\Omega} (\nabla \gamma + \nabla \gamma^T) : \nabla v_1 dx - \int_{\Omega} q_1 \text{div} \gamma dx = 0, \quad \forall \gamma \in H^1_{\Gamma_c}(\Omega), \\ - \int_{\Gamma_c} (\sigma(u_1, p_1) n - \Phi) \delta n ds - \int_{\Omega} \delta \text{div} v_1 dx = 0, \quad \forall \delta \in H^1(\Omega)^d. \end{cases}$$

Now we compute the other derivative, the derivative of the cost function  $J_2$  with respect to the variable  $\tau$ . We have,

$$\frac{\partial J_2}{\partial \tau}(\eta, \tau) \cdot \mu = \int_{\Gamma_c} (u_2 - f) u'_2 ds - \int_{\Gamma_i} (u_1 - \tau) \mu ds, \quad (2.26)$$

where  $u'_2 = \frac{\partial u_2}{\partial \tau}$  and  $p'_2 = \frac{\partial p_2}{\partial \tau}$ . Let

$$W_1 = \{v \in H^1(\Omega)^d / v|_{\Gamma_i} = 0\}.$$

We have then,

$$\begin{aligned} \frac{\partial \mathcal{L}}{\partial u_2} \cdot h &= \int_{\Gamma_c} (u_2 - f) h ds + \int_{\Omega} (\nabla h + \nabla h^T) : \nabla v_2 dx \\ &\quad + \int_{\Gamma_i} ((\nabla h + \nabla h^T) n) v_2 ds - \int_{\Omega} q_2 \text{div} h dx = 0, \quad \forall h \in W_1, \end{aligned} \quad (2.27)$$

$$\frac{\partial \mathcal{L}}{\partial p_2} \cdot k = - \int_{\Omega} k \text{div} v_2 dx - \int_{\Gamma_i} k n v_2 ds = 0, \quad \forall k \in L^2(\Omega). \quad (2.28)$$

Using the Green's formula, and summing (2.27) and (2.28), we obtain

$$\begin{aligned} &\int_{\Gamma_c} (u_2 - f) h ds - \int_{\Omega} \text{div}(\nabla v_2 + \nabla v_2^T) h dx + \int_{\Gamma_c} ((\nabla v_2 + \nabla v_2^T) n) h ds \\ &\quad + \int_{\Gamma_i} \sigma(h, k) n v_2 ds + \int_{\Omega} \nabla q_2 h dx - \int_{\Gamma_c} (q_2 n) h ds - \int_{\Omega} k \text{div} v_2 dx = 0. \end{aligned}$$

Therefore, we get for all  $(h, k) \in W_1 \times L^2(\Omega)$ ,

$$-\int_{\Omega} \operatorname{div}(\nabla v_2 + \nabla v_2^T) h dx + \int_{\Omega} \nabla q_2 h dx + \int_{\Gamma_c} ((\sigma(v_2, q_2)n - (f - u_2)) h ds + \int_{\Gamma_i} \sigma(h, k) n v_2 ds - \int_{\Omega} k \operatorname{div} v_2 dx = 0.$$

Finally, from this equality, we deduce the following problem

$$\begin{cases} \Delta v_2 - \nabla q_2 = 0 & \text{in } \Omega, \\ \operatorname{div} v_2 = 0 & \text{in } \Omega, \\ v_2 = 0 & \text{on } \Gamma_i, \\ \sigma(v_2, q_2)n = f - u_2 & \text{on } \Gamma_c. \end{cases}$$

The weak formulation associated to this problem is,

$$-\int_{\Omega} \sigma(v_2, q_2) : \nabla \varphi dx = \int_{\Gamma_c} (f - u_2) \varphi ds + \int_{\Gamma_i} \sigma(v_2, q_2)n \varphi ds, \quad \forall \varphi \in H^1(\Omega).$$

Taking  $\varphi = u'_2$ , we obtain,

$$\int_{\Omega} \sigma(v_2, q_2) : \nabla u'_2 dx = \int_{\Gamma_c} (f - u_2) u'_2 ds + \int_{\Gamma_i} (\sigma(v_2, q_2)n) u'_2 ds, \quad (2.29)$$

with the solution  $(u'_2, q'_2)$  verify

$$\begin{cases} \Delta u'_2 - \nabla p'_2 = 0 & \text{in } \Omega, \\ \operatorname{div} u'_2 = 0 & \text{in } \Omega, \\ u'_2 = \mu & \text{on } \Gamma_i, \\ \sigma(u'_2, p'_2)n = 0 & \text{on } \Gamma_c. \end{cases}$$

The weak formulation associated of this problem is

$$\int_{\Omega} \sigma(u'_2, p'_2) : \nabla \vartheta dx = \int_{\Gamma_i} (\sigma(u'_2, p'_2)n) \vartheta ds, \quad \forall \vartheta \in H^1(\Omega)^d,$$

if we replace  $\vartheta$  by  $v_2$ , we obtain

$$\int_{\Omega} \sigma(u'_2, p'_2) : \nabla v_2 dx = \int_{\Gamma_i} (\sigma(u'_2, p'_2)n) v_2 ds. \quad (2.30)$$

From (2.29) and (2.30), and the boundary condition  $v_2|_{\Gamma_i} = 0$ , we have

$$\int_{\Gamma_c} (u_2 - f) u'_2 ds = \int_{\Gamma_i} (\sigma(v_2, q_2)n) \mu ds.$$

Thus,

$$\frac{\partial J_2}{\partial \tau}(\eta, \tau) \cdot \mu = \int_{\Gamma_i} (\sigma(v_2, q_2)n) \mu ds - \int_{\Gamma_i} (u_1 - \tau) \mu ds, \quad \forall \mu \in H^{\frac{1}{2}}(\Gamma_i)^d.$$



## A.2 Proposition 2.4.1 : Derivation of the sensitivity formula.

For fixed  $(\eta, \tau) \in H^{\frac{1}{2}}(\Gamma_i)^d \times H^{\frac{3}{2}}(\Gamma_i)^d$ , let us define the Lagrangian  $\mathcal{L}'$  by :

$$\begin{aligned} \mathcal{L}'(\phi, \lambda_1, \pi_1, \lambda_2, \pi_2, u_1, p_1, u_2, p_2) &= \int_{\Omega} |\sigma(u_2, p_2) - \sigma(u_1, p_1)|^2 H_{\varepsilon, \beta}(\phi) dx \\ &+ \mu \int_{\Omega} \delta_{\varepsilon, \beta}(\phi) |\nabla \phi| dx + \int_{\Omega} (\sigma(u_1, p_1) : \nabla \lambda_1) H_{\varepsilon, \beta}(\phi) dx - \int_{\Gamma_i} \eta \lambda_1 ds \\ &- \int_{\Omega} \pi_1 \operatorname{div} u_1 H_{\varepsilon, \beta}(\phi) dx + \int_{\Omega} (\sigma(u_2, p_2) : \nabla \lambda_2) H_{\varepsilon, \beta}(\phi) dx - \int_{\Gamma_c} \Phi \lambda_2 ds \\ &- \int_{\Omega} \pi_2 \operatorname{div} u_2 H_{\varepsilon, \beta}(\phi) dx, \end{aligned}$$

where the control  $\phi \in \mathcal{S}$ , the state variables  $(u_1, u_2, p_1, p_2) \in V_f \times W_{\tau} \times L^2(\Omega) \times L^2(\Omega)$ , the adjoint variables  $(\lambda_1, \lambda_2) \in H_{\Gamma_c}^1(\Omega) \times H_{\Gamma_i}^1(\Omega)$  and  $(\pi_1, \pi_2) \in L^2(\Omega) \times L^2(\Omega)$ .

The differentiation of the functional  $\mathcal{J}_3(\eta, \tau; \phi)$  with respect to  $\phi$  in some direction  $\psi \in H^1(\Omega)$  yields

$$\begin{aligned} \frac{\partial \mathcal{J}_3}{\partial \phi}(\eta, \tau; \phi) \cdot \psi &= \int_{\Omega} |\sigma(u_2, p_2) - \sigma(u_1, p_1)|^2 \delta_{\varepsilon, \beta}(\phi) \psi dx \\ &+ 2 \int_{\Omega} (\sigma(u_2, p_2) - \sigma(u_1, p_1)) : (\sigma(u'_2, p'_2) - \sigma(u'_1, p'_1)) H_{\varepsilon, \beta}(\phi) dx \\ &+ \mu \int_{\Omega} \delta'_{\varepsilon, \beta}(\phi) |\nabla \phi| \psi dx + \mu \int_{\Omega} \delta_{\varepsilon, \beta}(\phi) \frac{\nabla \phi \nabla \psi}{|\nabla \phi|} dx, \quad \forall \psi \in H^1(\Omega)^d, \end{aligned} \quad (2.31)$$

where we have used the notations

$$(u'_1, p'_1) = \left( \frac{\partial u_1}{\partial \phi} \psi, \frac{\partial p_1}{\partial \phi} \psi \right) \quad \text{and} \quad (u'_2, p'_2) = \left( \frac{\partial u_2}{\partial \phi} \psi, \frac{\partial p_2}{\partial \phi} \psi \right).$$

We know that  $(u_1, p_1)$  solves the variational equation

$$\int_{\Omega} (\sigma(u_1, p_1) : \nabla v_1) H_{\varepsilon, \beta}(\phi) dx = \int_{\Gamma_i} \eta v_1 ds, \quad \forall v_1 \in H_{\Gamma_c}^1(\Omega).$$

Then,  $(u'_1, p'_1)$  fulfills the following weak formulation

$$\int_{\Omega} (\sigma(u'_1, p'_1) : \nabla v_1) H_{\varepsilon, \beta}(\phi) dx + \int_{\Omega} (\sigma(u_1, p_1) : \nabla v_1) \delta_{\varepsilon, \beta}(\phi) \psi dx = 0, \quad \forall v_1 \in H_{\Gamma_c}^1(\Omega).$$

Now, we derive the Lagrangian  $\mathcal{L}'$  with respect to  $u_1$  and with respect to  $p_1$ , we get

$$\begin{cases} \frac{\partial \mathcal{L}'}{\partial u_1} h_1 = -2 \int_{\Omega} (\nabla h_1 + \nabla h_1^T) : (\sigma(u_2, p_2) - \sigma(u_1, p_1)) H_{\varepsilon, \beta}(\phi) dx \\ \quad + \int_{\Omega} (\nabla h_1 + \nabla h_1^T) : \nabla \lambda_1 H_{\varepsilon, \beta}(\phi) dx - \int_{\Omega} \pi_1 \operatorname{div} h_1 dx = 0, \quad \forall h_1 \in H_{\Gamma_c}^1(\Omega), \\ \frac{\partial \mathcal{L}'}{\partial p_1} k_1 = 2 \int_{\Omega} (k_1 I_d) : (\sigma(u_2, p_2) - \sigma(u_1, p_1)) H_{\varepsilon, \beta}(\phi) dx - \int_{\Omega} k_1 \operatorname{div} \lambda_1 H_{\varepsilon, \beta}(\phi) dx \\ = 0, \quad \forall k_1 \in L^2(\Omega). \end{cases} \quad (2.32)$$

If the pair  $(h_1, k_1)$  is replaced by  $(u'_1, p'_1)$  in (2.32) and because of  $\operatorname{div} u_1 = 0$  implies  $\operatorname{div} u'_1 = 0$ , using the weak formulation for the couple  $(u'_1, p'_1)$ , we get

$$-2 \int_{\Omega} (\sigma(u_2, p_2) - \sigma(u_1, p_1)) : \sigma(u'_1, p'_1) H_{\varepsilon, \beta}(\phi) dx = \int_{\Omega} (\sigma(u_1, p_1) : \nabla \lambda_1) \delta_{\varepsilon, \beta}(\phi) \psi dx, \quad (2.33)$$

where  $(\lambda_1, \pi_1)$  solves the adjoint state problem

$$\left\{ \begin{array}{l} -2 \int_{\Omega} (\sigma(u_2, p_2) - \sigma(u_1, p_1)) : (\nabla h_1 + \nabla h_1^T) H_{\varepsilon, \beta}(\phi) dx - \int_{\Omega} \pi_1 \operatorname{div} h_1 H_{\varepsilon, \beta}(\phi) dx \\ \quad + \int_{\Omega} ((\nabla h_1 + \nabla h_1^T) : \nabla \lambda_1) H_{\varepsilon, \beta}(\phi) dx = 0, \quad \forall h_1 \in H_{L^c}^1(\Omega), \\ 2 \int_{\Omega} (\sigma(u_2, p_2) - \sigma(u_1, p_1)) : (k_1 I_d) H_{\varepsilon, \beta}(\phi) dx - \int_{\Omega} k_1 \operatorname{div} \lambda_1 H_{\varepsilon, \beta}(\phi) dx = 0, \\ \quad \forall k_1 \in L^2(\Omega). \end{array} \right.$$

In the same way, we find that

$$2 \int_{\Omega} (\sigma(u_2, p_2) - \sigma(u_1, p_1)) : \sigma(u'_2, p'_2) H_{\varepsilon, \beta}(\phi) dx = \int_{\Omega} (\sigma(u_2, p_2) : \nabla \lambda_2) \delta_{\varepsilon, \beta}(\phi) \psi dx, \quad (2.34)$$

where  $(\lambda_2, \pi_2)$  solves the adjoint problem

$$\left\{ \begin{array}{l} 2 \int_{\Omega} (\sigma(u_2, p_2) - \sigma(u_1, p_1)) : (\nabla h_2 + \nabla h_2^T) H_{\varepsilon, \beta}(\phi) dx - \int_{\Omega} \pi_2 \operatorname{div} h_2 H_{\varepsilon, \beta}(\phi) dx \\ \quad + \int_{\Omega} ((\nabla h_2 + \nabla h_2^T) : \nabla \lambda_2) H_{\varepsilon, \beta}(\phi) dx = 0, \quad \forall h_2 \in H_{L^i}^1(\Omega), \\ -2 \int_{\Omega} (\sigma(u_2, p_2) - \sigma(u_1, p_1)) : (k_2 I_d) H_{\varepsilon, \beta}(\phi) dx - \int_{\Omega} k_2 \operatorname{div} \lambda_2 H_{\varepsilon, \beta}(\phi) dx = 0, \\ \quad \forall k_2 \in L^2(\Omega). \end{array} \right.$$

Using (2.33) and (2.34), we obtain

$$\begin{aligned} \frac{\partial \mathcal{J}_3}{\partial \phi}(\eta, \tau; \phi) \cdot \psi &= \int_{\Omega} |\sigma(u_2, p_2) - \sigma(u_1, p_1)|^2 \delta_{\varepsilon, \beta}(\phi) \psi dx + \mu \int_{\Omega} \delta'_{\varepsilon, \beta}(\phi) |\nabla \phi| \psi dx \\ &\quad + \mu \int_{\Omega} \delta_{\varepsilon, \beta}(\phi) \frac{\nabla \phi \nabla \psi}{|\nabla \phi|} dx + \int_{\Omega} (\sigma(u_1, p_1) : \nabla \lambda_1) \delta_{\varepsilon, \beta}(\phi) \psi dx \\ &\quad + \int_{\Omega} (\sigma(u_2, p_2) : \nabla \lambda_2) \delta_{\varepsilon, \beta}(\phi) \psi dx. \end{aligned}$$

On the one hand, we have

$$\int_{\Omega} \operatorname{div}(\delta_{\varepsilon, \beta}(\phi) \frac{\nabla \phi}{|\nabla \phi|}) \psi dx = - \int_{\Omega} \delta_{\varepsilon, \beta}(\phi) \frac{\nabla \phi}{|\nabla \phi|} \nabla \psi dx + \int_{\partial \Omega} \frac{\delta_{\varepsilon, \beta}(\phi)}{|\nabla \phi|} \frac{\partial \phi}{\partial n} \psi ds,$$

and on the other hand,

$$\int_{\Omega} \operatorname{div}(\delta_{\varepsilon, \beta}(\phi) \frac{\nabla \phi}{|\nabla \phi|}) \psi dx = \int_{\Omega} \delta'_{\varepsilon, \beta}(\phi) |\nabla \phi| \psi dx + \int_{\Omega} \delta_{\varepsilon, \beta}(\phi) \operatorname{div}(\frac{\nabla \phi}{|\nabla \phi|}) \psi dx.$$

Then, if  $\phi$  satisfies the boundary condition

$$\frac{\delta_{\varepsilon, \beta}(\phi)}{|\nabla \phi|} \frac{\partial \phi}{\partial n} = 0, \quad \text{on } \partial \Omega,$$

one can conclude that

$$\begin{aligned} \frac{\partial \mathcal{J}_3}{\partial \phi}(\eta, \tau; \phi) \cdot \psi &= \int_{\Omega} |\sigma(u_2, p_2) - \sigma(u_1, p_1)|^2 \delta_{\varepsilon, \beta}(\phi) \psi dx \\ &\quad + \int_{\Omega} [\sigma(u_1, p_1) : \nabla \lambda_1 + (\sigma(u_2, p_2) : \nabla \lambda_2)] \delta_{\varepsilon, \beta}(\phi) \psi dx \\ &\quad - \mu \int_{\Omega} \delta_{\varepsilon, \beta}(\phi) \operatorname{div}(\frac{\nabla \phi}{|\nabla \phi|}) \psi dx. \end{aligned}$$

# A Three-player Nash game for point-wise source identification in Cauchy-Stokes problems

*“ As far as the laws of  
mathematics refer to reality,  
they are not certain, and as far  
as they are certain, they do not  
refer to reality. ”*

---

Albert Einstein

**Abstract.** We consider linear steady Stokes flow under the action of a finite number of particles located inside the flow domain. The particles exert point-wise forces on the fluid, and are unknown in number, location and magnitude. We are interested in the determination of these point-wise forces, using only a single pair of partially available Cauchy boundary measurements. The inverse problem then couples two harsh problems : identification of point-wise sources and recovery of missing boundary data. We reformulate it as a three-player Nash game. The first two players aim at recovering the Dirichlet and Neumann missing data, while the third one aims at the point-forces reconstruction of the number, location and magnitude of the point-forces. To illustrate the efficiency and robustness of the proposed algorithm, we finally present several numerical experiments for different geometries and source distribution, including the case of noisy measurements.

**keyword :** Data completion, Point-force detection, Topological sensitivity, Nash game.

The results presented in this chapter lead to the paper :  
A. Habbal, M. Kallel, and M. Ouni. A Three-player Nash game for point-wise source identification in Cauchy-Stokes problems. Submitted.

---

## Contents

---

<b>3.1</b>	<b>Introduction</b>	<b>61</b>
<b>3.2</b>	<b>An identifiability result for the inverse point-forces Cauchy-Stokes problem</b>	<b>63</b>
<b>3.3</b>	<b>A game formulation of the coupled data completion and point-forces identification problems</b>	<b>65</b>
3.3.1	Relaxation step	66
3.3.2	Localization of the source position.	68
	Topological sensitivity method	68
3.3.3	Identification of the source intensity.	73
3.3.4	The three-player Nash algorithm	74
<b>3.4</b>	<b>Numerical experiments</b>	<b>77</b>
<b>3.5</b>	<b>Conclusion</b>	<b>81</b>

---

---

### 3.1 Introduction

Consider a bounded open domain  $\Omega \subset \mathbb{R}^d$  ( $d=2, 3$ ) occupied by an incompressible viscous fluid, with a smooth enough boundary  $\partial\Omega$ . We assume that the fluid flow is under the action of a finite number of point-wise forces  $F$  located inside  $\Omega$ .

The source term  $F$  is assumed to be a linear combination of Dirac distributions accounting for the collection of the point-wise forces :

$$F = \sum_{k=1}^m \lambda_k \delta_{P_k}, \quad (3.1)$$

where  $m$  is the total number of point-wise forces,  $\delta_{P_k}$  denotes the classical Dirac distribution with origin the point  $P_k$ , and  $\lambda_k \in \mathbb{R}^d$  is a constant vector. The parameters  $P_k$  and  $\lambda_k$  stand respectively for the position and the magnitude of the  $k$ th point-wise force.

In this work, we assume that the vectors  $\lambda_k$  are nonzero and that the positions  $P_k$  are well separated and satisfy the following :

$$\begin{aligned} P_k \neq P_{k'}, \quad \forall k \neq k' \text{ and } \lambda_k \neq 0 \quad \forall k, k' \in \{1, \dots, m\}, \\ \text{dist}(P_k, \partial\Omega) \geq d_0 > 0, \quad \forall k \in \{1, \dots, m\}. \end{aligned} \quad (3.2)$$

The Cauchy-Stokes inverse problem consists then in a coupled inverse problem : identification of point-wise sources, and recovery of missing boundary data.

The first inverse problem is a classical point-wise source reconstruction. Namely, from given velocity  $G$  and fluid stress forces  $\Phi$  prescribed on  $\Gamma_c$ , where  $\Gamma_c$  is a part of the boundary  $\partial\Omega$ , one has to identify the unknown source-term  $F^*$ , that is, to find the number, the location and the magnitude of these point-wise forces such that the fluid velocity  $u$  and the pressure  $p$  are solution of the following Stokes problem :

$$(\mathcal{CS}) \left\{ \begin{array}{ll} -\text{div}(\sigma(u, p)) = F^* & \text{in } \Omega, \\ \text{div} u = 0 & \text{in } \Omega, \\ u = G & \text{on } \Gamma_c, \\ \sigma(u, p)n = \Phi & \text{on } \Gamma_c, \end{array} \right.$$

where  $n$  is the unit outward normal vector on the boundary, and  $\sigma(u, p)$  the fluid stress tensor defined as follows :

$$\sigma(u, p) = -pI_d + 2\nu D(u)$$

with  $D(u) = \frac{1}{2}(\nabla u + \nabla u^T)$  being the linear strain tensor,  $I_d$  denotes the  $d \times d$  identity matrix and  $\nu > 0$  is a viscosity coefficient that remains constant for all values of applied shear stress. For simplicity and without loss of generality, from now on, the viscosity to be equal unity.

Additionally to the inverse problem of detecting the unknown point-wise sources, one has to complete the boundary data, that is to recover the missing traces of the velocity  $u$  and of the normal stress  $\sigma(u, p).n$  over  $\Gamma_i$ , the inaccessible part of the boundary. This inverse problem is of Cauchy type, a family of problems known to be severely ill-posed in the sense of Hadamard [59], even regardless of the point-wise force identification, because the existence of solution is not guaranteed for arbitrary Cauchy data and depends on their *compatibility*, and even if a solution exists, it is unstable

---

with respect to small perturbations of the Cauchy data.

For the Cauchy problem, there exists a prolific dedicated literature. An excerpt of popular approaches are the least-square penalty techniques, as used in [48] and in the earlier paper [50], Tikhonov regularization methods [38], quasi reversibility methods [28], alternating iterative methods [72, 63] and control type methods [10, 2]. Recently, an approach based on game theory, using decentralized strategies, was proposed in [56]. The same approach has been investigated in [36] for the solution of coupled conductivity identification and data completion in cardiac electrophysiology, and in [57] to solve the problem of detecting unknown cavities immersed in a stationary viscous fluid using partial boundary measurements.

The point-wise force identification for the Stokes system was, in contrast, paid much less attention. The authors in [7] introduced an approach based on considering a reciprocity gap functional for *Stokeslets* located outside  $\Omega$ . In [49], the authors proposed to detect the point-force locations by minimizing tracking (a difference to a distributed state known all over  $\Omega$ ) and energy functionals. Their algorithm is based on a relaxation technique and on topological sensitivity analysis. We shall follow the same lines for the source identification algorithmic part of our coupled inverse problem. To the best of our knowledge, there are no papers which address algorithmic aspects in solving the present coupled point-wise source identification and boundary data recovery problems for the steady Stokes flows. The paper [78] addresses the coupled inverse problem of identifying wells and recovering boundary data, but with the help of a number of interior measurements. We can also mention an ancient work made by El Badia and Ha-Duong [44] for an inverse source problem for elliptic equations. Its application aims to identify electrostatic dipoles in the human head where the boundary data are generated via electrodes placed on the head's part. The authors give a uniqueness result and an algebraic method for computing the number of dipoles and their characteristics.

The paper is organized as follows. In section 2, we introduce the identifiability problem for the Cauchy-Stokes case, and we provide an identifiability result. Then, using a relaxed formulation in section 3, we formulate a Nash game approach to tackle the coupled problem of detecting the unknown point-forces and recovering the missing boundary data. A topological sensitivity analysis method is used in order to determine the optimal location of the point-sources. We present what we think is a fairly new algorithm. Optimization (sub)tasks are performed by means of descend methods, so *ad hoc* adjoint state methods are provided to compute the gradients.

Finally, Section 4 illustrates the efficiency and robustness of the proposed overall method, where different numerical experiments are presented and discussed. We end paper by a short concluding section.

**Some notation :** Let  $\Omega$  be a bounded domain in  $\mathbb{R}^d$ , with Lipschitz boundary  $\partial\Omega$ . Let  $I_c$  be an open part of  $\partial\Omega$  and we put  $I_i = \partial\Omega \setminus I_c$ . For any subset  $\Gamma = I_c$  or  $I_i$ , the space of function in  $H^1(\Omega)$  vanishing on  $\Gamma$  is denoted by  $H^1_\Gamma(\Omega)$ . By  $H^{\frac{1}{2}}(\Gamma)$ , we denote the space of traces of functions of  $H^1(\Omega)$  over  $\Gamma$ . Furthermore, we will use the special space  $H^{\frac{1}{2}}_{00}(\Gamma)$ , which consists of functions from  $H^{\frac{1}{2}}(\Gamma)$  vanishing on  $\partial\Omega \setminus \Gamma$ . This is a subspace of  $H^{\frac{1}{2}}(\Gamma)$  and its dual space is then denoted by  $(H^{\frac{1}{2}}_{00}(\Gamma))'$ .

## 3.2 An identifiability result for the inverse point-forces Cauchy-Stokes problem

The source identifiability problem amounts to ask whether a unique pair of over specified boundary data, for instance the Cauchy data  $(G, \Phi)$ , could reconstruct a unique source, and if not, how much of such pairs is necessary to a unique reconstruction.

Our identifiability result is given by the following theorem :

**Theorem 3.2.1** *Let be  $\Omega \subset \mathbb{R}^d$  an open bounded Lipschitz domain and  $\Gamma_c$  a non-empty open subset of the boundary  $\partial\Omega$ . Consider two point-wise source terms  $F_1$  and  $F_2$  of the form (3.1), whose magnitudes and locations satisfy the requirements stated in (3.2).*

*For  $i = 1, 2$ , let be  $(u_i, p_i)$  the solution of the following :*

$$\left\{ \begin{array}{ll} -\operatorname{div}(\sigma(u_i, p_i)) & = F_i \quad \text{in } \Omega, \\ \operatorname{div} u_i & = 0 \quad \text{in } \Omega, \\ u_i & = G \quad \text{on } \Gamma_c, \\ \sigma(u_i, p_i)n & = \Phi \quad \text{on } \Gamma_c. \end{array} \right. \quad (3.3)$$

where the Cauchy data  $(G, \Phi) \in H^{\frac{1}{2}}(\Gamma_c)^d \times (H_{00}^{\frac{1}{2}}(\Gamma_c)^d)'$  are assumed to be compatible for the two Cauchy-Stokes problems. Then  $F_1 = F_2$ , that is,

$$m_1 = m_2 = m, \quad \{(\lambda_{k,1}, P_{k,1}), 1 \leq k \leq m\} = \{(\lambda_{k',2}, P_{k',2}), 1 \leq k' \leq m\}.$$

*Proof :* An identifiability result is proved for the Dirac-Stokes problem in [7] using the reciprocity gap. In our general framework, proofs of identifiability usually follow the same classical steps by properly using the unique continuation property, notably for second order elliptic PDES. We follow the same lines, with slight adaption to our Cauchy-Stokes problem.

Let  $(u_i, p_i)$ ,  $i=1,2$  be solutions to the system (3.3), and we define  $(v, q) = (u_1 - u_2, p_1 - p_2)$  and  $F = F_1 - F_2$ , where

$$F = \sum_{k=1}^{m_1} \lambda_{k,1} \delta_{P_{k,1}} - \sum_{k'=1}^{m_2} \lambda_{k',2} \delta_{P_{k',2}}, \quad \forall k, k' = 1, \dots, m_i \text{ and } i = 1, 2.$$

It is straightforward to see that  $(v, q)$  is a solution of

$$(\mathcal{P}) \left\{ \begin{array}{ll} -\operatorname{div}(\sigma(v, q)) & = F \quad \text{in } \Omega, \\ \operatorname{div} v & = 0 \quad \text{in } \Omega, \\ v & = 0 \quad \text{on } \Gamma_c, \\ \sigma(v, q)n & = 0 \quad \text{on } \Gamma_c. \end{array} \right.$$

Consider  $(\mathcal{B}_{k,i})_{k=1, \dots, m_i}$  for  $i = 1, 2$ , a family of open balls such that

$$0 < \epsilon \ll 1, \quad \mathcal{B}_{k,i} = B(P_{k,i}, \epsilon) \subset \Omega, \quad \text{and } \mathcal{B}_{k,i} \cap \mathcal{B}_{k',i} = \emptyset, \text{ if } k \neq k'. \quad (3.4)$$

Thus  $F$  vanishes as restricted to  $\Omega_H = \Omega \setminus ((\cup_{k=1}^{m_1} \mathcal{B}_{k,1}) \cup (\cup_{k'=1}^{m_2} \mathcal{B}_{k',2}))$ .

From the unique continuation theorem for the steady Stokes equation established in [47], we obtain  $v = 0$  and  $q = 0$  in  $\Omega_H$ . Let us suppose that  $m_1 > m_2$ , and as the

positions  $P_k$  are well separated and satisfy (3.2), then there exists a source  $P_{m_0,1} \neq P_{k',2}$ ,  $k' = 1, \dots, m_2$ , and we define  $\Omega_0 = \Omega \setminus ((\cup_{k \neq m_0} \mathcal{B}_{k,1}) \cup (\cup_{k'=1}^{m_2} \mathcal{B}_{k',2}))$  with  $k = 1, \dots, m_1$ . We denote  $\mathcal{O} = \mathcal{B}_{m_0,1} \subset \Omega$ . Thus, the solution  $(v, q)$  of the problem  $(\mathcal{P})$ , which is null in  $\Omega_0 \setminus \mathcal{O}$ , satisfies the following system in  $\mathcal{O}$ ;

$$\begin{cases} -\operatorname{div}(\sigma(v, q)) = \lambda_{m_0,1} \delta_{P_{m_0,1}} & \text{in } \mathcal{O}, \\ \operatorname{div} v = 0 & \text{in } \mathcal{O}, \\ v = 0 & \text{on } \partial\mathcal{O}. \end{cases} \quad (3.5)$$

Let us consider now the solution  $(v_s, q_s)$  that satisfies :

$$\begin{cases} -\operatorname{div}(\sigma(v_s, q_s)) = \lambda_{m_0,1} \delta_{P_{m_0,1}} & \text{in } \mathbb{R}^d, \\ \operatorname{div} v_s = 0 & \text{in } \mathbb{R}^d, \end{cases}$$

and  $(v_r, q_r)$  which solves

$$\begin{cases} -\operatorname{div}(\sigma(v_r, q_r)) = 0 & \text{in } \mathcal{O}, \\ \operatorname{div} v_r = 0 & \text{in } \mathcal{O}, \\ v_r = -v_s & \text{on } \partial\mathcal{O}. \end{cases}$$

Thus, the solution  $(v_s, q_s)$  is given by

$$(v_s, q_s) = (U * (\lambda_{m_0,1} \delta_{P_{m_0,1}}), P * (\lambda_{m_0,1} \delta_{P_{m_0,1}})) = (U(\cdot - P_{m_0,1}) \cdot \lambda_{m_0,1}, P(\cdot - P_{m_0,1}) \cdot \lambda_{m_0,1}),$$

where the pair  $(U, P)$  is the fundamental solution of the Stokes equation. It is given (see e.g. [7]), for  $d = 2$ , by

$$\begin{cases} U_{ij}(x) = \frac{1}{4\pi\nu} \left( \delta_{ij} \log\left(\frac{1}{|x|}\right) + \frac{x_i x_j}{|x|^2} \right), \quad i, j = 1, 2 \\ P_i(x) = \frac{1}{2\pi} \frac{x_i}{|x|^2}, \quad i = 1, 2 \end{cases}$$

and, for  $d = 3$ ,

$$\begin{cases} U_{ij}(x) = \frac{1}{8\pi\nu} \left( \delta_{ij} \left( \frac{1}{|x|} \right) + \frac{x_i x_j}{|x|^3} \right), \quad i, j = 1, 2, 3 \\ P_i(x) = \frac{1}{4\pi} \frac{x_i}{|x|^3}, \quad i = 1, 2, 3. \end{cases}$$

Then, we can deduce that the solution  $(v, q)$  of the problem  $(\mathcal{P})$ , and which satisfies (3.5), can be written  $(v, q) = (v_r + v_s, q_r + q_s)$  in  $\mathcal{O}$ . Besides, we have  $(v_s, q_s)$  is an analytic solution in  $\mathcal{O} \setminus P_{m_0,1}$ , implies that  $v_s$  is analytic on the boundary of  $\mathcal{O}$ , then  $v_r$  is an analytic function in  $\mathcal{O} \setminus P_{m_0,1}$ . Therefore, the fluid velocity  $v$ , which is null in  $\Omega_0 \setminus \mathcal{O}$ , is an analytic function in  $\mathcal{O} \setminus P_{m_0,1}$ . This would imply that  $\lambda_{m_0,1} = 0$ , which by assumption is impossible.

We proceed analogously, for the case  $m_2 > m_1$ . Thus,  $m = m_1 = m_2$ .

Now, let us suppose

$$\{P_{1,1}, \dots, P_{m,1}\} \neq \{P_{1,2}, \dots, P_{m,2}\},$$



and we assume that  $\mathcal{O}$  is a subset of  $\Omega$  such that  $\{\cup_{k=1}^m (P_{k,1} \cup P_{k,2})\} \in \mathcal{O}$ . In the same way, we deduce that the solution  $v$  is an analytic function in  $\mathcal{O} \setminus \{\cup_{k=1}^m (P_{k,1} \cup P_{k,2})\}$ , which is null in  $\Omega \setminus \mathcal{O}$ , and by application of the unique continuation property we conclude that  $v$  equal to zero in  $\mathcal{O}$ , that is,

$$\sum_{k=1}^m (\lambda_{k,1} \delta_{P_{k,1}} - \lambda_{k,2} \delta_{P_{k,2}}) = 0 \text{ in } \mathcal{O},$$

such that  $\lambda_{k,i} \neq 0$  for  $k = 1, \dots, m_1$  and  $i=1,2$ . Therefore, there exists a unique permutation  $\pi$  of the entries such that,

$$P_{k,1} = P_{\pi(k),2}, \forall k = \{1, \dots, m\}.$$

Finally, we conclude that  $F = \sum_{k=1}^m (\lambda_{k,1} - \lambda_{\pi(k),2}) \delta_{P_{k,2}}$ . Using the same arguments, we obtain  $\lambda_{k,1} = \lambda_{\pi(k),2}$ , with  $i=1,2$  and  $k = 1, \dots, m$ . ■

### 3.3 A game formulation of the coupled data completion and point-forces identification problems

The present section aims to introduce a new algorithm based on the game-theoretic approach to solving our coupled inverse problem of data completion and source identification. As the source term  $F$  belongs to  $H^s(\Omega)^d$  with  $s < -1$  for  $d = 2$  or  $s < -3/2$  for  $d = 3$ , one thus thinks of describing the two-dimensional case, although the presented method here can properly be applied to the 3-D case. A three-dimensional experiment is provided to illustrate the algorithm's efficiency and stability in section 4.

With the previous notations, let be  $G \in H^{\frac{1}{2}}(\Gamma_c)^2$  and  $\Phi \in (H_{00}^{\frac{1}{2}}(\Gamma_c)^2)'$  given Cauchy data. We recall that the inverse source-term problem amounts to find a collection of point-wise sources  $F^* \in H^s(\Omega)^2$  for  $s < -1$  such that the fluid velocity  $u$  and the pressure  $p$  are solution to the following Cauchy-Stokes problem :

$$(\mathcal{CS}) \begin{cases} -\operatorname{div}(\sigma(u, p)) = F^* & \text{in } \Omega, \\ \operatorname{div} u = 0 & \text{in } \Omega, \\ u = G & \text{on } \Gamma_c, \\ \sigma(u, p)n = \Phi & \text{on } \Gamma_c. \end{cases}$$

For any given  $\eta \in (H_{00}^{\frac{1}{2}}(\Gamma_i)^2)'$ ,  $\tau \in H^{\frac{1}{2}}(\Gamma_i)^2$  and  $F \in H^s(\Omega)^2$  for  $s < -1$ , we define the states  $(u_1, p_1) = (u_1(\eta, F), p_1(\eta, F)) \in L^2(\Omega)^2 \times L^2(\Omega)$  and  $(u_2, p_2) = (u_2(\tau, F), p_2(\tau, F)) \in L^2(\Omega)^2 \times L^2(\Omega)$  as the unique solution of the following Stokes mixed boundary value problem  $(\mathcal{P}_1)$  and  $(\mathcal{P}_2)$ ,

$$(\mathcal{P}_1) \begin{cases} -\operatorname{div}(\sigma(u_1, p_1)) = F & \text{in } \Omega, \\ \operatorname{div} u_1 = 0 & \text{in } \Omega, \\ u_1 = G & \text{on } \Gamma_c, \\ \sigma(u_1, p_1)n = \eta & \text{on } \Gamma_i, \end{cases} \quad (\mathcal{P}_2) \begin{cases} -\operatorname{div}(\sigma(u_2, p_2)) = F & \text{in } \Omega, \\ \operatorname{div} u_2 = 0 & \text{in } \Omega, \\ u_2 = \tau & \text{on } \Gamma_i, \\ \sigma(u_2, p_2)n = \Phi & \text{on } \Gamma_c. \end{cases}$$

The proof of the existence and uniqueness of the solutions to  $(\mathcal{P}_1)$  and  $(\mathcal{P}_2)$ , can be easily adapted from the proof given in [49] for the Dirichlet type boundary condition.

Since the source  $F$  given by (3.1) belongs to Hilbert space  $H^s(\Omega)^2$  with  $s < -1$ , a classical formulation of the problems  $(\mathcal{P}_1)$  and  $(\mathcal{P}_2)$ , well adapted to standard finite elements analysis is not possible. Nevertheless, to overcome this difficulty, we recourse to a relaxation technique, which consists in approximating the point-force support  $P_k$  by a small region, we could also use a subtraction method [7].

### 3.3.1 Relaxation step

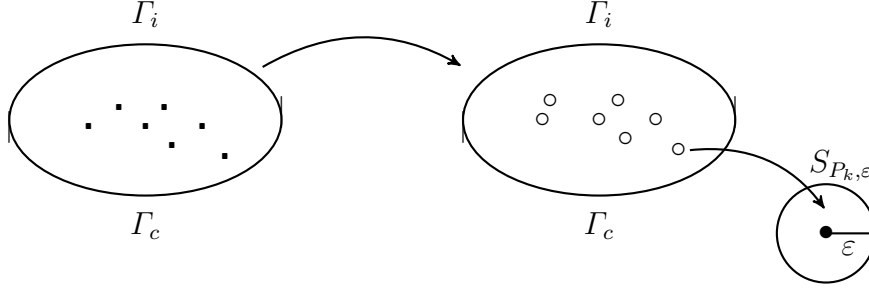


FIGURE 3.1 – Relaxation step

We consider the classical approximation of a Dirac function at a points  $P = \{P_1, \dots, P_m\}$  by the characteristic function of a small ball centred at  $P$  divided by its volume. Thus, instead of the source term  $F$  given by (3.1), we consider the following :

$$F_\epsilon = \sum_{k=1}^m \frac{\lambda_k}{|\mathcal{S}_{P_k, \epsilon}|} \chi_{\mathcal{S}_{P_k, \epsilon}}$$

where  $\chi_{\mathcal{S}_{P_k, \epsilon}}$  denotes the characteristic function of the ball  $\mathcal{S}_{P_k, \epsilon} = P_k + \epsilon\omega_k$ , with  $\epsilon > 0$  is small enough and  $\omega_k$  is bounded and smooth domain containing the origin. As the positions  $P_k$  are well separated and satisfy (3.2), we can suppose then that the region  $\mathcal{S}_{P_k, \epsilon}$  also do not intersect,

$$\mathcal{S}_{P_k, \epsilon} \cap \mathcal{S}_{P_{k'}, \epsilon} = \emptyset \text{ if } k \neq k'. \quad (3.6)$$

The set of admissible source term  $\mathcal{D}_{\text{ad}}$  is defined by :

$$\mathcal{D}_{\text{ad}} = \left\{ f \in L^2(\Omega); f = \sum_{k=1}^p \beta_k \chi_{\mathcal{S}_{z_k, \epsilon}}, \text{ such that } \mathcal{S}_{z_k, \epsilon} \subset \subset \Omega \right\}.$$

Problems  $(\mathcal{P}_1)$  and  $(\mathcal{P}_2)$  are then rephrased in terms of this more regular source term. Let  $(u_{1, \epsilon}, p_{1, \epsilon}) \in H^1(\Omega)^2 \times L^2(\Omega)$  and  $(u_{2, \epsilon}, p_{2, \epsilon}) \in H^1(\Omega)^2 \times L^2(\Omega)$  be the unique solutions of the respective relaxed BVPs  $(\mathcal{P}_{1, \epsilon})$  and  $(\mathcal{P}_{2, \epsilon})$ ,

$$\begin{aligned} (\mathcal{P}_{1, \epsilon}) \left\{ \begin{array}{ll} -\text{div}(\sigma(u_{1, \epsilon}, p_{1, \epsilon})) = F_\epsilon & \text{in } \Omega, \\ \text{div} u_{1, \epsilon} = 0 & \text{in } \Omega, \\ u_{1, \epsilon} = G & \text{on } \Gamma_c, \\ \sigma(u_{1, \epsilon}, p_{1, \epsilon})n = \eta & \text{on } \Gamma_i, \end{array} \right. \\ (\mathcal{P}_{2, \epsilon}) \left\{ \begin{array}{ll} -\text{div}(\sigma(u_{2, \epsilon}, p_{2, \epsilon})) = F_\epsilon & \text{in } \Omega, \\ \text{div} u_{2, \epsilon} = 0 & \text{in } \Omega, \\ \sigma(u_{2, \epsilon}, p_{2, \epsilon})n = \Phi & \text{on } \Gamma_c, \\ u_{2, \epsilon} = \tau & \text{on } \Gamma_i, \end{array} \right. \end{aligned}$$

where

$$F_\epsilon = \sum_{k=1}^m \frac{\lambda_k}{|\mathcal{S}_{P_k, \epsilon}|} \chi_{\mathcal{S}_{P_k, \epsilon}} \in \mathcal{D}_{\text{ad}} \quad (3.7)$$

is more regular source term, with  $\chi_{\mathcal{S}_{P_k, \epsilon}}$  is the characteristic function of the unknown region  $\mathcal{S}_{P_k, \epsilon}$ .

**Remark 3.3.1** *The existence and uniqueness of the solutions  $(\mathcal{P}_{1, \epsilon})$  and  $(\mathcal{P}_{2, \epsilon})$ , can be derived from the general theory on existence of solutions to the incompressible steady state Stokes equations, which can be found e.g. in [95, 40]; See also [22] which is suitable to the Stokes framework of the present paper. Moreover, the solutions  $(u_{1, \epsilon}, p_{1, \epsilon})$  and  $(u_{2, \epsilon}, p_{2, \epsilon})$  converge to the respective solutions  $(u_1, p_1)$  and  $(u_2, p_2)$  with the parameter  $\epsilon$ , the proof of this result can be handled by applying the same technique as in [49].*

Let  $\mathcal{I}_{\text{ad}} = \{(m; \lambda, P) \in \mathbb{N}^* \times \mathbb{R}^{2m} \times \Omega^m\}$ . Let  $\phi = (m; (\lambda_k, P_k)_{1 \leq k \leq m}) \in \mathcal{I}_{\text{ad}}$  be a source configuration corresponding to a source  $F$  of the form (1). Let us introduce the following three cost functionals :

$$\mathcal{J}_1(\eta, \tau; \phi) = \frac{1}{2} \|\sigma(u_{1, \epsilon}, p_{1, \epsilon})n - \Phi\|_{(H_{00}^{\frac{1}{2}}(\Gamma_c)^2)'}^2 + \frac{\alpha}{2} \|u_{1, \epsilon} - u_{2, \epsilon}\|_{H^{\frac{1}{2}}(\Gamma_i)^2}^2, \quad (3.8)$$

$$\mathcal{J}_2(\eta, \tau; \phi) = \frac{1}{2} \|u_{2, \epsilon} - G\|_{H^{\frac{1}{2}}(\Gamma_c)^2}^2 + \frac{\alpha}{2} \|u_{1, \epsilon} - u_{2, \epsilon}\|_{H^{\frac{1}{2}}(\Gamma_i)^2}^2, \quad (3.9)$$

$$\mathcal{J}_3(\eta, \tau; \phi) = \|\sigma(u_{1, \epsilon}, p_{1, \epsilon}) - \sigma(u_{2, \epsilon}, p_{2, \epsilon})\|_{L^2(\Omega)^2}^2, \quad (3.10)$$

where  $\alpha$  is given positive parameter (e.g.  $\alpha = 1$ ). Player (1) controls the strategy variable  $\eta \in (H_{00}^{\frac{1}{2}}(\Gamma_i)^2)'$  and aims at minimizing the cost  $\mathcal{J}_1$  and Player (2) controls the strategy variable  $\tau \in H^{\frac{1}{2}}(\Gamma_i)^2$  and aims at minimizing the cost  $\mathcal{J}_2$  : they are given Dirichlet (resp. Neumann) data and try to minimize the gap with the Neumann (resp. Dirichlet) remaining condition. The player (3) controls the strategy variable  $\phi \in \mathcal{I}_{\text{ad}}$  and aims at minimizing the Kohn-Vogelius type functional  $\mathcal{J}_3$ .

**Definition 3.3.1** *A triplet  $(\eta_N, \tau_N, \phi_N) \in (H_{00}^{\frac{1}{2}}(\Gamma_i)^2)' \times H^{\frac{1}{2}}(\Gamma_i)^2 \times \mathcal{I}_{\text{ad}}$  is a Nash equilibrium for the three players game if the following holds :*

$$\begin{cases} \mathcal{J}_1(\eta_N, \tau_N; \phi_N) \leq \mathcal{J}_1(\eta, \tau_N, \phi_N), & \forall \eta \in (H_{00}^{\frac{1}{2}}(\Gamma_i)^2)', \\ \mathcal{J}_2(\eta_N, \tau_N; \phi_N) \leq \mathcal{J}_2(\eta_N, \tau, \phi_N), & \forall \tau \in H^{\frac{1}{2}}(\Gamma_i)^2, \\ \mathcal{J}_3(\eta_N, \tau_N; \phi_N) \leq \mathcal{J}_3(\eta_N, \tau_N, \phi), & \forall \phi \in \mathcal{I}_{\text{ad}}. \end{cases} \quad (3.11)$$

The player 3 in charge of the inverse source-term problem has as a strategy  $\phi = (m; (\lambda_k, P_k)_{1 \leq k \leq m})$ , which is a solution of the following optimization problem,

$$\min_{\phi \in \mathcal{I}_{\text{ad}}} \mathcal{J}_3(\eta, \tau; \phi), \quad \text{when } (\eta, \tau) \in (H_{00}^{\frac{1}{2}}(\Gamma_i)^2)' \times H^{\frac{1}{2}}(\Gamma_i)^2.$$

In the following, the player (3) will play in two steps in order to determine the elements defining the source  $F$  introduced in (3.1); a first step enables to localize the source position  $P = \{P_1, \dots, P_m\}$ , or in other words after this relaxation step, the support of  $\mathcal{S} = \cup_{k=1}^m \mathcal{S}_{k, \epsilon}$ . Then, a second step uses the determined source position and compute the approximate value of the source intensity  $\Lambda = \{\lambda_1, \dots, \lambda_m\}$ .

### 3.3.2 Localization of the source position.

Here, the player (3) focuses on identifying the optimal location of the source-term with respect to the assumption (3.6). Therefore, the minimization problem of  $\mathcal{J}_3$  w.r.t.  $P$  can be formulated as a topological optimization one. Thus, the unknown region  $\mathcal{S}$  can be characterized as the solution to the following topological optimization problem, for fixed  $(\eta, \tau, \Lambda) \in (H_{00}^{\frac{1}{2}}(I_i)^2)' \times H^{\frac{1}{2}}(I_i)^2 \times \mathbb{R}^{2m}$ ,

$$\left\{ \begin{array}{l} \text{Find } \mathcal{S}^* = \cup_{k=1}^m \mathcal{S}_{P_k, \epsilon} \subset \Omega, \text{ such that} \\ \mathcal{S}^* = \arg \min_{\mathcal{S} \subset \Omega} \left\{ \mathcal{J}(\mathcal{S}) := \int_{\Omega} |\sigma(u_{1, \epsilon}, p_{1, \epsilon}) - \sigma(u_{2, \epsilon}, p_{2, \epsilon})|^2 dx \right\}, \end{array} \right.$$

where  $(u_{1, \epsilon}, p_{1, \epsilon})$  and  $(u_{2, \epsilon}, p_{2, \epsilon})$  are the solutions to respectively  $(\mathcal{P}_{1, \epsilon})$  and  $(\mathcal{P}_{2, \epsilon})$ . In order to solve this problem, we shall use a topological sensitivity analysis method. The concept of the topological derivative was proposed by Schumacher [45] in the case of compliance minimization. Next, Sokolowski et al. [91] extended it to more general shape functionals. It has been widely applied in literature for arbitrarily shaped perturbations and a general class of cost functionals related to PDEs. It consists in studying the variation of the cost function with respect to small perturbations of the topology of the domain. In our case, we want to apply the topological gradient computation to adding a source term of a given form to the Stokes equations. A topological gradient computation for a source term perturbation can be found in [49, 9].

#### Topological sensitivity method

This approach's main step consists of studying the variation of a given functional with respect to a small topological perturbation of the source term. For a given source term  $f$ , let  $\delta f_{P, \epsilon}$  be a finite topological perturbation of  $f$  on the form

$$\delta f_{P, \epsilon} = \begin{cases} \lambda & \text{in } \omega_{P, \epsilon} = \cup_{k=1}^m \omega_{P_k, \epsilon} \\ 0 & \text{in } \Omega \setminus \overline{\cup_{k=1}^m \omega_{P_k, \epsilon}} \end{cases}$$

where  $P = (P_1, \dots, P_m) \in \Omega^m$ , and  $\omega_{P_k, \epsilon}$ ,  $1 \leq k \leq m$  are small geometrical perturbation separated and have the geometry form  $\omega_{P_k, \epsilon} = P_k + \epsilon B$ , where  $\epsilon > 0$  is small enough and  $B$  is a fixed bounded domain containing the origin (e.g. the unit ball). The points  $P_k \in \Omega$ ,  $1 \leq k \leq m$ , determine the location of the geometric  $\omega_{P_k, \epsilon}$ . Then, the asymptotic expansion of the given cost function  $\mathcal{J}$  with respect to  $\epsilon$  takes the form,

$$\begin{aligned} \mathcal{J}(f + \delta f_{P, \epsilon}) - \mathcal{J}(f) &= \rho(\epsilon) \sum_{k=1}^m \mathcal{G}(P_k) + o(\rho(\epsilon)), \quad \forall P_k \in \Omega, \\ \lim_{\epsilon \rightarrow 0} \rho(\epsilon) &= 0, \quad \rho(\epsilon) > 0, \end{aligned} \quad (3.12)$$

where the function  $\mathcal{G}$  is the so-called topological gradient. Therefore, the source location would be identified in the region where the topological gradient is the most negative, that means that, the function  $\mathcal{J}$  will be decreased if we add source terms at points  $P_k$ ,  $1 \leq k \leq m$ .

Let us consider, for now, the case of a single support  $\mathcal{S}_{x_0, \epsilon} := \omega_{x_0, \epsilon}$  such that the perturbation  $\delta f_{\epsilon} := \delta f_{x_0, \epsilon}$  is given by

$$\delta f_{\epsilon} = \begin{cases} \lambda & \text{in } \mathcal{S}_{x_0, \epsilon}, \\ 0 & \text{in } \Omega \setminus \overline{\mathcal{S}_{x_0, \epsilon}}. \end{cases}$$

Then, we define the source function  $\mathcal{J}$  to be minimized,

$$\mathcal{J}(f + \delta f_\epsilon) := \mathcal{J}((u_1^\epsilon, p_1^\epsilon); (u_2^\epsilon, p_2^\epsilon)),$$

where

$$\mathcal{J}((u_1^\epsilon, p_1^\epsilon); (u_2^\epsilon, p_2^\epsilon)) = \int_{\Omega} |\sigma(u_1^\epsilon, p_1^\epsilon) - \sigma(u_2^\epsilon, p_2^\epsilon)|^2 dx,$$

and  $(u_1^\epsilon, p_1^\epsilon)$  and  $(u_2^\epsilon, p_2^\epsilon)$  are respective solutions of the following BVP,

$$\begin{aligned} (\mathcal{P}_1^\epsilon) \begin{cases} -\operatorname{div}(\sigma(u_1^\epsilon, p_1^\epsilon)) &= f + \delta f_\epsilon & \text{in } \Omega, \\ \operatorname{div} u_1^\epsilon &= 0 & \text{in } \Omega, \\ u_1^\epsilon &= G & \text{on } \Gamma_c, \\ \sigma(u_1^\epsilon, p_1^\epsilon)n &= \eta & \text{on } \Gamma_i, \end{cases} \\ (\mathcal{P}_2^\epsilon) \begin{cases} -\operatorname{div}(\sigma(u_2^\epsilon, p_2^\epsilon)) &= f + \delta f_\epsilon & \text{in } \Omega, \\ \operatorname{div} u_2^\epsilon &= 0 & \text{in } \Omega, \\ \sigma(u_2^\epsilon, p_2^\epsilon)n &= \Phi & \text{on } \Gamma_c, \\ u_2^\epsilon &= \tau & \text{on } \Gamma_i, \end{cases} \end{aligned}$$

Then, the weak solutions to problem  $(P_1^\epsilon)$  and  $(P_2^\epsilon)$  are defined by :

$$\begin{cases} \text{Find } (u_1^\epsilon, p_1^\epsilon) \in H^1(\Omega)^2 \times L^2(\Omega) \text{ such that,} \\ \mathcal{A}(u_1^\epsilon, \varphi_1) + \mathcal{B}(p_1^\epsilon, \varphi_1) = l_{1,\epsilon}(\varphi_1), \quad \forall \varphi_1 \in H_{\Gamma_c}^1(\Omega), \\ \mathcal{B}(\xi_1, u_1^\epsilon) = 0, \quad \forall \xi_1 \in L_0^2(\Omega), \end{cases} \quad (3.13)$$

$$\begin{cases} \text{Find } (u_2^\epsilon, p_2^\epsilon) \in H^1(\Omega)^2 \times L^2(\Omega) \text{ such that,} \\ \mathcal{A}(u_2^\epsilon, \varphi_2) + \mathcal{B}(p_2^\epsilon, \varphi_2) = l_{2,\epsilon}(\varphi_2), \quad \forall \varphi_2 \in H_{\Gamma_i}^1(\Omega), \\ \mathcal{B}(\xi_2, u_2^\epsilon) = 0, \quad \forall \xi_2 \in L_0^2(\Omega), \end{cases} \quad (3.14)$$

where

$$\mathcal{A}(u_i^\epsilon, \varphi_i) = \int_{\Omega} D(u_i^\epsilon) : \nabla \varphi_i dx, \quad \mathcal{B}(p_i^\epsilon, \varphi_i) = - \int_{\Omega} p_i^\epsilon \operatorname{div} \varphi_i dx$$

and

$$l_{1,\epsilon}(\varphi_1) = \int_{\Omega} (f + \delta f_\epsilon) \varphi_1 dx + \int_{\Gamma_i} \eta \varphi_1 ds, \quad l_{2,\epsilon}(\varphi_2) = \int_{\Omega} (f + \delta f_\epsilon) \varphi_2 dx + \int_{\Gamma_c} \Phi \varphi_2 ds.$$

We now consider the case where  $f = 0$ , then, the linear forms  $l_{1,0}$  and  $l_{2,0}$  can be defined as follows

$$l_{1,0}(\varphi_1) = \int_{\Gamma_i} \eta \varphi_1 ds, \quad l_{2,0}(\varphi_2) = \int_{\Gamma_c} \Phi \varphi_2 ds.$$

Next, we introduce the following Proposition which describes an adjoint method, for the computation of this first variation of our cost function  $\mathcal{J}$  with respect to  $\epsilon$ .

**Proposition 3.3.1** *Consider  $(u_1^\epsilon, p_1^\epsilon)$  and  $(u_2^\epsilon, p_2^\epsilon)$  solutions of the Problems (3.13) and (3.14), respectively. Suppose that the following assumptions hold :*

- (i)  $\mathcal{J}$  is Fréchet-differentiable with respect to  $(u_i, p_i)$ , for  $i = 1, 2$ .

– (ii) There exist two real numbers  $\delta l_1$  and  $\delta l_2$  such that

$$(l_{1,\epsilon} - l_{1,0})(v_1) = \rho(\epsilon)\delta l_1 + o(\rho(\epsilon)),$$

$$(l_{2,\epsilon} - l_{2,0})(v_2) = \rho(\epsilon)\delta l_2 + o(\rho(\epsilon)),$$

where  $(v_1, q_1)$  and  $(v_2, q_2)$  are solutions of the following weak formulations adjoint problems,

$$(\mathcal{AP}_1) \left\| \begin{aligned} \mathcal{A}(h_1, v_1) + \mathcal{B}(k_1, v_1) - \mathcal{B}(q_1, h_1) &= -\frac{\partial \mathcal{J}}{\partial u_1}((u_1^0, p_1^0); (u_2^0, p_2^0)).h1 \\ &\quad -\frac{\partial \mathcal{J}}{\partial p_1}((u_1^0, p_1^0); (u_2^0, p_2^0)).k1 \end{aligned} \right.$$

$$(\mathcal{AP}_2) \left\| \begin{aligned} \mathcal{A}(h_2, v_2) + \mathcal{B}(k_2, v_2) - \mathcal{B}(q_2, h_2) &= -\frac{\partial \mathcal{J}}{\partial u_2}((u_1^0, p_1^0); (u_2^0, p_2^0)).h2 \\ &\quad -\frac{\partial \mathcal{J}}{\partial p_2}((u_1^0, p_1^0); (u_2^0, p_2^0)).k2 \end{aligned} \right.$$

for all  $(h_1, k_1) \in H_{\Gamma_c}^1(\Omega) \times L^2(\Omega)$  and  $(h_2, k_2) \in H_{\Gamma_i}^1(\Omega) \times L^2(\Omega)$ .

Then the first variation of the cost function  $\mathcal{J}$  with respect to  $\epsilon$  is given by,

$$\mathcal{J}(\delta f_\epsilon) = \mathcal{J}(0) + \rho(\epsilon)(\delta l_1 + \delta l_2) + o(\rho(\epsilon)),$$

where  $\rho(\epsilon) = |\mathcal{S}_{x_0, \epsilon}|$ . The topological gradient  $\mathcal{G}$  at point  $x_0$  is given by :

$$\mathcal{G}(x_0) = -\lambda \cdot (v_1 + v_2)(x_0), \quad (3.15)$$

where  $\lambda$  is a constant vector and  $(v_i, q_i)$  is the solution of the adjoint problem  $(\mathcal{AP}_i)$ , with  $i=1,2$ .

*Proof.* Let us define the Lagrangian  $\mathcal{L}$  by,

$$\begin{aligned} \mathcal{L}_\epsilon(v_1, q_1, v_2, q_2, u_1, p_1, u_2, p_2) &= \mathcal{J}((u_1, p_1); (u_2, p_2)) + \mathcal{A}(u_1, v_1) + \mathcal{B}(p_1, v_1) \\ &\quad - \mathcal{B}(q_1, u_1) - l_{1,\epsilon}(v_1) + \mathcal{A}(u_2, v_2) + \mathcal{B}(p_2, v_2) - \mathcal{B}(q_2, u_2) - l_{2,\epsilon}(v_2), \end{aligned}$$

with  $(u_1, u_2, v_1, v_2) \in H^1(\Omega)^2 \times H^1(\Omega)^2 \times H_{\Gamma_c}^1(\Omega) \times H_{\Gamma_i}^1(\Omega)$  and  $(p_1, p_2, q_1, q_2) \in L^2(\Omega)^4$ .

Using (3.13) and (3.14), we obtain

$$\mathcal{J}(\delta f_\epsilon) = \mathcal{L}_\epsilon(v_1, q_1, v_2, q_2, u_1^\epsilon, p_1^\epsilon, u_2^\epsilon, p_2^\epsilon).$$

So the first variation of the cost function with respect to  $\epsilon$  is given by :

$$\begin{aligned} \mathcal{J}(\delta f_\epsilon) - \mathcal{J}(0) &= \mathcal{L}_\epsilon(v_1, q_1, v_2, q_2, u_1^\epsilon, p_1^\epsilon, u_2^\epsilon, p_2^\epsilon) - \mathcal{L}_0(v_1, q_1, v_2, q_2, u_1^0, p_1^0, u_2^0, p_2^0) \\ &= \mathcal{A}(u_1^\epsilon, v_1) + \mathcal{B}(p_1^\epsilon, v_1) - \mathcal{B}(q_1, u_1^\epsilon) - \mathcal{A}(u_1^0, v_1) - \mathcal{B}(p_1^0, v_1) + \mathcal{B}(q_1, u_1^0) \\ &\quad + \mathcal{A}(u_2^\epsilon, v_2) + \mathcal{B}(p_2^\epsilon, v_2) - \mathcal{B}(q_2, u_2^\epsilon) - \mathcal{A}(u_2^0, v_2) - \mathcal{B}(p_2^0, v_2) + \mathcal{B}(q_2, u_2^0) \\ &\quad - (l_1^\epsilon - l_1^0)(v_1) - (l_2^\epsilon - l_2^0)(v_2) + \mathcal{J}((u_1^\epsilon, p_1^\epsilon); (u_2^\epsilon, p_2^\epsilon)) - \mathcal{J}((u_1^0, p_1^0); (u_2^0, p_2^0)). \end{aligned}$$

Then, from the definition of  $\mathcal{A}$  and  $\mathcal{B}$ , we have

$$\begin{aligned}
& \mathcal{A}(u_1^\epsilon, v_1) + \mathcal{B}(p_1^\epsilon, v_1) - \mathcal{B}(q_1, u_1^\epsilon) - \mathcal{A}(u_1^0, v_1) - \mathcal{B}(p_1^0, v_1) + \mathcal{B}(q_1, u_1^0) \\
&= \int_{\Omega} D(u_1^\epsilon - u_1^0) : \nabla v_1 \, dx + \int_{\Omega} (p_1^\epsilon - p_1^0) \operatorname{div} v_1 \, dx - \int_{\Omega} q_1 \operatorname{div}(u_1^\epsilon - u_1^0) \, dx, \\
& \mathcal{A}(u_2^\epsilon, v_2) + \mathcal{B}(p_2^\epsilon, v_2) - \mathcal{B}(q_2, u_2^\epsilon) - \mathcal{A}(u_2^0, v_2) - \mathcal{B}(p_2^0, v_2) + \mathcal{B}(q_2, u_2^0) \\
&= \int_{\Omega} D(u_2^\epsilon - u_2^0) : \nabla v_2 \, dx + \int_{\Omega} (p_2^\epsilon - p_2^0) \operatorname{div} v_2 \, dx - \int_{\Omega} q_2 \operatorname{div}(u_2^\epsilon - u_2^0) \, dx.
\end{aligned}$$

Choosing  $(v_1, q_1)$  and  $(v_2, q_2)$  as the solutions of the adjoints problems  $(\mathcal{AP}_1)$  and  $(\mathcal{AP}_2)$ ,

$$\begin{aligned}
& \int_{\Omega} D(u_1^\epsilon - u_1^0) : \nabla v_1 \, dx + \int_{\Omega} (p_1^\epsilon - p_1^0) \operatorname{div} v_1 \, dx - \int_{\Omega} q_1 \operatorname{div}(u_1^\epsilon - u_1^0) \, dx = \\
& \quad - \frac{\partial \mathcal{J}}{\partial u_1}((u_1^0, p_1^0); (u_2^0, p_2^0)) \cdot (u_1^\epsilon - u_1^0) - \frac{\partial \mathcal{J}}{\partial p_1}((u_1^0, p_1^0); (u_2^0, p_2^0)) \cdot (p_1^\epsilon - p_1^0), \\
& \int_{\Omega} D(u_2^\epsilon - u_2^0) : \nabla v_2 \, dx + \int_{\Omega} (p_2^\epsilon - p_2^0) \operatorname{div} v_2 \, dx - \int_{\Omega} q_2 \operatorname{div}(u_2^\epsilon - u_2^0) \, dx = \\
& \quad - \frac{\partial \mathcal{J}}{\partial u_2}((u_1^0, p_1^0); (u_2^0, p_2^0)) \cdot (u_2^\epsilon - u_2^0) - \frac{\partial \mathcal{J}}{\partial p_2}((u_1^0, p_1^0); (u_2^0, p_2^0)) \cdot (p_2^\epsilon - p_2^0).
\end{aligned}$$

Thus, we have

$$\begin{aligned}
\mathcal{J}(\delta f_\epsilon) - \mathcal{J}(0) &= - \frac{\partial \mathcal{J}}{\partial u_1}((u_1^0, p_1^0); (u_2^0, p_2^0)) \cdot (u_1^\epsilon - u_1^0) - \frac{\partial \mathcal{J}}{\partial p_1}((u_1^0, p_1^0); (u_2^0, p_2^0)) \cdot (p_1^\epsilon - p_1^0) \\
& \quad - \frac{\partial \mathcal{J}}{\partial u_2}((u_1^0, p_1^0); (u_2^0, p_2^0)) \cdot (u_2^\epsilon - u_2^0) - \frac{\partial \mathcal{J}}{\partial p_2}((u_1^0, p_1^0); (u_2^0, p_2^0)) \cdot (p_2^\epsilon - p_2^0) \\
& \quad - (l_1^\epsilon - l_1^0)(v_1) - (l_2^\epsilon - l_2^0)(v_2) + \mathcal{J}((u_1^\epsilon, p_1^\epsilon); (u_2^\epsilon, p_2^\epsilon)) - \mathcal{J}((u_1^0, p_1^0); (u_2^0, p_2^0))
\end{aligned}$$

• *Variation of the linear form.* We are interested here in the asymptotic analysis of the variation

$$\begin{aligned}
(l_{1,\epsilon} - l_{1,0})(v_1) &= \int_{\Omega} \delta f_\epsilon v_1 \, dx = \int_{\mathcal{S}_{x_0,\epsilon}} \lambda v_1 \, dx, \\
&= |\mathcal{S}_{x_0,\epsilon}| \lambda v_1(x_0) + o(\epsilon).
\end{aligned} \tag{3.16}$$

where  $(v_1, q_1)$  is the solution of the adjoint problem  $(\mathcal{AP}_1)$ . The same, we have

$$(l_{2,\epsilon} - l_{2,0})(v_1) = |\mathcal{S}_{x_0,\epsilon}| \lambda v_2(x_0) + o(\epsilon), \tag{3.17}$$

where  $(v_2, q_2)$  is the solution of the adjoint problem  $(\mathcal{AP}_2)$ .

• *Variation of the cost function.* Let us now turn to the asymptotic analysis of the variation of the Kohn-Vogelius functional given by

$$\mathcal{J}((u_1^\epsilon, p_1^\epsilon); (u_2^\epsilon, p_2^\epsilon)) = \int_{\Omega} |\sigma(u_1^\epsilon, p_1^\epsilon) - \sigma(u_2^\epsilon, p_2^\epsilon)|^2 \, dx.$$

Thus, this functional  $\mathcal{J}$  can be decomposed as

$$\mathcal{J}((u_1^\epsilon, p_1^\epsilon); (u_2^\epsilon, p_2^\epsilon)) = \mathfrak{J}_1(u_1^\epsilon, p_1^\epsilon) + \mathfrak{J}_2(u_2^\epsilon, p_2^\epsilon) - 2\mathfrak{J}_{12}(u_1^\epsilon, p_1^\epsilon; (u_2^\epsilon, p_2^\epsilon)),$$

with

$$\mathfrak{J}_1(u_1^\epsilon, p_1^\epsilon) = \int_{\Omega} |\sigma(u_1^\epsilon, p_1^\epsilon)|^2 dx,$$

$$\mathfrak{J}_2(u_2^\epsilon, p_2^\epsilon) = \int_{\Omega} |\sigma(u_2^\epsilon, p_2^\epsilon)|^2 dx,$$

$$\mathfrak{J}_{12}((u_1^\epsilon, p_1^\epsilon); (u_2^\epsilon, p_2^\epsilon)) = \int_{\Omega} \sigma(u_1^\epsilon, p_1^\epsilon) \sigma(u_2^\epsilon, p_2^\epsilon) dx.$$

Variation of  $\mathfrak{J}_1$  :

$$\begin{aligned} \mathfrak{J}_1(u_1^\epsilon, p_1^\epsilon) - \mathfrak{J}_1(u_1^0, p_1^0) &= \int_{\Omega} |\sigma(u_1^\epsilon, p_1^\epsilon)|^2 dx - \int_{\Omega} |\sigma(u_1^0, p_1^0)|^2 dx \pm 2 \int_{\Omega} |\sigma(u_1^0, p_1^0)|^2 dx \\ &= \int_{\Omega} |\sigma(u_1^\epsilon, p_1^\epsilon) - \sigma(u_1^0, p_1^0)|^2 dx + 2 \int_{\Omega} \sigma(u_1^\epsilon, p_1^\epsilon) \sigma(u_1^0, p_1^0) dx - 2 \int_{\Omega} |\sigma(u_1^0, p_1^0)|^2 dx. \end{aligned}$$

Posing  $(w_i^\epsilon, \xi_i^\epsilon) = (u_i^\epsilon - u_i^0, p_i^\epsilon - p_i^0)$  for  $i=1,2$ , we obtain

$$\mathfrak{J}_1(u_1^\epsilon, p_1^\epsilon) - \mathfrak{J}_1(u_1^0, p_1^0) = \int_{\Omega} |\sigma(w_1^\epsilon, \xi_1^\epsilon)|^2 dx + 2 \int_{\Omega} \sigma(u_1^0, p_1^0) \sigma(w_1^\epsilon, \xi_1^\epsilon) dx. \quad (3.18)$$

Variation of  $\mathfrak{J}_2$  : In the same way, we find that

$$\mathfrak{J}_2(u_2^\epsilon, p_2^\epsilon) - \mathfrak{J}_2(u_2^0, p_2^0) = \int_{\Omega} |\sigma(w_2^\epsilon, \xi_2^\epsilon)|^2 dx + 2 \int_{\Omega} \sigma(u_2^0, p_2^0) \sigma(w_2^\epsilon, \xi_2^\epsilon) dx. \quad (3.19)$$

Variation of  $\mathfrak{J}_{12}$  :

$$\begin{aligned} \mathfrak{J}_{12}((u_1^\epsilon, p_1^\epsilon); (u_2^\epsilon, p_2^\epsilon)) - \mathfrak{J}_{12}((u_1^0, p_1^0); (u_2^0, p_2^0)) &= \int_{\Omega} \sigma(u_1^\epsilon, p_1^\epsilon) \sigma(u_2^\epsilon, p_2^\epsilon) dx \\ &\quad - \int_{\Omega} \sigma(u_1^0, p_1^0) \sigma(u_2^0, p_2^0) dx. \end{aligned}$$

Then, we have

$$\begin{aligned} \mathfrak{J}_{12}((u_1^\epsilon, p_1^\epsilon); (u_2^\epsilon, p_2^\epsilon)) - \mathfrak{J}_{12}((u_1^0, p_1^0); (u_2^0, p_2^0)) &= \int_{\Omega} \sigma(w_1^\epsilon, \xi_1^\epsilon) \sigma(w_2^\epsilon, \xi_2^\epsilon) dx \\ &\quad + \int_{\Omega} \sigma(u_1^0, p_1^0) \sigma(w_2^\epsilon, \xi_2^\epsilon) dx + \int_{\Omega} \sigma(u_2^0, p_2^0) \sigma(w_1^\epsilon, \xi_1^\epsilon) dx \end{aligned} \quad (3.20)$$

Combining the variations (3.18), (3.19) and (3.20), we obtain

$$\begin{aligned} \mathcal{J}((u_1^\epsilon, p_1^\epsilon); (u_2^\epsilon, p_2^\epsilon)) - \mathcal{J}((u_1^0, p_1^0); (u_2^0, p_2^0)) &= \int_{\Omega} |\sigma(w_1^\epsilon, \xi_1^\epsilon)|^2 dx \\ &\quad + \int_{\Omega} |\sigma(w_2^\epsilon, \xi_2^\epsilon)|^2 dx - 2 \int_{\Omega} \sigma(w_1^\epsilon, \xi_1^\epsilon) \sigma(w_2^\epsilon, \xi_2^\epsilon) dx \\ &\quad + 2 \int_{\Omega} (\sigma(u_1^0, p_1^0) - \sigma(u_2^0, p_2^0)) \sigma(w_1^\epsilon, \xi_1^\epsilon) dx \\ &\quad - 2 \int_{\Omega} (\sigma(u_1^0, p_1^0) - \sigma(u_2^0, p_2^0)) \sigma(w_2^\epsilon, \xi_2^\epsilon) dx. \end{aligned}$$

Therefore,

$$\begin{aligned} \mathcal{J}((u_1^\epsilon, p_1^\epsilon); (u_2^\epsilon, p_2^\epsilon)) - \mathcal{J}((u_1^0, p_1^0); (u_2^0, p_2^0)) - \frac{\partial \mathcal{J}}{\partial u_1}((u_1^0, p_1^0); (u_2^0, p_2^0)) \cdot w_1^\epsilon \\ - \frac{\partial \mathcal{J}}{\partial p_1}((u_1^0, p_1^0); (u_2^0, p_2^0)) \cdot \xi_1^\epsilon - \frac{\partial \mathcal{J}}{\partial u_2}((u_1^0, p_1^0); (u_2^0, p_2^0)) \cdot w_2^\epsilon \\ - \frac{\partial \mathcal{J}}{\partial p_2}((u_1^0, p_1^0); (u_2^0, p_2^0)) \cdot \xi_2^\epsilon = \mathcal{I}(\epsilon), \end{aligned}$$



where

$$\mathcal{I}(\epsilon) = \|\sigma(w_1^\epsilon, \xi_1^\epsilon)\|_{0,\Omega}^2 + \|\sigma(w_2^\epsilon, \xi_2^\epsilon)\|_{0,\Omega}^2 - 2 \int_{\Omega} \sigma(w_1^\epsilon, \xi_1^\epsilon) \sigma(w_2^\epsilon, \xi_2^\epsilon) dx.$$

We will then prove that  $\mathcal{I}(\epsilon) = o(\rho(\epsilon))$ . Thus, the topological asymptotic expansion of the functional  $\mathcal{J}$  with respect to  $\epsilon$  is given by

$$\mathcal{J}(\delta f_\epsilon) - \mathcal{J}(0) = -|\mathcal{S}_{x_0,\epsilon}| \lambda(v_1 + v_2)(x_0) + o(|\mathcal{S}_{x_0,\epsilon}|),$$

then the topological gradient  $\mathcal{G}$  at point  $x_0$  is given by

$$\mathcal{G}(x_0) = -\lambda(v_1 + v_2)(x_0).$$

Let's now show that  $\mathcal{I}(\epsilon) = o(|\mathcal{S}_{x_0,\epsilon}|)$ . Consider  $(w_1^\epsilon, \xi_1^\epsilon) = (u_1^\epsilon - u_1^0, p_1^\epsilon - p_1^0)$  solution of the following problem,

$$\begin{cases} -\operatorname{div}(\sigma(w_1^\epsilon, \xi_1^\epsilon)) = \delta f_\epsilon & \text{in } \Omega, \\ \operatorname{div} w_1^\epsilon = 0 & \text{in } \Omega, \\ w_1^\epsilon = 0 & \text{on } \Gamma_c, \\ \sigma(w_1^\epsilon, \xi_1^\epsilon)n = 0 & \text{on } \Gamma_i. \end{cases}$$

This problem is well-posed and has a unique solution in  $H^1(\Omega)^2 \times L^2(\Omega)$ , see e.g. [34]. Using ([22], theorem 5.2), there exists a positive constant  $C$  such that,

$$\begin{aligned} \|w_1^\epsilon\|_{1,\Omega} + \|\xi_1^\epsilon\|_{0,\Omega} &\leq C \|\delta f_\epsilon\|_{0,\Omega} \\ &\leq C \|\lambda\| (\rho(\epsilon))^{\frac{1}{2}}. \end{aligned} \quad (3.21)$$

The same for the solution  $(w_2^\epsilon, \xi_2^\epsilon)$ . Using these latter results, we obtain an estimation of the third term of  $\mathcal{I}$ . We deduce then that  $\mathcal{I}(\epsilon) = o(\rho(\epsilon))$ . ■

### 3.3.3 Identification of the source intensity.

In this subsection, the player (3) assumes to be known the position  $P = x_0$  defining a source-term  $F_\epsilon$  that satisfies (3.7) and focuses on identifying the source intensity  $\lambda_k$ . To this end, player (3) must minimize the functional  $\mathcal{J}_3$  with respect to  $\lambda$ . So the source intensity can be characterized as the solution of the following minimization problem,

$$\lambda^* = \arg \min_{\lambda \in \mathbb{R}^d} \left\{ \mathcal{J}_3(\eta, \tau; \phi) := \int_{\Omega} |\sigma(u_{1,\epsilon}, p_{1,\epsilon}) - \sigma(u_{2,\epsilon}, p_{2,\epsilon})|^2 dx \right\},$$

where  $(u_{1,\epsilon}, p_{1,\epsilon})$  and  $(u_{2,\epsilon}, p_{2,\epsilon})$  solve respectively problems  $(\mathcal{P}_{1,\epsilon})$  and  $(\mathcal{P}_{2,\epsilon})$ . In order to perform the partial optimization problem of  $\mathcal{J}_3(\eta, \tau; \phi)$  w.r.t the source intensity  $\lambda$  with  $(\eta, \tau)$  given by players (1) and (2), one needs to compute the derivative of  $\mathcal{J}_3$  w.r.t.  $\lambda$ . We have the following :

**Proposition 3.3.2** *We have the following partial derivative,*

$$\frac{\partial \mathcal{J}_3}{\partial \lambda} \cdot \varphi = -\frac{1}{|\mathcal{S}_{x_0,\epsilon}|} \int_{\mathcal{S}_{x_0,\epsilon}} (z_1 + z_2)(x) \cdot \varphi dx, \quad \forall \varphi \in \mathbb{R},$$

where  $(z_1, \pi_1) \in H_{\Gamma_c}^1(\Omega) \times L^2(\Omega)$  and  $(z_2, \pi_2) \in H_{\Gamma_i}^1(\Omega) \times L^2(\Omega)$  are respective solutions of the adjoints problems,

$$\left\{ \begin{array}{l} 2 \int_{\Omega} (\sigma(u_{1,\epsilon}, p_{1,\epsilon}) - \sigma(u_{2,\epsilon}, p_{2,\epsilon})) : (\nabla h_1 + \nabla h_1^T) dx - \int_{\Omega} \pi_1 \operatorname{div} h_1 dx \\ \quad + \int_{\Omega} ((\nabla h_1 + \nabla h_1^T) : \nabla z_1) dx = 0, \quad \forall h_1 \in H_{\Gamma_c}^1(\Omega), \\ -2 \int_{\Omega} (\sigma(u_{1,\epsilon}, p_{1,\epsilon}) - \sigma(u_{2,\epsilon}, p_{2,\epsilon})) : (k_1 I_d) dx - \int_{\Omega} k_1 \operatorname{div} z_1 dx = 0, \\ \quad \forall k_1 \in L^2(\Omega), \end{array} \right. \quad (3.22)$$

$$\left\{ \begin{array}{l} -2 \int_{\Omega} (\sigma(u_{1,\epsilon}, p_{1,\epsilon}) - \sigma(u_{2,\epsilon}, p_{2,\epsilon})) : (\nabla h_2 + \nabla h_2^T) dx - \int_{\Omega} \pi_2 \operatorname{div} h_2 dx \\ \quad + \int_{\Omega} ((\nabla h_2 + \nabla h_2^T) : \nabla z_2) dx = 0, \quad \forall h_2 \in H_{\Gamma_i}^1(\Omega), \\ 2 \int_{\Omega} (\sigma(u_{1,\epsilon}, p_{1,\epsilon}) - \sigma(u_{2,\epsilon}, p_{2,\epsilon})) : (k_2 I_d) dx - \int_{\Omega} k_2 \operatorname{div} z_2 dx = 0, \\ \quad \forall k_2 \in L^2(\Omega), \end{array} \right. \quad (3.23)$$

and where  $(u_{1,\epsilon}, p_{1,\epsilon})$  and  $(u_{2,\epsilon}, p_{2,\epsilon})$  are the solutions to respectively  $(\mathcal{P}_{1,\epsilon})$  and  $(\mathcal{P}_{2,\epsilon})$ .

### 3.3.4 The three-player Nash algorithm

We are now ready to state the three-player identification/completion Nash game. As aforementioned, players (1) and (2) aim at solving the Cauchy problem, while player (3) is aimed at minimizing a Kohn-Vogelius type energy, intended to identify the elements of the source-term. The game is of Nash type, which means that it is static with complete information [56] and hence its solution is a Nash equilibrium (NE), see Definition 3.3.1.

Given a triplet  $(\eta, \tau; \phi) \in (H_{00}^{\frac{1}{2}}(\Gamma_i)^2)' \times H^{\frac{1}{2}}(\Gamma_i)^2 \times \mathcal{I}_{\text{ad}}$ , and we define  $(u_{1,\epsilon}, p_{1,\epsilon}) := (u_{1,\epsilon}(\eta, \phi), p_{1,\epsilon}(\eta, \phi))$  be the solution to the approximate Stokes problem  $(\mathcal{P}_{1,\epsilon})$  and  $(u_{2,\epsilon}, p_{2,\epsilon}) := (u_{2,\epsilon}(\tau, \phi), p_{2,\epsilon}(\tau, \phi))$  the solution to the approximate Stokes problem  $(\mathcal{P}_{2,\epsilon})$ , then the three players and their respective costs are defined as follows :

- Player (1) has control on the Neumann strategies  $\eta \in (H_{00}^{\frac{1}{2}}(\Gamma_i)^2)'$ , and its cost functional is given by

$$\mathcal{J}_1(\eta, \tau; \phi) = \frac{1}{2} \|\sigma(u_{1,\epsilon}, p_{1,\epsilon})n - \Phi\|_{(H_{00}^{\frac{1}{2}}(\Gamma_c)^2)'}^2 + \frac{1}{2} \|u_{1,\epsilon} - u_{2,\epsilon}\|_{H^{\frac{1}{2}}(\Gamma_i)^2}^2 \quad (3.24)$$

- Player (2) has control on the Dirichlet strategies  $\tau \in H^{\frac{1}{2}}(\Gamma_i)^2$ , and its cost functional is given by

$$\mathcal{J}_2(\eta, \tau; \phi) = \frac{1}{2} \|u_{2,\epsilon} - f\|_{H^{\frac{1}{2}}(\Gamma_c)^2}^2 + \frac{1}{2} \|u_{1,\epsilon} - u_{2,\epsilon}\|_{H^{\frac{1}{2}}(\Gamma_i)^2}^2 \quad (3.25)$$

- Player (3) has control on the elements  $\phi \in \mathcal{I}_{\text{ad}}$  defining the unknown source, and its cost functional is given by

$$\mathcal{J}_3(\eta, \tau; \phi) = \int_{\Omega} |\sigma(u_{1,\epsilon}, p_{1,\epsilon}) - \sigma(u_{2,\epsilon}, p_{2,\epsilon})|^2 dx \quad (3.26)$$

In algorithm 3.3.1 below, we describe the main steps in computing the Nash equilibrium, with a version where the Cauchy data of the Dirichlet type  $G$  are possibly perturbed by a noise with some magnitude  $\sigma$ , yielding for the Cauchy problem a noisy Dirichlet data  $G^\sigma$ .

The topological gradient and the gradient with fixed step methods are used to solve step I and II respectively. In step II, in order to solve the problems of partial optimization of  $\mathcal{J}_1$ ,  $\mathcal{J}_2$  and  $\mathcal{J}_3$ , we need to calculate the gradient of these costs with respect to their respective strategies  $\eta$ ,  $\tau$  and  $\lambda$ . The fast computation of the latter is classical, and led by means of an adjoint state method, as shown by the proposition 3.3.2 and 3.3.3, the proof of the proposition 3.3.3 is given in ([57], Appendix A. 1).

**Proposition 3.3.3** [57] *We have the following two partial derivatives :*

$$\left\{ \begin{array}{l} \frac{\partial \mathcal{J}_1}{\partial \eta} \cdot \psi = - \int_{\Gamma_i} \psi \lambda_1 ds, \quad \forall \psi \in (H_{00}^{\frac{1}{2}}(\Gamma_i)^2)', \\ \text{with } (\lambda_1, \kappa_1) \in H_{\Gamma_c}^1(\Omega) \times L^2(\Omega) \quad \text{solution of the adjoint problem :} \\ \left\{ \begin{array}{l} \int_{\Gamma_c} (\sigma(u_{1,\epsilon}, p_{1,\epsilon})n - \Phi)((\nabla \gamma + \nabla \gamma^T)n) ds + \int_{\Gamma_i} (u_{1,\epsilon} - u_{2,\epsilon}) \gamma ds \\ \quad + \int_{\Omega} (\nabla \gamma + \nabla \gamma^T) : \nabla \lambda_1 dx - \int_{\Omega} \kappa_1 \operatorname{div} \gamma dx = 0, \quad \forall \gamma \in H_{\Gamma_c}^1(\Omega). \\ - \int_{\Gamma_c} (\sigma(u_{1,\epsilon}, p_{1,\epsilon})n - \Phi) \delta n ds - \int_{\Omega} \delta \operatorname{div} \lambda_1 dx = 0, \quad \forall \delta \in L^2(\Omega), \end{array} \right. \end{array} \right. \quad (3.27)$$

$$\left\{ \begin{array}{l} \frac{\partial \mathcal{J}_2}{\partial \tau} \cdot \mu = \int_{\Gamma_i} (\sigma(\lambda_2, \kappa_2)n - (u_{1,\epsilon} - u_{2,\epsilon})) \mu ds, \quad \forall \mu \in H^{\frac{1}{2}}(\Gamma_i)^2, \\ \text{with } (\lambda_2, \kappa_2) \in H^1(\Omega)^2 \times L^2(\Omega) \quad \text{solution of the adjoint problem :} \\ \left\{ \begin{array}{l} \int_{\Omega} (\nabla \lambda_2 + \nabla \lambda_2^T) : \nabla \varphi dx - \int_{\Omega} \kappa_2 \operatorname{div} \varphi dx = \int_{\Gamma_c} (G - u_{2,\epsilon}) \varphi ds, \\ \quad \forall \varphi \in H_{\Gamma_i}^1(\Omega), \\ \int_{\Omega} \xi \operatorname{div} \lambda_2 dx = 0, \quad \forall \xi \in L^2(\Omega), \end{array} \right. \end{array} \right. \quad (3.28)$$

where, by a classical convention,  $\nabla u : \nabla v = \operatorname{Tr}(\nabla u \nabla v^T) = \sum_{i,j} \frac{\partial u_i}{\partial x_j} \frac{\partial v_i}{\partial x_j}$ .

---

**Algorithm 3.3.1:** Computation of the Nash equilibrium

---

**Data:**  $\epsilon_S > 0$  a convergence tolerance,  $K_{max}$  a computational budget per Nash iteration,  $N_{max}$  a maximum Nash iterations,  $\sigma$  a noise level and  $\rho(\sigma)$  a-tuned-function which depends on the noise.

Set  $n = 0$ , choose an initial source intensity  $\lambda^{(0)}$  and  $F_\epsilon = 0$  ;

**while**  $\|u_2 - G\|_{0,\Gamma_c} > \rho(\sigma)$  **do**

Set  $k = 0$  and choose an initial guess  $(\eta^{(0)}, \tau^{(0)}) \in (H_{00}^{\frac{1}{2}}(\Gamma_i)^2)' \times H^{\frac{1}{2}}(\Gamma_i)^2$  ;

Compute  $\bar{\eta}^{(k)}$  solution of  $\min_{\eta} \mathcal{J}_1(\eta, \tau^{(k)}; F_\epsilon)$ .

Compute (in parallel)  $\bar{\tau}^{(k)}$  solution of  $\min_{\tau} \mathcal{J}_2(\eta^{(k)}, \tau; F_\epsilon)$ .

Evaluate  $(\eta^{(k+1)}, \tau^{(k+1)}) = \alpha(\eta^{(k)}, \tau^{(k)}) + (1 - \alpha)(\bar{\eta}^{(k)}, \bar{\tau}^{(k)})$ , with  $0 \leq \alpha < 1$ .

– Step I : Set  $F_\epsilon = 0$ , and use the one-shot algorithm to determine the set of optimal locations  $P^{(n)} = \{P_1, \dots, P_{m^{(n)}}\}$  :

- Solve two well-posed mixed forward problems :

$$(\mathcal{P}_1^0) \begin{cases} -\operatorname{div}(\sigma(u_1^{0,k+1}, p_1^{0,k+1})) = 0 & \text{in } \Omega, \\ \operatorname{div} u_1^{0,k+1} = 0 & \text{in } \Omega, \\ u_1^{0,k+1} = G & \text{on } \Gamma_c, \\ \sigma(u_1^{0,k+1}, p_1^{0,k+1})n = \eta^{(k+1)} & \text{on } \Gamma_i, \end{cases}$$

$$(\mathcal{P}_2^0) \begin{cases} -\operatorname{div}(\sigma(u_2^{0,k+1}, p_2^{0,k+1})) = 0 & \text{in } \Omega, \\ \operatorname{div} u_2^{0,k+1} = 0 & \text{in } \Omega, \\ \sigma(u_2^{0,k+1}, p_2^{0,k+1})n = \Phi & \text{on } \Gamma_c, \\ u_2^{0,k+1} = \tau^{(k+1)} & \text{on } \Gamma_i. \end{cases}$$

- Solve the adjoint problems  $(\mathcal{AP}_1)$  and  $(\mathcal{AP}_2)$  with respective solutions  $v_1$  and  $v_2$ .
- Compute the topological gradient  $\mathcal{G}$  using Formula (3.15), i.e.

$$\mathcal{G}(x) = -\lambda^{(k)}.(v_1 + v_2)(x), \quad \forall x \in \Omega.$$

- Seek

$$P^{(n)} = \arg \min_{x \in \Omega} \mathcal{J}_3(\eta^{(k+1)}, \tau^{(k+1)}; (\lambda^{(k)}, x)).$$

– Step II : Solve the Nash game between  $\eta$ ,  $\tau$  and  $\lambda$  : Set  $k = 1$ ,

- Step 1 : Evaluate  $F_\epsilon^{(n,k)} = \sum_{i=1}^{m^{(n)}} \frac{1}{|\mathcal{S}_{P_i, \epsilon}|} \lambda_i^{(k-1)} \chi_{\mathcal{S}_{P_i, \epsilon}}$ .
- Step 2 : Compute  $\bar{\eta}^{(k)}$  solution of  $\min_{\eta} \mathcal{J}_1(\eta, \tau^{(k)}; (\lambda^{(k-1)}, P^{(n)}))$ .
- Step 3 : Compute (in parallel)  $\bar{\tau}^{(k)}$  solution of  $\min_{\tau} \mathcal{J}_2(\eta^{(k)}, \tau; (\lambda^{(k-1)}, P^{(n)}))$ .
- Step 4 : Compute (in parallel)  $\bar{\lambda}^{(k)}$  solution of  $\min_{\lambda} \mathcal{J}_3(\eta^{(k)}, \tau^{(k)}; (\lambda, P^{(n)}))$ .
- Step 5 : For  $0 \leq \alpha < 1$ , set

$$S^{(k+1)} = (\eta^{(k+1)}, \tau^{(k+1)}, \lambda^{(k)}) = \alpha(\eta^{(k)}, \tau^{(k)}, \lambda^{(k-1)}) + (1 - \alpha)(\bar{\eta}^{(k)}, \bar{\tau}^{(k)}, \bar{\lambda}^{(k)}).$$

While  $\|S^{(k+1)} - S^{(k)}\| > \epsilon_S$  and  $k < N_{max}$ , set  $k = k + 1$ , return back to step 1.

**end**

---

### 3.4 Numerical experiments

In this section, we illustrate the numerical results obtained using the 3-costs functionals described in the previous section 3.3. In order to test the efficiency of the proposed numerical method, we solve the source Cauchy-Stokes problem in the 2-D situations : the annular domain and a geometry with corners are considered. Then, we present an example of numerical reconstruction in the three-dimensional 3-D case. In our numerical experiments, we use L2 norms to estimate errors and calculate the gradient of the cost functionals.

Given a known the elements defining the source term  $F_\epsilon^*$ , that is  $\phi^* = (\lambda, P)$ , we solve the following Stokes problem :

$$\begin{cases} -\operatorname{div}(\sigma(u, p)) = F_\epsilon^* & \text{in } \Omega, \\ \operatorname{div} u = 0 & \text{in } \Omega, \\ u = G & \text{on } \Gamma_c, \\ \beta u + \gamma \sigma(u, p)n = \beta H + \gamma \Psi & \text{on } \Gamma_i, \end{cases} \quad (3.29)$$

where the (phantom) exact solution  $(u, p)$  is used to build the remaining Cauchy data  $\Phi = \sigma(u, p)n|_{\Gamma_c}$ , and the exact missing data  $u|_{\Gamma_i}$  and  $\sigma(u, p)n|_{\Gamma_i}$ . The two latter data together with the known elements defining  $F_\epsilon^*$  are used to compute the following relative errors :

$$\begin{aligned} err_D &= \frac{\|\tau_N - u|_{\Gamma_i}\|_{0, \Gamma_i}}{\|u|_{\Gamma_i}\|_{0, \Gamma_i}}, & err_N &= \frac{\|\eta_N - \sigma(u, p)n|_{\Gamma_i}\|_{0, \Gamma_i}}{\|\sigma(u, p)n|_{\Gamma_i}\|_{0, \Gamma_i}}, \\ err_P &= \frac{\|P_{ex} - P_{op}\|_2}{\|P_{ex}\|_2}, & err_\lambda &= \frac{\|\Lambda_{ex} - \Lambda_{op}\|_2}{\|\Lambda_{ex}\|_2}, \end{aligned} \quad (3.30)$$

where  $(\eta_N, \tau_N; \phi_N)$  is the approximate Nash equilibrium output from Algorithm 3.3.1, and  $\|\cdot\|_2$  represents the Euclidean norm. These metrics are used to assess the efficiency of our approach. The stability w.r.t. noise was stressed by solving the coupled problem with noisy perturbations of the Dirichlet data  $G^\sigma = G(1 + \sigma\delta)$ , with  $\delta$  is a random real number taken from the uniform distribution over the interval  $[-1, 1]$ .

An arbitrary initial guess such as  $S^{(0)} = (\eta^{(0)}, \tau^{(0)}, \lambda^{(0)}) = (0, 0, 0.1)$  and  $F_\epsilon = 0$  are chosen to start the algorithm, and the relaxation parameter  $\alpha$  is set to 0.25. The pointwise forces identified are represented in the domain  $\Omega$  as a disc of radius  $\epsilon = 0.07$ .

The solvers for Stokes, the computation of the topological gradient and adjoint systems, and the minimization algorithms as well, were implemented using the Finite Element package FreeFem++ [61].

#### Example 1 : An annular domain.

We consider an annular domain  $\Omega$  with circular boundary components  $\Gamma_i$  and  $\Gamma_c$ , both centered at  $(0, 0)$  and with radii  $R_i = 1$  and  $R_c = 2$ , respectively. In this example, we choose  $(\beta, \gamma) = (0, 1)$ , and the Cauchy data  $\sigma(u, p)n|_{\Gamma_c}$  is generated via the solution of the problem (3.29), with  $G|_{\Gamma_c} = (y^2, x^2)$  and  $\Psi|_{\Gamma_i} = -(x, y)$ .

---

**Test-case A.**

The exact source-term is located at  $P_{ex} = (1.8, 0)$ , with an intensity source  $\Lambda_{ex} = (0.2, 0.2)$ .

We applied our algorithm 1, presented in section 3.3, to compute the Nash equilibrium. Figure 3.5 presents the obtained results. We remark that these results are in good accordance with the exact source  $F_\epsilon$  and missing data.

For the case of noisy Dirichlet data  $G^\sigma$  given over  $\Gamma_c$ , it can be seen from the profiles presented in Figure 3.6 and the Table 3.4 that the boundary data recovery is overall stable with respect to the noise magnitude, in particular the computed components of the normal stress are more sensitive than the velocity one, and the estimated elements defining  $F_\epsilon$ , identified source and their intensity forces, are also acceptable.

The relative errors defined by formulas (3.30) are summarized in Table 3.1 for the test-case A.

Table 3.1 – Test-case A.  $L^2$  relative errors on missing data on  $\Gamma_i$  (on Dirichlet and Neumann data), and the relative errors on the identified source position and on the identified source intensity for various noise levels.

Noise level	$err_D$	$err_N$	$err_P$	$err_\Lambda$
$\sigma = 0\%$	0.003	0.060	0.010	0.018
$\sigma = 1\%$	0.008	0.087	0.010	0.155
$\sigma = 3\%$	0.015	0.147	0.043	0.169

**Test-case B. The case of multiple points-forces.**

In this test-case, we try to detect and locate multiple point-forces. We propose to identify four pointwise forces, located respective at the points  $P_1 = (1.8, 0)$ ,  $P_2 = (0, 1.8)$ ,  $P_3 = (-1.8, 0)$  and  $P_4 = (0, -1.8)$ , and their exact intensity force  $\lambda_i$  is equal to  $(0.2, 0.2)$ ,  $i=1, \dots, 4$ .

We suppose that the number  $m$  of the region  $\mathcal{S}_{P_i, \epsilon}$ ,  $i=1, \dots, m$ , is unknown. We observe from Figure 3.7(a)(b) that our proposed algorithm is able to determine the number of the small region inside  $\Omega$  and gives a good approximation of the locations and the recovery intensity for each components of the source-term, as well as the recovered data Figure 3.7(c)-(f). The recovery of missing boundary data and the estimated value of  $P$  and  $\lambda$  are stable with respect to noisy Dirichlet measurements, as shown Figure 3.8 and Table 3.5, where the table 3.5 presents the different error at convergence.

To assess our algorithm and results against the so-called inverse crime, that possibly arises when the same model is used to synthesize Cauchy data and to solve the corresponding inverse problem, resulting in possible artificial outperformance, we synthesized Cauchy data using different meshes, see Figure 3.2. All our numerical experiments produced results of the same good quality than the results presented in Figure 3.7, see Figure 3.9.

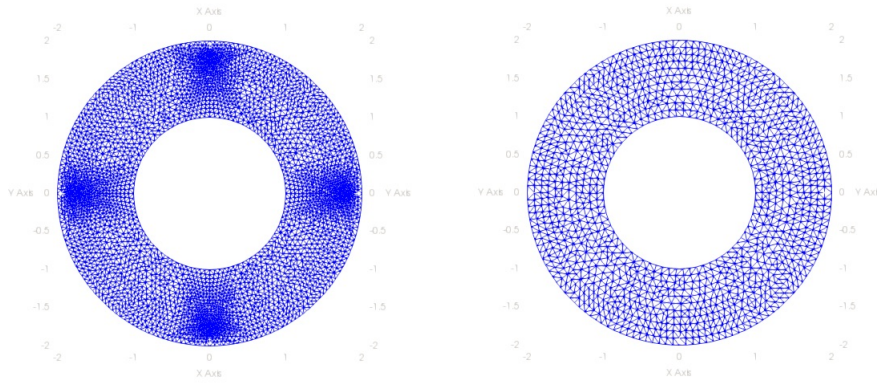


FIGURE 3.2 – Test case B. (Left) Mesh used for solving the direct problem, in order to construct the synthetic data. (Right) Mesh used for solving the coupled inverse problem, with P2-P1 finite element.

## Example 2 : A geometry with corners.

The domain is a centered square  $] - 0.5, 0.5[ \times ] - 0.5, 0.5[$ , the finite element discretization of the domain boundary  $\partial\Omega$  is constituted of 160 vertices. We impose here  $(\beta, \gamma) = (1, 0)$ , and  $G = H = (2y^2 - 1/2, 0)$  prescribed over  $\partial\Omega$ . Overspecified Cauchy data are prescribed on the boundaries  $y \in \{-\frac{1}{2}, \frac{1}{2}\}$  and  $x = -1/2$  of the square and the underspecified boundary data  $u|_{\Gamma_i} = u(1/2, y)$  and its stress force are sought.

### Test-case C.

The exact source-term is located at  $P_{ex} = (-0.3, -0.25)$ , with intensity  $\Lambda_{ex} = (0.25, 0.2)$ .

The numerically obtained results are shown in Figure 3.10. Figure 3.10(a) presents the iso-values of the topological gradient, the source support  $\mathcal{S}_{x_0, \epsilon}$  can be located in the areas where the topological gradient is negative. The estimated intensity and the determined position are very satisfactory, as shown Figure 3.10(b). The numerical Dirichlet solution is a good approximation for the exact solution one, see Figure 3.10(c)(d). Then, concerning the numerical Neumann solution, see Figure 3.10(e)(f), it can be seen that the estimates deviate from the exact one, especially near the endpoints of the boundary which is the region of singularities, in the corners. There is also a remarkable stability with respect to noisy data of both the estimated elements and the recovered boundary data, see Figure 3.11 and Table 3.6.

The relative errors presented in Table 3.2 show the performance of our method with respect to noisy Dirichlet measurements.

A numerical study concerning the sensitivity of the reconstruction according to the position of the source term in the domain has been studied. The Figure 3.3 shows that the relative errors increase when the source term becomes closer to the inaccessible boundary  $\Gamma_i$ .

Table 3.2 – Test-case C.  $L^2$  relative errors on missing data on  $I_i$  (on Dirichlet and Neumann data), and the relative errors on the identified source position and on the identified source intensity for various noise levels.

Noise level	$err_D$	$err_N$	$err_P$	$err_\Lambda$
$\sigma = 0\%$	0.011	0.097	0.071	0.009
$\sigma = 1\%$	0.011	0.102	0.136	0.029
$\sigma = 3\%$	0.021	0.106	0.184	0.058

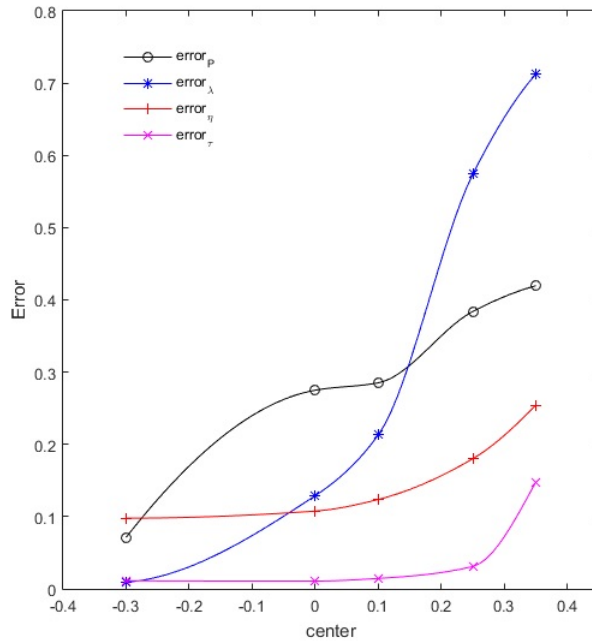


FIGURE 3.3 – Test case C. Sensitivity of the reconstruction w.r.t. the distance to the inaccessible boundary  $I_i$ , the distance of the center of  $\mathcal{S}_{P,\epsilon}$  from  $I_i$ , for  $y = -0.25$ .

### The 3D case.

We present hereafter an example of numerical reconstruction in the three dimensional case. The domain  $\Omega$  is a cube  $(0, 1)^3$ , such that its boundary splitted into two parts  $\Gamma_i$  and  $\Gamma_c$ , where  $\Gamma_i = \{(x, y, z) \in \partial\Omega; \text{ such that } x = 1\}$  represents the inaccessible part and  $\Gamma_c = \partial\Omega \setminus \Gamma_i$  is the accessible part, where the Cauchy data is available. We try so to detect a source  $F_\epsilon$  located in  $P_{ex} = (0.25, 0.25, 0.25)$  and with a source intensity  $\lambda_{ex} = (0.25, 0.2, 0)$ . The Cauchy data on  $\Gamma_c$  are numerically simulated by solving the following Dirichlet problem :

$$\begin{cases} -\operatorname{div}(\sigma(u, p)) = F_\epsilon^* & \text{in } \Omega, \\ \operatorname{div}u = 0 & \text{in } \Omega, \\ u = G & \text{on } \partial\Omega, \end{cases}$$

where  $G$  is a given function. Then, applying our algorithm 3.3 in order to find the Nash equilibrium, which is expected to approximate the coupled problem solution. The finite element computations are performed with 4,096 nodes and 20,250 tetrahedral



elements. The cost of computation is quite expensive, to overcome this difficulty, we use `ffddm` which implements a class of parallel solvers in FreeFem. The obtained results are presented in Table 3.3, with noise free Dirichlet data over  $\Gamma_c$ . The Figure 3.4 represents the iso-values of the topological gradient at convergence.

Table 3.3 –  $L^2$  relative errors of reconstructed solution in the whole domain and missing data on  $\Gamma_i$  (on Dirichlet and Neumann data), and the relative errors on the identified source position and on the identified source intensity for noise-free, where  $err_{u_i} = \|u_{i,\epsilon} - u\|_{0,\Omega} / \|u\|_{0,\Omega}$ , for  $i = 1, 2$ .

$err_{u_1}$	$err_{u_2}$	$err_\tau$	$err_\eta$	$err_P$	$err_\Lambda$
0.008	0.026	0.031	0.224	0.2	0.056

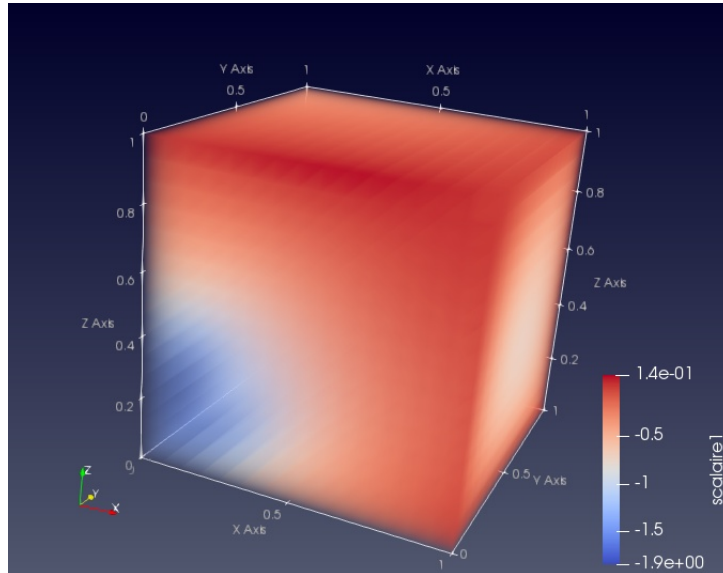


FIGURE 3.4 – The iso-values of the topological gradient at convergence,  $P_{op} = (0.2, 0.2, 0.2)$  and  $\Lambda_{op} = (0.233, 0.204, 0.005)$ . Exact values :  $P_{ex} = (0.25, 0.25, 0.25)$  and  $\Lambda_{ex} = (0.25, 0.2, 0)$ .

### 3.5 Conclusion

we have addressed, in the present paper, the problem of identifying the location and magnitude of a finite but unknown number of point-wise sources, in a linear steady Stokes problem with missing boundary data. Such a reconstruction problem couples two inverse problems of different classes, the recovery of missing boundary data (the Cauchy problem), and the identification of point-wise sources. Each of these two inverse problems is known to be severely ill-posed by its own, and designing efficient and stable algorithms is challenging. In our case, the problem of designing efficient and robust algorithms is worsened by the coupling of the two ill-posed problems, and by the fact

---

that we consider as available only a single pair of over-specified data (and not the classical Dirichlet-to-Neumann whole map).

Due to the identification/recovery coupling, classical methods fail, mainly because of being too specific to each of the source identification or data recovery problems. Hence our recourse to game theory, which is, by its very nature, able to address such antagonistic situations. Previous successful reframing of data recovery inverse problems as Nash games has fostered the formulation of the coupled source identification and data recovery problems as Nash games.

We have proposed here to formulate the coupled inverse problems as a static with complete information Nash game. First, we have relaxed the point-wise source identification problem to gain some regularity on the velocity and pressure state variables, and we have introduced three players and three cost functionals. The two first, named Dirichlet-Neumann players, were dedicated to ensure the data completion while the third one was dedicated to ensure the detection of the sources. We postulated that the sought solution of the coupled problem could be found as a Nash equilibrium of the three-player game.

This formulation resulted in the design of a novel algorithm, which is composed of two main steps. In the first step, the third player seeks to identify the number and location of the sources using a topological gradient method. In the second one, the two Dirichlet-Neumann players solve the data completion, in a parallel task with the third player, which minimizes a Kohn-Vogelius like functional in order to identify the different sources magnitudes.

The efficiency and robustness of our coupled reconstruction algorithm was proved against several numerical experiments led for different two- and three-dimensional test-cases.

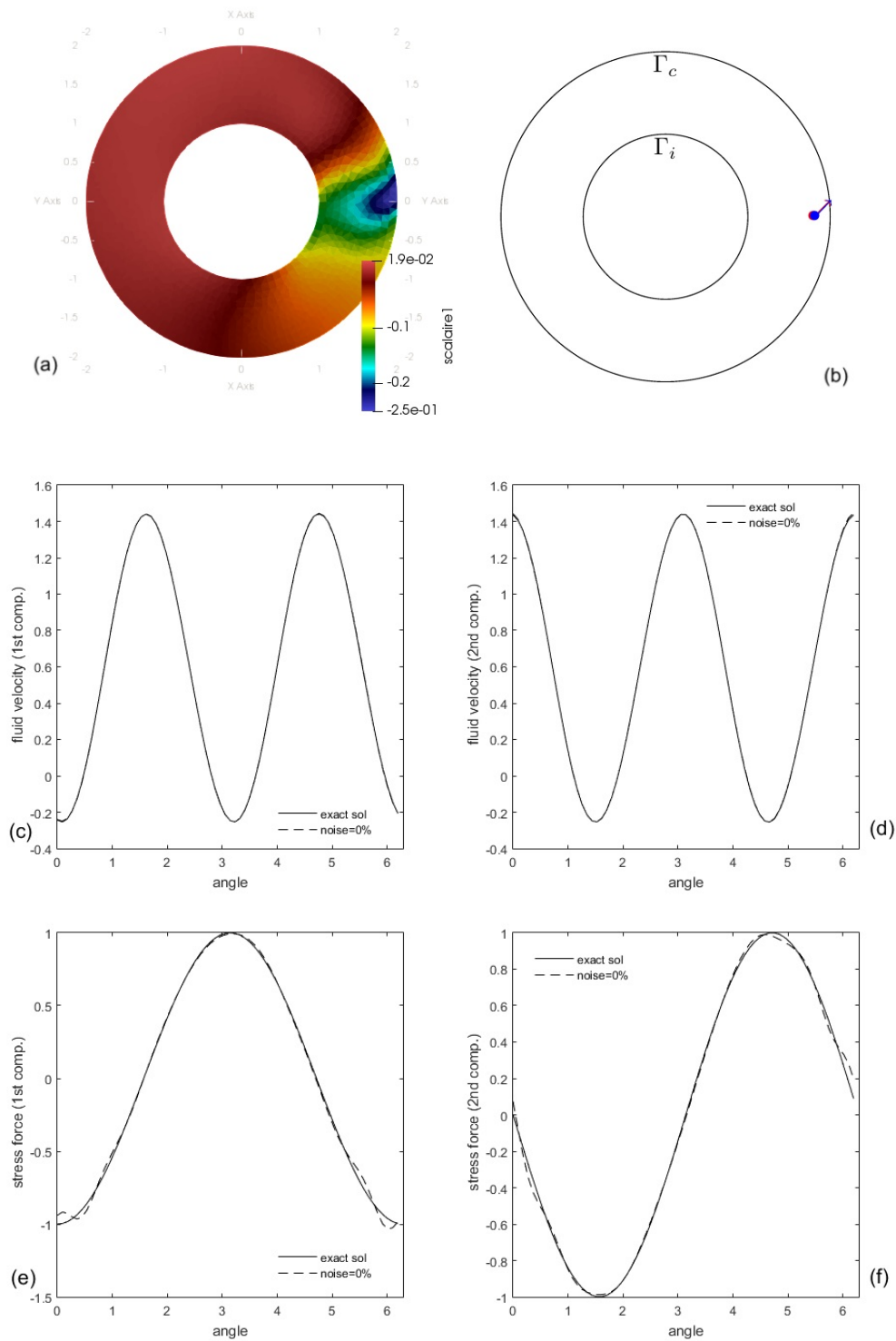


FIGURE 3.5 – Test case A. Reconstruction of the point-forces and missing boundary data with noise free Dirichlet data over  $\Gamma_c$ . (a) the iso-values of the topological gradient at convergence. (b) exact elements defining the source-term -red vector- and computed one -blue vector- (c) exact -line- and computed -dashed line- first component of the velocity over  $\Gamma_i$ . (d) exact -line- and computed -dashed line- second component of the velocity over  $\Gamma_i$ . (e) exact -line- and computed -dashed line- first component of the normal stress over  $\Gamma_i$  (f) exact -line- and computed -dashed line- second component of the normal stress over  $\Gamma_i$ .

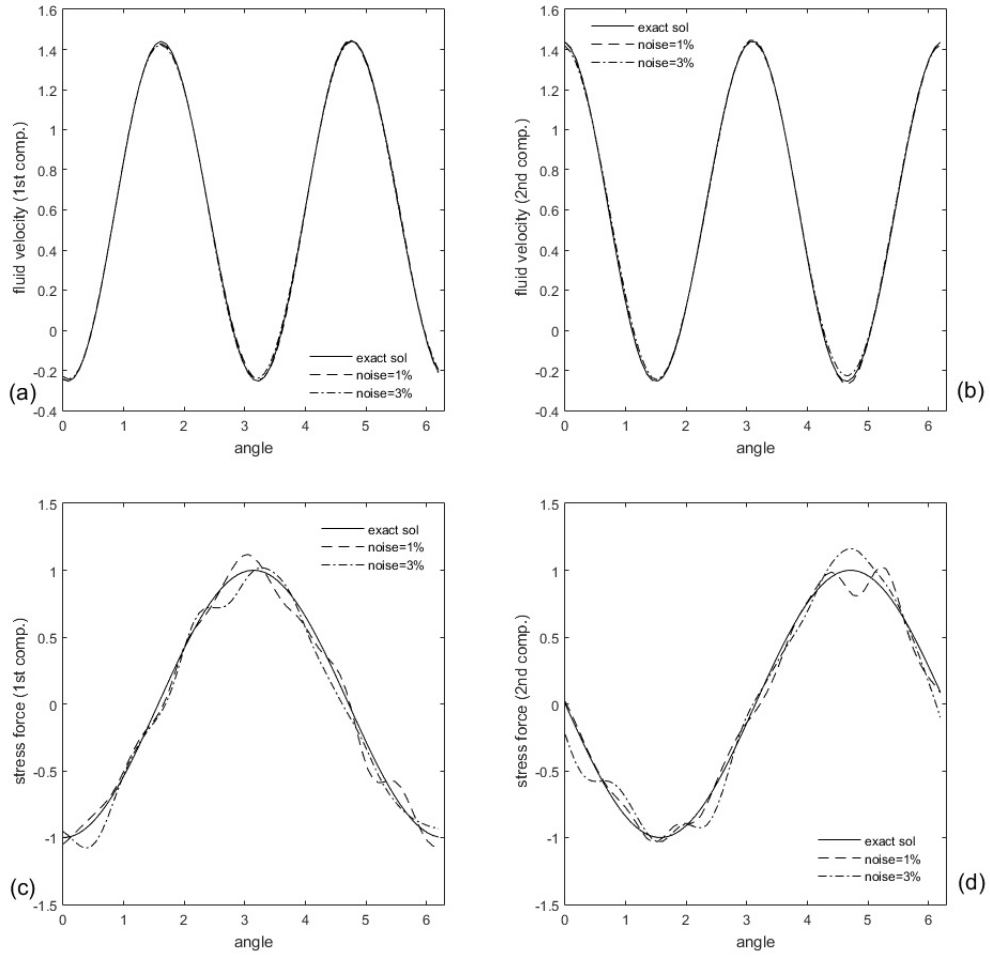


FIGURE 3.6 – Test case A. Reconstruction of the missing boundary data with noisy Dirichlet data over  $I_C$  with noise levels  $\sigma = \{1\%, 3\%\}$ . **(a)** exact and computed first components of the velocity over  $I_i$  **(b)** exact and computed second components of the velocity over  $I_i$  **(c)** exact and computed first components of the normal stress over  $I_i$  **(d)** exact and computed second components of the normal stress over  $I_i$ .

Table 3.4 – Test-case A. Identified source position and their intensity for various noise levels.

Noise level	$\sigma = 0\%$	$\sigma = 1\%$	$\sigma = 3\%$	
$P_{op}$	(1.81,-2e-09)	(1.81,-2.e-09)	(1.84,-0.066)	$P_{ex} = (1.8, 0)$
$\Lambda_{op}$	(0.195,0.202)	(0.161,0.179)	(0.2,0.152)	$\Lambda_{ex} = (0.2, 0.2)$

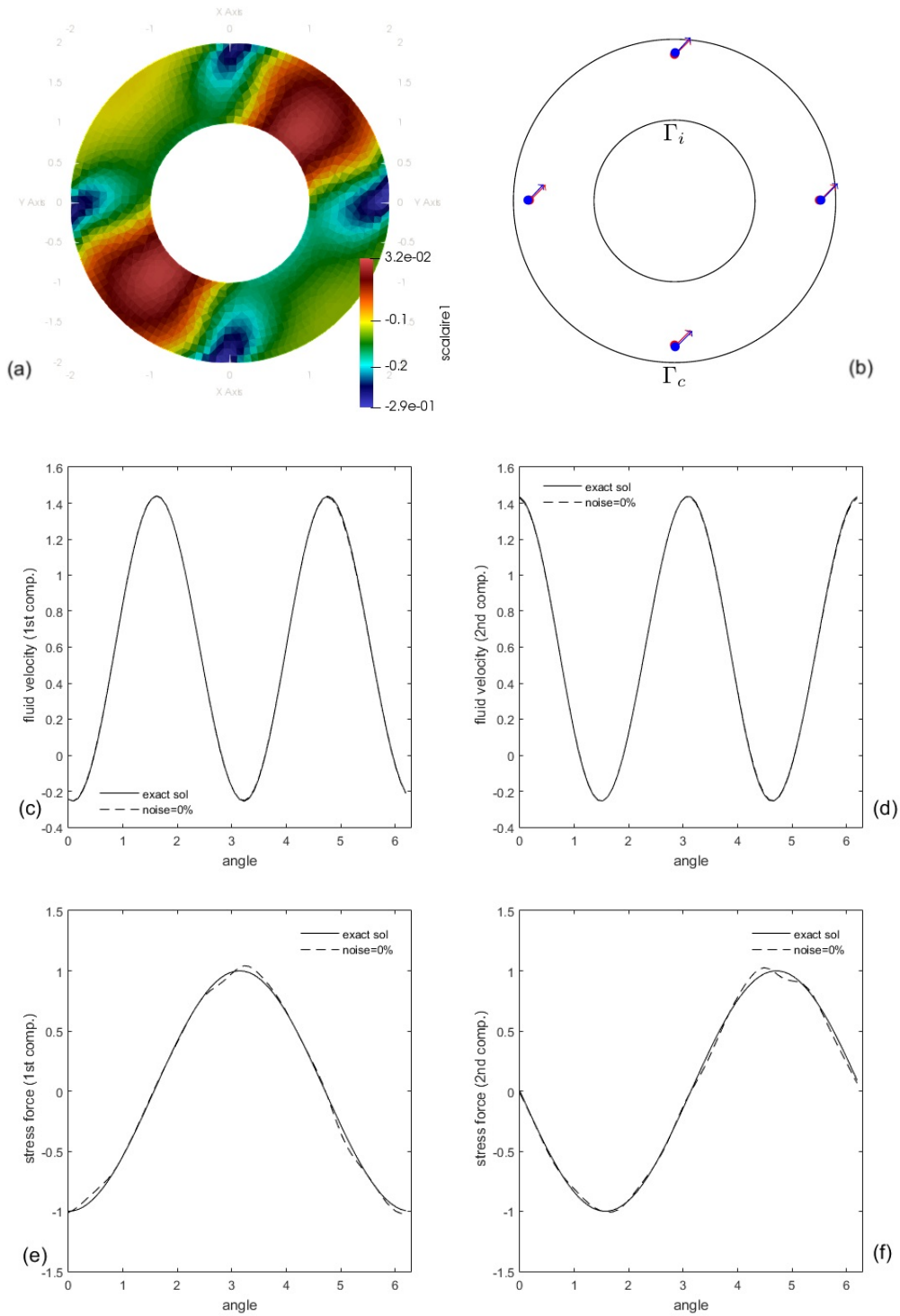


FIGURE 3.7 – Test case B. Reconstruction of the point-forces and missing boundary data with noise free Dirichlet data over  $\Gamma_c$ . (a) the iso-values of the topological gradient at convergence. (b) exact elements defining the source-term -red vector- and computed one -blue vector- (c) exact -line- and computed -dashed line- first component of the velocity over  $\Gamma_i$ . (d) exact -line- and computed -dashed line- second component of the velocity over  $\Gamma_i$ . (e) exact -line- and computed -dashed line- first component of the normal stress over  $\Gamma_i$  (f) exact -line- and computed -dashed line- second component of the normal stress over  $\Gamma_i$ .

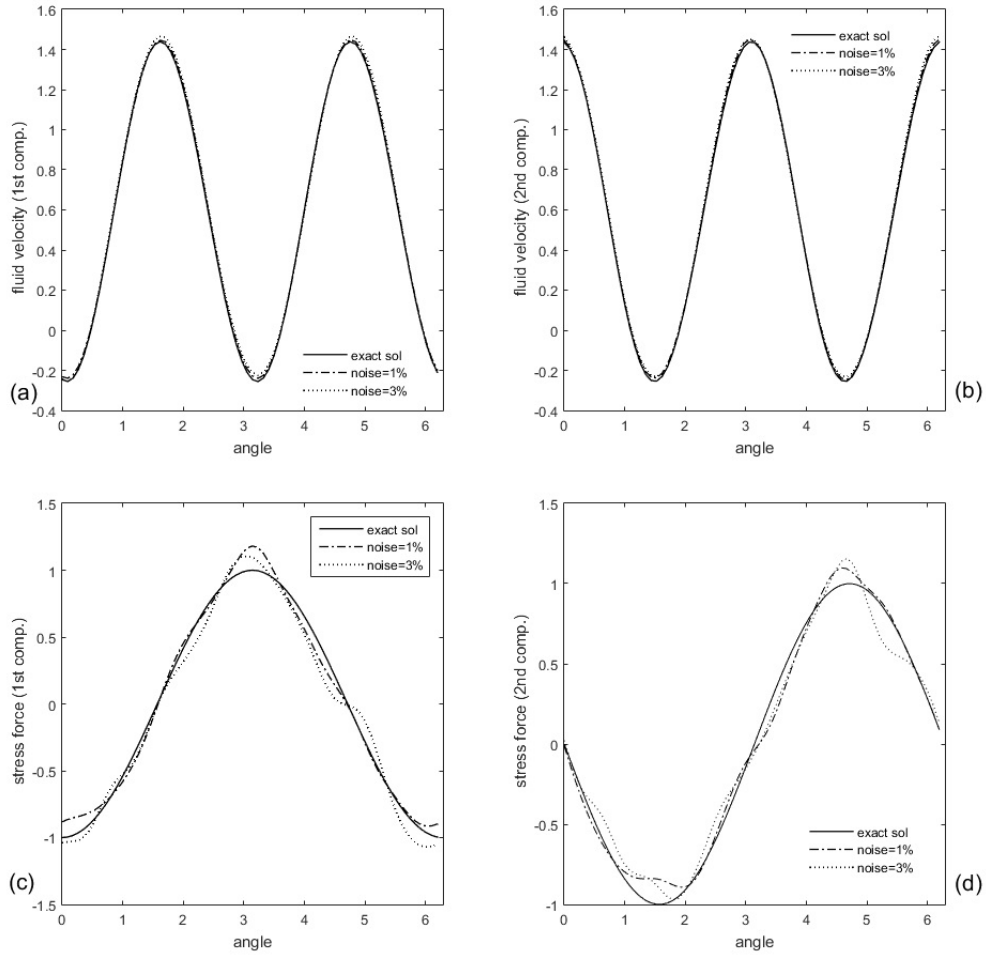


FIGURE 3.8 – Test case B. Reconstruction of the missing boundary data with noisy Dirichlet data over  $\Gamma_C$  with noise levels  $\sigma = \{1\%, 3\%\}$ . **(a)** exact and computed first components of the velocity over  $\Gamma_i$  **(b)** exact and computed second components of the velocity over  $\Gamma_i$  **(c)** exact and computed first components of the normal stress over  $\Gamma_i$  **(d)** exact and computed second components of the normal stress over  $\Gamma_i$ .

Table 3.5 – Test-case B.  $L^2$  relative errors on missing data on  $\Gamma_i$  (on Dirichlet and Neumann data), and the relative errors on the identified source position and on the identified source intensity for various noise levels.

Noise level	$err_D$	$err_N$	$err_P$	$err_\Lambda$
$\sigma = 0\%$	0.005	0.056	0.010	0.049
$\sigma = 1\%$	0.013	0.113	0.010	0.181
$\sigma = 3\%$	0.025	0.141	0.043	0.24

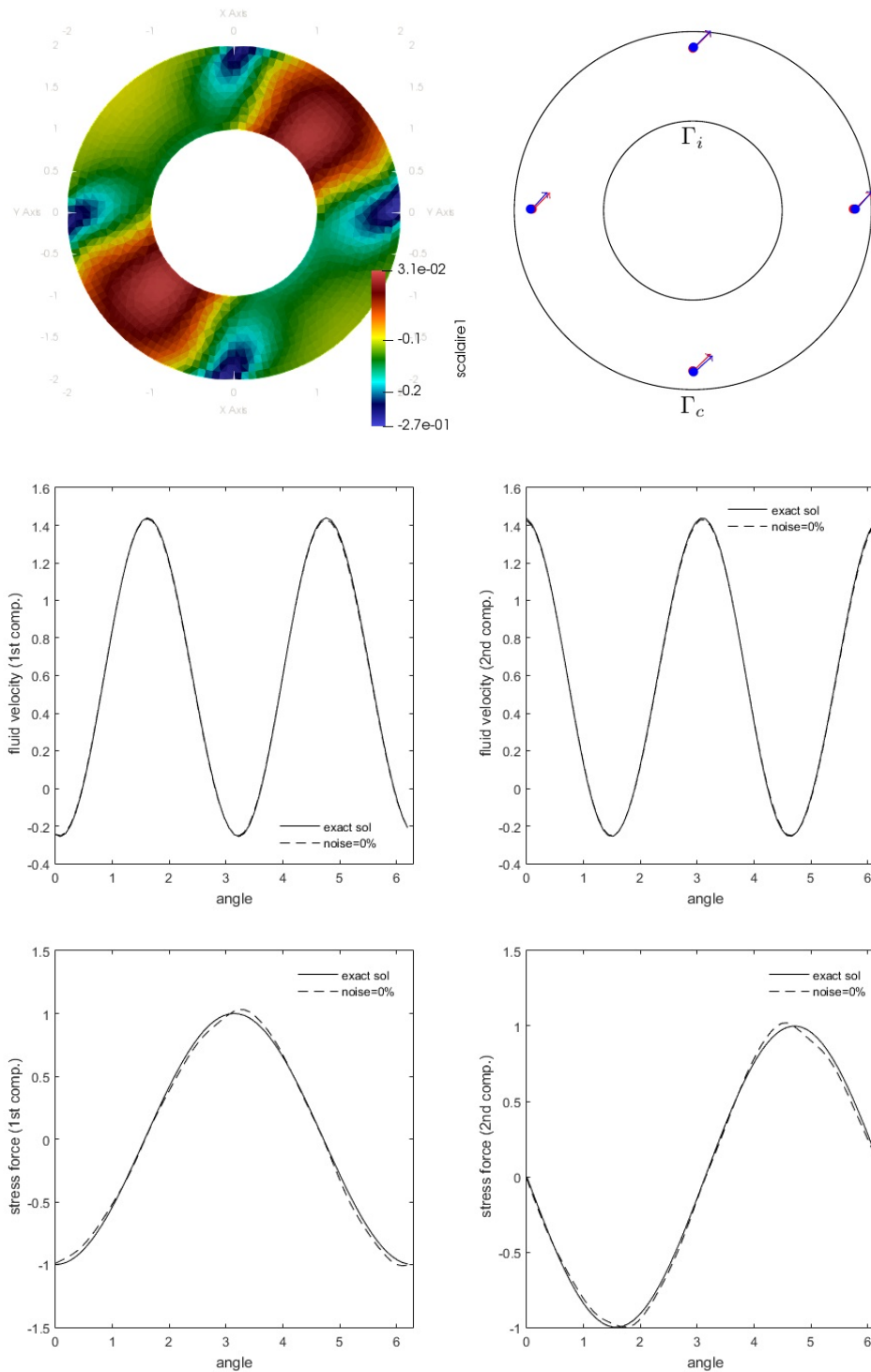


FIGURE 3.9 – Test case B : Assessing Inverse-Crime-Free reconstruction. Test case B. Top : the iso-values of the topological gradient at convergence, and the exact and optimal elements defining the source-term. Middle : the two components of the velocity on  $\Gamma_i$ . Bottom : the two components of the normal stress on  $\Gamma_i$  ( $err_\tau = 0.00768152$ ,  $err_\eta = 0.0713575$ ,  $err_P = 0.0105486$ , and  $err_\Lambda = 0.0560551$ ).

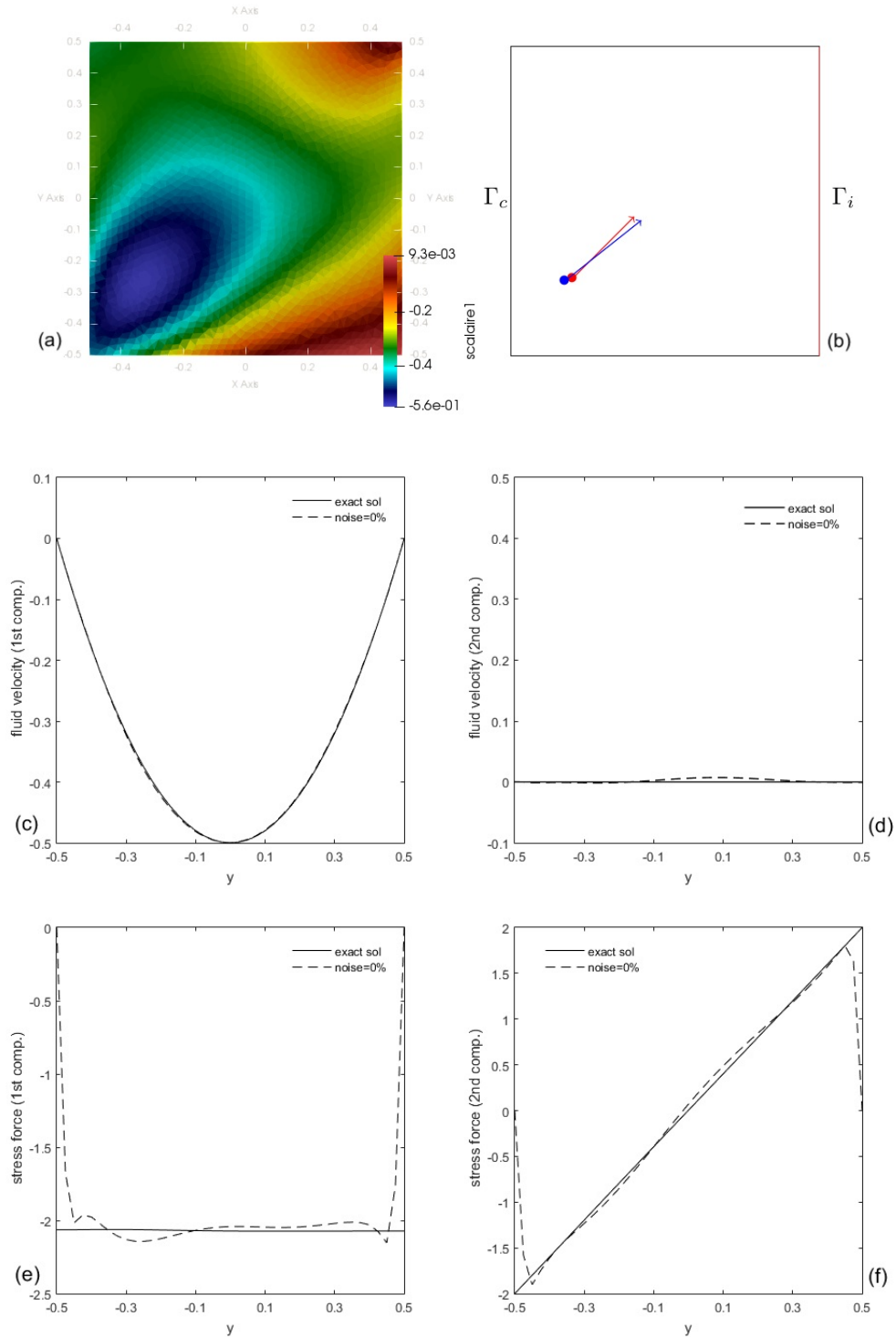


FIGURE 3.10 – Test case C. Reconstruction of the point-forces and missing boundary data with noise free Dirichlet data over  $\Gamma_c$ . (a) the iso-values of the topological gradient at convergence. (b) exact elements defining the source-term -red vector- and computed one -blue vector- (c) exact -line- and computed -dashed line- first component of the velocity over  $\Gamma_i$ . (d) exact -line- and computed -dashed line- second component of the velocity over  $\Gamma_i$ . (e) exact -line- and computed -dashed line- first component of the normal stress over  $\Gamma_i$  (f) exact -line- and computed -dashed line- second component of the normal stress over  $\Gamma_i$ .



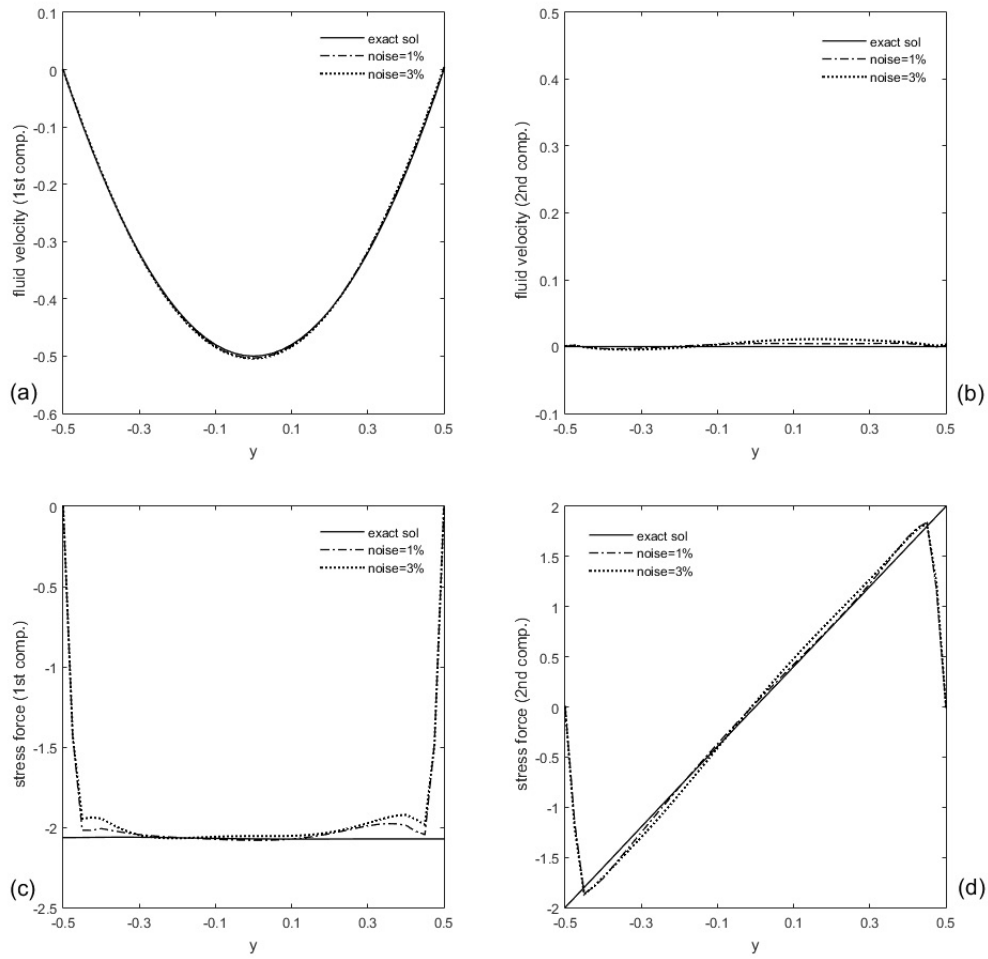


FIGURE 3.11 – Test case C. Reconstruction of the missing boundary data with noisy Dirichlet data over  $I_c$  with noise levels  $\sigma = \{1\%, 3\%\}$ . **(a)** exact and computed first components of the velocity over  $I_i$  **(b)** exact and computed second components of the velocity over  $I_i$  **(c)** exact and computed first components of the normal stress over  $I_i$  **(d)** exact and computed second components of the normal stress over  $I_i$ .

Table 3.6 – Test-case C. Identified source position and their intensity for various noise levels.

Noise level $\sigma = 0\%$	$\sigma = 1\%$	$\sigma = 3\%$	
$P_{op}$	(-0.326,-0.259)	(-0.339,-0.285)	$P_{ex} = (-0.3, -0.25)$
$\Lambda_{op}$	(0.248,0.197)	(0.24,0.199)	$\Lambda_{ex} = (0.25, 0.2)$ .

# A Nash-game approach to joint data completion and location of small inclusions in Stokes flow

*“ If people do not believe that mathematics is simple, it is only because they do not realize how complicated life is. ”*

---

John Louis von Neumann

**Abstract.** We consider the coupled inverse problem of data completion and the determination of the best locations of an unknown number of small objects immersed in a stationary viscous fluid. We carefully introduce a novel method to solve this problem based on a game theory approach. A new algorithm is provided to recovering the missing data and the number of these objects and their approximate location simultaneously. The detection problem is formulated as a topological one. We present two test-cases that illustrate the efficiency of our original strategy to deal with the ill-posed problem.

**keywords :** Geometric inverse problem, Data completion, Calculus of variations, Topological sensitivity, Nash games.

The results presented in this chapter lead to the paper :  
A. Habbal, M. Kallel, and M. Ouni. A Nash-game approach to joint data completion and location of small inclusions in Stokes flow. Accepted for publication in the *ARIMA* journal in December 2020.

---

## Contents

---

<b>4.1</b>	<b>Introduction and motivation</b>	<b>92</b>
<b>4.2</b>	<b>Data completion and localization of small objects</b>	<b>93</b>
4.2.1	The topological gradient method	95
4.2.2	Application to the model problem	96
<b>4.3</b>	<b>Numerical simulations.</b>	<b>102</b>
<b>4.4</b>	<b>Conclusion</b>	<b>104</b>

---

---

## 4.1 Introduction and motivation

Geometric inverse problems are central in various fields of industrial, biological, and biomedical processes. Challenging theoretical and computational problems arising in fluid mechanics have been intensively investigated, see e.g. [25]. In the present paper, we study a geometric identification problem related to Stokes flows. The problem amounts to determining the unknown number of small objects located in a stationary viscous fluid and their approximate locations, using partial boundary measurements. The latter are of Cauchy type data, available only on the -accessible- part of the outer boundary. Then, the inverse problem under consideration here consists of a coupled inverse problem of object detection and data completion. The identifiability result for the inverse inclusion Cauchy-Stokes problem, with a homogeneous Neumann condition imposed on the unknown geometry, of Habbal et al. [57] implies that a single pair of compatible- measurements is enough to recover the unknown objects and the missing boundary data on the remaining -inaccessible- part of the exterior boundary. It is well known that the considered inverse problems are ill-posed, in Hadamard's sense [59]. The problem's ill-posed character is worsened by the coupling, and is critically related to the solution's instability. Ill-posedness makes classical numerical methods usually inappropriate, and consequently, some regularization techniques have to be used to solve the problem numerically. In order to address the present coupled ill-posedness, we use a game-theoretic framework, following the works [56, 57]. We then suggest an alternating minimization approach, where the coupled inverse problem is formulated as a three players non-cooperative Nash game. The two first players are associated with the data completion while the third one is in charge of identifying the number of small objects and their location. The small size assumption made on the objects allows deriving an asymptotic expansion of an involved functional. To solve the identification problem, we use the topological gradient notion. Topological sensitivity analysis related to Stokes equations has been investigated in the past by several authors. Various other mathematical approaches in different frameworks are available to solve the obstacle inverse problem, such that the level-set approach, shape gradient method, and homogenization theory.

Let us introduce a preliminary mathematical description of the problem. Consider a bounded open domain  $\Omega \subset \mathbb{R}^d$  ( $d=2,3$ ), which is filled with a viscous incompressible fluid. We assume that a finite number of the objects included in the domain  $\Omega$ , and we also suppose that these unknown objects are well separated and have the geometry form :  $\mathcal{O}_{z_k, \epsilon} = z_k + \epsilon \mathcal{B}_k; \forall k \in \{1, \dots, m\}$ , where  $\epsilon$  is the shared diameter and  $\mathcal{B}_k$  is bounded and smooth domain containing the origin. The points  $z_k \in \Omega$  determine the location of the unknown objects inside  $\Omega$ . Finally, we suppose that for  $k \in \{1, \dots, m\}$ , the object  $\mathcal{O}_{z_k, \epsilon}$  is far from the exterior boundary  $\partial\Omega$ , which is composed of two disjoint components  $I_i$  and  $I_c$ , see Figure-4.1.

The problem we study then is to detect some small objects (location of the inclusions), from given fluid velocity  $f$  and stress forces  $\Phi$  prescribed only on the accessible part  $I_c$  of the boundary. We denote  $\mathcal{O}_\epsilon^* = \cup_{k=1}^m \mathcal{O}_{z_k, \epsilon}^*$  and we consider the following

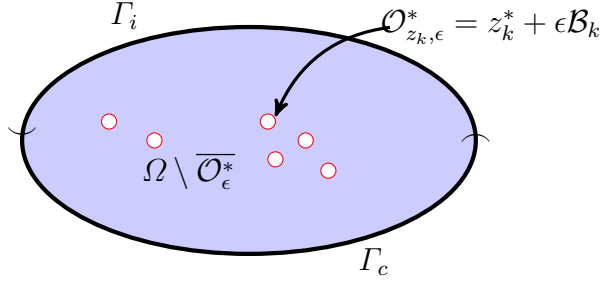


FIGURE 4.1 – An example of the geometric configuration of the problem : The whole domain  $\Omega$ , the inclusions  $\mathcal{O}_\epsilon^*$ , and two parts of the boundary  $\Gamma_c$  and  $\Gamma_i$ .

problem :

$$\begin{cases} \Delta u - \nabla p = 0 & \text{in } \Omega \setminus \overline{\mathcal{O}_\epsilon^*}, \\ \operatorname{div} u = 0 & \text{in } \Omega \setminus \overline{\mathcal{O}_\epsilon^*}, \\ \sigma(u, p)n = 0 & \text{on } \partial\mathcal{O}_\epsilon^*, \\ u = f & \text{on } \Gamma_c, \\ \sigma(u, p)n = \Phi & \text{on } \Gamma_c, \end{cases} \quad (4.1)$$

where  $u$  denote the velocity field,  $p$  the pressure, and  $\sigma(u, p)$  represents the stress tensor defined by :

$$\sigma(u, p) = 2\nu\mathcal{D}(u) - pI_d,$$

with  $\nu$  is the kinematic viscosity of the fluid,  $\mathcal{D}(u) = 1/2(\nabla u + {}^t\nabla u)$  is the deformation tensor, and  $I_d$  is the identity matrix.

This work aims to recover the missing data of fluid velocity  $u$  and stress forces  $\sigma(u, p)n$  over  $\Gamma_i$  the inaccessible part of the boundary from available measurements on the accessible part  $\Gamma_c$ , in addition determine the number of the small objects included in a flow domain and their approximate locations. Section 2 presents an original approach to jointly solving data completion and object detection problems using a Nash game strategy. A topological sensitivity analysis method is used in order to determine the optimal locations of these inclusions, and a new algorithm is provided. In section 3, we illustrate the efficiency of the proposed method by treating two different situations.

## 4.2 Data completion and localization of small objects

Assuming that the Cauchy data  $f$  and  $\Phi$  belongs to  $H^{\frac{1}{2}}(\Gamma_c)^d \times (H_{00}^{\frac{1}{2}}(\Gamma_c)^d)'$ . For given functions  $\eta \in (H_{00}^{\frac{1}{2}}(\Gamma_i)^d)'$ ,  $\tau \in H^{\frac{1}{2}}(\Gamma_i)^d$ , and  $\mathcal{O}_\epsilon = \cup_{k=1}^m z_k + \epsilon\mathcal{B}_k \subset \Omega$ , we define  $(u_1^\epsilon, p_1^\epsilon) = (u_1^\epsilon(\eta), p_1^\epsilon(\eta))$ ,  $(u_2^\epsilon, p_2^\epsilon) = (u_2^\epsilon(\tau), p_2^\epsilon(\tau))$ , and  $(u_3^\epsilon, p_3^\epsilon) = (u_3^\epsilon(\tau), p_3^\epsilon(\tau))$  as the unique weak solutions of the following Stokes mixed boundary value problems :

$$\begin{cases}
(\mathcal{P}_1^\epsilon) \left\{ \begin{array}{l}
\text{Find } (u_1^\epsilon, p_1^\epsilon) \in (H^1(\Omega \setminus \overline{\mathcal{O}_\epsilon}))^d \times L^2(\Omega \setminus \overline{\mathcal{O}_\epsilon}) \text{ such that :} \\
-div(\sigma(u_1^\epsilon, p_1^\epsilon)) = 0 \quad \text{in } \Omega \setminus \overline{\mathcal{O}_\epsilon}, \\
\operatorname{div} u_1^\epsilon = 0 \quad \text{in } \Omega \setminus \overline{\mathcal{O}_\epsilon}, \\
\sigma(u_1^\epsilon, p_1^\omega) n = 0 \quad \text{on } \partial\mathcal{O}_\epsilon, \\
u_1^\epsilon = f \quad \text{on } \Gamma_c, \\
\sigma(u_1^\epsilon, p_1^\epsilon) n = \eta \quad \text{on } \Gamma_i.
\end{array} \right. \\
(\mathcal{P}_2^\epsilon) \left\{ \begin{array}{l}
\text{Find } (u_2^\epsilon, p_2^\epsilon) \in (H^1(\Omega \setminus \overline{\mathcal{O}_\epsilon}))^d \times L^2(\Omega \setminus \overline{\mathcal{O}_\epsilon}) \text{ such that :} \\
-div(\sigma(u_2^\epsilon, p_2^\epsilon)) = 0 \quad \text{in } \Omega \setminus \overline{\mathcal{O}_\epsilon}, \\
\operatorname{div} u_2^\epsilon = 0 \quad \text{in } \Omega \setminus \overline{\mathcal{O}_\epsilon}, \\
\sigma(u_2^\epsilon, p_2^\epsilon) n = 0 \quad \text{on } \partial\mathcal{O}_\epsilon, \\
u_2^\epsilon = \tau \quad \text{on } \Gamma_i, \\
\sigma(u_2^\epsilon, p_2^\epsilon) n = \Phi \quad \text{on } \Gamma_c.
\end{array} \right. \\
(\mathcal{P}_3^\epsilon) \left\{ \begin{array}{l}
\text{Find } (u_3^\epsilon, p_3^\epsilon) \in (H^1(\Omega \setminus \overline{\mathcal{O}_\epsilon}))^d \times L^2_0(\Omega \setminus \overline{\mathcal{O}_\epsilon}) \text{ such that :} \\
-div(\sigma(u_3^\epsilon, p_3^\epsilon)) = 0 \quad \text{in } \Omega \setminus \overline{\mathcal{O}_\epsilon}, \\
\operatorname{div} u_3^\epsilon = 0 \quad \text{in } \Omega \setminus \overline{\mathcal{O}_\epsilon}, \\
\sigma(u_3^\epsilon, p_3^\omega) n = 0 \quad \text{on } \partial\mathcal{O}_\epsilon, \\
u_3^\epsilon = \tau \quad \text{on } \Gamma_i, \\
u_3^\epsilon = f \quad \text{on } \Gamma_c.
\end{array} \right.
\end{cases}$$

In order to solve the inverse problem (4.1), we use the simplest class of games. Let us present the following three costs : For  $(\eta, \tau; \mathcal{Z}) \in (H_{00}^{\frac{1}{2}}(\Gamma_i)^d)' \times H^{\frac{1}{2}}(\Gamma_i)^d \times \Omega$ ,

$$\mathcal{J}_1(\eta, \tau; \mathcal{Z}) = \frac{1}{2} \|\sigma(u_1^\epsilon, p_1^\epsilon) n - \Phi\|_{(H_{00}^{\frac{1}{2}}(\Gamma_c)^d)'}^2 + \frac{1}{2} \|u_1^\epsilon - u_2^\epsilon\|_{H^{\frac{1}{2}}(\Gamma_i)^d}^2, \quad (4.2)$$

$$\mathcal{J}_2(\eta, \tau; \mathcal{Z}) = \frac{1}{2} \|u_2^\epsilon - f\|_{H^{\frac{1}{2}}(\Gamma_c)^d}^2 + \frac{1}{2} \|u_1^\epsilon - u_2^\epsilon\|_{H^{\frac{1}{2}}(\Gamma_i)^d}^2, \quad (4.3)$$

$$\mathcal{J}_3(\eta, \tau; \mathcal{Z}) = 2\nu \|\mathcal{D}(u_3^\epsilon) - \mathcal{D}(u_2^\epsilon)\|_{L^2(\Omega \setminus \overline{\mathcal{O}_\epsilon})}^2. \quad (4.4)$$

We shall say that there are three players : Player 1 and 2 control the respective strategies  $\eta \in (H_{00}^{\frac{1}{2}}(\Gamma_i)^d)'$  and  $\tau \in H^{\frac{1}{2}}(\Gamma_i)^d$ , and try to minimize their own cost, namely,  $\mathcal{J}_1$  for Player 1 and  $\mathcal{J}_2$  for Player 2, such that each cost functional split into a classical least square term depending only on  $\eta$  in  $\mathcal{J}_1$  and  $\tau$  in  $\mathcal{J}_2$ , and a common coupling term  $\frac{1}{2} \|u_1^\epsilon - u_2^\epsilon\|_{H^{\frac{1}{2}}(\Gamma_i)^d}^2$ , which depends on both  $\eta$  and  $\tau$ , and has a regularization effect in the partial minimization. Player 3 controls the strategy variable  $\mathcal{Z} = \{z_1, \dots, z_m\} \in \Omega$ , where no information on the number  $m$  is given, and tries to minimize a cost functional  $\mathcal{J}_3$  of Kohn-Vogelius type, which basically relies on an identifiability result.

We seek the solution of the original coupled problem as a Nash equilibrium, defined as follows :

**Definition 4.2.1** *A triplet  $(\eta_N, \tau_N, \mathcal{Z}_N) \in (H_{00}^{\frac{1}{2}}(\Gamma_i)^d)' \times H^{\frac{1}{2}}(\Gamma_i)^d \times \Omega$  is a Nash equilibrium for the three players game involving the costs  $\mathcal{J}_1$ ,  $\mathcal{J}_2$  and  $\mathcal{J}_3$  if :*

$$(NE) \left\{ \begin{array}{l}
\mathcal{J}_1(\eta_N, \tau_N, \mathcal{Z}_N) \leq \mathcal{J}_1(\eta, \tau_N, \mathcal{Z}_N), \quad \forall \eta \in (H_{00}^{\frac{1}{2}}(\Gamma_i)^d)', \\
\mathcal{J}_2(\eta_N, \tau_N, \mathcal{Z}_N) \leq \mathcal{J}_2(\eta_N, \tau, \mathcal{Z}_N), \quad \forall \tau \in H^{\frac{1}{2}}(\Gamma_i)^d, \\
\mathcal{J}_3(\eta_N, \tau_N, \mathcal{Z}_N) \leq \mathcal{J}_3(\eta_N, \tau_N, \mathcal{Z}), \quad \forall \mathcal{Z} \in \Omega.
\end{array} \right.$$

---

**Remark 4.2.1** *If we consider the case where possible object locations are known, concentrating only on the data completion problem, then the existence of a two-players Nash equilibrium can be proved by using the partial ellipticity of  $\mathcal{J}_1$  and  $\mathcal{J}_2$  with respect to  $\eta$  and  $\tau$ , respectively [56, 57]. This property allows us to restrict the search for Nash equilibria to bounded subsets of the strategy spaces, which remains consistent with the classical results of conditional stability of the Cauchy problem [3]. The existence of a three-players Nash equilibrium is much less easy to prove and is out of the scope of the present paper.*

**Remark 4.2.2** *We sometimes use the improper notation  $\mathcal{Z} \in \Omega$  to stipulate that  $\mathcal{Z}$  is made of a collection of points in  $\Omega$  whose size is unknown.*

The minimization problem  $\min_{\mathcal{Z} \in \Omega} \mathcal{J}_3$  can be formulated as a topological optimization problem as follows : for fixed  $\eta \in (H_{00}^{\frac{1}{2}}(I_i)^d)'$  and  $\tau \in H^{\frac{1}{2}}(I_i)^d$ ,

$$(\mathcal{P}_\epsilon) \left\{ \begin{array}{l} \text{Find } \mathcal{Z}^* = \{z_1^*, \dots, z_m^*\} \in \Omega, \text{ such that :} \\ \mathcal{J}(\Omega \setminus \overline{\mathcal{O}_\epsilon^*}) = \min_{\mathcal{Z} \in \Omega} \mathcal{J}(\Omega \setminus \overline{\mathcal{O}_\epsilon}), \end{array} \right.$$

where  $\mathcal{O}_\epsilon^* = \cup_{k=1}^m z_k^* + \epsilon \mathcal{B}_k \subset \Omega$ , and  $\mathcal{J}$  is defined by

$$\mathcal{J}(\Omega \setminus \overline{\mathcal{O}_\epsilon}) = \mathcal{J}_{KV}(u_2^\epsilon, u_3^\epsilon) := \mathcal{J}_3(\eta, \tau; \mathcal{Z}). \quad (4.5)$$

In order to solve the optimization problem  $(\mathcal{P}_\epsilon)$  above, we will use the notion of topological gradient. The topological gradient method has been known as an efficient approach to solving geometric optimization problems. It consists of studying the variation of a cost function with respect to modifying the topology of the domain  $\Omega$ . For simplicity in what follows, we will consider the case of a single object  $\mathcal{O}_{z,\epsilon}$ . Notice that in the case of several inclusions, the results presented below are still valid.

### 4.2.1 The topological gradient method

The topological sensitivity analysis consists in the study of the variations of a design functional  $\mathcal{J}$  with respect to the insertion of a small inclusion  $\mathcal{O}_{z,\epsilon}$  at the point  $z$ . Then, an asymptotic expansion of the function  $\mathcal{J}$  can be obtained in the following form : for  $\epsilon > 0$

$$\begin{aligned} \mathcal{J}(\Omega_{z,\epsilon}) &= \mathcal{J}(\Omega) + \rho(\epsilon) \delta \mathcal{J}(z) + o(\rho(\epsilon)), \quad \forall z \in \Omega, \\ \lim_{\epsilon \rightarrow 0} \rho(\epsilon) &= 0, \quad \rho(\epsilon) > 0, \end{aligned}$$

where  $\Omega_{z,\epsilon} = \Omega \setminus \overline{\mathcal{O}_{z,\epsilon}}$  and the function  $\delta \mathcal{J}(z)$  is the so-called topological gradient. This function  $\delta \mathcal{J}(z)$  provides an information for creating a small hole located at  $z$ . Hence, it can be used like a descent direction in an optimization process. Therefore, to minimize the cost function, one has to create small hole at the location  $z$  when  $\delta \mathcal{J}$  is the most negative.

The concept of the topological derivative was introduced by Schumacher [45] in the case of compliance minimization. Next, Sokolowski et al [91] extended it to a more general shape functionals. Various kinds of topology optimization problems have been solved efficiently by using the topological gradient method. It has been widely applied

in literature for arbitrarily shaped perturbations and a general class of cost functionals related to PDEs : the elasticity equations [52], Laplace equations [9], Maxwell equations [79], and stokes system [25], with a homogeneous boundary conditions prescribed on the boundary of the objects.

An adaptation of the adjoint method to the topological context is developed in [52]. We now present the following proposition that describes a generalized adjoint method for the computation of the first variation of a given cost functional.

**Proposition 4.2.1** *Let  $\mathcal{V}$  be a Hilbert space. For  $\epsilon \in [0, \xi)$ ,  $\xi \geq 0$ , consider a function  $u_\epsilon \in \mathcal{V}$  that's solution of a variational problem of the form*

$$\mathcal{A}_\epsilon(u_\epsilon, v) = l_\epsilon(v), \quad \forall v \in \mathcal{V}$$

where  $\mathcal{A}_\epsilon$  and  $l_\epsilon$  are a bilinear form and a linear form on  $\mathcal{V}$ , respectively. For all  $\epsilon \in [0, \xi)$ , consider a functional  $j(\epsilon) = J_\epsilon(u_\epsilon)$ , where  $J_\epsilon$  is Fréchet differentiable at the point  $u_0$  and its derivative being denoted  $DJ(u_0)$ . Suppose that the following hypotheses hold :

(i)- *There exist two numbers  $\delta a$ ,  $\delta l$  and a function  $\rho(\epsilon) \geq 0$  such that*

$$(\mathcal{A}_\epsilon - \mathcal{A}_0)(u_0, v_\epsilon) = \rho(\epsilon)\delta a + o(\rho(\epsilon)),$$

$$(l_\epsilon - l_0)(v_\epsilon) = \rho(\epsilon)\delta l + o(\rho(\epsilon)),$$

$$\lim_{\epsilon \rightarrow 0} \rho(\epsilon) = 0,$$

where  $v_\epsilon$  is an adjoint state satisfying,

$$\mathcal{A}_\epsilon(w, v_\epsilon) = -DJ(u_0)w, \quad \forall w \in \mathcal{V}.$$

(ii)- *There exist a real number  $\delta J$  such that*

$$J_\epsilon(u_\epsilon) = J_0(u_0) + DJ(u_0)(u_\epsilon - u_0) + \rho(\epsilon)\delta J + o(\rho(\epsilon)).$$

Then, the first variation of the cost function with respect to  $\epsilon$  is given by

$$j(\epsilon) = j(0) + \rho(\epsilon)(\delta a + \delta l + \delta J) + o(\rho(\epsilon)).$$

## 4.2.2 Application to the model problem

The aim here is to derive an asymptotic expansion for our functional  $\mathcal{J}$  defined in (4.5) following the same steps described in the proposition 4.2.1 above. Then, we shall give explicitly the variations  $\delta a$ ,  $\delta l$ ,  $\delta \mathcal{J}_{KV}$ .

We start by defining the -control free- Sobolev state spaces : Given  $g \in H^{\frac{1}{2}}(\Gamma_i)^d$  and  $\phi \in H^{\frac{1}{2}}(\partial\Omega)$ ,

$$\mathcal{V}_{1,g}^\epsilon = \{v \in H^1(\Omega_{z,\epsilon})^d, \text{ such that } \operatorname{div} v = 0 \text{ in } \Omega_{z,\epsilon} \text{ and } v|_{\Gamma_i} = g\},$$

and

$$\mathcal{V}_{2,\phi}^\epsilon = \{v \in H^1(\Omega_{z,\epsilon})^d, \text{ such that } \operatorname{div} v = 0 \text{ in } \Omega_{z,\epsilon} \text{ and } v|_{\partial\Omega} = \phi\}.$$



The variational formulations associated to problems  $(\mathcal{P}_2^\epsilon)$  and  $(\mathcal{P}_3^\epsilon)$  can be stated respectively as follows :

$$\left\| \begin{array}{l} \text{Find } u_2^\epsilon \in \mathcal{V}_{1,\tau}^\epsilon \text{ such that :} \\ \mathcal{A}_{1,\epsilon}(u_2^\epsilon, v) = l_{1,\epsilon}(v), \quad \forall v \in \mathcal{V}_{1,0}^\epsilon, \end{array} \right. \quad (4.6)$$

$$\left\| \begin{array}{l} \text{Find } u_3^\epsilon \in W = \{\phi \in \mathcal{V}_{1,\tau}^\epsilon / \phi|_{\Gamma_c} = f\} \text{ such that :} \\ \mathcal{A}_{2,\epsilon}(u_3^\epsilon, v) = l_{2,\epsilon}(v), \quad \forall v \in \mathcal{V}_{2,0}^\epsilon, \end{array} \right. \quad (4.7)$$

where

$$\mathcal{A}_{1,\epsilon}(u_2^\epsilon, v) = 2\nu \int_{\Omega_{z,\epsilon}} \mathcal{D}(u_2^\epsilon) : \mathcal{D}(v) \, dx,$$

$$\mathcal{A}_{2,\epsilon}(u_3^\epsilon, v) = 2\nu \int_{\Omega_{z,\epsilon}} \mathcal{D}(u_3^\epsilon) : \mathcal{D}(v) \, dx,$$

$$l_{1,\epsilon}(v) = \int_{\Gamma_c} \Phi v \, ds,$$

and

$$l_{2,\epsilon}(v) = 0.$$

Note that for  $\epsilon = 0$ , we have  $\Omega_0 = \Omega$ , and  $(u_2^0, p_2^0) \in H^1(\Omega)^d \times L^2(\Omega)$  and  $(u_3^0, p_3^0) \in H^1(\Omega)^d \times L_0^2(\Omega)$  solve the respective boundary value problems :

$$(\mathcal{P}_2^0) \left\{ \begin{array}{l} \text{Find } (u_2^0, p_2^0) \in H^1(\Omega)^d \times L^2(\Omega) \text{ such that :} \\ -\text{div}(\sigma(u_2^0, p_2^0)) = 0 \quad \text{in } \Omega, \\ \text{div} u_2^0 = 0 \quad \text{in } \Omega, \\ u_2^0 = \tau \quad \text{on } \Gamma_i, \\ \sigma(u_2^0, p_2^0)n = \Phi \quad \text{on } \Gamma_c, \end{array} \right.$$

$$(\mathcal{P}_3^0) \left\{ \begin{array}{l} \text{Find } (u_3^0, p_3^0) \in H^1(\Omega)^d \times L_0^2(\Omega) \text{ such that :} \\ -\text{div}(\sigma(u_3^0, p_3^0)) = 0 \quad \text{in } \Omega, \\ \text{div} u_3^0 = 0 \quad \text{in } \Omega, \\ u_3^0 = \tau \quad \text{on } \Gamma_i, \\ u_3^0 = f \quad \text{on } \Gamma_c. \end{array} \right.$$

VARIATION OF THE BILINEAR FORM  $\mathcal{A}_{1,\epsilon}$  AND  $\mathcal{A}_{2,\epsilon}$  :

In order to obtain an asymptotic expansion of the variation of the bilinear form, we will use a simplified technique proposed in [25] for the Stokes system. We can also use a truncation technique, which is developed in [52] for elasticity equations, with a Neumann boundary condition on  $\partial\mathcal{O}_{z,\epsilon}$ .

Variation of  $\mathcal{A}_{1,\epsilon}$  : We are interested in the asymptotic analysis of the variation

$$\begin{aligned}
(\mathcal{A}_{1,\epsilon} - \mathcal{A}_{1,0})(u_2^0, v_1^\epsilon) &= -\mathcal{A}_{1,\epsilon}(u_2^\epsilon - u_2^0, v_1^\epsilon) + (l_{1,\epsilon}(v_1^\epsilon) - l_{1,0}(v_1^\epsilon)) \\
&= -\mathcal{A}_{1,\epsilon}(u_2^\epsilon - u_2^0, v_1^\epsilon) \\
&= -2\nu \int_{\Omega_{z,\epsilon}} \mathcal{D}(u_2^\epsilon - u_2^0) : \mathcal{D}(v_1^\epsilon) dx \\
&= \int_{\partial\mathcal{O}_{z,\epsilon}} \sigma(u_2^0, p_2^0)n v_1^\epsilon ds.
\end{aligned}$$

According to fundamental assumption (i) carefully formulated in proposition 4.2.1, we search to find a real number  $\delta a_1 \in \mathbb{R}$  and a scalar function positive  $\rho$  such that

$$\begin{aligned}
\int_{\partial\mathcal{O}_{z,\epsilon}} \sigma(u_2^0, p_2^0)n v_1^\epsilon ds &= \rho(\epsilon)\delta a_1 + o(\rho(\epsilon)), \\
\lim_{\epsilon \rightarrow 0} \rho(\epsilon) &= 0.
\end{aligned}$$

To this end, we start by splitting the integral above,

$$\begin{aligned}
\int_{\partial\mathcal{O}_{z,\epsilon}} \sigma(u_2^0, p_2^0)n v_1^\epsilon ds &= \int_{\partial\mathcal{O}_{z,\epsilon}} \sigma(u_2^0, p_2^0)n v_1^0 ds + \int_{\partial\mathcal{O}_{z,\epsilon}} \sigma(u_2^0, p_2^0)n (v_1^\epsilon - v_1^0) ds \\
&= \mathcal{I}_1 + \mathcal{I}_2.
\end{aligned}$$

Next, properly using the obtained estimates by Ben Abda et al [25] for each term  $\mathcal{I}_1$  and  $\mathcal{I}_2$ , which are written as follows

$$\mathcal{I}_1 = -2\nu\epsilon^2|\mathcal{B}|\mathcal{D}(u_2^0)(z) : \mathcal{D}(v_1^0)(z) + o(\epsilon^2),$$

and

$$\mathcal{I}_2 = 2\nu\epsilon^2|\mathcal{B}|\mathcal{D}(u_2^0)(z) : \mathcal{D}(v_1^0)(z) - \epsilon^2\mathcal{D}(u_2^0)(z) : \int_{\partial\mathcal{B}} \mu(y)y^T ds + o(\epsilon^2),$$

where  $\mu \in H^{-\frac{1}{2}}(\partial\mathcal{B})^d$  is the solution to the boundary integral equation :  $\forall y \in \partial\mathcal{B}$ ,

$$-\frac{\mu(y)}{2} + \int_{\partial\mathcal{B}} [2\nu\mathcal{D}_y(E)(x-y)\mu(x)n(y) - P(x-y)\mu(x)n(y)] ds(x) = -2\nu\mathcal{D}(v_1^0)(z)n(y),$$

with  $(E, P)$  is the fundamental solution to the stokes system in  $\mathbb{R}^2$ . Therefore, we deduce

$$(\mathcal{A}_{1,\epsilon} - \mathcal{A}_{1,0})(u_2^0, v_1^\epsilon) = -\epsilon^2\mathcal{D}(u_2^0)(z) : \int_{\partial\mathcal{B}} \mu(y)y^T ds + o(\epsilon^2).$$

If  $\mathcal{B} = \mathcal{B}(0, 1)$ , using the same technique as that used in [25], we obtain

$$\delta a_1 = -4\nu\mathcal{D}(u_2^0)(z) : \mathcal{D}(v_1^0)(z),$$

where  $v_1^0 \in \mathcal{V}_{1,0}^0$  is the solution to the associated adjoint problem :

$$\mathcal{A}_{1,0}(w, v_1^0) = -\partial_{u_2^0}\mathcal{J}_{KV}(u_2^0, u_3^0)w, \quad \forall w \in \mathcal{V}_{1,0}^0.$$

Variation of  $\mathcal{A}_{2,\epsilon}$  : Let us mention that the same bilinear form is available also for the  $(\mathcal{P}_3^\epsilon)$ , namely,  $\mathcal{A}_{1,\epsilon} \equiv \mathcal{A}_{2,\epsilon}$ . Thus, the variation of  $\mathcal{A}_{1,\epsilon}$  associated to  $(\mathcal{P}_3^\epsilon)$  is written as follows :

$$(\mathcal{A}_{2,\epsilon} - \mathcal{A}_{2,0})(u_3^0, v_2^\epsilon) = -4\nu\pi\epsilon^2\mathcal{D}(u_3^0)(z) : \mathcal{D}(v_2^0)(z),$$

where  $v_2^0 \in \mathcal{V}_{2,0}^0$  is the solution to the associated adjoint problem :

$$\mathcal{A}_{2,0}(w, v_2^0) = -\partial_{u_3^0} \mathcal{J}_{KV}(u_2^0, u_3^0)w, \quad \forall w \in \mathcal{V}_{2,0}^0.$$

VARIATION OF THE LINEAR FORM  $l_{1,\epsilon}$  AND  $l_{2,\epsilon}$  :

Since  $l_{1,\epsilon}$  and  $l_{2,\epsilon}$  are independent of  $\epsilon$ , it follows trivially that  $\delta l_1 = \delta l_2 = 0$ .

VARIATION OF THE COST FUNCTIONAL  $\mathcal{J}_{KV}$  :

Let us now turn to the asymptotic analysis of the variation of the Kohn-Vogeluis functional given by

$$\mathcal{J}_{KV}(u_2^\epsilon, u_3^\epsilon) = 2\nu \int_{\Omega_{z,\epsilon}} \mathcal{D}(u_3^\epsilon - u_2^\epsilon) : \mathcal{D}(u_3^\epsilon - u_2^\epsilon) dx.$$

One can decompose this above functional as follows :

$$\mathcal{J}_{KV}(u_2^\epsilon, u_3^\epsilon) = \mathfrak{J}_1(u_2^\epsilon) + \mathfrak{J}_2(u_3^\epsilon) - 2\mathfrak{J}_{12}(u_2^\epsilon, u_3^\epsilon),$$

where

$$\begin{aligned} \mathfrak{J}_1(u_2^\epsilon) &= 2\nu \int_{\Omega_{z,\epsilon}} \mathcal{D}(u_2^\epsilon) : \mathcal{D}(u_2^\epsilon) dx, \\ \mathfrak{J}_2(u_3^\epsilon) &= 2\nu \int_{\Omega_{z,\epsilon}} \mathcal{D}(u_3^\epsilon) : \mathcal{D}(u_3^\epsilon) dx, \\ \mathfrak{J}_{12}(u_2^\epsilon, u_3^\epsilon) &= 2\nu \int_{\Omega_{z,\epsilon}} \mathcal{D}(u_2^\epsilon) : \mathcal{D}(u_3^\epsilon) dx. \end{aligned}$$

*Variation of  $\mathfrak{J}_1$*  : The variation of  $\mathfrak{J}_1$  reads

$$\begin{aligned} \mathfrak{J}_1(u_2^\epsilon) - \mathfrak{J}_1(u_2^0) &= 2\nu \int_{\Omega_{z,\epsilon}} \mathcal{D}(u_2^\epsilon) : \mathcal{D}(u_2^\epsilon) dx - 2\nu \int_{\Omega} \mathcal{D}(u_2^0) : \mathcal{D}(u_2^0) dx \\ &= 2\nu \int_{\Omega_{z,\epsilon}} \mathcal{D}(u_2^\epsilon - u_2^0) : \mathcal{D}(u_2^\epsilon) dx + 2\nu \int_{\Omega_{z,\epsilon}} \mathcal{D}(u_2^\epsilon - u_2^0) : \mathcal{D}(u_2^0) dx \\ &\quad - 2\nu \int_{\mathcal{O}_{z,\epsilon}} \mathcal{D}(u_2^0) : \mathcal{D}(u_2^0) dx \end{aligned}$$

Using the Green formula applied to the problem  $(\mathcal{P}_2^\epsilon)$ , we get

$$2\nu \int_{\Omega_{z,\epsilon}} \mathcal{D}(u_2^\epsilon - u_2^0) : \mathcal{D}(u_2^\epsilon) dx = \int_{\Gamma_c} \Phi(u_2^\epsilon - u_2^0) ds.$$

Then, it follows that

$$\begin{aligned} \mathfrak{J}_1(u_2^\epsilon) - \mathfrak{J}_1(u_2^0) &= 2\nu \int_{\Omega_{z,\epsilon}} \mathcal{D}(u_2^\epsilon - u_2^0) : \mathcal{D}(u_2^0) dx - 2\nu \int_{\mathcal{O}_{z,\epsilon}} \mathcal{D}(u_2^0) : \mathcal{D}(u_2^0) dx \\ &\quad + \int_{\Gamma_c} \Phi(u_2^\epsilon - u_2^0) ds. \end{aligned} \tag{4.8}$$

Variation of  $\mathfrak{J}_2$  : The variation of  $\mathfrak{J}_2$  reads

$$\begin{aligned}\mathfrak{J}_2(u_3^\epsilon) - \mathfrak{J}_2(u_3^0) &= 2\nu \int_{\Omega_{z,\epsilon}} \mathcal{D}(u_3^\epsilon) : \mathcal{D}(u_3^\epsilon) dx - 2\nu \int_{\Omega} \mathcal{D}(u_3^0) : \mathcal{D}(u_3^0) dx \\ &= 2\nu \int_{\Omega_{z,\epsilon}} \mathcal{D}(u_3^\epsilon - u_3^0) : \mathcal{D}(u_3^\epsilon) dx + 2\nu \int_{\Omega_{z,\epsilon}} \mathcal{D}(u_3^\epsilon - u_3^0) : \mathcal{D}(u_3^0) dx \\ &\quad - 2\nu \int_{\mathcal{O}_{z,\epsilon}} \mathcal{D}(u_3^0) : \mathcal{D}(u_3^0) dx\end{aligned}$$

Using the Green formula, one can get from  $(\mathcal{P}_3^\epsilon)$  that

$$2\nu \int_{\Omega_{z,\epsilon}} \mathcal{D}(u_3^\epsilon - u_3^0) : \mathcal{D}(u_3^\epsilon) dx = 0.$$

Then, we obtain

$$\mathfrak{J}_2(u_2^\epsilon) - \mathfrak{J}_2(u_2^0) = 2\nu \int_{\Omega_{z,\epsilon}} \mathcal{D}(u_3^\epsilon - u_3^0) : \mathcal{D}(u_3^0) dx - 2\nu \int_{\mathcal{O}_{z,\epsilon}} \mathcal{D}(u_3^0) : \mathcal{D}(u_3^0) dx. \quad (4.9)$$

Variation of  $\mathfrak{J}_{12}$  : The variation of  $\mathfrak{J}_{12}$  reads

$$\mathfrak{J}_{12}(u_2^\epsilon, u_3^\epsilon) - \mathfrak{J}_{12}(u_2^0, u_3^0) = 2\nu \int_{\Omega_{z,\epsilon}} \mathcal{D}(u_2^\epsilon) : \mathcal{D}(u_3^\epsilon) dx - 2\nu \int_{\Omega} \mathcal{D}(u_2^0) : \mathcal{D}(u_3^0) dx.$$

Using the Green formula applied to  $(\mathcal{P}_2^\epsilon)$  and  $(\mathcal{P}_2^0)$ , we obtain

$$\begin{aligned}2\nu \int_{\Omega_{z,\epsilon}} \mathcal{D}(u_2^\epsilon) : \mathcal{D}(u_3^\epsilon) dx &= \int_{\Gamma_c} \Phi f ds + \int_{\Gamma_i} \sigma(u_2^\epsilon, p_2^\epsilon) n \tau ds. \\ 2\nu \int_{\Omega} \mathcal{D}(u_2^0) : \mathcal{D}(u_3^0) dx &= \int_{\Gamma_c} \Phi f ds + \int_{\Gamma_i} \sigma(u_2^0, p_2^0) n \tau ds.\end{aligned}$$

Then, we deduce

$$\mathfrak{J}_{12}(u_2^\epsilon, u_3^\epsilon) - \mathfrak{J}_{12}(u_2^0, u_3^0) = \int_{\Gamma_i} \sigma(u_2^\epsilon - u_2^0, p_2^\epsilon - p_2^0) n \tau ds. \quad (4.10)$$

Combining the variation (4.8), (4.9) and (4.10), the variation of the functional  $\mathcal{J}_{KV}$  becomes

$$\begin{aligned}\mathcal{J}_{KV}(u_2^\epsilon, u_3^\epsilon) - \mathcal{J}_{KV}(u_2^0, u_3^0) &= -2\nu \int_{\mathcal{O}_{z,\epsilon}} \mathcal{D}(u_2^0) : \mathcal{D}(u_2^0) dx - 2\nu \int_{\mathcal{O}_{z,\epsilon}} \mathcal{D}(u_3^0) : \mathcal{D}(u_3^0) dx \\ &\quad + 2\nu \int_{\Omega_{z,\epsilon}} \mathcal{D}(u_2^\epsilon - u_2^0) : \mathcal{D}(u_2^0) dx + 2\nu \int_{\Omega_{z,\epsilon}} \mathcal{D}(u_3^\epsilon - u_3^0) : \mathcal{D}(u_3^0) dx \\ &\quad + \int_{\Gamma_c} \Phi(u_2^\epsilon - u_2^0) ds - 2 \int_{\Gamma_i} \sigma(u_2^\epsilon - u_2^0, p_2^\epsilon - p_2^0) n \tau ds.\end{aligned}$$

Then for  $\epsilon \in [0, \xi)$ , we get

$$\begin{aligned}D\mathcal{J}_{KV}(u_2^0, u_3^0)(u_2^\epsilon - u_2^0, u_3^\epsilon - u_3^0) &= 2\nu \int_{\Omega_{z,\epsilon}} \mathcal{D}(u_2^\epsilon - u_2^0) : \mathcal{D}(u_2^0) dx \\ &\quad + 2\nu \int_{\Omega_{z,\epsilon}} \mathcal{D}(u_3^\epsilon - u_3^0) : \mathcal{D}(u_3^0) dx + \int_{\Gamma_c} \Phi(u_2^\epsilon - u_2^0) ds \\ &\quad - 2 \int_{\Gamma_i} \sigma(u_2^\epsilon - u_2^0, p_2^\epsilon - p_2^0) n \tau ds.\end{aligned}$$

Thus, we have

$$\begin{aligned} \mathcal{J}_{KV}(u_2^\epsilon, u_3^\epsilon) - \mathcal{J}_{KV}(u_2^0, u_3^0) &= D\mathcal{J}_{KV}(u_2^0, u_3^0)(u_2^\epsilon - u_2^0, u_3^\epsilon - u_3^0) \\ &\quad - 2\nu \int_{\mathcal{O}_{z,\epsilon}} \mathcal{D}(u_2^0) : \mathcal{D}(u_2^0) dx - 2\nu \int_{\mathcal{O}_{z,\epsilon}} \mathcal{D}(u_3^0) : \mathcal{D}(u_3^0) dx. \end{aligned} \quad (4.11)$$

Next, the second term on the right hand side of (4.11) may be written as

$$\begin{aligned} 2\nu \int_{\mathcal{O}_{z,\epsilon}} \mathcal{D}(u_2^0) : \mathcal{D}(u_2^0) dx &= 2\nu \int_{\mathcal{O}_{z,\epsilon}} \mathcal{D}(u_2^0)(z) : \mathcal{D}(u_2^0)(z) dx \\ &\quad + 2\nu \int_{\mathcal{O}_{z,\epsilon}} [\mathcal{D}(u_2^0) - \mathcal{D}(u_2^0)(z)] : \mathcal{D}(u_2^0) dx \\ &\quad + 2\nu \int_{\mathcal{O}_{z,\epsilon}} \mathcal{D}(u_2^0)(z) : [\mathcal{D}(u_2^0) - \mathcal{D}(u_2^0)(z)] dx. \end{aligned}$$

Using the Taylor theorem and the change of variables  $x = z + \epsilon y$ , we obtain

$$2\nu \int_{\mathcal{O}_{z,\epsilon}} \mathcal{D}(u_2^0) : \mathcal{D}(u_2^0) dx = 2\nu\epsilon^2 |\mathcal{B}| \mathcal{D}(u_2^0)(z) : \mathcal{D}(u_2^0)(z) + o(\epsilon^2).$$

The same way for the third term, we have

$$2\nu \int_{\mathcal{O}_{z,\epsilon}} \mathcal{D}(u_3^0) : \mathcal{D}(u_3^0) dx = 2\nu\epsilon^2 |\mathcal{B}| \mathcal{D}(u_3^0)(z) : \mathcal{D}(u_3^0)(z) + o(\epsilon^2).$$

Thus,

$$\delta\mathcal{J}_{KV} = -2\nu\pi(|\mathcal{D}(u_2^0)(z)|^2 + |\mathcal{D}(u_3^0)(z)|^2).$$

Now, we are ready to give the main result of this paper.

**Theorem 4.2.1** *If  $d = 2$ , the function  $\mathcal{J}$  has the following asymptotic expansion*

$$\mathcal{J}(\Omega_{z,\epsilon}) - \mathcal{J}(\Omega) = \pi\epsilon^d(\delta a_1(u_2^0, v_1^0) + \delta a_2(u_3^0, v_2^0) + \delta\mathcal{J}_{KV}(u_2^0, u_3^0)) + o(\epsilon^d),$$

where  $\forall z \in \Omega$ , we have

$$\begin{cases} \delta a_1(u_2^0, v_1^0) &= -4\nu\mathcal{D}(u_2^0)(z) : \mathcal{D}(v_1^0)(z), \\ \delta a_2(u_3^0, v_2^0) &= -4\nu\mathcal{D}(u_3^0)(z) : \mathcal{D}(v_2^0)(z), \\ \delta\mathcal{J}_{KV}(u_2^0, u_3^0) &= -2(|\mathcal{D}(u_2^0)(z)|^2 + |\mathcal{D}(u_3^0)(z)|^2), \end{cases}$$

with  $v_1^0 \in \mathcal{V}_{1,0}^0$  and  $v_2^0 \in \mathcal{V}_{2,0}^0$  are solutions to the adjoint equations associated respectively to the  $(\mathcal{P}_2^0)$  and  $(\mathcal{P}_3^0)$  :

$$\mathcal{A}_{1,0}(w, v_1^0) = -\partial_{u_2^0}\mathcal{J}(u_2^0, u_3^0)w, \quad \forall w \in \mathcal{V}_{1,0}^0,$$

$$\mathcal{A}_{2,0}(w, v_2^0) = -\partial_{u_3^0}\mathcal{J}(u_2^0, u_3^0)w, \quad \forall w \in \mathcal{V}_{2,0}^0.$$

We now present a novel algorithm dedicated to the Nash equilibrium computation, which is described below. The algorithm is divided into two main steps : In the

first, Player 3 seeks to identify the number and the best locations of the objects by minimizing  $\mathcal{J}_3$  and using a one-shot algorithm based on a topological derivative. In the second one, players 1 and 2 play a Nash subgame in order to precondition the Cauchy problem and tackle its ill-posedness. To save overall computation time, we consider parallel implementations for the computation of the two-players Nash equilibrium based on the alternating minimization algorithm introduced in [12]; we can also assume that the players solve their partial optimization problems sequentially, not simultaneously. Those algorithms are similar to alternating and parallel Schwarz methods. A fixed-step gradient method is used to solve the partial optimization problems of  $\mathcal{J}_1$  and  $\mathcal{J}_2$ .

---

**Algorithm 4.2.1:** Computation of the Nash equilibrium  $(\eta_N, \tau_N, \mathcal{Z}_N)$

---

Given : convergence tolerances  $\varepsilon_S, \varepsilon_N, Nmax$  a computational budget per Nash iteration,  $Kmax$  a maximum Nash iterations.

Set  $k = 0$  and choose an initial guess  $S^{(0)} = (\eta^{(0)}, \tau^{(0)}) \in (H_{00}^{\frac{1}{2}}(I_i)^d)' \times H^{\frac{1}{2}}(I_i)^d$  :

- Step I : Fix an initial shape  $\mathcal{O}_k = \emptyset$  and use the one-shot algorithm to determine

$$\mathcal{Z}^{(k+1)} = \operatorname{argmin}_{x \in \Omega} \mathcal{J}_3(\eta^{(k)}, \tau^{(k)}; x).$$

- Step II : Solve the Nash game between  $\eta$  and  $\tau$  : Set  $p = 0$ .

Set  $\Omega^{(k+1)} = \Omega \setminus \overline{\mathcal{O}_{k+1}}$ , where  $\mathcal{O}_{k+1} = \bigcup_{i=1}^{m_k} \mathcal{B}(z_i, r)$ .

1. Compute  $\bar{\eta}^{(p)}$ , which solves  $\min_{\eta} \mathcal{J}_1(\eta, \tau^{(p)}; \mathcal{Z}^{(k+1)})$ .

Evaluate  $\eta^{(p+1)} = \alpha \eta^{(p)} + (1 - \alpha) \bar{\eta}^{(p)}$ , with  $0 \leq \alpha < 1$ .

2. Compute  $\bar{\tau}^{(p)}$ , which solves  $\min_{\tau} \mathcal{J}_2(\eta^{(p)}, \tau; \mathcal{Z}^{(k+1)})$ .

Evaluate  $\tau^{(p+1)} = \alpha \tau^{(p)} + (1 - \alpha) \bar{\tau}^{(p)}$ , with  $0 \leq \alpha < 1$ .

3. Set  $S^{(p+1)} = (\eta^{(p+1)}, \tau^{(p+1)})$ .

While  $\|S^{(p+1)} - S^{(p)}\| > \varepsilon_S$  and  $p < Nmax$ , set  $p = p + 1$ , return back to step 1.

- Step III : Compute  $r_k = \|u_2^{(k)} - f\|_{0, \Gamma_c}$ , where  $(u_2^{(k)}, p_2^{(k)})$  is the solution of the problem  $(\mathcal{P}_2^\varepsilon)$ . If  $r_k < \varepsilon_N$  stop. Otherwise  $k = k + 1$ , go to Step I.
- 

### 4.3 Numerical simulations.

In this section, we will present some numerical reconstructions in two dimensions to show the efficiency of our novel approach, using synthetic data generated via a finite element resolution of boundary value problem, corresponding to a homogeneous Neumann condition on the boundary  $\partial\mathcal{O}_\varepsilon^*$  with the code *FreeFem++* [61].

The exterior boundary is assumed to be the rectangle  $\Omega = [-0.5, 0.5] \times [-0.25, 0.25]$ , which will be split in two components : the inaccessible part of the boundary  $I_i = \{0.5\} \times [-0.25, 0.25]$  and the accessible part  $I_c = \partial\Omega \setminus I_i$ , where the Cauchy data are available.

In the following, the subscripts *ex* and *opt* denote, respectively, exact and optimal values.

**Case A- Single object :** First, we start testing the detection of a single circle  $\mathcal{O}^* = \mathcal{C}(z_{ex}, r)$  centered at  $z_{ex} = (-0.3, -0.15)$  and  $r = 0.025$ .

Figure 4.2 presents the evolution of the three costs functionals as functions of overall Nash iterations for unnoisy data. We observe that during the early Nash iteration process, Player 1 shows a fast decrease of its cost  $\mathcal{J}_1$  then stagnates around 0.005, while the other players 2 and 3 continuously improve their own cost  $\mathcal{J}_2$  and  $\mathcal{J}_3$  respectively. The fact that each player controls only his strategy, while there is a strong dependence of each player's cost on the joint strategy, justifies the game theory framework employed to formulate the iterative negotiation between the costs. Typical of a static Nash equilibrium, the three players then proceed in the negotiation until none of them can unilaterally improve its cost, a behavior which is observed around iteration 18. The detection is quite efficient, see Figure 4.3(a)-(b), where 3(a) presents the iso-values of the topological gradient and 3(b) presents the obtained domain at convergence. Figure 4.4 show the reconstructed Dirichlet and Neumann boundary data. It can be seen that the reconstructed Dirichlet data give a good approximation for the exact one, while the reconstructed Neumann data deviate from the exact one, especially near the endpoints of the unspecified boundary, which is the region of singularities. At convergence, the approximate location  $z_{opt}$  is equal to  $(-0.294, -0.174)$  and the relative error on Dirichlet data  $\frac{\|\tau_{opt} - u_{ex}\|_{L^2(\Gamma_i)}}{\|u_{ex}\|_{L^2(\Gamma_i)}}$  and Neumann data  $\frac{\|\eta_{opt} - \sigma(u_{ex}, p_{ex})n\|_{L^2(\Gamma_i)}}{\|\sigma(u_{ex}, p_{ex})n\|_{L^2(\Gamma_i)}}$  are equal to 0.003 and 0.073 respectively.

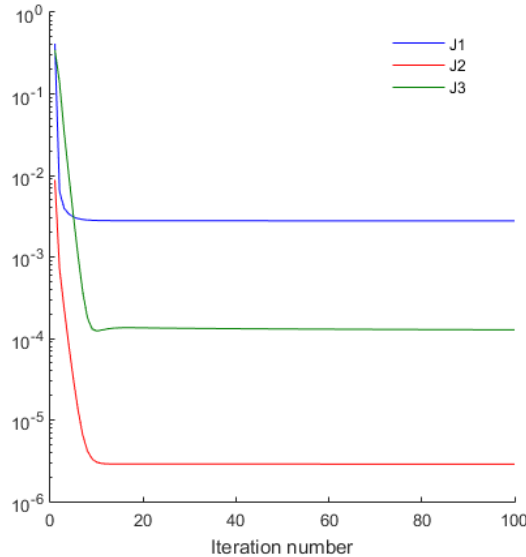


FIGURE 4.2 – Case A- . Plots of the three costs  $\mathcal{J}_1$ ,  $\mathcal{J}_2$  and  $\mathcal{J}_3$  as functions of overall Nash iterations

**Case B- Two objects :** For this test, we want to detect two circles  $\mathcal{O}_1^*$  and  $\mathcal{O}_2^*$  centered respectively at  $(-0.4, -0.15)$  and  $(-0.4, 0.15)$ , with shared radius  $r = 0.025$ .

The numerical results are illustrated in Figure 4.5 and 4.6. Figure 4.5 shows the iso-values of the topological gradient and the obtained domain at convergence. The optimal locations are equal to  $(-0.422006, -0.160662)$  and  $(-0.416224, 0.159772)$ . In Figure 4.6, we present the reconstruction of the missing Dirichlet and Neumann boundary data.

## 4.4 Conclusion

In the present work, we addressed the coupled inverse problem of recovering the missing boundary data and determining the best locations of an unknown number of small objects included in a stationary viscous fluid. To treat this problem, we have proposed to formulate it as static with complete information Nash game, where the two first players target the data completion while the third one seeks to determine the number and the locations of the objects. The latter problem (identification) is formulated as a topological one. Topological sensitive analysis related to a considered Kohn-Vogelius functional has been investigated. Then we have introduced a new algorithm for computing the Nash equilibrium for three players. We have then presented two test-cases, which showed that small inclusions close to the accessible part of the boundary could be recovered, as well as the missing boundary data on the inaccessible part.

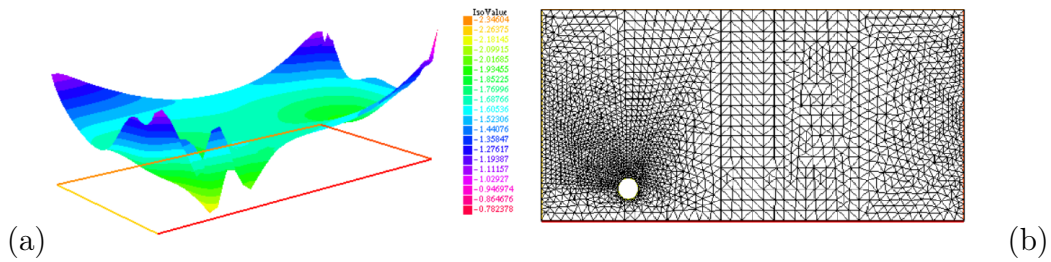


FIGURE 4.3 – Case A- Detection of a single object (for unnoisy data). (a) the iso-values of the topological gradient at convergence (b) the approximate location  $z_{opt}$  is equal to  $(-0.294, -0.174)$ , while the exact one  $z_{ex}$  is equal to  $(-0.3, -0.15)$ .



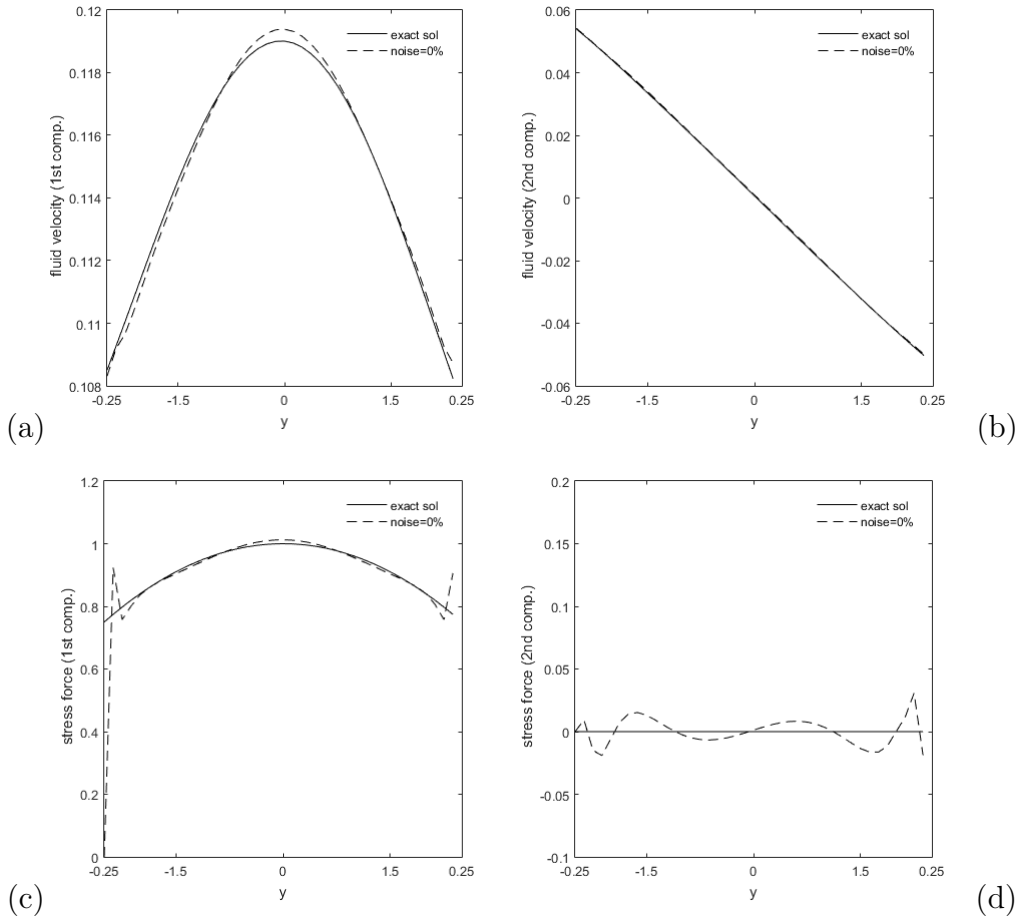


FIGURE 4.4 – Case A- Reconstruction of the missing boundary data (for unnoisy data). (a) exact -line- and computed -dashed line- first component of the velocity over  $I_i$  (b) exact -line- and computed -dashed line- second component of the velocity over  $I_i$  (c) exact -line- and computed -dashed line- first component of the normal stress over  $I_i$  (d) exact -line- and computed -dashed line- second component of the normal stress over  $I_i$ .

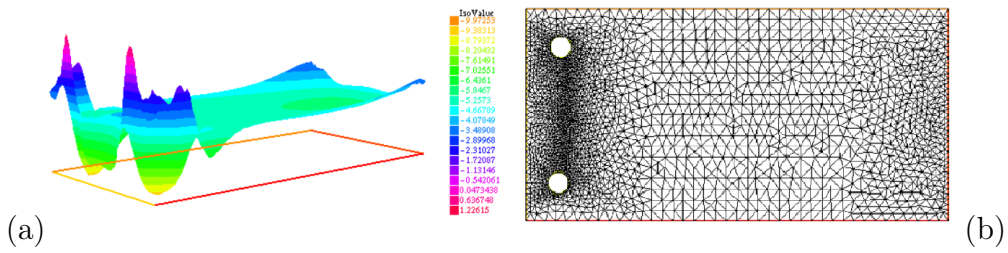


FIGURE 4.5 – Case B- Detection of two objects (for unnoisy data). (a) the iso-values of the topological gradient at convergence (b) the approximate locations are equal to  $z_{opt}^1 = (-0.422006, -0.160662)$  and  $z_{opt}^2 = (-0.416224, 0.159772)$ , while the exact ones are equal to  $z_{ex}^1 = (-0.4, -0.15)$  and  $z_{ex}^2 = (-0.4, 0.15)$ .

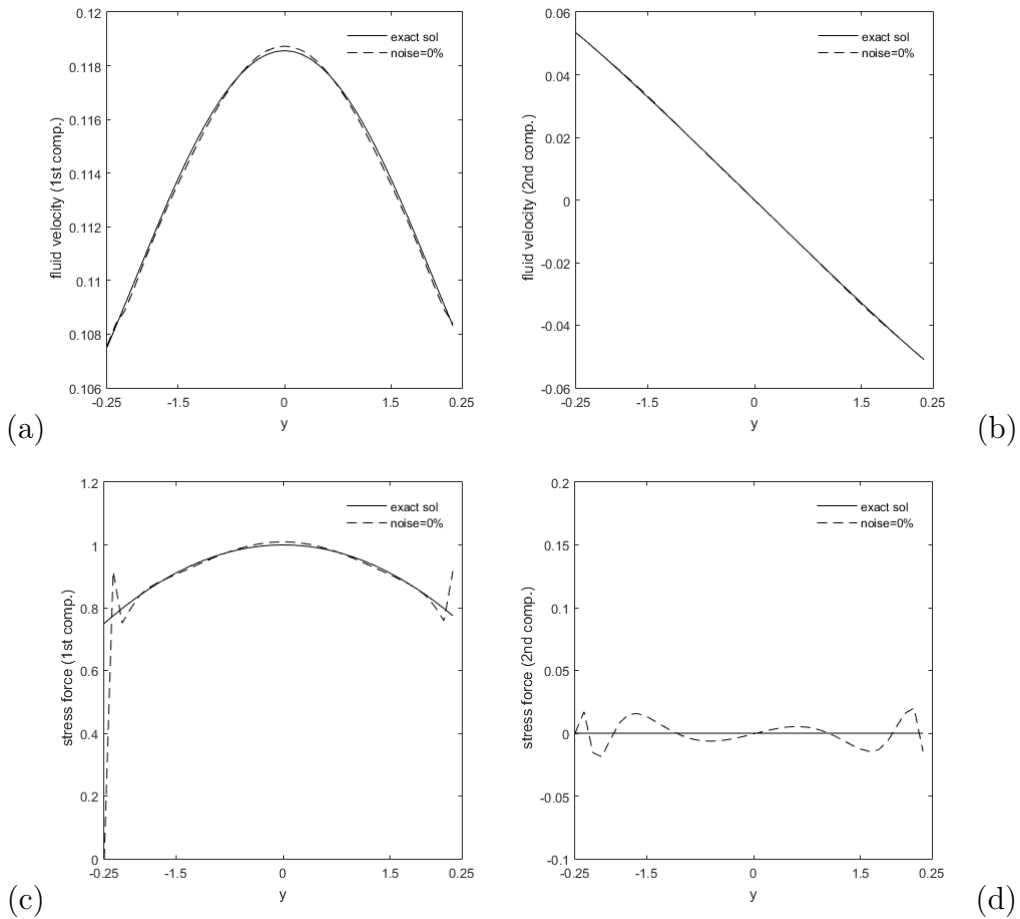


FIGURE 4.6 – Case B- Reconstruction of the missing boundary data (for unnoisy data). (a) exact -line- and computed -dashed line- first component of the velocity over  $I_i$  (b) exact -line- and computed -dashed line- second component of the velocity over  $I_i$  (c) exact -line- and computed -dashed line- first component of the normal stress over  $I_i$  (d) exact -line- and computed -dashed line- second component of the normal stress over  $I_i$ .

# A Nash game strategy to model the nonlinear Cauchy-Stokes problems : Quasi-Newtonian flow

*“ The definition of insanity is doing the same thing over and over again, but expecting different results. ”*

---

Albert Einstein

**Abstract.** In this work, two iterative procedures (conjugate gradient- classic method CM- and Nash game method NGM) for obtaining a solution to the Cauchy-Stokes problem in quasi-Newtonian fluid flow obeying the Carreau law are presented and compared. This model is well known to be severely ill-posed. Each of the two strategies reduces the ill-posed problem to solving a series of well-posed mixed BVPs. The state equations are nonlinear due to the non-linearity of the fluid viscosity function, and their numerical treatment demands some particular algorithms during the overall iterations. Two schemes are presented to solve the nonlinear state equations, the first is a fixed-point algorithm FPA, and the second is a novel one-shot scheme NS that we proposed described a new way for solving the nonlinear Cauchy problem. We present numerical results that illustrate the proposed methods' efficiency and robustness for solving our inverse problem. A comparison of the numerical results was performed to show our new scheme's performance. This paper also contributes to recovering the location and shape of some objects immersed in the flow domain and the missing boundary data simultaneously. A Nash game formulation of this nonlinear geometric Cauchy-Stokes problem and a new algorithm for its solution is given. The numerical experiments performed using the finite-element method show the game-based algorithm's relevance and efficiency.

**keywords :** Cauchy problem, quasi-Newtonian flow, data completion, Nash game, geometric inverse problem.

The content of this chapter is a work in progress, in collaboration with Abderrahmane Habbal and Moez Kallel.

---

## Contents

---

<b>5.1</b>	<b>Introduction</b>	<b>109</b>
<b>5.2</b>	<b>Data completion problem for the quasi-Newtonian flow</b>	<b>110</b>
5.2.1	The direct Problem	111
5.2.2	Existence of the Cauchy-Stokes solution	115
5.2.3	A control-type method for solving the nonlinear Cauchy-Stokes problem	116
5.2.4	A Nash game formulation of the nonlinear Cauchy-Stokes problem	119
5.2.5	A one-shot algorithm to deal with nonlinear Cauchy problems	122
<b>5.3</b>	<b>Extension for a nonlinear coupled problem : Data completion and Geometry identification</b>	<b>124</b>
<b>5.4</b>	<b>Numerical results</b>	<b>128</b>
5.4.1	Data completion problem.	128
5.4.2	Application to coupled problem : Data completion and geometry identification	131
<b>5.5</b>	<b>Conclusion</b>	<b>133</b>

---

---

## 5.1 Introduction

This work is concerned with reconstructing a nonlinear Stokes flow governed by the partial differential equations PDEs, which arises in modeling flows of, for example, biological or polymeric fluids, where the viscosity varied upon the imposed strain tensor. Our nonlinear Cauchy-Stokes problem here is given by

$$\begin{cases} -\operatorname{div}(2\nu(I(u))D(u)) + \nabla p = 0 & \text{in } \Omega, \\ \operatorname{div} u = 0 & \text{in } \Omega, \\ u = f & \text{on } \Gamma_c, \\ \sigma(u, p)n = \Phi & \text{on } \Gamma_c, \end{cases} \quad (5.1)$$

where  $\Omega$  is the flow region, a bounded open domain in  $\mathbb{R}^d$  ( $d=2, 3$ ) with a sufficiently smooth boundary  $\partial\Omega$ , and  $\Gamma_c$  is an accessible part of  $\partial\Omega$ . The motion of our incompressible fluid is described by the velocity  $u$  and pressure  $p$ . The stress tensor  $\sigma(u, p)$  defined as follows :

$$\sigma(u, p) = -pI_d + 2\nu(I(u))D(u) \quad (5.2)$$

with  $D(u) = \frac{1}{2}(\nabla u + \nabla u^T)$  represents the deformation (rate-of-strain) tensor, the shear rate  $I$  is defined by  $I(u) = \frac{1}{2}D(u) : D(u)$ , and the function  $\nu$  describes the nonlinear viscosity of the fluid. The fluid flows satisfying (5.2) for a function  $\nu$  to be typically specified are called quasi-Newtonian.

Some classical examples of  $\nu$  are given by ; (a) *The Carreau law*

$$\nu(z) = \nu_\infty + (\nu_0 - \nu_\infty)(1 + \lambda z)^{\frac{r-2}{2}},$$

(b) *the power law*

$$\nu(z) = \nu_0 z^{\frac{r-2}{2}},$$

where  $\lambda > 0$  is a constant,  $\nu_0$  and  $\nu_\infty$  are positive constants assumed to satisfy  $\nu_0 > \nu_\infty \geq 0$  and  $1 < r < \infty$  is a fluid characteristic real parameter. Note that,  $r = 2$  in both models of  $\nu$  leads to  $\nu = \nu_0$ , that is, the power law and the Carreau's law reduces to a Newtonian fluid model. When  $r < 2$ , the fluid is said, *shear thinning* or *pseudo-plastic*. This designates the fact that the system's viscosity decreases as the shear rate is increased : the power law is quite similar to the case of Carreau's law with  $\nu_\infty = 0$  and tends to zero. Shear-thinning is the most common type of non-Newtonian behavior of fluids and is seen in many industrial and everyday applications. When  $r > 2$ , the viscosity increases with the shear strain, and the fluid is said *shear thickening* or *dilatant*.

The Cauchy problem is a difficult issue, and it is ill-posed in the Hadamard sense [59]. In fact, the existence of solutions for arbitrary Cauchy data cannot be guaranteed, and even it exists, it does not depend continuously on the data. The linear elliptic Cauchy problems are already discussed in many published works by several numerical approaches, which were carefully considered, for instance, classical numerical methods [2, 10, 72], and game theory approaches [56, 55, 57]. What concerns nonlinear elliptic Cauchy problems, the level set approach proposed in [42], which is based on a Tikhonov regularization method. In [73], the authors proposed two iterative methods based on the segmenting Mann iteration applied to fixed point equations. The first approach consists of transforming the nonlinear Cauchy problem into a linear Cauchy

---

problem and analyzing a linear fixed point equation. A nonlinear fixed point equation is considered on the second approach, and a thoroughly nonlinear iterative method is investigated. Avdonin et al used in [14] an iterative method for solving a nonlinear elliptic Cauchy problem in glaciology. In [66], the authors used a game strategy to solve the image inpainting problem as a nonlinear Cauchy problem. However, to the best of our knowledge, there are no papers devoted to the present problem (5.1), which consists of recovering in quasi-Newtonian fluid flow models the missing data on the inaccessible part  $\partial\Omega \setminus \Gamma_c$ , i.e., nonlinear Cauchy-Stokes problem.

A secondary problem is also studied in the quasi-Newtonian flow framework, where we supposed that there is  $\omega^*$  an unknown object immersed in the flow domain  $\Omega$ . Thus, the considered problem here is finding the location and shape of this object  $\omega^*$ , using incomplete measurements on the boundary. For this case, we're gonna complete the missing boundary data and recover the inclusion(s). In particular, with  $r = 2$ , we properly recover the linear inverse inclusion Cauchy-stokes problem [57].

The manuscript is organized as follows : In Section 2, the nonlinear mixed boundary value problem's solution's existence and uniqueness are proved. A density result for compatible data of the nonlinear Cauchy problem is demonstrated. Next, we rephrased the data completion problem as an optimization one, and we presented two different approaches, a control-type regularized and a Nash game approach. To solve the nonlinear state equations, we proposed a novel one-shot scheme. Then, we compared it with the classic algorithm of the fixed-point. In section 3, we formulated the joint completion/detection problem as three players, and we proposed a new algorithm for its numerical solution. Some numerical examples presented in Section 4 corroborate the proposed methods' efficiency and robustness for the data completion and the coupled problems.

## 5.2 Data completion problem for the quasi-Newtonian flow

In this section, we focus on the problem of reconstructing velocity  $u$  and pressure  $p$  from partial boundary measurements, which described as a solution of the following system :

$$\begin{cases} -\operatorname{div}(2\nu(I(u))D(u)) + \nabla p = 0 & \text{in } \Omega, \\ \operatorname{div} u = 0 & \text{in } \Omega, \\ u = f & \text{on } \Gamma_c, \\ \sigma(u, p)n = \Phi & \text{on } \Gamma_c, \end{cases} \quad (5.3)$$

where  $f$  and  $\Phi$  are given functions that will be specified later. The data completion problem, which is a reformulation of the nonlinear Cauchy-Stokes one, amounts to find  $\eta^* = \sigma(u, p)n|_{\Gamma_i}$  and  $\tau^* = u|_{\Gamma_i}$ , where  $\Gamma_i = \partial\Omega \setminus \Gamma_c$ .

The Stokes equation with different boundary conditions, Dirichlet or a combination of a Dirichlet-Neumann boundary condition, can be formulated variationally. In the following subsection, we present the existence and uniqueness result of a weak solution for the following direct nonlinear mixed boundary-value problem : for a given function  $\eta$ ,

$$(\mathcal{P}_d) \begin{cases} -\operatorname{div}(2\nu(I(u))D(u)) + \nabla p = 0 & \text{in } \Omega, \\ \operatorname{div} u = 0 & \text{in } \Omega, \\ u = f & \text{on } \Gamma_c, \\ \sigma(u, p)n = \eta & \text{on } \Gamma_i. \end{cases}$$

We limit ourselves in this work to the Quasi-Newtonian flows whose viscosity obeys the Carreau law, but the presented methods can properly be applied to other laws.

### 5.2.1 The direct Problem

The well-posedness of the direct quasi-Newtonian fluid flow problem and its standard finite element approximation are well demonstrated precisely in [18, 39] for homogeneous Dirichlet boundary conditions. In this paragraph, we formulate the variational model associated to nonlinear mixed boundary-value problem  $(\mathcal{P}_d)$ , and we also indicate how the existence and uniqueness of solution is obtained.

Before giving the weak formulation of the direct problem  $(\mathcal{P}_d)$ . Let us introduce some notations that will be used throughout this paper : The Lebesgue space is denoted as usual  $L^p(\Omega)$ ,  $1 \leq p \leq \infty$ , with norms  $\|\cdot\|_{L^p}$ . For any non-negative integer  $m$  and real number  $p \geq 1$ , the classical Sobolev spaces  $W^{m,p}(\Omega)$  is defined to be

$$W^{m,p}(\Omega) = \left\{ u \in L^p(\Omega) \mid \forall \alpha \text{ such that } |\alpha| \leq m, D^\alpha u \in L^p(\Omega) \right\}.$$

For  $p \in ]1, 2]$ , we let

$$\begin{aligned} \chi^p &= (W^{1,p}(\Omega))^d, \\ \chi_g^p &= \{v \in \chi^p, \text{ such that } v|_{\Gamma_c} = g\}, \\ \chi_\phi^p &= \{v \in \chi^p, \text{ such that } v|_{\Gamma_i} = \phi\}, \end{aligned}$$

and

$$\chi_{g,\operatorname{div}}^p = \left\{ v \in \chi^p, \text{ such that } \operatorname{div} v = 0 \text{ in } \Omega \text{ and } v|_{\Gamma_c} = g \right\}.$$

From the Sobolev trace theorem [31], a necessary and sufficient condition for the boundary condition  $f$  and  $\eta$  to satisfy  $f = u|_{\Gamma_c}$  and  $\eta = \sigma(u, p)n|_{\Gamma_i}$  when  $u \in \chi^p$  is  $f \in \chi_{\Gamma_c}^p = W^{1-\frac{1}{p},p}(\Gamma_c)^d$ , and  $\eta$  belongs to the dual space of trace  $\chi'_{\Gamma_i} = (W^{1-\frac{1}{p},p}(\Gamma_i)^d)'$ .

The variational principle corresponding to the equations  $(\mathcal{P}_d)$  with viscosity well specified is

$$(\mathcal{O}_m) \begin{cases} \text{Find } u \in V \text{ such that,} \\ \mathfrak{J}(u) = \inf_{w \in V} \mathfrak{J}(w) \end{cases}$$

where

$$\mathfrak{J}(w) = \int_{\Omega} \int_0^{I(w)} \nu(t) dt dx - \int_{\Gamma_i} \eta w ds, \quad \forall w \in V,$$

and

$$V = \left\{ v \in X \text{ such that } \operatorname{div} v = 0 \text{ in } \Omega \text{ and } v|_{\Gamma_c} = f \right\},$$

with  $X$  is a functional space to be specified depending on the viscosity function  $\nu$ . Now, when the quasi-Newtonian flow obeying the Carreau law, the functional  $\mathfrak{J}$  takes the following form :

$$\mathfrak{J}(w) = \int_{\Omega} \left[ \frac{\nu_{\infty}}{2} |D(w)|^2 + \frac{2}{\lambda r} (\nu_0 - \nu_{\infty}) \left[ \left(1 + \frac{\lambda}{2} |D(w)|^2\right)^{\frac{r}{2}} - 1 \right] \right] dx - \int_{\Gamma_i} \eta w ds, \quad \forall w \in V,$$

these terms are well bounded when  $w \in W^{1,p}(\Omega)^d$  with  $p = r$  if  $\nu_{\infty} = 0$ , otherwise  $p = \max(2, r)$ . Hereafter, we consider then the case where  $\nu_{\infty} > 0$  and  $1 < r \leq 2$ , which implies that  $X := \chi^p$  is the Hilbert space  $H^1(\Omega)^d$  (i.e.  $p = 2$  and  $V = \chi_{f,\text{div}}^2$ ), and the spaces  $\chi_{\Gamma_c}$ ,  $\chi'_{\Gamma_i}$  are respectively  $H^{\frac{1}{2}}(\Gamma_c)^d$  and  $(H^{\frac{1}{2}}(\Gamma_i)^d)'$ . Therefore, we assume that the function  $\nu$  satisfies the structural hypothesis stated in Hypothesis 5.2.1 below :

**Assumptions 5.2.1** *We assume that the nonlinearity  $\nu$  satisfies the following conditions :*

(i)  $\nu \in \mathcal{C}^1(\mathbb{R}_+)$ .

(ii) *There exist constants  $m_{\nu}, M_{\nu} > 0$  such that*

$$m_{\nu} \leq \nu(t) \leq M_{\nu}, \quad \forall t \geq 0.$$

(iii) *There exist constants  $C_1, C_2 > 0$  such that, for all  $\tau, \omega \in \mathbb{R}^{d \times d}$*

$$|\nu(|\tau|)\tau - \nu(|\omega|)\omega| \leq C_1 |\tau - \omega|, \quad (5.4)$$

$$C_2 |\tau - \omega|^2 \leq (\nu(|\tau|)\tau - \nu(|\omega|)\omega) : (\tau - \omega). \quad (5.5)$$

It is easy to see that the direct weak formulation of  $(\mathcal{P}_d)$  is the Euler-Lagrange equation of  $\mathfrak{J}$ , if  $u$  is solution of  $(\mathcal{O}_m)$ , then  $u$  solves the direct weak formulation of  $(\mathcal{P}_d)$ . Conversely, if  $u$  is a weak solution, then it is a minimum of  $\mathfrak{J}$ , which is characterized by  $\mathfrak{J}'(u).v = 0$  for all  $v \in \chi^2$ ,  $\text{div} v = 0$  and  $v = 0$  on  $\Gamma_c$ . Multiplying the first equation of  $(\mathcal{P}_d)$  by any test function  $\varphi$  that must belong to  $\chi_0^2$ , integrating over  $\Omega$  and performing an integration by parts, we obtain the following weak form

$$\int_{\Omega} 2\nu(I(u))D(u) : \nabla \varphi dx - \int_{\Omega} p \text{div} \varphi dx = \int_{\Gamma_i} \eta \varphi ds, \quad \forall \varphi \in \chi_0^2, \quad (5.6)$$

that is, for all  $\varphi \in \chi_0^2$  satisfies  $\text{div} \varphi = 0$ ,

$$\int_{\Omega} 2\nu(I(u))D(u) : \nabla \varphi dx - \int_{\Gamma_i} \eta \varphi ds = 0.$$

Therefore, the functional  $\mathfrak{J}$  is Gâteaux differentiable (see Proposition 2.1 of Baranger and Najib [18]).

**Proposition 5.2.1** *The optimization problem  $(\mathcal{O}_m)$  admits a unique solution  $u \in \chi_{f,\text{div}}^2$ .*



*Proof.* We start by proving that the potential  $\mathfrak{J}$  is continuous. Let  $h$  be a function in  $\chi_0^2$ , then we have

$$\mathfrak{J}(u+h) - \mathfrak{J}(u) = \int_{\Omega} \int_0^{I(u+h)} \nu(t) dt dx - \int_{\Omega} \int_0^{I(u)} \nu(t) dt dx - \int_{\Gamma_i} \eta h ds.$$

We define now a function  $H : \mathbb{R}^+ \rightarrow \mathbb{R}^+$  by  $\int_0^z \nu(t) dt$ , and graciously according to the Mean-Value Theorem applied for the continuous function  $H$ , we deduce that there exists  $0 < \alpha < 1$  such that

$$H(I(v+h)) - H(I(v)) = H'(Q) (I(v+h) - I(v)),$$

with

$$Q = \alpha I(v+h) + (1-\alpha)I(v).$$

Therefore,

$$\begin{aligned} \mathfrak{J}(v+h) - \mathfrak{J}(v) &= \int_{\Omega} H'(Q) (I(v+h) - I(v)) dx - \int_{\Gamma_i} \eta h ds \\ &= \int_{\Omega} \nu(Q) (I(v+h) - I(v)) dx - \int_{\Gamma_i} \eta h ds \\ &= \frac{1}{2} \int_{\Omega} \nu(Q) (|D(v+h)|^2 - |D(v)|^2) dx - \int_{\Gamma_i} \eta h ds \\ &= \frac{1}{2} \int_{\Omega} \nu(Q) (2D(v) : D(h) + |D(h)|^2) dx - \int_{\Gamma_i} \eta h ds. \end{aligned}$$

Applying the condition (ii) and the continuity of the trace operator from  $H^1(\Omega)^d$  to  $L^2(\Gamma_i)$ , for all  $h \in \chi_0^2$  we have

$$|\mathfrak{J}(v+h) - \mathfrak{J}(v)| \leq (c_1 \|D(v)\|_{L^2(\Omega)} + c_2 \|\eta\|_{L^2(\Gamma_i)} + c_3 \|h\|_{H^1(\Omega)^d}) \|h\|_{H^1(\Omega)^d}.$$

where  $c_1$ ,  $c_2$  and  $c_3$  are positive constants. Thus, this inequality implies that the functional  $\mathfrak{J}$  is continuous. Next, we show that the functional  $\mathfrak{J}$  is strongly convex. Clearly,

$$\begin{aligned} \mathfrak{J}''(v; \psi, h) &= \frac{d}{dt} \left\{ \int_{\Omega} \nu(I(v+th)) D(v+th) : D(\psi) dx \right\}_{t=0}, \\ &= \int_{\Omega} \nu(I(v)) D(h) : D(\psi) dx + \frac{1}{2} \int_{\Omega} \nu'(I(v)) (D(v) : D(h)) (D(v) : D(\psi)) dx, \end{aligned}$$

Now, for  $h = \psi$  we get

$$\mathfrak{J}''(v; \psi, \psi) = \int_{\Omega} \nu(I(v)) |D(\psi)|^2 dx + \frac{1}{2} \int_{\Omega} \nu'(I(v)) (D(v) : D(\psi))^2 dx.$$

Not since  $1 < r \leq 2$ , we have that  $\nu' < 0$ , and from the Cauchy-Schwartz inequality,

$$\begin{aligned} \mathfrak{J}''(v; \psi, \psi) &\geq \int_{\Omega} (\nu(I(v)) + \nu'(I(v))I(v)) |D(\psi)|^2 dx, \\ &\geq \int_{\Omega} F(I(v)) |D(\psi)|^2 dx, \end{aligned}$$

with  $F(t) = \nu(t) + \nu'(t)t$ , where,

$$\nu(t) = \nu_{\infty} + (\nu_0 - \nu_{\infty})(1 + \lambda t)^{\frac{r-2}{2}},$$

$$\nu'(t) = \frac{(r-2)\lambda}{2}(\nu_0 - \nu_\infty)(1 + \lambda t)^{\frac{r-4}{2}}.$$

Thus,

$$F(t) = \nu_\infty + (\nu_0 - \nu_\infty)(1 + \lambda t)^{\frac{r-2}{2}} + \frac{(r-2)\lambda}{2}(\nu_0 - \nu_\infty)(1 + \lambda t)^{\frac{r-4}{2}}t,$$

or as long as  $1 < r \leq 2$ , we have that  $(r-2)\lambda t \geq (r-2)(1 + \lambda t)$ .

Therefore,

$$\begin{aligned} F(t) &\geq \nu_\infty + (\nu_0 - \nu_\infty)(1 + \lambda t)^{\frac{r-2}{2}} + \frac{(r-2)}{2}(\nu_0 - \nu_\infty)(1 + \lambda t)^{\frac{r-2}{2}}, \\ &= \nu_\infty + \frac{r}{2}(\nu_0 - \nu_\infty)(1 + \lambda t)^{\frac{r-2}{2}}, \\ &\geq \nu_\infty + \frac{r}{2}(\nu_0 - \nu_\infty) > 0, \end{aligned}$$

which implies that there exists  $\delta > 0$  such that,

$$\mathfrak{J}''(v; \psi, \psi) \geq \delta \|D(\psi)\|_{L^2(\Omega)}^2,$$

using Poincaré-Wirtinger's inequality, we obtain

$$\mathfrak{J}''(v; \psi, \psi) \geq c' \|\psi\|_{H^1(\Omega)^d}^2, \quad \forall \psi \in \chi_0^2.$$

Then, we conclude that  $\mathfrak{J}$  is a strongly convex function. Therefore, the optimization problem  $(\mathcal{O}_m)$  admits a unique solution  $v \in \chi_{f,\text{div}}^2$ , for  $1 < r \leq 2$ .  $\blacksquare$

Now, we consider the mixed weak formulation of  $(\mathcal{P}_d)$ . Since we will be working with the pressure, and according to the second term of (5.6), it is convenient to introduce the pressure space  $\mathcal{M}^2 := L^2(\Omega)$ .

Thus, the mixed weak formulation of the Stokes problem  $(\mathcal{P}_d)$  writes

$$\left\{ \begin{array}{l} \text{Find } (u, p) \in \chi_f^2 \times \mathcal{M}^2 \text{ such that :} \\ \mathfrak{A}(u; u, \varphi) + \mathfrak{B}(\varphi, p) = l(\varphi), \quad \forall \varphi \in \chi_0^2 \\ \mathfrak{B}(u, q) = 0, \quad \forall q \in \mathcal{M}^2 \end{array} \right. \quad (5.7)$$

where

$$\mathfrak{A}(u; u, \varphi) = \int_{\Omega} 2\nu(I(u))D(u) : \nabla \varphi \, dx,$$

$$\mathfrak{B}(u, q) = - \int_{\Omega} q \operatorname{div} u \, dx,$$

$$l(\varphi) = \int_{\Gamma_i} \eta \varphi \, ds.$$

Furthermore, the above problem (5.7) can appear as a saddle-point formulation of the minimization problem  $(\mathcal{O}_m)$  under the incompressibility constraint  $\operatorname{div} u = 0$ . Let us introduce the following Lagrangian functional on  $\chi_f^2 \times L^2(\Omega)$  :

$$\begin{aligned} \mathfrak{L}(w, q) &:= \mathfrak{J}(w) + \mathfrak{B}(w, q) \\ &= \int_{\Omega} \int_0^{I(w)} \nu(t) \, dt \, dx - \int_{\Omega} q \operatorname{div} w \, dx - \int_{\Gamma_i} \eta w \, ds. \end{aligned}$$

The lagrangian  $\mathfrak{L}$  is convex and coercive with respect to  $u$ , due to the strong convexity of the functional  $\mathfrak{J}$  and linear with respect to  $p$  and then concave. Moreover, the lagrangian  $\mathfrak{L}$  is Gâteaux-differentiable with respect each variable  $u$  and  $p$ , hence  $\mathfrak{L}$  is weakly lower semi-continuous in  $u$  and weakly upper semi-continuous in  $p$ . According to Ekeland and Temam ([43] Proposition 2.4 page 164), the functional  $\mathfrak{L}$  admits at least one saddle-point  $(u^*, p^*)$  on  $\chi_f^2 \times L^2(\Omega)$ , which satisfies :

$$\begin{aligned}\mathfrak{L}(u^*, p^*) &= \min_{u \in \chi_f^2} \sup_{p \in L^2(\Omega)} \mathfrak{L}(u, p) \\ &= \max_{p \in L^2(\Omega)} \inf_{u \in \chi_f^2} \mathfrak{L}(u, p).\end{aligned}$$

Then, from the existence of the saddle-point of the lagrangian  $\mathfrak{L}$  and the existence and uniqueness of the solution of the minimization problem  $(\mathcal{O}_m)$ , the uniqueness of  $u$  of the saddle-point of the lagrangian is ensured but not the uniqueness of the Lagrange multiplier part  $p$  which is in  $L^2(\Omega)$ . Whereas the Neumann type condition on the part of the boundary implies the uniqueness of the direct problem's pressure. This yields the existence and uniqueness of a weak solution  $(u^*, p^*)$  associated to  $(\mathcal{P}_d)$ .

## 5.2.2 Existence of the Cauchy-Stokes solution

Existence solution to the Cauchy-Stokes problem (5.3) is not guaranteed for any pair of data and depends on the compatibility of  $f$  and  $\Phi$ . They are said compatible if the corresponding Cauchy problem has a solution. For a fixed  $f \in H^{\frac{1}{2}}(\Gamma_c)^d$ , we show in the Lemma 5.2.1 below that the set of compatible data  $\Phi$  with  $f$  is dense in  $(H^{\frac{1}{2}}(\Gamma_c)^d)'$ .

**Lemma 5.2.1** *Let  $(f, \Phi)$  the data on  $\Gamma_c$ . For fixed  $f \in H^{\frac{1}{2}}(\Gamma_c)^d$ , and  $(u, p) \in H^1(\Omega)^d \times L^2(\Omega)$  satisfies the Cauchy problem, then, the set*

$$\mathcal{D} = \{\Phi \in (H^{\frac{1}{2}}(\Gamma_c)^d)', \text{ such that } f \text{ and } \Phi \text{ are compatible}\},$$

*is dense in  $(H^{\frac{1}{2}}(\Gamma_c)^d)'$ .*

*Proof.* We assume that  $f = 0$ , and let  $(u, p)$  be the solution of the following problem,

$$\begin{cases} -\operatorname{div}(2\nu(I(u))D(u)) + \nabla p = 0 & \text{in } \Omega, \\ \operatorname{div} u = 0 & \text{in } \Omega, \\ u = 0 & \text{on } \Gamma_c, \\ \sigma(u, p)n = \Phi & \text{on } \Gamma_c. \end{cases}$$

Denote by  $\mathcal{D}_0$  the set of compatible data  $\Phi$  with the Dirichlet condition  $f = 0$  on  $\Gamma_c$ ,

$$\mathcal{D}_0 = \{\Phi \in (H^{\frac{1}{2}}(\Gamma_c)^d)', \text{ such that } 0 \text{ and } \Phi \text{ are compatible}\}.$$

Let  $\lambda \in \mathcal{D}_0^\perp$ , then  $\lambda \in H^{\frac{1}{2}}(\Gamma_c)^d$  such that

$$(\lambda, \phi) = 0, \quad \forall \phi \in \mathcal{D}_0. \quad (5.8)$$

Now, we consider the following direct nonlinear BVP :

$$\begin{cases} -\operatorname{div}(2\nu(I(u_0))D(u_0)) + \nabla p_0 = 0 & \text{in } \Omega, \\ \operatorname{div} u_0 = 0 & \text{in } \Omega, \\ u_0 = 0 & \text{on } \Gamma_c, \\ \sigma(u_0, p_0)n = \xi & \text{on } \Gamma_i, \end{cases} \quad (5.9)$$

where  $\xi \in (H^{\frac{1}{2}}(\Gamma_c)^d)'$ , and let  $(v, q)$  be the unique solution of the following linear mixed BVP,

$$\begin{cases} -\operatorname{div}(2\nu(I(u_0))D(v)) + \nabla q = 0 & \text{in } \Omega, \\ \operatorname{div} v = 0 & \text{in } \Omega, \\ v = \lambda & \text{on } \Gamma_c, \\ -qn + 2\nu(I(u_0))D(v)n = 0 & \text{on } \Gamma_i. \end{cases} \quad (5.10)$$

From the second Green's formula applied to  $(u_0, p_0)$  and  $(v, q)$ , we conclude that

$$\int_{\partial\Omega} (\sigma(u_0, p_0)nv - \sigma(v, q)nu_0) ds = 0.$$

The integral is defined in the sense of duality. It flows from  $u_0|_{\Gamma_c} = 0$  and  $\sigma(v, q)n|_{\Gamma_i} = 0$  that

$$\int_{\Gamma_i} \xi v ds = 0, \quad \forall \xi \in (H^{\frac{1}{2}}(\Gamma_c)^d)',$$

which implies  $v|_{\Gamma_i} = 0$ . Therefore, the solution  $(v, q)$  satisfies the upcoming system,

$$\begin{cases} -\operatorname{div}(2\nu(I(u_0))D(v)) + \nabla q = 0 & \text{in } \Omega, \\ \operatorname{div} v = 0 & \text{in } \Omega, \\ v = 0 & \text{on } \Gamma_i, \\ -qn + 2\nu(I(u_0))D(v)n = 0 & \text{on } \Gamma_i. \end{cases}$$

Thus, thanks to the unique continuation property for the linear Stokes system [47], we have  $v = 0$  in  $\Omega$ , and consequently  $\lambda = 0$ .

For any fixed  $f \neq 0$ . Under the assumption  $f \in H^{\frac{1}{2}}(\Gamma_c)^d$ , let  $\tilde{f} \in H^1(\Omega)^d$  in order that  $\tilde{f}|_{\Gamma_c} = f$ , and  $\operatorname{div} \tilde{f} = 0$  in  $\Omega$ . Then, we reduced the Dirichlet condition  $u|_{\Gamma_c} = f$  to a homogeneous condition. The Cauchy problem (5.3) can be written with unknown function  $(w, p)$  as follows :

$$\begin{cases} -\operatorname{div}(2\nu(I(w + \tilde{f}))D(w + \tilde{f})) + \nabla p = 0 & \text{in } \Omega, \\ \operatorname{div} w = 0 & \text{in } \Omega, \\ w = 0 & \text{on } \Gamma_c, \\ \sigma(w + \tilde{f}, p)n = \Phi & \text{on } \Gamma_c. \end{cases}$$

Therefore, the density result in this case can be obtained by the same previous arguments of the fixed data  $f = 0$ . ■

**Remark 5.2.1** For a fixed  $\Phi \in (H^{\frac{1}{2}}(\Gamma_c)^d)'$ , we can put into service the same process of Lemma 5.2.1 proof to demonstrate a particular case for  $\Phi = 0$ , that is, the set  $\mathcal{D}_0 = \{f \in H^{\frac{1}{2}}(\Gamma_c)^d, \text{ such that } f \text{ and } 0 \text{ are compatible}\}$  is dense in  $H^{\frac{1}{2}}(\Gamma_c)^d$ . However, this march is useless for any fixed  $\Phi \neq 0$ , due to the nonlinear function.

### 5.2.3 A control-type method for solving the nonlinear Cauchy-Stokes problem

In this subsection, we propose to use a control-type regularized data recovery process that generalized the method given in [2] for the linear case. Then, we reformulate the considered nonlinear Cauchy-Stokes problem (5.3) as an optimization one.

For any given  $\eta \in (H^{\frac{1}{2}}(\Gamma_i^d))'$  and  $\tau \in H^{\frac{1}{2}}(\Gamma_i^d)$ , we define the states  $(u_1(\eta), p_1(\eta)) \in \chi^2 \times \mathcal{M}^2$  and  $(u_2(\tau), p_2(\tau)) \in \chi^2 \times \mathcal{M}^2$  as the unique weak solutions, respectively, of the following mixed boundary value problems  $(\mathcal{SP}_1)$  and  $(\mathcal{SP}_2)$  :

$$\begin{aligned}
(\mathcal{SP}_1) \quad & \left\{ \begin{array}{ll} -\operatorname{div}(2\nu(I(u_1))D(u_1)) + \nabla p_1 = 0 & \text{in } \Omega, \\ \operatorname{div} u_1 = 0 & \text{in } \Omega, \\ u_1 = f & \text{on } \Gamma_c, \\ \sigma(u_1, p_1)n = \eta & \text{on } \Gamma_i, \end{array} \right. \\
(\mathcal{SP}_2) \quad & \left\{ \begin{array}{ll} -\operatorname{div}(2\nu(I(u_2))D(u_2)) + \nabla p_2 = 0 & \text{in } \Omega, \\ \operatorname{div} u_2 = 0 & \text{in } \Omega, \\ \sigma(u_2, p_2)n = \Phi & \text{on } \Gamma_c, \\ u_2 = \tau & \text{on } \Gamma_i. \end{array} \right.
\end{aligned}$$

Following the work in [2], the unknown data  $(\eta, \tau)$  can be characterized as the solution of the following minimization problem :

$$(\eta^*, \tau^*) = \arg \min_{(\eta, \tau)} \mathcal{J}(\eta, \tau), \quad (5.11)$$

where the cost functional  $\mathcal{J}$  is defined below, and splits into a classical least square term, prescribing the gap between the Neumann known data  $\Phi$  and the stress forces of the solution of the boundary value problem  $(\mathcal{SP}_1)$  on  $\Gamma_c$ , and a regularization term over  $\Gamma_i$ . Thus,  $\mathcal{J}$  could be renamed into a "Neumann-gap" cost  $\mathbb{J}_N$ , which is given by :

$$\begin{aligned}
\mathcal{J}(\eta, \tau) := \mathbb{J}_N(u_1(\eta), p_1(\eta); u_2(\tau), p_2(\tau)) &= \frac{1}{2} \int_{\Gamma_c} (\sigma(u_1(\eta), p_1(\eta))n - \Phi)^2 ds \\
&+ \frac{1}{2} \int_{\Gamma_i} (u_1(\eta) - u_2(\tau))^2 ds.
\end{aligned}$$

**Proposition 5.2.2** *For a pair of -compatible- measurements  $(f, \Phi) \in H^{\frac{1}{2}}(\Gamma_c^d) \times (H^{\frac{1}{2}}(\Gamma_c^d))'$ , we assume that the problem (5.3) admits a unique solution. Then, solving the nonlinear Cauchy-Stokes problem (5.3) is equivalent to solving the minimization problem (5.11) and*

$$\inf_{(\eta, \tau) \in (H^{\frac{1}{2}}(\Gamma_i^d))' \times H^{\frac{1}{2}}(\Gamma_i^d)} \mathcal{J}(\eta, \tau) = 0.$$

**Proof.** We assume that the nonlinear Cauchy-Stokes problem admits a unique solution. Let  $(u, p)$  be a solution of (5.3), such that  $\eta_0 = \sigma(u, p)n|_{\Gamma_i}$  and  $\tau_0 = u|_{\Gamma_i}$ . Then, we have,

$$\mathcal{J}(\eta_0, \tau_0) = \mathbb{J}_N(u_1(\eta_0), p_1(\eta_0); u_2(\tau_0), p_2(\tau_0)) = 0.$$

Conversely, let  $(\eta^*, \tau^*)$  solution of the minimization problem (5.11). Then, we have

$$0 \leq \mathcal{J}(\eta^*, \tau^*) \leq \mathcal{J}(\eta_0, \tau_0).$$

This implies that,  $\sigma(u_1(\eta^*), p_1(\eta^*))n|_{\Gamma_c} = \Phi$ , that is  $(u_1(\eta^*), p_1(\eta^*)) = (u, p)$  in  $\Omega$  and the condition  $u_1(\eta^*)|_{\Gamma_i} = \tau^*$ . Thus, the solution  $(u_1(\eta^*), p_1(\eta^*))$  satisfies the upcoming system,

$$\left\{ \begin{array}{ll} -\operatorname{div}(2\nu(I(u_1))D(u_1)) + \nabla p_1 = 0 & \text{in } \Omega, \\ \operatorname{div} u_1 = 0 & \text{in } \Omega, \\ u_1 = \tau^* & \text{on } \Gamma_i, \\ \sigma(u_1, p_1)n = \Phi & \text{on } \Gamma_c, \end{array} \right. \quad (5.12)$$

multiplying the first equation of (5.12) by  $v_1 \in \chi^2$  and the first equation of  $(\mathcal{SP}_2)$  by  $v_2 \in \chi^2$ , and using Green's formula, we obtain

$$\begin{aligned} \int_{\Omega} 2\nu(I(u_1))D(u_1) : \nabla(v_1) dx - \int_{\Omega} p_1 \operatorname{div} v_1 dx &= \int_{\Gamma_c} \Phi v_1 ds + \int_{\Gamma_i} \sigma(u_1, p_1) n v_1 ds, \\ \int_{\Omega} 2\nu(I(u_2))D(u_2) : \nabla(v_2) dx - \int_{\Omega} p_2 \operatorname{div} v_2 dx &= \int_{\Gamma_c} \Phi v_2 ds + \int_{\Gamma_i} \sigma(u_2, p_2) n v_2 ds, \end{aligned}$$

we replace now  $v_1$  and  $v_2$  by  $u_1 - u_2$ , we get

$$2 \int_{\Omega} (\nu(I(u_1))D(u_1) - \nu(I(u_2))D(u_2)) : D(u_1 - u_2) dx = 0. \quad (5.13)$$

It follows from condition (iii) and Poincaré-Wirtinger's inequality that  $u_1(\eta^*) = u_2(\tau^*)$ . Hence, by assumption of uniqueness of the Cauchy Stokes solution, we have that  $u_1(\eta^*) = u_2(\tau^*) = u(\eta_0, \tau_0)$ .  $\blacksquare$

**Remark 5.2.2** *Other functional  $\mathbb{J}_D$ , referring to the "Dirichlet-gap" cost, may be considered here, where the classical least square term on  $\Gamma_c$  is the gap between the Dirichlet known data  $f$  and the trace of the solution of the boundary value problem  $(\mathcal{SP}_2)$  over  $\Gamma_c$ . In this way  $\mathbb{J}_D$  is given by :*

$$\mathbb{J}_D(u_1(\eta), p_1(\eta); u_2(\tau), p_2(\tau)) = \frac{1}{2} \int_{\Gamma_c} (u_2(\tau) - f)^2 ds + \frac{1}{2} \int_{\Gamma_i} (u_1(\eta) - u_2(\tau))^2 ds. \quad (5.14)$$

*Conjointly, the "Dirichlet-gap" cost  $\mathbb{J}_D$  responds to the same process shown in this subsection.*

The optimization process which will be evolved here require the components of the gradient of  $\mathcal{J}$ . The computation of this latter may be efficiently calculated employing an adjoint state method. We presented it in proposition 5.2.3 below. Let us now define the following Lagrangian :

$$\begin{aligned} \mathcal{L}(\eta, \tau, u_1, p_1, \varphi, \xi) &= \frac{1}{2} \int_{\Gamma_c} (\sigma(u_1, p_1) n - \Phi)^2 ds + \frac{1}{2} \int_{\Gamma_i} (u_1 - \tau)^2 ds \\ &+ \int_{\Omega} 2\nu(I(u_1))D(u_1) : \nabla \varphi dx - \int_{\Omega} p_1 \operatorname{div} \varphi dx - \int_{\Gamma_i} \eta \varphi ds - \int_{\Omega} \xi \operatorname{div} u_1 dx, \end{aligned}$$

for every  $(u_1, \varphi) \in \chi^2 \times \chi_0^2$ ,  $(p_1, \xi) \in L^2(\Omega) \times L^2(\Omega)$ , and  $(\eta, \tau) \in (H^{\frac{1}{2}}(\Gamma_i)^d)' \times H^{\frac{1}{2}}(\Gamma_i)^d$ .

**Proposition 5.2.3** *The gradient of the functional  $\mathcal{J}$  is given by*

$$\begin{cases} \frac{\partial \mathcal{J}}{\partial \eta}(\eta, \tau) \gamma = - \int_{\Gamma_i} z_1 \gamma ds, & \forall \gamma \in (H^{\frac{1}{2}}(\Gamma_i)^d)', \\ \frac{\partial \mathcal{J}}{\partial \tau}(\eta, \tau) \delta = - \int_{\Gamma_i} (u_1 - \tau) \delta ds, & \forall \delta \in H^{\frac{1}{2}}(\Gamma_i)^d, \end{cases}$$

with  $(z_1, r_1) \in \chi_0^2 \times L^2(\Omega)$  solution of the adjoint problem :

$$\left\{ \begin{array}{l} \int_{\Gamma_c} (\sigma(u_1, p_1)n - \Phi)(\nu'(I(u_1))(D(u_1) : D(h_1))D(u_1)n + 2\nu(I(u_1))D(h_1)n)ds \\ \quad + \int_{\Gamma_i} (u_1 - \tau)h_1 ds + \int_{\Omega} 2\nu'(I(u_1))(D(u_1) : D(h_1))(D(u_1) : \nabla(z_1))dx \\ \quad + \int_{\Omega} 2\nu(I(u_1))D(h_1) : \nabla(z_1)dx - \int_{\Omega} r_1 \operatorname{div} h_1 dx = 0, \quad \forall h_1 \in \chi_0^2. \\ - \int_{\Gamma_c} (\sigma(u_1, p_1)n - \Phi)k_1 n ds - \int_{\Omega} k_1 \operatorname{div} z_1 dx = 0, \quad \forall k_1 \in L^2(\Omega). \end{array} \right. \quad (5.15)$$

In the numerical treatment, we used a fixed-point algorithm for the resolution of the nonlinear state equations ( $\mathcal{SP}_1$ ) (resp. ( $\mathcal{SP}_2$ )) described as follows :

- Choose  $\epsilon \in ]0, \xi)$  a convergence tolerance and  $(u_{1,0}, p_{1,0})$  a Newtonian solution.
- Iteration : For  $n \in \mathbb{N}$  :
  - Given  $u_{1,n-1}$  ; Find  $(u_{1,n}, p_{1,n}) \in \chi_f^2 \times \mathcal{M}^2$  such that

$$\left\{ \begin{array}{l} \mathcal{A}(u_{1,n-1}; u_{1,n}, v) + \mathcal{B}(v, p_{1,n}) = \int_{\Gamma_i} \eta v ds, \quad \forall v \in \chi_0^2, \\ \mathcal{B}(u_{1,n}, q) = 0, \quad \forall q \in \mathcal{M}^2, \end{array} \right. \quad (5.16)$$

where,

$$\mathcal{A}(u_{1,n-1}; u_{1,n}, v) = \int_{\Omega} 2\nu(I(u_{1,n-1}))D(u_{1,n}) : \nabla v dx,$$

and

$$\mathcal{B}(v, p_{1,n}) = - \int_{\Omega} p_{1,n} \operatorname{div} v dx.$$

- If  $\|u_{1,n} - u_{1,n-1}\| < \epsilon$ , stop. Otherwise  $u_{1,n-1} = u_{1,n}$ , repeat the solving of (5.16).

Let us consider a convergent sequence situation  $u_{1,n}$  in order to apply an iterative reconstruction procedure for the minimization problem's numerical resolution  $\min_{(\eta, \tau)} \mathcal{J}(\eta, \tau)$ . Consequently, due to the fixed-point algorithm and this assumption of convergence, we propose a novel algorithm inspired by the classical method of the conjugate gradient for a linear criterion. We describe in Algorithm 5.2.1 below the main steps of the method, supposing that the Cauchy data of the Dirichlet type  $f$  are noisy and we denote by  $\sigma$  the level of noise.

## 5.2.4 A Nash game formulation of the nonlinear Cauchy-Stokes problem

Following the previous subsection and conforming to the game theory vocabulary, the Neumann and Dirichlet controls  $\eta$  and  $\tau$  cooperate to optimize either the Neumann-gap and Dirichlet-gap costs. Consider then a two-player Nash game : Player 1, referring to the "Neumann-gap" while Player 2, referring to the "Dirichlet-gap" with two different strategies. Those two players play a static game with complete information.

---



---

**Algorithm 5.2.1:** Conjugate Gradient Method

**Data:**  $\varepsilon > 0$  a convergence tolerance,  $K_{max}$  a maximum number of iterations.

Set  $k=0$  and choose an initial guess  $(\eta^{(0)}, \tau^{(0)}) \in (H^{\frac{1}{2}}(\Gamma_i)^d)' \times H^{\frac{1}{2}}(\Gamma_i)^d$  ;

**while**  $\|u_2^{(k)} - f\|_{\Gamma_c} \geq \varepsilon$  **do**

- Solve the Stokes problem ( $\mathcal{SP}_1$ ) and the adjoint problem (5.15).
- Evaluate the gradient

$$\nabla \mathcal{J}(\eta^*, \tau^*) = -(z_1^{(k)}, u_{1,n}^{(k)} - \tau^{(k)})|_{\Gamma_i}.$$

- Determine the descent direction  $d_k$  given by :

$$\begin{cases} \beta_{k-1} = (\int_{\Gamma_i} \nabla \mathcal{J}(\eta^{(k)}, \tau^{(k)})^2 ds) / (\int_{\Gamma_i} \nabla \mathcal{J}(\eta^{(k-1)}, \tau^{(k-1)})^2 ds), \\ \text{with } \beta_{-1} = 0 \text{ and } d_k = (d_{1,k}, d_{2,k}) = -\nabla \mathcal{J}(\eta^{(k)}, \tau^{(k)}) + \beta_{k-1} d_{k-1}, \end{cases}$$

in order to find

$$(\eta^{(k+1)}, \tau^{(k+1)}) = (\eta^{(k)}, \tau^{(k)}) + \alpha_k d_k,$$

$\alpha_k$  is explicitly evaluated by :

$$\alpha_k = \frac{I_1^{(k)}}{I_2^{(k)}}$$

where

$$\begin{aligned} I_1^{(k)} = & \int_{\Gamma_c} (-p_{1,n}^{(k)} n + 2\nu(I(u_{1,n-1}^{(k)}))D(u_{1,n}^{(k)})n - \Phi)(-q_1^{(k)} n + 2\nu(I(u_{1,n-1}^{(k)}))D(v_1^{(k)})n) ds \\ & + \int_{\Gamma_i} (u_{1,n}^{(k)} - \tau^{(k)})(v_1^{(k)} - d_{2,k}) ds, \end{aligned}$$

$$I_2^{(k)} = \int_{\Gamma_c} (-q_1^{(k)} n + 2\nu(I(u_{1,n-1}^{(k)}))D(v_1^{(k)})n)^2 ds + \int_{\Gamma_i} (v_1^{(k)} - d_{2,k})^2 ds,$$

with  $(v_1^{(k)}, q_1^{(k)})$  is the weak solution of

$$\begin{cases} -\operatorname{div}(2\nu(I(v_1^{(k)}))D(v_1^{(k)})) + \nabla q_1^{(k)} = 0 & \text{in } \Omega, \\ \operatorname{div} v_1^{(k)} = 0 & \text{in } \Omega, \\ v_1^{(k)} = 0 & \text{on } \Gamma_c, \\ \sigma(v_1^{(k)}, q_1^{(k)})n = d_{1,k} & \text{on } \Gamma_i. \end{cases}$$

**end**

---

More explicitly, the "Neumann-gap" player's objective is to optimize (with strategy  $\eta$ ) the succeeding cost,

$$\mathcal{J}_1(\eta, \tau) = \frac{1}{2} \int_{\Gamma_c} (-p_1 n + 2\nu(I(u_1))D(u_1)n - \Phi)^2 ds + \frac{1}{2} \int_{\Gamma_i} (u_1 - \tau)^2 ds, \quad (5.17)$$

however, the "Dirichlet-gap" player's one is to optimize (with strategy  $\tau$ ) the cost

$$\mathcal{J}_2(\eta, \tau) = \frac{1}{2} \int_{\Gamma_c} (u_2 - f)^2 ds + \frac{1}{2} \int_{\Gamma_i} (u_1 - \tau)^2 ds, \quad (5.18)$$



where  $(u_1, p_1)$  and  $(u_2, p_2)$  are the solutions to respectively  $(\mathcal{SP}_1)$  and  $(\mathcal{SP}_2)$ . The considered two players solve, in parallel, their respective partial optimization problems, by seeking to converge towards an equilibrium that represents a compromise between them. This equilibrium situation is known in the game theory vocabulary as Nash equilibrium, which is defined as follows :

**Definition 5.2.1** *A strategy pair  $(\eta_N, \tau_N) \in (H^{\frac{1}{2}}(I_i^d))' \times H^{\frac{1}{2}}(I_i^d)$  is called, for the two-player game :*

– *Nash equilibrium if the following holds :*

$$\begin{cases} \mathcal{J}_1(\eta_N, \tau_N) \leq \mathcal{J}_1(\eta, \tau_N), & \forall \eta \in (H^{\frac{1}{2}}(I_i^d))', \\ \mathcal{J}_2(\eta_N, \tau_N) \leq \mathcal{J}_2(\eta_N, \tau), & \forall \tau \in H^{\frac{1}{2}}(I_i^d). \end{cases}$$

– *Pareto optimal Nash equilibrium if there does not exist another Nash equilibrium  $(\eta_n, \tau_n) \in (H^{\frac{1}{2}}(I_i^d))' \times H^{\frac{1}{2}}(I_i^d)$  such that :*

$$\mathcal{J}_1(\eta_n, \tau_n) \leq \mathcal{J}_1(\eta_N, \tau_N) \text{ and } \mathcal{J}_2(\eta_n, \tau_n) \leq \mathcal{J}_2(\eta_N, \tau_N).$$

The proposed game formulation has a separable structure. Indeed, the players' criteria are formed of individual costs, in the sense that for each cost, we try to optimize it with respect to a single variable where the information coming from the others is fixed. In [56], the authors showed in the linear case that this separable structure is privileged since it eases proving the existence and uniqueness of Nash equilibrium and proving a convergence result concerning noisy data. Graciously to this structure of the criteria, it can evidently show that when the nonlinear Cauchy-Stokes problem has a unique solution  $(u, p)$ , the pair  $(\eta_c, \tau_c) = (\sigma(u, p)n|_{I_i}, u|_{I_i})$  is the unique Pareto optimal Nash equilibrium.

From the computational viewpoint, we consider a classical alternating minimization algorithm with relaxation [12]. It is also referred to as the inertial Nash equilibration process, which computes the Nash equilibrium described in Algorithm 5.2.2 below.

---

**Algorithm 5.2.2:** Nash equilibrium algorithm

---

**Data:**  $\xi > 0$  a convergence tolerance, a relaxation factor  $0 \leq \alpha < 1$ .

Set  $k = 0$ . Starting from an initial guess  $S^{(0)} = (\eta^{(0)}, \tau^{(0)}) \in (H^{\frac{1}{2}}(I_i^d))' \times H^{\frac{1}{2}}(I_i^d)$

**while**  $\|S^{(k+1)} - S^{(k)}\| > \xi$  **do**

• Step 1 : Compute  $\bar{\eta}^{(k)}$  solution of

$$\min_{\eta} \mathcal{J}_1(\eta, \tau^{(k)}).$$

• Step 2 : Compute (in parallel)  $\bar{\tau}^{(k)}$  solution of

$$\min_{\tau} \mathcal{J}_2(\eta^{(k)}, \tau).$$

• Step 3 : Set  $S^{(k+1)} = (\eta^{(k+1)}, \tau^{(k+1)}) = \alpha(\eta^{(k)}, \tau^{(k)}) + (1 - \alpha)(\bar{\eta}^{(k)}, \bar{\tau}^{(k)})$ .

**end**

---

We used the fixed step gradient method to solve the partial optimization problem in steps 1 and 2 above. For that, we need to evaluate the gradients of the costs  $\mathcal{J}_1$  and

$\mathcal{J}_2$ , respectively, to their strategies. The adjoint state method is employed to compute the components of the gradient. Let us define the lagragian  $\mathcal{L}'$  as follows :

$$\begin{aligned} \mathcal{L}'(\eta, \tau, u_1, p_1, u_2, p_2, v_1, q_1, u_2, p_2) &= \frac{1}{2} \int_{\Gamma_c} (\sigma(u_1, p_1)n - \Phi)^2 ds + \frac{1}{2} \int_{\Gamma_c} (u_2 - f)^2 ds \\ &+ \frac{1}{2} \int_{\Gamma_i} (u_1 - u_2)^2 ds + \int_{\Omega} 2\nu(I(u_1))D(u_1) : \nabla v_1 dx - \int_{\Omega} p_1 \operatorname{div} v_1 dx \\ &- \int_{\Gamma_i} \eta v_1 ds - \int_{\Omega} q_1 \operatorname{div} u_1 dx + \int_{\Omega} 2\nu(I(u_2))D(u_2) : \nabla v_2 dx - \int_{\Omega} p_2 \operatorname{div} v_2 dx \\ &- \int_{\Gamma_c} \Phi v_2 ds - \frac{1}{\epsilon} \int_{\Gamma_i} (u_2 - \tau) v_2 ds - \int_{\Omega} q_2 \operatorname{div} u_2 dx, \end{aligned}$$

for every  $(u_1, u_2, v_1, v_2) \in \chi^2 \times \chi^2 \times \chi_0^2 \times \chi^2$ ,  $(p_1, p_2, q_1, q_2) \in (L^2(\Omega))^4$ , and  $(\eta, \tau) \in (H^{\frac{1}{2}}(\Gamma_i)^d)' \times H^{\frac{1}{2}}(\Gamma_i)^d$ , and with  $\epsilon \ll 1$ .

**Proposition 5.2.4** *We have the following two partial derivatives :*

$$\begin{aligned} (\mathcal{A}_1) \left\{ \begin{array}{l} \frac{\partial \mathcal{J}_1}{\partial \eta} \psi = - \int_{\Gamma_i} \psi v_1 ds, \quad \forall \psi \in (H^{\frac{1}{2}}(\Gamma_i)^d)', \\ \text{with } (v_1, q_1) \in \chi_0^2 \times L^2(\Omega) \text{ solution of the adjoint problem :} \\ \left\{ \begin{array}{l} \int_{\Gamma_c} (\sigma(u_1, p_1)n - \Phi)(\nu'(I(u_1))(D(u_1) : D(h_1))D(u_1)n + 2\nu(I(u_1))D(h_1)n) ds \\ + \int_{\Gamma_i} (u_1 - \tau)h_1 ds + \int_{\Omega} 2\nu'(I(u_1))(D(u_1) : D(h_1))(D(u_1) : \nabla(v_1))dx \\ + \int_{\Omega} 2\nu(I(u_1))D(h_1) : \nabla(v_1)dx - \int_{\Omega} q_1 \operatorname{div} h_1 dx = 0, \quad \forall h_1 \in \chi_0^2. \\ - \int_{\Gamma_c} (\sigma(u_1, p_1)n - \Phi)k_1 n ds - \int_{\Omega} k_1 \operatorname{div} v_1 dx = 0, \quad \forall k_1 \in L^2(\Omega), \end{array} \right. \end{array} \right. \\ \\ (\mathcal{A}_2) \left\{ \begin{array}{l} \frac{\partial \mathcal{J}_2}{\partial \tau} \mu = \int_{\Gamma_i} \left( \frac{1}{\epsilon} v_2 - (u_1 - \tau) \right) \mu ds, \quad \forall \mu \in H^{\frac{1}{2}}(\Gamma_i)^d, \\ \text{with } (v_2, q_2) \in \chi^2 \times L^2(\Omega) \text{ solution of the adjoint problem :} \\ \left\{ \begin{array}{l} \int_{\Gamma_c} (u_2 - f)h_2 ds + \int_{\Omega} 2\nu'(I(u_2))(D(u_2) : D(h_2))(D(u_2) : \nabla(v_2))dx \\ + \int_{\Omega} 2\nu(I(u_2))D(h_2) : \nabla(v_2)dx - \int_{\Omega} q_2 \operatorname{div} h_2 dx - \frac{1}{\epsilon} \int_{\Gamma_i} h_2 v_2 ds = 0, \quad \forall h_2 \in \chi^2, \\ - \int_{\Omega} k_2 \operatorname{div} v_2 dx = 0, \quad \forall k_2 \in L^2(\Omega). \end{array} \right. \end{array} \right. \end{aligned}$$

where  $(u_1, p_1)$  and  $(u_2, p_2)$  are the solutions, respectively to  $(\mathcal{SP}_1)$  and  $(\mathcal{SP}_2)$ .

In order to solve the state equations  $(\mathcal{SP}_1)$  and  $(\mathcal{SP}_2)$ , we employed the fixed-point algorithm described in the previous subsection.

### 5.2.5 A one-shot algorithm to deal with nonlinear Cauchy problems :

Due to the non-linearity of the viscosity function, we need to use specific algorithms to solve the nonlinear boundary value problems  $(\mathcal{SP}_1)$  and  $(\mathcal{SP}_2)$  during the

reconstruction procedure. In this context, we propose a novel one-shot scheme for solving these nonlinear state equations. It is about a new way to study the nonlinear Cauchy type problems, which gives hope to treat nonlinear state equations with a very advantageous cost compared with a classical resolution such as a fixed-point method.

More explicitly, this novel purpose consists precisely of reconstructing two linear well-posed problems. In each one  $(\mathcal{P}_i)$  for  $i \neq j \in \{1, 2\}$ , we displace the variable  $u_i$  in the viscosity function by  $u_j$ . This technique aims to linearize the problems without forgetting that they come from the same Cauchy problem. In fact, we define  $(w_1, \xi_1) = (w_1(\eta), \xi_1(\eta))$  and  $(w_2, \xi_2) = (w_2(\tau), \xi(\tau))$  as the respective solutions to the following linear mixed boundary value problem,

$$\begin{aligned} (\mathcal{P}_1^*) \left\{ \begin{array}{l} -\operatorname{div}(2\nu(I(w_2))D(w_1)) + \nabla\xi_1 = 0 \quad \text{in } \Omega, \\ \operatorname{div}w_1 = 0 \quad \text{in } \Omega, \\ w_1 = f \quad \text{on } \Gamma_c, \\ \sigma(w_1, \xi_1)n = \eta \quad \text{on } \Gamma_i, \end{array} \right. \\ (\mathcal{P}_2^*) \left\{ \begin{array}{l} -\operatorname{div}(2\nu(I(w_1))D(w_2)) + \nabla\xi_2 = 0 \quad \text{in } \Omega, \\ \operatorname{div}w_2 = 0 \quad \text{in } \Omega, \\ \sigma(w_2, \xi_2)n = \Phi \quad \text{on } \Gamma_c, \\ w_2 = \tau \quad \text{on } \Gamma_i. \end{array} \right. \end{aligned}$$

These two systems are generally distinct for any values of  $\eta$  and  $\tau$ . But when they coincide, the Cauchy problem (5.3) is solved. In this fact, we start by introducing the two cost functionals, that measure the gap between these two problems  $(\mathcal{P}_1^*)$  and  $(\mathcal{P}_2^*)$  : For  $\eta \in (H^{\frac{1}{2}}(\Gamma_i)^d)'$  and  $\tau \in H^{\frac{1}{2}}(\Gamma_i)^d$ ,

$$\begin{aligned} \mathbb{J}^1(\eta, \tau) &= \frac{1}{2} \int_{\Gamma_c} ((-\xi_1(\eta)I_d + 2\nu(I(w_2(\tau)))D(w_1(\eta)))n - \Phi)^2 ds + \frac{1}{2} \int_{\Gamma_i} (w_1(\eta) - w_2(\tau))^2 ds, \\ \mathbb{J}^2(\eta, \tau) &= \frac{1}{2} \int_{\Gamma_c} (w_2(\tau) - f)^2 ds + \frac{1}{2} \int_{\Gamma_i} (w_1(\eta) - w_2(\tau))^2 ds. \end{aligned}$$

Proceeding in the same manner, the nonlinear Cauchy-Stokes problem is formulated as a two-player Nash-game. The two players here solve in parallel the associated BVPs  $(\mathcal{P}_1^*)$  and  $(\mathcal{P}_2^*)$ . Naturally, each tries minimizing his own cost ;  $\mathbb{J}^1$  for player 1 and  $\mathbb{J}^2$  for player 2. This game's best strategy is defined as an equilibrium situation where none of the players has the interest to minimize its cost function. Consequently, the optimum found is called Nash equilibrium, given by Definition 5.2.1. For the equilibrium computation, in this case, we used Algorithm 5.2.2 described above, where the gradients for this case are given in the following proposition.

**Proposition 5.2.5** *We have the following two partial derivatives :*

$$(\mathcal{AP}_1) \left\{ \begin{array}{l} \frac{\partial \mathcal{J}_1}{\partial \eta} \psi = - \int_{\Gamma_i} \psi \lambda_1 ds, \quad \forall \psi \in (H^{\frac{1}{2}}(\Gamma_i)^d)', \\ \text{with } (\lambda_1, \kappa_1) \in \chi_0^2 \times L^2(\Omega) \quad \text{solution of the adjoint problem :} \\ \left\{ \begin{array}{l} \int_{\Gamma_c} ((-\xi I_d + 2\nu(I(w_2))D(w_1))n - \Phi)(\nu(I(w_2))(\nabla\gamma + \nabla\gamma^T)n) ds + \int_{\Gamma_i} (w_1 - \tau)\gamma ds \\ \quad + \int_{\Omega} \nu(I(w_2))(\nabla\gamma + \nabla\gamma^T) : \nabla\lambda_1 dx - \int_{\Omega} \kappa_1 \operatorname{div}\gamma dx = 0, \quad \forall \gamma \in \chi_0^2. \\ - \int_{\Gamma_c} ((-\xi I_d + 2\nu(I(w_2))D(w_1))n - \Phi)\delta n ds - \int_{\Omega} \delta \operatorname{div}\lambda_1 dx = 0, \quad \forall \delta \in L^2(\Omega), \end{array} \right. \end{array} \right.$$



---


$$(\mathcal{P}_2) \left\{ \begin{array}{ll} -\operatorname{div}(2\nu(I(u_2^\omega))D(u_2^\omega)) + \nabla p_2^\omega = 0 & \text{in } \Omega \setminus \bar{\omega}, \\ \operatorname{div} u_2^\omega = 0 & \text{in } \Omega \setminus \bar{\omega}, \\ \sigma(u_2^\omega, p_2^\omega)n = 0 & \text{on } \partial\omega, \\ \sigma(u_2^\omega, p_2^\omega)n = \Phi & \text{on } \Gamma_c, \\ u_2^\omega = \tau & \text{on } \Gamma_i. \end{array} \right.$$

Adopting the two-player Nash game strategy precendently stated in subsection 5.2.4 to solve here our coupled inverse problem. Therefore, three players are defined which play non-cooperatively a Nash game : the players 1 and 2 control the strategies  $\eta \in (H^{\frac{1}{2}}(\Gamma_i)^d)'$  and  $\tau \in H^{\frac{1}{2}}(\Gamma_i)^d$ , respectively, and play a Nash subgame to minimize the "Neumann-gap" cost  $\mathcal{J}_1$  and the "Dirichlet-gap" cost  $\mathcal{J}_2$ , while the player 3 has a control on  $\omega \in \mathcal{D}_{\text{ad}}$  and aims at minimizing the Kohn-Vogelius cost  $\mathcal{J}_3$ , to which we added the regularizing term  $\mu|\partial\omega|$  which prevents from obtaining too irregular contours. In this setting, solving the coupled inverse problem (5.19) amounts to find a Nash equilibrium, defined as a triplet of strategies  $(\eta^*, \tau^*, \omega^*) \in (H^{\frac{1}{2}}(\Gamma_i)^d)' \times H^{\frac{1}{2}}(\Gamma_i)^d \times \mathcal{D}_{\text{ad}}$ , such that

$$\left\{ \begin{array}{l} \eta^* = \arg \min_{\eta} \mathcal{J}_1(\eta, \tau^*, \omega^*), \\ \tau^* = \arg \min_{\tau} \mathcal{J}_2(\eta^*, \tau, \omega^*), \\ \omega^* = \arg \min_{\omega} \mathcal{J}_3(\eta^*, \tau^*, \omega). \end{array} \right. \quad (5.20)$$

Now, we suppose that the Nash equilibrium for the three players exists. To evaluate it then we use Algorithm 5.3.1 described below, which is mainly based on the ideas of Habbal et al. [57]. This algorithm is divided into two main steps : In step I, called a preconditioning Nash subgame, we solve a fixed shape's data completion problem. From the two-player Nash equilibrium obtained in step I, we move to step II, where the third player solves the minimization problem to detect the inclusion's shape and location.

---

**Algorithm 5.3.1:** Nash game algorithm for the Three-players

---

**Data:** convergence tolerances  $\xi > 0$ ,  $\sigma$  a noise level,  $\rho(\sigma)$  a-tuned-function which depends on the noise and  $0 \leq t < 1$  a relaxation factor.

Set  $n = 0$  and choose an initial shape  $\omega^{(0)} \in \mathcal{D}_{\text{ad}}$  ;

**while**  $\|u_2 - f^\sigma\|_{0, \Gamma_c} > \rho(\sigma)$  **do**

– Step I : A Nash subgame between  $\eta$  and  $\tau$  : Set  $k = 0$ .

Initial guess :  $S^{(0)} = (\eta^{(0)}, \tau^{(0)}) \in (H^{\frac{1}{2}}(\Gamma_i)^d)' \times H^{\frac{1}{2}}(\Gamma_i)^d$ .

1. Compute  $\bar{\eta}^{(k)}$  solution of  $\min_{\eta} \mathcal{J}_1(\eta, \tau^{(k)}; \omega^{(n)})$ ,

2. Compute (in parallel)  $\bar{\tau}^{(k)}$  solution of  $\min_{\tau} \mathcal{J}_2(\bar{\eta}^{(k)}, \tau; \omega^{(n)})$ ,

3. Set  $S^{(k+1)} = (\eta^{(k+1)}, \tau^{(k+1)}) = t(\eta^{(k)}, \tau^{(k)}) + (1-t)(\bar{\eta}^{(k)}, \bar{\tau}^{(k)})$ .

4. If  $\|S^{(k+1)} - S^{(k)}\| > \xi$ , then, set  $k = k + 1$  and repeat step 1.

– Step II : Compute  $\omega^{(n+1)}$  solution of  $\min_{\omega} \mathcal{J}_3(\eta^{(k+1)}, \tau^{(k+1)}; \omega)$ .

**end**

---

In step II, the level set approach has been used to represent the boundaries of the inclusions. This approach is an original development one for the curve and surface evolution [90]. For a given admissible shape  $\omega \subset \mathcal{D}_{\text{ad}}$  included in  $\Omega$ , we assume that there exists an implicit function  $\phi$ , the so-called level set function, which satisfies,

$$\begin{cases} \phi(x) < 0 & \text{in } \omega, \\ \phi(x) > 0 & \text{in } \Omega \setminus \bar{\omega}, \\ \phi(x) = 0 & \text{on } \partial\omega. \end{cases}$$

For the Heaviside and Dirac delta distributions, used in the level set approach and for the regularity reasons, we used smoothed versions of these distributions denoted respectively by  $H_{\varepsilon,\beta}(\cdot)$  and  $\delta_{\varepsilon,\beta}(\cdot)$ , in terms of continuous functions defined over  $\Omega$  considered as follows : for  $s \in \mathbb{R}$ ,

$$H_{\varepsilon,\beta}(s) = \begin{cases} 1 & \text{if } s > \varepsilon, \\ \frac{1}{2}\left(1 + \frac{s}{\varepsilon} + \frac{1}{\pi}\sin\left(\frac{\pi s}{\varepsilon}\right)\right) & \text{if } |s| \leq \varepsilon, \\ 0 & \text{if } s < -\varepsilon, \end{cases}$$

$$\delta_{\varepsilon,\beta}(s) = \begin{cases} \frac{1}{2\varepsilon}\left(1 + \cos\left(\frac{\pi s}{\varepsilon}\right)\right) & \text{if } |s| \leq \varepsilon, \\ 0 & \text{if } |s| > \varepsilon, \end{cases}$$

where  $\varepsilon > 0$  is small enough parameters.

Denoting by  $\tilde{\mathcal{J}}_3$  the new form of the cost functional  $\mathcal{J}_3$  in term of the level set function to be minimized

$$\min_{\phi} \left\{ \tilde{\mathcal{J}}_3(\eta, \tau; \phi) := \int_{\Omega} |\sigma(u_2^{\phi}, p_2^{\phi}) - \sigma(u_1^{\phi}, p_1^{\phi})|^2 H_{\varepsilon,\beta}(\phi) dx + \mu \int_{\Omega} \delta_{\varepsilon,\beta}(\phi) |\nabla\phi| dx \right\}, \quad (5.21)$$

where  $\sigma(u_i^{\phi}, p_i^{\phi}) = 2\nu(I(u_i^{\phi}))D(u_i^{\phi}) - p_i^{\phi}I_d$ , for  $i = 1, 2$ ,  $(u_1^{\phi}, p_1^{\phi})$  and  $(u_2^{\phi}, p_2^{\phi})$  are solutions of the following weak formulations problems

$$(\mathcal{P}_{1_{\varepsilon,\beta}}) \left\{ \begin{array}{l} \text{Find } (u_1^{\phi}, p_1^{\phi}) \in \chi_{f,\text{div}}^2 \times L^2(\Omega) \text{ such that} \\ \int_{\Omega} 2\nu(I(u_1^{\phi}))D(u_1^{\phi}) : \nabla(v_1)H_{\varepsilon,\beta}(\phi) dx - \int_{\Omega} p_1^{\phi} \text{div}v_1 H_{\varepsilon,\beta}(\phi) dx = \int_{\Gamma_i} \eta v_1 ds, \\ \forall v_1 \in \chi_0^2, \end{array} \right.$$

$$(\mathcal{P}_{2_{\varepsilon,\beta}}) \left\{ \begin{array}{l} \text{Find } (u_2^{\phi}, p_2^{\phi}) \in \kappa_{\tau,\text{div}}^2 \times L^2(\Omega) \text{ such that} \\ \int_{\Omega} 2\nu(I(u_2^{\phi}))D(u_2^{\phi}) : \nabla(v_2)H_{\varepsilon,\beta}(\phi) dx - \int_{\Omega} p_2^{\phi} \text{div}v_2 H_{\varepsilon,\beta}(\phi) dx = \int_{\Gamma_c} \Phi v_2 ds, \\ \forall v_2 \in \kappa_0^2. \end{array} \right.$$

The numerical resolution of (5.21) required the computation of the gradient of  $\tilde{\mathcal{J}}_3$ . Following the same lines as for the linear case [57] and using the Lagrangian method, we obtain for  $\phi \in H^1(\Omega)$  such that  $|\nabla\phi| \neq 0$  and with the boundary condition  $\frac{\partial\phi}{\partial n} = 0$  over  $\partial\Omega$ , the partial derivative of  $\tilde{\mathcal{J}}_3(\eta, \tau; \phi)$  with respect to  $\phi$ , in any direction  $\psi \in H^1(\Omega)$  :

$$\begin{aligned} \left(\frac{\partial\tilde{\mathcal{J}}_3}{\partial\phi}(\eta, \tau; \phi), \psi\right) &= \int_{\Omega} \delta_{\varepsilon,\beta}(\phi) \left[ |\sigma(u_2^{\phi}, p_2^{\phi}) - \sigma(u_1^{\phi}, p_1^{\phi})|^2 - \mu \text{div}\left(\frac{\nabla\phi}{|\nabla\phi|}\right) \right. \\ &\quad \left. + 2\nu(I(u_1^{\phi}))D(u_1^{\phi}) : \nabla\lambda_1 - p_1 \text{div}\lambda_1 + 2\nu(I(u_2^{\phi}))D(u_2^{\phi}) : \nabla\lambda_2 - p_2 \text{div}\lambda_2 \right] \psi dx, \end{aligned}$$

where  $(\lambda_1, \pi_1) \in \chi_0^2 \times L^2(\Omega)$  and  $(\lambda_2, \pi_2) \in \kappa_0^r \times L^2(\Omega)$  are respective solutions of the adjoints problems,

$$\left\{ \begin{array}{l} 2 \int_{\Omega} (\sigma(u_2^\phi, p_2^\phi) - \sigma(u_1^\phi, p_1^\phi)) : (2\nu'(I(u_1^\phi))(D(u_1) : D(h_1))D(u_1^\phi) + 2\nu(I(u_1^\phi))D(h_1))H_{\varepsilon,\beta}(\phi)dx \\ \quad + \int_{\Omega} (2\nu'(I(u_1^\phi))(D(u_1^\phi) : D(h_1))D(u_1^\phi) : \nabla\lambda_1 + 2\nu(I(u_1^\phi))D(h_1) : \lambda_1)H_{\varepsilon,\beta}(\phi)dx \\ \quad - \int_{\Omega} \pi_1 \operatorname{div} h_1 H_{\varepsilon,\beta}(\phi)dx = 0, \quad \forall h_1 \in \chi_0^2, \\ 2 \int_{\Omega} (\sigma(u_2^\phi, p_2^\phi) - \sigma(u_1^\phi, p_1^\phi)) : (k_1 I_d)H_{\varepsilon,\beta}(\phi)dx - \int_{\Omega} k_1 \operatorname{div} \lambda_1 H_{\varepsilon,\beta}(\phi)dx = 0, \\ \quad \forall k_1 \in L^2(\Omega), \end{array} \right. \quad (5.22)$$

$$\left\{ \begin{array}{l} 2 \int_{\Omega} (\sigma(u_2^\phi, p_2^\phi) - \sigma(u_1^\phi, p_1^\phi)) : (2\nu'(I(u_2^\phi))(D(u_2) : D(h_2))D(u_2^\phi) + 2\nu(I(u_2^\phi))D(h_2))H_{\varepsilon,\beta}(\phi)dx \\ \quad + \int_{\Omega} (2\nu'(I(u_2^\phi))(D(u_2^\phi) : D(h_2))D(u_2^\phi) : \nabla\lambda_2 + 2\nu(I(u_2^\phi))D(h_2) : \lambda_2)H_{\varepsilon,\beta}(\phi)dx \\ \quad - \int_{\Omega} \pi_2 \operatorname{div} h_2 H_{\varepsilon,\beta}(\phi)dx = 0, \quad \forall h_2 \in \kappa_0^2, \\ -2 \int_{\Omega} (\sigma(u_2^\phi, p_2^\phi) - \sigma(u_1^\phi, p_1^\phi)) : (k_2 I_d)H_{\varepsilon,\beta}(\phi)dx - \int_{\Omega} k_2 \operatorname{div} \lambda_2 H_{\varepsilon,\beta}(\phi)dx = 0, \\ \quad \forall k_2 \in L^2(\Omega), \end{array} \right. \quad (5.23)$$

and where  $(u_1^\phi, p_1^\phi)$  and  $(u_2^\phi, p_2^\phi)$  are the solutions to respectively  $(\mathcal{P}_{1\varepsilon,\beta})$  and  $(\mathcal{P}_{2\varepsilon,\beta})$ .

The Euler-Lagrange equation associated to the minimization problem  $\min_{\phi \in \mathcal{S}} \mathcal{J}_3(\eta, \tau; \phi)$ , ( $\mathcal{S} = H^1(\Omega)$ ) reads :

$$\left\{ \begin{array}{l} \delta_{\varepsilon,\beta}(\phi) \left[ |\sigma(u_2^\phi, p_2^\phi) - \sigma(u_1^\phi, p_1^\phi)|^2 - \mu \operatorname{div} \left( \frac{\nabla \phi}{|\nabla \phi|} \right) \right. \\ \quad \left. + \sigma(u_1^\phi, p_1^\phi) : \nabla \lambda_1 + \sigma(u_2^\phi, p_2^\phi) : \nabla \lambda_2 \right] = 0, \quad \text{in } \Omega, \\ \frac{\partial \phi}{\partial n} = 0, \quad \text{on } \partial \Omega. \end{array} \right. \quad (5.24)$$

The nonlinear equation above is solved as the stationary state of the evolution equation in order to make the level set function dynamically changes in times :

$$\left\{ \begin{array}{l} \frac{\partial \phi}{\partial t} + \delta_{\varepsilon,\beta}(\phi) \left[ |\sigma(u_2^\phi, p_2^\phi) - \sigma(u_1^\phi, p_1^\phi)|^2 - \mu \operatorname{div} \left( \frac{\nabla \phi}{|\nabla \phi|} \right) \right. \\ \quad \left. + \sigma(u_1^\phi, p_1^\phi) : \nabla \lambda_1 + \sigma(u_2^\phi, p_2^\phi) : \nabla \lambda_2 \right] = 0, \quad \text{in } \mathbb{R}^+ \times \Omega, \\ \frac{\partial \phi}{\partial n} = 0, \quad \text{on } \mathbb{R}^+ \times \partial \Omega, \\ \phi(0, x) = \phi_0(x), \quad \text{in } \Omega, \end{array} \right. \quad (5.25)$$

where  $\phi_0$  is a given initial condition. The numerical solution associated with the problem (5.25) above will be achieved using a finite-element method and a semi-implicit Euler scheme.

---

## 5.4 Numerical results

All the PDEs are numerically solved in this work using the Finite Element package FreeFem++ [61]. The domain boundary is split into two parts  $\Gamma_c$  and  $\Gamma_i$  :  $\Gamma_i$  is the inaccessible part where the fluid velocity and the stress forces are missing, and  $\Gamma_c$  is the accessible part where the Cauchy data  $f$  and  $\Phi$  are available. These latter are generated via a finite element solution of the mixed boundary value problem in each test-case.

In order to study the robustness of our algorithms, we add white noise to the Dirichlet data  $f = u_{ex}$  over  $\Gamma_c$ , as follows

$$f^\sigma = f + \sigma N,$$

where  $\sigma$  representing the percentage of noise, and  $N$  being a Gaussian-or-uniform white noise. For the Carreau law, we assume that :  $r = 3/2$ ,  $\lambda = 1$ ,  $\nu_\infty = 1/2$ , and  $\nu_0 = 1$ .

### 5.4.1 Data completion problem.

This paragraph illustrates the numerical results obtained using two approaches, the control type method and the Nash game one, described in subsection 5.2.3 and 5.2.4. To test these approaches' efficiency and compare them, we solve the Cauchy-Stokes problem in two 2D-situations. We will present here three test-cases, named A, B, and C.

Our goal is to find the missing data over the inaccessible  $\Gamma_i$  part of the boundary  $\partial\Omega$  : the fluid velocity and the stress forces. We start from an initial guess  $(\eta_0, \tau_0) = (0, 0)$ .

**Test-case A.** In this example, the nonlinear Cauchy-Stokes problem is solved in an annular domain  $\Omega$ , centered in  $(0, 0)$ , and discretized by a mesh of 180 vertices on  $\Gamma_c$  and 90 vertices on  $\Gamma_i$ . The inner boundary, circle of radius  $R_i = 1$ , is considered as  $\Gamma_i$ , while the outer circle, of radius  $R_c = 2$ , indicates the accessible part  $\Gamma_c$ . The Cauchy data here are numerically simulated by solving the following problem,

$$(\mathcal{P}_{ex}^1) \left\{ \begin{array}{ll} -\operatorname{div}(2\nu(I(u))D(u)) + \nabla p = 0 & \text{in } \Omega, \\ \operatorname{div} u = 0 & \text{in } \Omega, \\ \sigma(u, p)n = 0 & \text{on } \Gamma_c, \\ \sigma(u, p)n = \Psi & \text{on } \Gamma_i, \end{array} \right.$$

where  $\Psi$  is a given function, and in order to solve this problem  $(\mathcal{P}_{ex}^1)$ , we used the fixed-point algorithm.

Figure 5.1 represents the iso-values of the exact solution ; fluid velocity and corresponding pressure. The two components of the fluid velocity and the normal stress are presented in Figure 5.4 for unnoisy data, compared with the corresponding exacts solution, using the conjugate gradient algorithm 5.2.1 described in subsection 5.2.3.

In this test-case A, the proposed algorithms 5.2.1 and 5.2.2 are tested for two types of noise : Gaussian noise and uniform noise. Figures 5.5 and 5.8 show the reconstructed



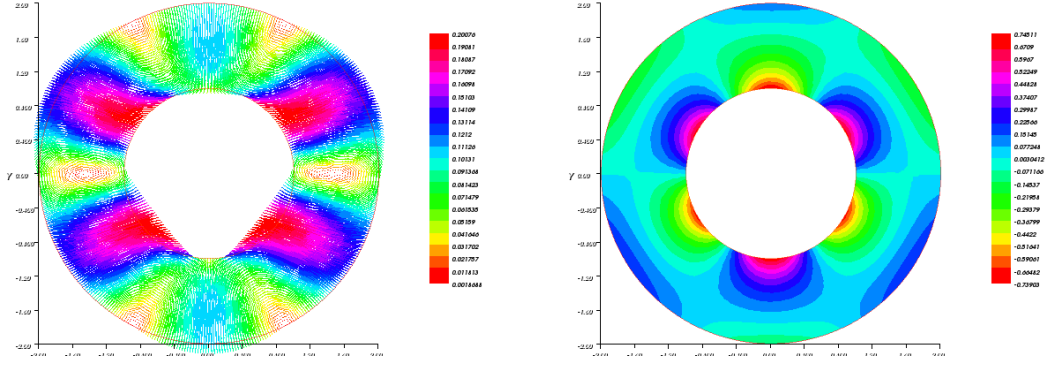


FIGURE 5.1 – Test case A. Iso-values of the velocity (left) and pressure (right) fields.

fluid velocity and normal stress for different values of noise  $\sigma$  as well as the exact ones, when we added, respectively, the uniform noise and the Gaussian noise, to the Dirichlet data over  $\Gamma_c$ . These letter results are obtained by a classical method.

We repeated the same test for the Nash game algorithm by using two different schemes to solve the state equations  $(\mathcal{SP}_1)$  and  $(\mathcal{SP}_2)$  : The first is the fixed-point algorithm FPA, and the second is our new proposed one-shot scheme NS, which consists to change the viscosity function  $\nu(u_1)$  in  $(\mathcal{SP}_1)$  by  $\nu(u_2)$  (resp.  $\nu(u_2)$  in  $(\mathcal{SP}_2)$  by  $\nu(u_1)$ ), that is, solving the state equations  $(\mathcal{P}_1^*)$  and  $(\mathcal{P}_2^*)$  instead of  $(\mathcal{SP}_1)$  and  $(\mathcal{SP}_2)$ . At convergence, using the fixed-point algorithm (respectively, NS), the relative  $L^2$ -errors on missing Dirichlet data is equal to 0.0015 (respectively, 0.0015), and Neumann data is equal to 0.0082 (respectively, 0.0081) for the case of unnoisy data. In Figures 5.6 and 5.7, the missing data  $\eta_N$  and  $\tau_N$  are presented at the convergence of the Nash game algorithm 5.2.2 for two different schemes with various noise levels. These results show remarkable stability with respect to a uniform noise.

Table 2 shows different errors on the reconstructed missing data for different uniform noise levels, and the following formulas compute these errors :

$$err_\tau = \frac{\|u_{ex} - \tau_{op}\|_{\Gamma_i}}{\|u_{ex}\|_{\Gamma_i}}, \quad err_\eta = \frac{\|\sigma(u_{ex}, p_{ex})n - \eta_{op}\|_{\Gamma_i}}{\|\sigma(u_{ex}, p_{ex})n\|_{\Gamma_i}}, \quad (5.26)$$

where  $(u_{ex}, p_{ex})$  is the solution to  $(\mathcal{P}_{ex}^1)$ , and the pair  $(\eta_{op}, \tau_{op})$  is the numerical Cauchy solution. On the one hand, according to the game method, a remarkable advantage is clearly observed for high noise levels. On the other hand, the relative errors obtained by testing two different schemes, the fixed-point and the novel schemes, are almost identical. So, for this reason, a comparison in CPUs time is performed. Let us note that the Nash game algorithm's benefit is that the players solve their partial optimization problems parallelly at each overall iteration. Consequently, to save computation time, parallel implementations are considered using the package FreeFem++ MPI. All experiments are performed on a Personal computer ; i.e., the CPU's obtained values are approximate to make simply the desired comparison. The obtained values are presented in Table 3 at convergence for noisy Dirichlet data, for the case of a uniform noise, and show our new scheme's performance.

Likewise that the precedent results concerning a uniform noise, we obtain the upcoming Figures 5.9-5.10 and Tables 4-5, which show nice stability with respect to a gaussian noise, according to two different schemes (fixed-point algorithm and novel scheme) using a Nash game strategy.

**Test-case B.** To illustrate the case where  $I_i$  touches  $I_c$ , we consider a unit disk domain, where the Cauchy data are available only on half the external boundary. The latter are generated via a finite element solution of the following mixed boundary value problem

$$(\mathcal{P}_{ex}^2) \begin{cases} -\operatorname{div}(2\nu(I(u))D(u)) + \nabla p = 0 & \text{in } \Omega, \\ \operatorname{div} u = 0 & \text{in } \Omega, \\ u = f & \text{on } I_c, \\ \sigma(u, p)n = H & \text{on } I_i, \end{cases}$$

where  $f$  and  $H$  are given functions. Several tests are carried out for various finite element meshes to show the convergence of our two algorithms ; the classic and the Nash game approaches. Figure 5.11 depicts the Dirichlet and Neumann reconstructed data for various numbers of nodes on the boundary  $M = \{100, 150, 200\}$ , with the control-type method. It can be possible to observe that the recovered Dirichlet data remains a good approximation for the exact solution, while the recovered Neumann data deviate from the exact one in the neighborhood of  $I_i$  endpoint, which is the region of singularity.

The same reconstructions are presented in Figure 5.12 using Nash game algorithm 5.2.2 with our proposed scheme to solve the state equations. In order to compare these two approaches for this test-case, we compute different errors indicators, which are presented in Table 6, where  $(u, p)$  is the solution of  $(\mathcal{P}_{ex}^2)$ .

**Test-case C.** To build a specific geometry of an artery close to being realistic for numerical simulation in 2D, the idea is to construct a mesh from a photo using Photoshop-or-Matlab and a script in FreeFem++, or GMSH to create the artery's initial mesh. In this case, the obtained mesh is given in figure 5.2(a). In which we assumed that the domain boundary is divided into two parts, namely,  $I_i = \sum_{k=1}^3 I_{i_k}$  where the outlet boundary conditions are unknown, and  $I_c = I_{c_1} \cup I_{c_2}$  which is the artery wall and the inlet side, where the Cauchy data are available. These latter are generated via the solution of the upcoming nonlinear mixed boundary problem,

$$(\mathcal{P}_{ex}^3) \begin{cases} -\operatorname{div}(2\nu(I(u))D(u)) + \nabla p = 0 & \text{in } \Omega, \\ \operatorname{div} u = 0 & \text{in } \Omega, \\ u = f & \text{on } I_{c_1}, \\ u = f & \text{on } I_i, \\ \sigma(u, p)n = 0 & \text{on } I_{c_2}, \end{cases}$$

where  $f$  is a given function. Figure 5.2(b) represents the exact velocity isoline of the above problem  $(\mathcal{P}_{ex}^3)$ . To recover the unknown outlet boundary conditions, Dirichlet and Neumann data, we employed the Nash game algorithm for two-player 5.2.2. The obtained results of the missing data over  $I_i$  are illustrated in figure 5.13, in comparison with the corresponding exact solutions for unnoisy data.

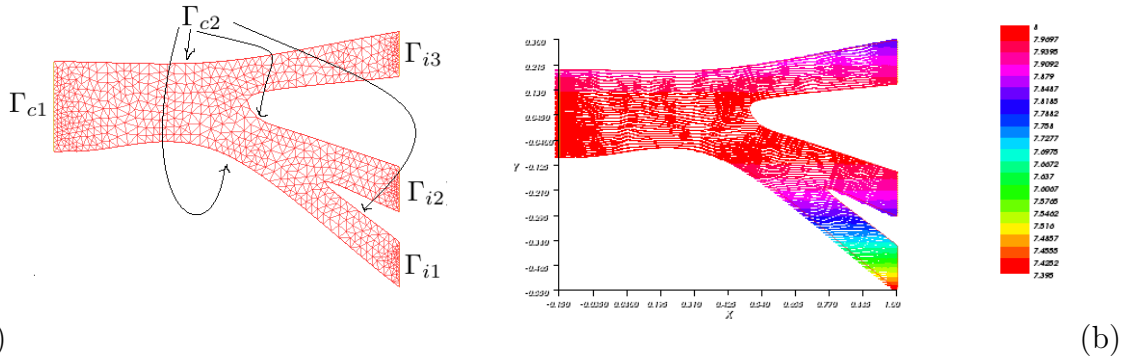


FIGURE 5.2 – Test case C. (Left) Mesh used for solving the coupled inverse problem. (Right) Iso-values of the velocity field.

## 5.4.2 Application to coupled problem : Data completion and geometry identification

A numerical study is performed for two 2D test-cases to illustrate the Nash game algorithm's efficiency for three players, which consists of recovering the inclusions and the missing data, Dirichlet and Neumann data on the inaccessible part.

**The domain :**  $\Omega = ]-\frac{1}{2}, \frac{1}{2}[ \times ]-\frac{1}{2}, \frac{1}{2}[$

**The boundaries :**  $I_i = \{\frac{1}{2}\} \times ]-\frac{1}{2}, \frac{1}{2}[$ ;  $I_c = \partial\Omega \setminus I_i$

**Normal stress :**  $\Phi(x, y) = -2(y^2 - 1/4; 0)$  prescribed over  $\partial\Omega$

The Cauchy data are generated via the solution of the following direct problem :

$$(\mathcal{P}_{ex}^4) \begin{cases} -\operatorname{div}(2\nu(I(u))D(u)) + \nabla p = 0 & \text{in } \Omega \setminus \overline{\omega^*}, \\ \operatorname{div} u = 0 & \text{in } \Omega \setminus \overline{\omega^*}, \\ \sigma(u, p)n = 0 & \text{on } \partial\omega^*, \\ \sigma(u, p)n = \Phi, & \text{on } \partial\Omega. \end{cases}$$

To start our Nash equilibrium algorithm 5.3.1, an initial guess  $(\eta^{(0)}, \tau^{(0)})$  is chosen equal to  $(0, 0)$ , and an initial contour  $\phi^{(0)}$  is defined by a periodic function, as several holes spread over the entire domain, see Figure 5.14(a). We re-initialize the level set function to a signed distance function during the evolution for maintaining stable curve evolution and guaranteeing desired results.

**Test-case D.** In this test case, we try to detect a disk  $\omega^* = B(c, r)$  centered at  $c = (-0.15, -0.15)$  and with a radius  $r$  of 0.15.

To illustrate the convergence of the Nash Equilibrium Algorithm for the three players, we present in Figure 5.3 the evolution of the three objective functionals as functions of overall Nash iterations for noise-free. We remark that during the early Nash iterations process, the three players show a fast decrease in their costs before stagnating.

In Figure 5.14, we present the recovered Dirichlet/ Neumann data results and the optimal shape of the inclusion for different noise levels. Notice that the reconstruction

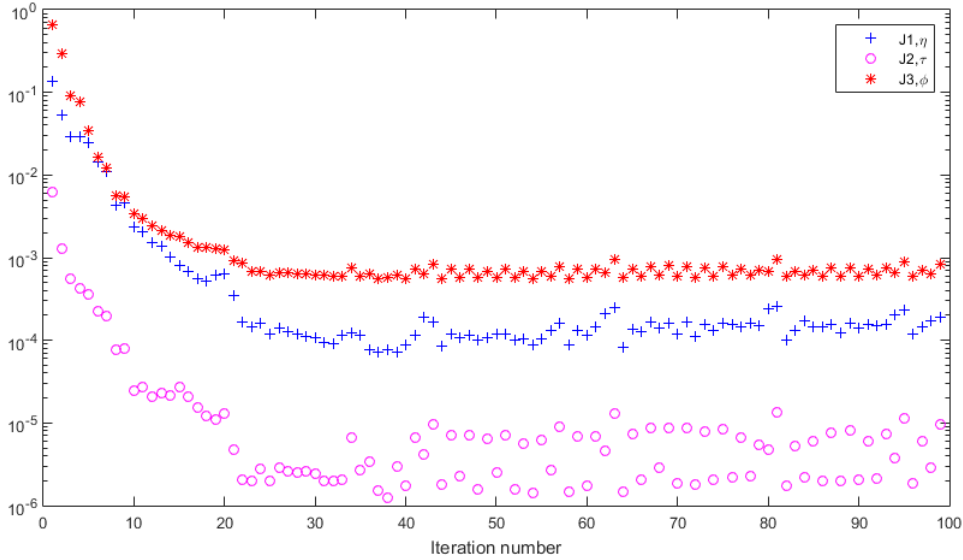


FIGURE 5.3 – Test case D. Plots of the three costs  $\mathcal{J}_1$ ,  $\mathcal{J}_2$  and  $\tilde{\mathcal{J}}_3$  as functions of overall Nash iterations.

of the missing data is in good agreement with the expected one. The profile shape also shows a remarkable stability w.r.t the Gaussian noise.

Table 1 represents the relative errors on Dirichlet and Neumann missing data, which are defined in (5.26), and the detected contours  $err_\omega$ , with respect to noisy Dirichlet measurements, where  $err_\omega = mes(\omega^* \cup \omega_N) - mes(\omega^* \cap \omega_N)/mes(\omega^*)$ .

Table 5.1 – Test-case D.  $L^2$ -errors on missing data over  $\Gamma_i$ , and the error between the reconstructed and the real shape of the inclusion for various noise levels.

Noise level	$\sigma = 1\%$	$\sigma = 3\%$	$\sigma = 5\%$	$\sigma = 8\%$
$err_\tau$	0.0222	0.0282	0.0405	0.0691
$err_\eta$	0.0466	0.0860	0.1038	0.1270
$err_\omega$	0.0831	0.1020	0.1163	0.1548

**Test-case E.** Here, we want to detect two object, a disk  $\omega_1^* = B(c, r)$  centered at  $c = (0.2, 0.25)$ , with a radius  $r$  of 0.1, and an ellipse  $\omega_2^*$ , in which the equation of its curve is :  $\frac{(x - x_1)^2}{a^2} + \frac{(y - y_1)^2}{b^2} = 1$ , where  $(a, b) = (0.15, 0.07)$  and  $(x_1, y_1) = (-0.2, -0.1)$ .

In Figure 5.15, we present the obtained results illustrating our algorithm's stability dedicated to the computation of Nash equilibrium for three players, the missing data over  $\Gamma_i$ , and the identified shape at convergence for different noise levels (for a Gaussian noise).

---

## 5.5 Conclusion

This paper has addressed the nonlinear Cauchy type problems for a quasi-Newtonian flow where the fluid viscosity is assumed to be a nonlinear function dependent on the deformation tensor. The Cauchy problem is ill-posed in the sense of Hadamard. Their ill-posedness is related to the instability issue, and designing efficient and stable algorithms is challenging.

Firstly, we have considered two different data recovering strategies : The first method is a control-type one that is a variational conjugate gradient iterative procedure is used. The second approach consists of formulating the data completion problem as a static game with complete information. Each one reduces the ill-posed problem to solving two well-posed nonlinear mixed BVPs. The numerical implementation of these approaches is accomplished using the finite-element method for solving, at each iteration, the state equations for a nonlinear Stokes system and the corresponding adjoint ones. Since the state equations are nonlinear, specific algorithms are required to solve them, such as Newton's or a fixed-point algorithm. We have proposed a novel one-shot scheme representing a new way to solve a nonlinear Cauchy problem. Next, we compare it with a fixed-point algorithm. The numerical results show that the Nash game approach outperforms the classic method, in terms of accuracy for noise-free, as well as for noisy Dirichlet data measurements (from a data completion viewpoint on the inaccessible part of the boundary), and that the one-shot scheme NS outperforms the fixed-point algorithm FPA, in terms of CPU times.

This work's second contribution is the numerical resolution of a delicate problem, which identifies unknown cavities immersed in a quasi-Newtonian fluid flow obeying the Carreau law, using partial boundary measurements. Following the ideas introduced earlier in [57] to solve the geometric Cauchy problem for the linear Stokes system, we reformulate the coupled problem as a three players Nash game : the two first players dedicate to the missing data, while the third one is functionally related to the geometric identification problem. Numerical experiments for two test-cases were performed and showed the efficiency of our 3-player Nash game algorithm.

Table 5.2 – Control type (classic) compared to Nash (game) algorithms. Relative L2-errors on missing data on  $I_i$  (on Dirichlet and Neumann data) are shown for various noise levels (w.r.t a uniform noise).

Noise level	$\sigma = 0\%$	$\sigma = 3\%$	$\sigma = 5\%$	$\sigma = 10\%$	$\sigma = 15\%$
Reconstructed data	D-N	D-N	D-N	D-N	D-N
Classic method	0.0054-0.0150	0.0195-0.0623	0.0293-0.0773	0.0507-0.1328	0.0916-0.1678
NGM-FPA	0.0015-0.0082	0.0124-0.0552	0.0158-0.0598	0.0185-0.0688	0.0236-0.0819
NGM-NS	0.0015-0.0081	0.0123-0.0544	0.0159-0.0600	0.0188-0.0689	0.0232-0.0815

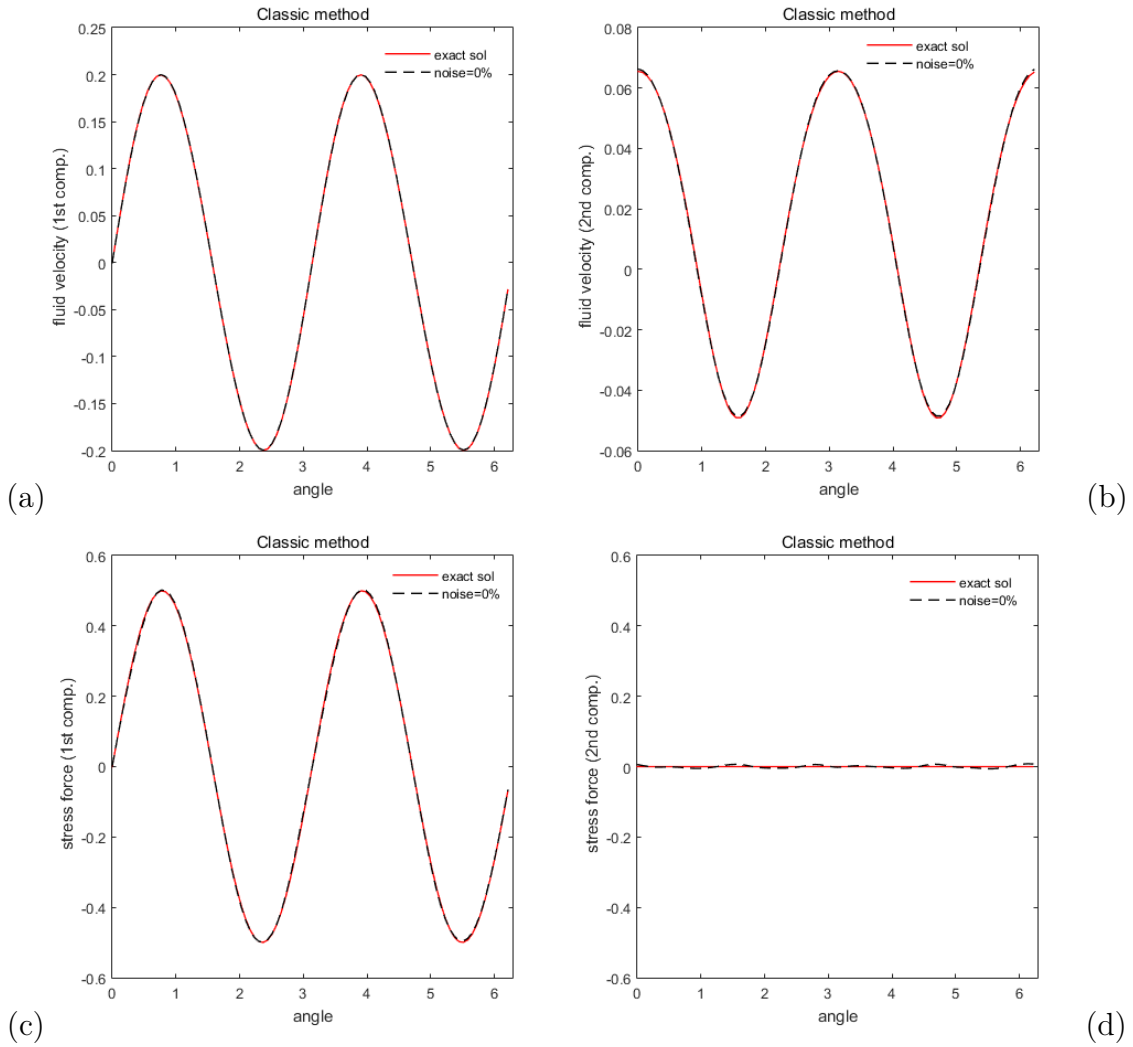


FIGURE 5.4 – Test case-A "Classic Method". Reconstruction of the missing boundary data from unnoisy data. **(a)** exact and computed first components of the velocity over  $I_i$  **(b)** exact and computed second components of the velocity over  $I_i$  **(c)** exact and computed first components of the normal stress over  $I_i$  **(d)** exact and computed second components of the normal stress over  $I_i$ .

Table 5.3 – Test case A. A CPU time performance's comparison, between the fixed-point algorithm and the new scheme, through CPUs' results (w.r.t a uniform noise).

Noise level	$\sigma = 0\%$	$\sigma = 3\%$	$\sigma = 5\%$	$\sigma = 10\%$	$\sigma = 15\%$
CPU	CPU	CPU	CPU	CPU	CPU
NGM-FPA	3870	1850	1512	792	578
NGM-NS	2511	1195	1084	492	358

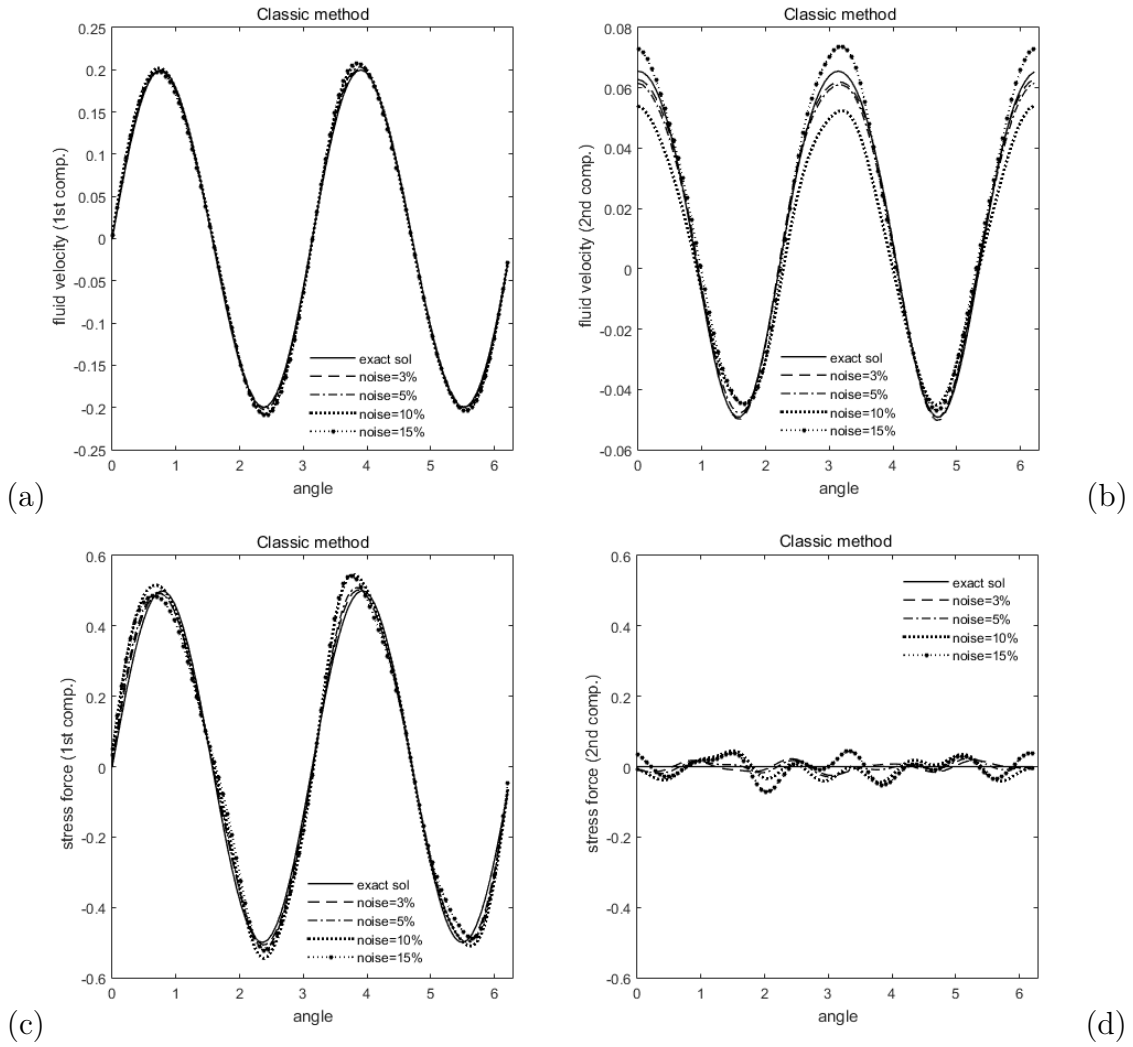


FIGURE 5.5 – Test case-A "Classic Method". Reconstruction of the missing boundary data with noisy Dirichlet data over  $I_c$  with noise levels  $\sigma = \{3\%, 5\%, 10\%, 15\%\}$ . (a) exact and computed first components of the velocity over  $I_i$  (b) exact and computed second components of the velocity over  $I_i$  (c) exact and computed first components of the normal stress over  $I_i$  (d) exact and computed second components of the normal stress over  $I_i$  (w.r.t a uniform noise).

Table 5.4 – Test case-A "Control type (classic) compared to Nash (game) algorithms". Relative L2-errors on missing data on  $I_i$  (on Dirichlet and Neumann data) are shown for various noise levels (w.r.t a Gaussian noise).

Noise level	$\sigma = 1\%$	$\sigma = 3\%$	$\sigma = 5\%$	$\sigma = 8\%$
Reconstructed data	D-N	D-N	D-N	D-N
Classic method	0.0270-0.0659	0.1242-0.2237	0.1293-0.2346	0.1261-0.3108
NGM- FPA	0.0145-0.0486	0.018-0.063	0.0221-0.0740	0.0278-0.0927
NGM-NS	0.0108-0.0404	0.0189-0.0606	0.0193-0.0636	0.0216-0.0711

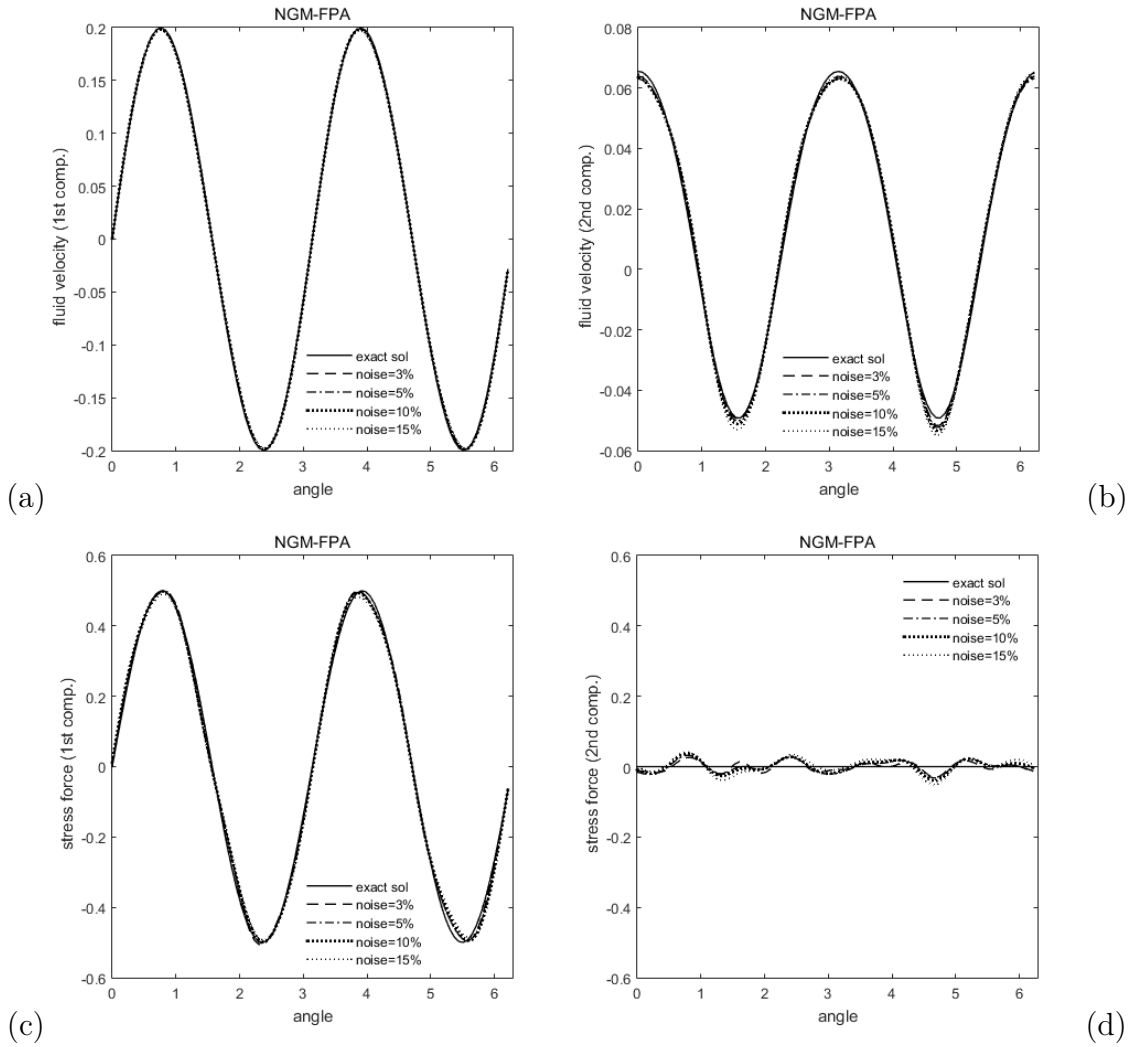


FIGURE 5.6 – Test case-A "NGM-FPA". Reconstruction of the missing boundary data with noisy Dirichlet data over  $L_c$  with noise levels  $\sigma = \{3\%, 5\%, 10\%, 15\%\}$ . **(a)** exact and computed first components of the velocity over  $I_i$  **(b)** exact and computed second components of the velocity over  $I_i$  **(c)** exact and computed first components of the normal stress over  $I_i$  **(d)** exact and computed second components of the normal stress over  $I_i$  (w.r.t a uniform noise).

Table 5.5 – Test case-A. A CPU time performance's comparison, between the fixed-point algorithm and the new scheme, through CPUs' results (w.r.t a Gaussian noise).

Noise level	$\sigma = 1\%$	$\sigma = 3\%$	$\sigma = 5\%$	$\sigma = 8\%$
CPU	CPU	CPU	CPU	CPU
NGM-FPA	2556	1798	5952	4922
NGM-NS	1444	925	703	688



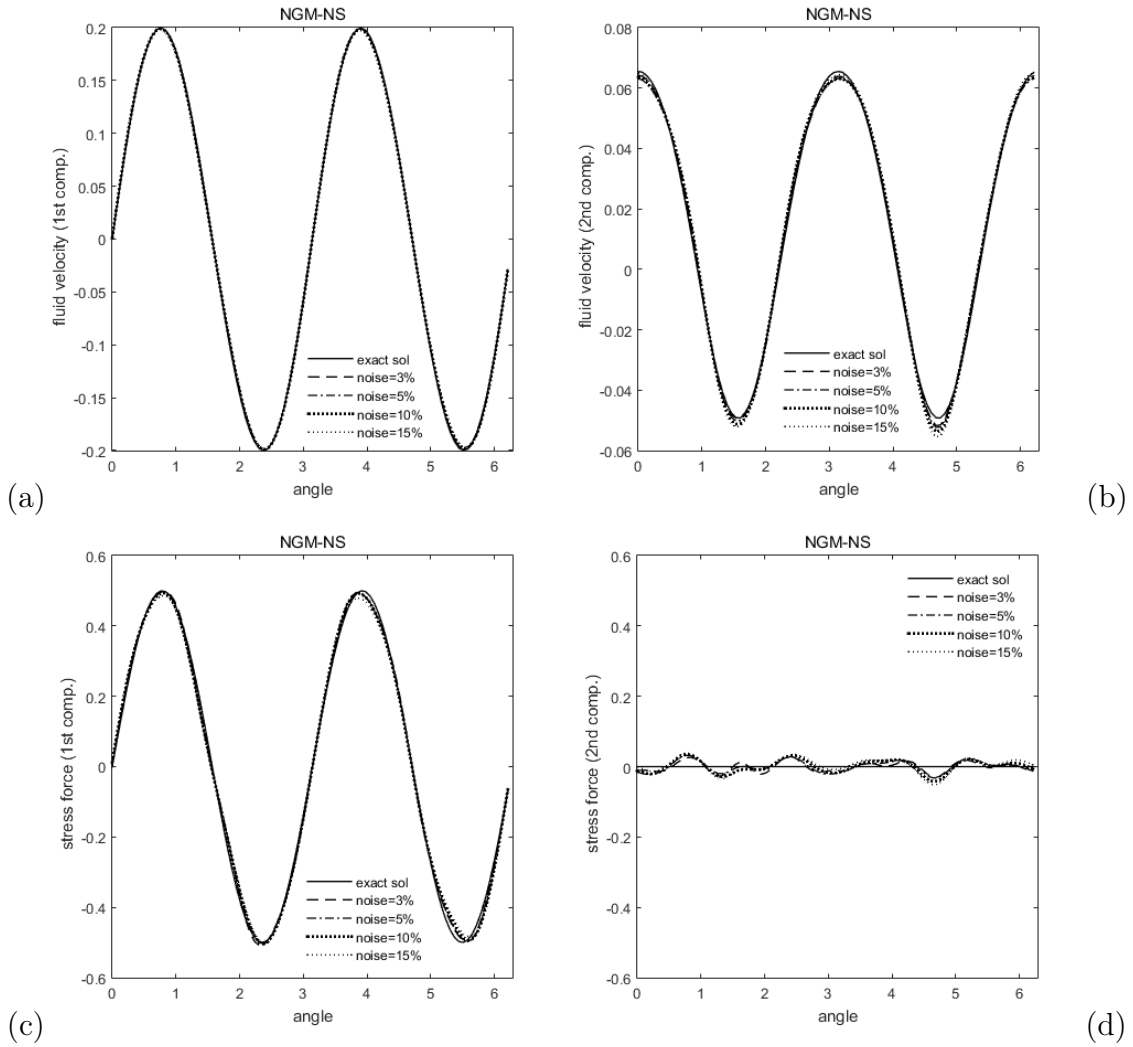


FIGURE 5.7 – Test case-A "NGM-NS". Reconstruction of the missing boundary data with noisy Dirichlet data over  $L_C$  with noise levels  $\sigma = \{3\%, 5\%, 10\%, 15\%\}$ . (a) exact and computed first components of the velocity over  $I_i$  (b) exact and computed second components of the velocity over  $I_i$  (c) exact and computed first components of the normal stress over  $I_i$  (d) exact and computed second components of the normal stress over  $I_i$  (w.r.t a uniform noise).

Table 5.6 – Test case B "The mesh refinement effect". Relative L2-errors on missing data on  $I_i$  (on Dirichlet and Neumann data) with noise free Dirichlet data over  $L_C$ , for various  $M = \{100, 150, 200\}$ .

	$M = 100$	$M = 150$	$M = 200$
Reconstructed data	D-N	D-N	D-N
Classic method	0.0114-0.0901	0.0116-0.0806	0.0169-0.0764
NGM-NS	0.0068-0.0789	0.0070-0.0669	0.0093-0.0645

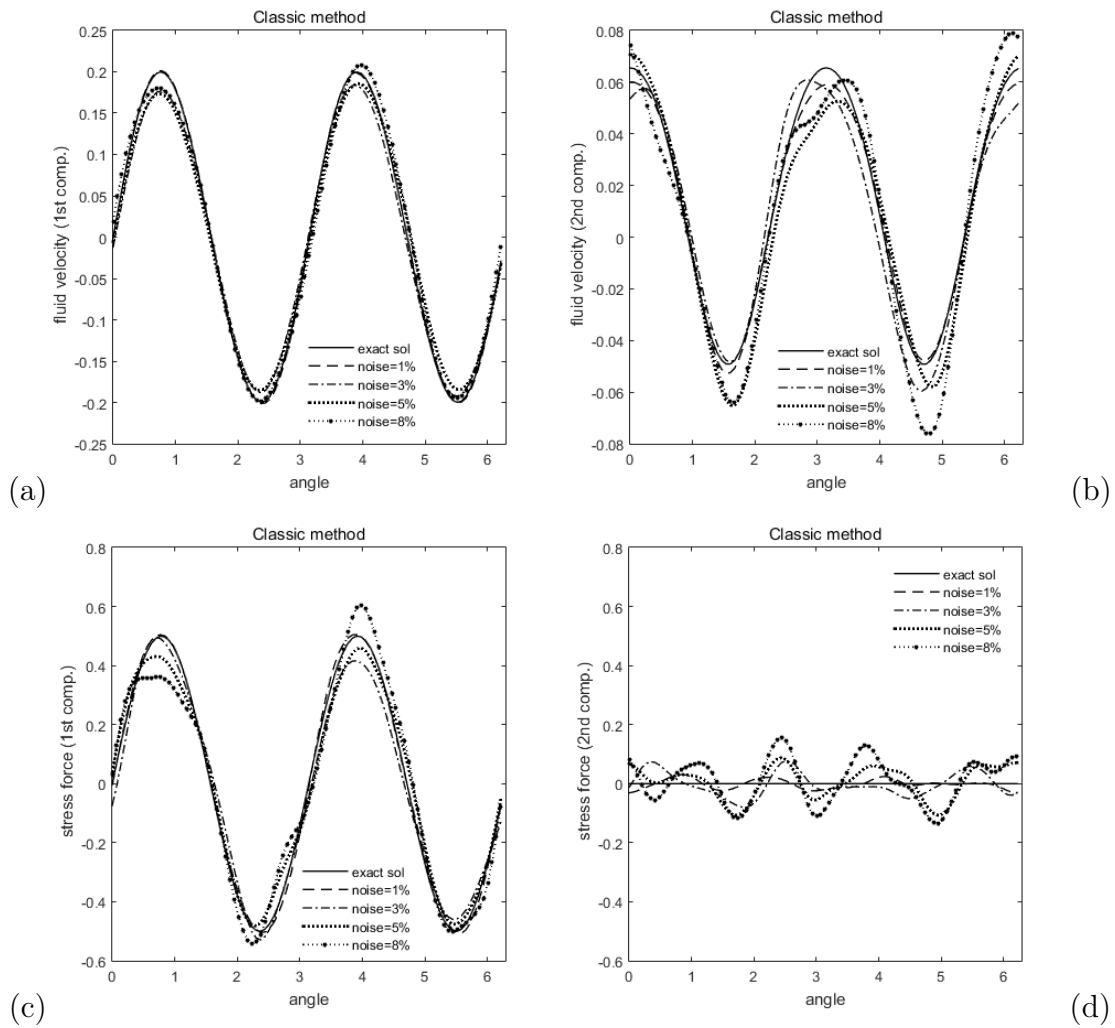


FIGURE 5.8 – Test case-A "Classic Method". Reconstruction of the missing boundary data with noisy Dirichlet data over  $I_c$  with noise levels  $\sigma = \{1\%, 3\%, 5\%, 8\%\}$ . **(a)** exact and computed first components of the velocity over  $I_i$  **(b)** exact and computed second components of the velocity over  $I_i$  **(c)** exact and computed first components of the normal stress over  $I_i$  **(d)** exact and computed second components of the normal stress over  $I_i$  (w.r.t a Gaussian noise).

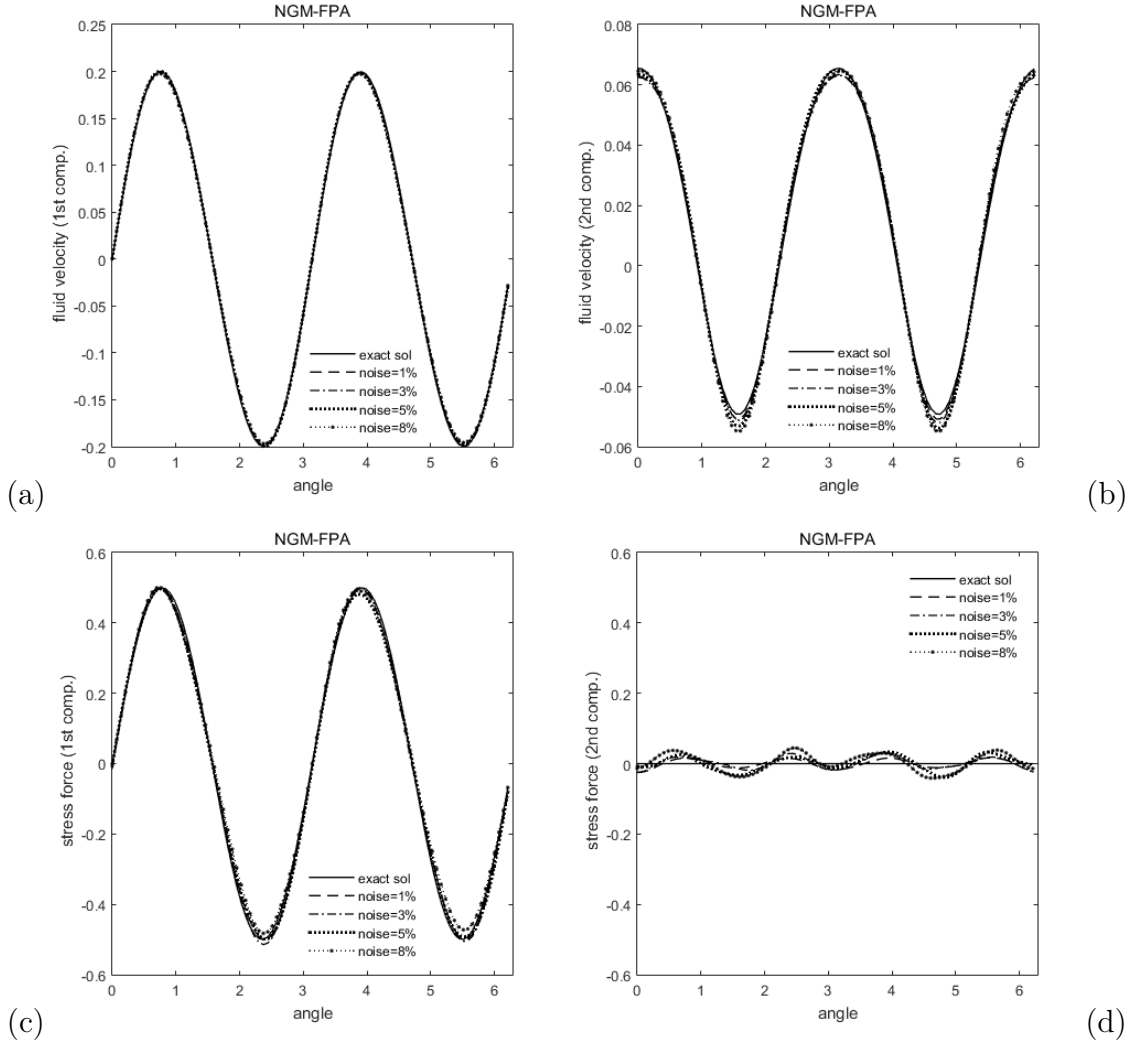


FIGURE 5.9 – Test case A "NGM-FPA". Reconstruction of the missing boundary data with noisy Dirichlet data over  $I_c$  with noise levels  $\sigma = \{1\%, 3\%, 5\%, 8\%\}$ . (a) exact and computed first components of the velocity over  $I_i$  (b) exact and computed second components of the velocity over  $I_i$  (c) exact and computed first components of the normal stress over  $I_i$  (d) exact and computed second components of the normal stress over  $I_i$  (w.r.t a Gaussian noise).

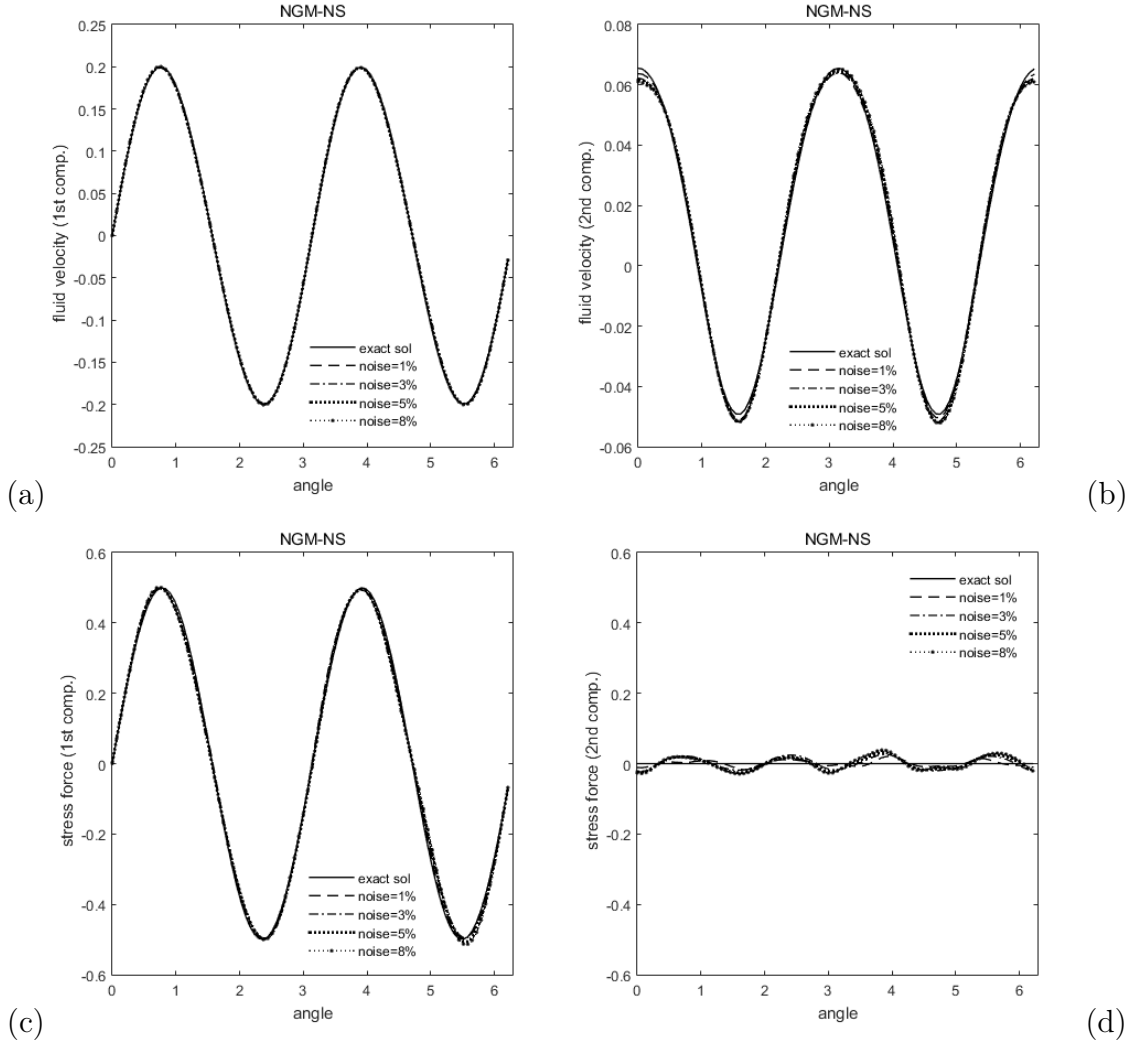


FIGURE 5.10 – Test case-A "NGM-NS". Reconstruction of the missing boundary data with noisy Dirichlet data over  $I_c$  with noise levels  $\sigma = \{1\%, 3\%, 5\%, 8\%\}$ . (a) exact and computed first components of the velocity over  $I_i$  (b) exact and computed second components of the velocity over  $I_i$  (c) exact and computed first components of the normal stress over  $I_i$  (d) exact and computed second components of the normal stress over  $I_i$  (w.r.t a Gaussian noise).

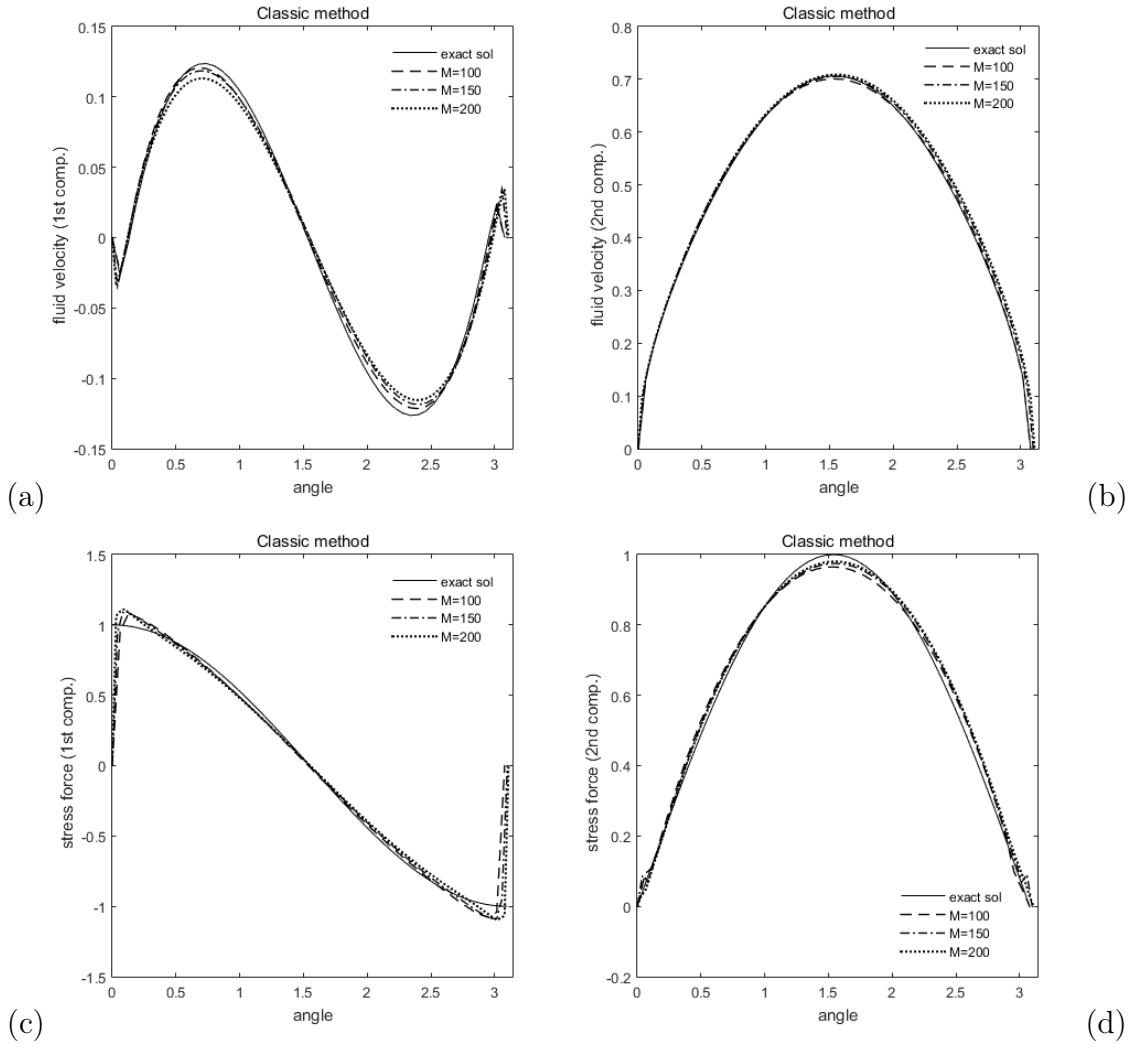


FIGURE 5.11 – Test case B "Classic Method". Reconstruction of the missing boundary data with noise free Dirichlet data over  $I_c$ . (a) exact -line- and computed -dashed line- first component of the velocity over  $I_i$  (b) exact -line- and computed -dashed line- second component of the velocity over  $I_i$  (c) exact -line- and computed -dashed line- first component of the normal stress over  $I_i$  (d) exact -line- and computed -dashed line- second component of the normal stress over  $I_i$ .

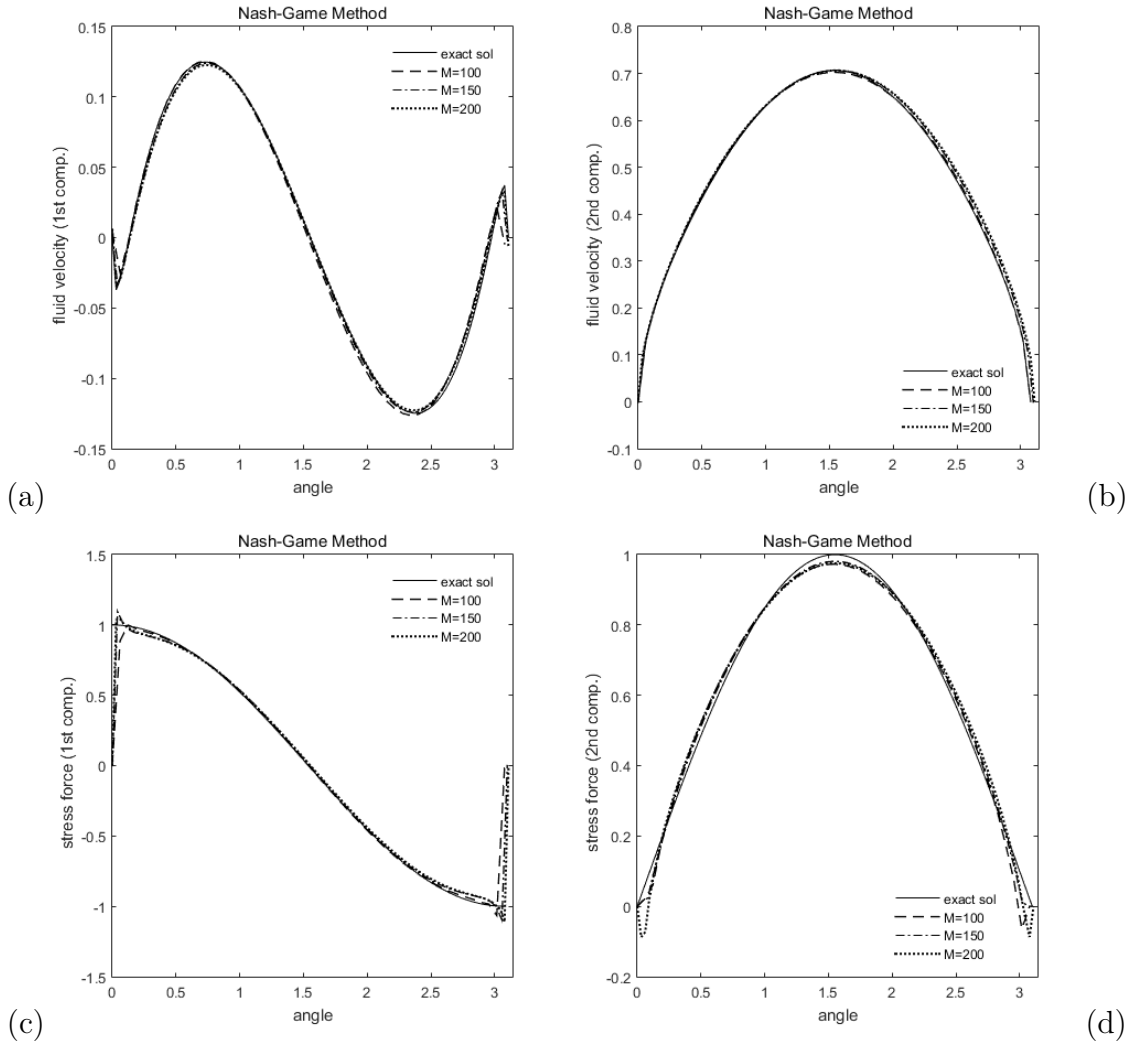


FIGURE 5.12 – Test case B "NGM-NS". Reconstruction of the missing boundary data with noise free Dirichlet data over  $I_c$ . **(a)** exact -line- and computed -dashed line- first component of the velocity over  $I_i$  **(b)** exact -line- and computed -dashed line- second component of the velocity over  $I_i$  **(c)** exact -line- and computed -dashed line- first component of the normal stress over  $I_i$  **(d)** exact -line- and computed -dashed line- second component of the normal stress over  $I_i$ .

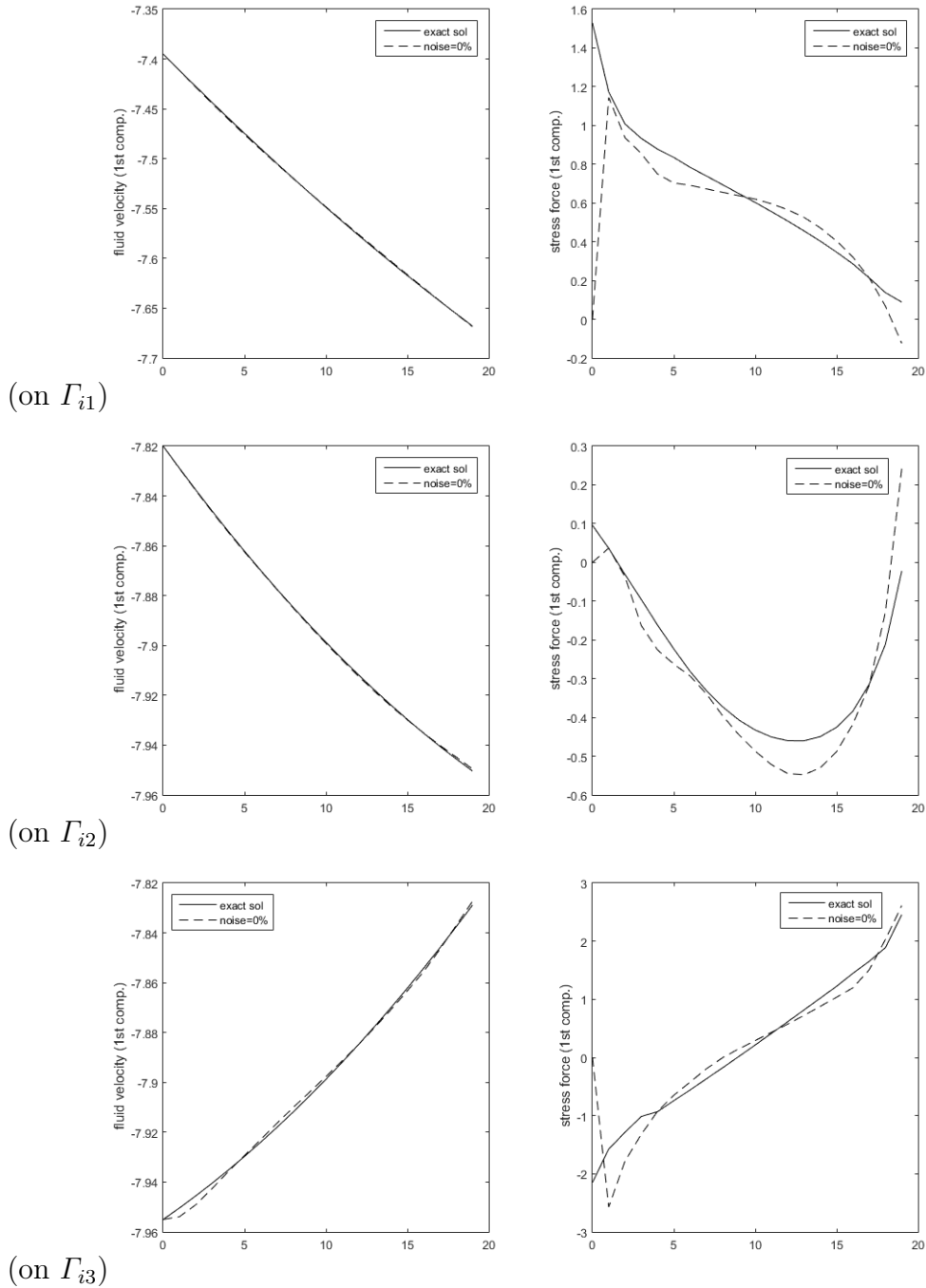


FIGURE 5.13 – Test case-C. Reconstruction of the missing boundary data from unnoisy data using Nash game algorithm. The exact and computed first component of the velocity and the normal stress, respectively : (Top) over  $\Gamma_{i1}$ , (Middle) over  $\Gamma_{i2}$  and (Bottom) over  $\Gamma_{i3}$ .

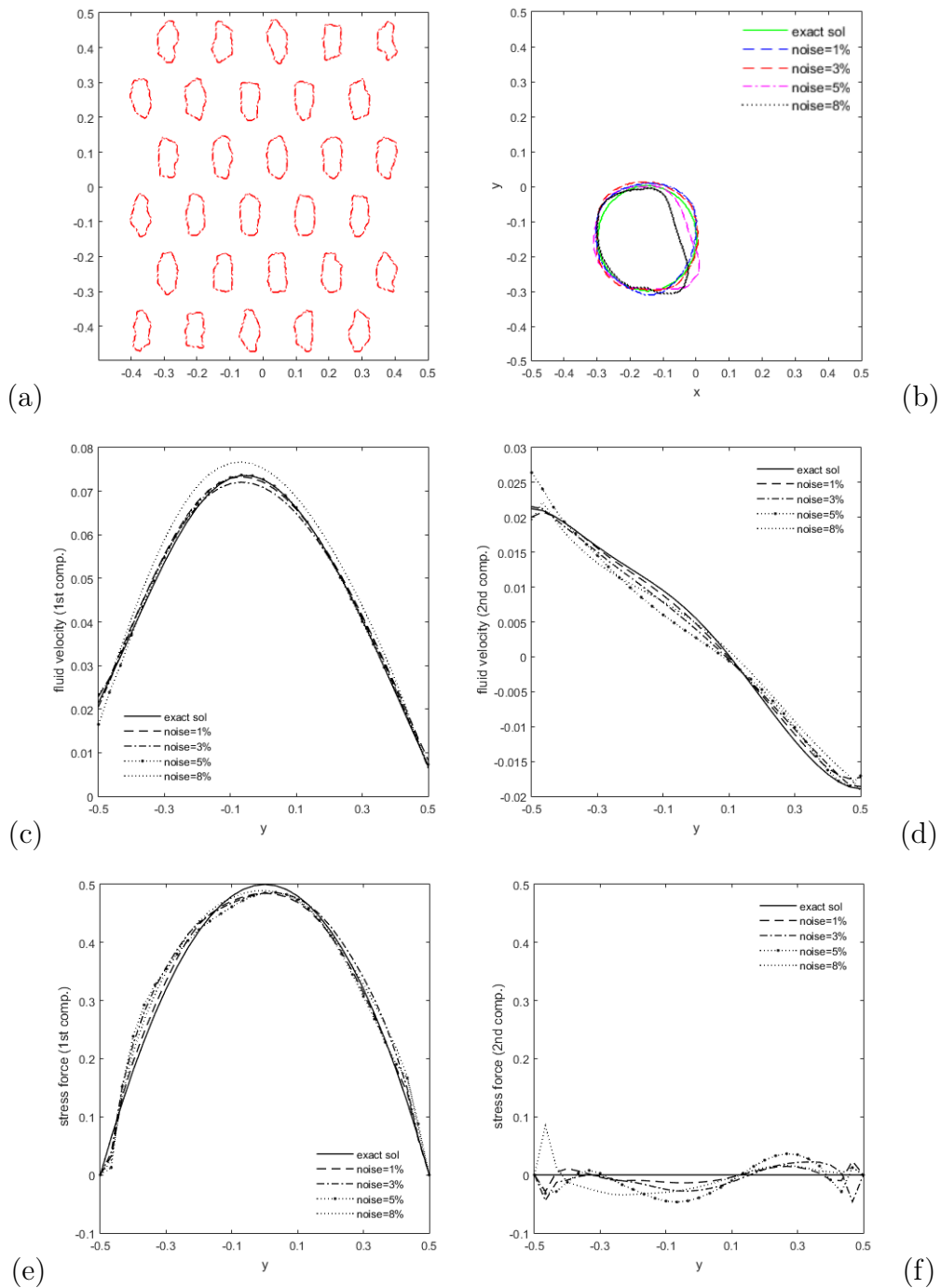


FIGURE 5.14 – Test case D. Reconstruction of the inclusion shape and missing boundary data with noisy Dirichlet data over  $I_c$  with noise levels  $\sigma = \{1\%, 3\%, 5\%, 8\%\}$ . **(a)** initial contour is  $\phi^{(0)}$  **(b)** exact inclusion shape -green line- and computed ones for different noise levels **(c)** exact and computed first components of the velocity over  $I_i$  **(d)** exact and computed second components of the velocity over  $I_i$  **(e)** exact and computed first components of the normal stress over  $I_i$  **(f)** exact and computed second components of the normal stress over  $I_i$ .



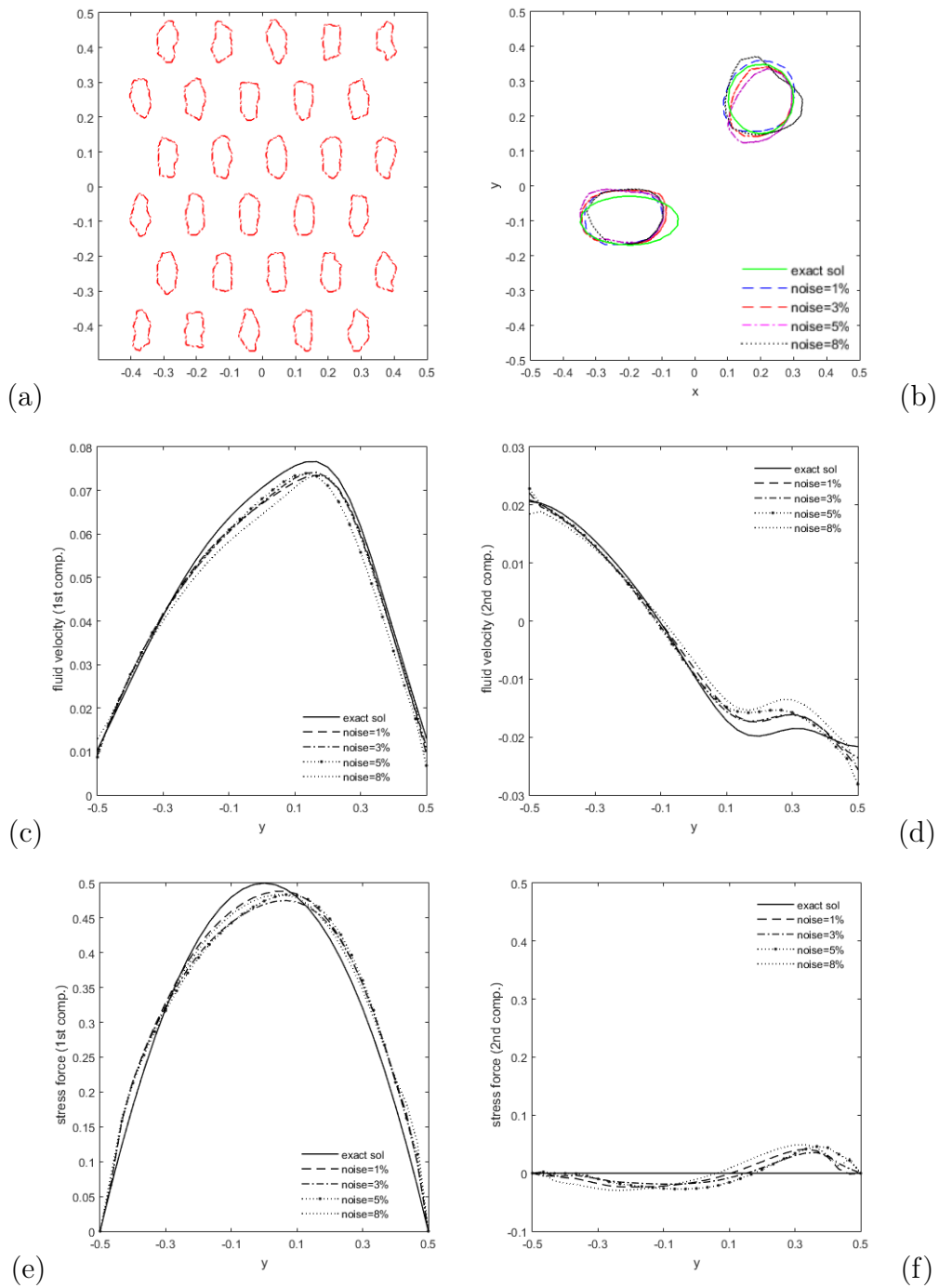


FIGURE 5.15 – Test case E. Reconstruction of the inclusion shape and missing boundary data with noisy Dirichlet data over  $I_c$  with noise levels  $\sigma = \{1\%, 3\%, 5\%, 8\%\}$ . **(a)** initial contour is  $\phi^{(0)}$  **(b)** exact inclusion shape -green line- and computed ones for different noise levels **(c)** exact and computed first components of the velocity over  $I_i$  **(d)** exact and computed second components of the velocity over  $I_i$  **(e)** exact and computed first components of the normal stress over  $I_i$  **(f)** exact and computed second components of the normal stress over  $I_i$ .

# Conclusion and perspectives

The inverse problems, such as identifying parameters, geometries, or sources, are known to be severely ill-posed in Hadamard's sense. The ill-posedness is related to the instability problem, which requires precisely regularized numerical methods. In this thesis, we have used the simplest class of games to model such situations. We have shown that this new formulation of the game could effectively deal with these problems and treat even those previously inaccessible, coupling ill-posedness.

In the first part of the thesis, we have assumed that the steady Stokes equations govern the fluid motion, the case of Newtonian fluids. We have proposed three original algorithms in a game theory framework for solving inverse problems of inclusions (or sources) identification coupled to the reconstruction of missing data, using only a single pair of Dirichlet and Neumann boundary measurements. Then, 3-players and their corresponding criteria are defined. The two first-named Dirichlet and Neumann players were dedicated to ensuring the data completion, while the third one was dedicated to ensuring the identification problem. The 3-players play a static game with complete information. We considered as a solution to the game the so-called Nash equilibrium. In chapter 2, to solve the inclusions detection and data completion jointly, we have proposed to use the level-set strategy to follow the evolution of the boundary of the shape to be recovered during the identification procedure. Thus, the third player in charge of the inverse inclusion problem controls the level-set function instead of the open subset. The first algorithm that we have proposed to solve this coupled problem is composed of two steps : First, compute the 2-player Nash equilibrium for a fixed level-set. This step, which we call a preconditioning Nash subgame, is dedicated to enforce the data completion part to precondition the Cauchy problem and tackle its ill-posedness. Second, the third player receives the optimal Dirichlet-Neumann solution and seeks to identify the inclusions' location and shape. A second algorithm has been introduced to solve the data completion and sources identification simultaneously in chapter 3. The third player, here in charge of identifying point-wise sources, controls the number, location, and magnitude of the point-forces as a strategy variable. For that, the third player plays en two-step ; first, seeks to find the number and locations of the sources using a topological gradient method, then aims to identify the sources' different magnitudes, parallel with the Dirichlet-Neumann players, which solve the data recovery problem. The 3-player Nash game algorithm naturally has been applied to detecting some unknown objects immersed in a stationary viscous fluid using partial boundary measurements in chapter 4. For this problem, the third player used a topological gradient method in order to determine its strategy : the number of objects and their relative locations.

The purpose of the second part is to extend those results to the class of nonli-

---

near Stokes models arising in quasi-Newtonian fluids. We have investigated two approaches, a control-types method and a Nash game algorithm, to a nonlinear Cauchy-stokes problem in chapter 5. The developed model is nonlinear with respect to the fluid velocity because of the non-linearity of the viscosity function, which varies upon the deformation tensor. The numerical procedure of this non-linearity demands particular algorithms. In this framework, we have proposed a new scheme to treat this non-linearity appropriately, and we have compared it with the fixed-point algorithm. The numerical results showed excellent performance in terms of the CPU of our proposed scheme. Finally, we have considered extending the Nash game strategy to the nonlinear coupled problem of geometric identification and data completion.

**Possible future work :** It might be fascinating to extend the Nash game strategy to other inverse problems and other operators, e.g., the Cauchy problem for Stokes or Navier-Stokes equations coupled with identifying the fluid's viscosity, Navier-Stokes or Darcy-stokes equations coupled with the heat equation, i.e., parameter identification (missing boundary data and temperature of the fluid on the part of the pipeline wall to control the material's condition) or leak detection, etc. We can also study another type of non-cooperative game like the Stackelberg game. It is a non-symmetric game where the players communicate hierarchically by designating them as a leader and the others as followers.

# Bibliography

- [1] R. Aboulaïch, A. Ben Abda, and M. Kallel. Missing boundary data reconstruction via an approximate optimal control. *Inverse Problems and Imaging*, 2 :411–426, 2008. [9](#), [12](#)
- [2] R. Aboulaïch, A. Ben Abda, and M. Kallel. A control type method for solving the cauchy–stokes problem. *Applied Mathematical Modelling*, 37 :4295–4304, 2013. [9](#), [11](#), [12](#), [26](#), [29](#), [62](#), [109](#), [116](#), [117](#)
- [3] G. Alessandrini, L. Rondi, E. Rosset, and S. Vessella. The stability for the cauchy problem for elliptic equations. *Inverse Problems*, 25 :123004, 2009. [16](#), [29](#), [95](#)
- [4] G. Allaire, F. Jouve, and A.-M. Toader. Structural optimization using sensitivity analysis and a level-set method. *Journal of computational physics*, 194(1) :363–393, 2004. [39](#)
- [5] C. Alvarez, C. Conca, L. Friz, O. Kaviani, and J. H. Ortega. Identification of immersed obstacles via boundary measurements. *Inverse Problems*, 21(5) :1531–1552, 2005. [26](#), [27](#), [32](#)
- [6] CJS Alves, R. Kress, and AL Silvestre. Integral equations for an inverse boundary value problem for the two-dimensional stokes equations. *Journal of Inverse and Ill-posed Problems jiiip*, 15(5) :461–481, 2007. [27](#)
- [7] CJS Alves and AL Silvestre. On the determination of point-forces on a stokes system. *Mathematics and Computers in Simulation*, 66 :385–397, 2004. [62](#), [63](#), [64](#), [66](#)
- [8] S. Amstutz. The topological asymptotic for the navier-stokes equations. *Society for Industrial and Applied Mathematics (SIAM)*, 11 :401–425, 2005. [20](#)
- [9] S. Amstutz, I. Horchani, and M. Masmoudi. Crack detection by the topological gradient method. *Control Cybernet*, 34 :81–101, 2005. [20](#), [68](#), [96](#)
- [10] S. Andrieux, T.N. Baranger, and A. Ben Abda. Solving cauchy problems by minimizing an energy-like functional. *Inverse problems*, 22(1) :115, 2006. [9](#), [12](#), [26](#), [62](#), [109](#)
- [11] S. Andrieux and A. Ben Abda. The reciprocity gap : a general concept for flaws identification problems. *Mechanics research communications*, 20(5) :415–420, 1993. [27](#)
- [12] H. Attouch, J. Bolte, and P. Redont. Alternating proximal algorithms for weakly coupled convex minimization problems. applications to dynamical games and pde’s. *J. Convex Anal.*, 15 :485–506, 2008. [30](#), [102](#), [121](#)
- [13] G. Aubert and P. Kornprobst. Mathematical problems in image processing : Partial differential equations and the calculus of variations. *Applied Mathematical Sciences*, 2006. [17](#), [35](#)

- [14] S. Avdonin, V. Kozlov, D. Maxwell, and M. Truffer. Iterative methods for solving a nonlinear boundary inverse problem in glaciology. *J. Inverse Ill-Posed Probl.*, 17 :239–258, 2009. [21](#), [110](#)
- [15] M. Azaiez, F. Ben Belgacem, and H. El Fekih. On cauchy’s problem : Ii. completion, regularization and approximation. *Inverse Problems*, 22 :1307–1336, 2006. [8](#)
- [16] M. Badra, F. Caubet, and M. Dambrine. Detecting an obstacle immersed in a fluid by shape optimization methods. *Math. Models Methods Appl. Sci.*, 21(10) :2069–2101, 2011. [26](#)
- [17] A. Ballerini. Stable determination of an immersed body in a stationary stokes fluid. *Inverse Problems*, 26 :125015(25pp), 2010. [26](#)
- [18] J. Baranger and K. Najib. Analyse numerique des ecoulements quasi-newtoniens dont la viscosite obeit a la loi puissance ou la loi de carreau. *Numerische Mathematik*, 58 :35–49, 1990. [20](#), [21](#), [111](#), [112](#)
- [19] T.N. Baranger and S. Andrieux. An optimization approach for the cauchy problem in linear elasticity. *Structural and Multidisciplinary Optimization*, 35 :141–152, 2008. [9](#)
- [20] J.W. Barrett and W.B. Liu. Finite element error analysis of a quasi-newtonian flow obeying the carreau or power law. *Numerische Mathematik*, 64 :433–453, 1993. [20](#)
- [21] J.W. Barrett and W.B. Liu. Quasi-norm error bounds for the finite element approximation of a non-newtonian flow. *Numerische Mathematik*, 68 :437–456, 1994. [20](#), [21](#)
- [22] G. Bastay, T. Johansson, V.A. Kozlov, and D. Lesnic. An alternating method for the stationary stokes system. *ZAMM*, 86 :268–280, 2006. [9](#), [31](#), [67](#), [73](#)
- [23] A. Ben Abda, F. Ben Hassen, J. Leblond, and M. Mahjoub. Sources recovery from boundary data : a model related to electroencephalography. *Mathematical and Computer Modelling*, 49 :2213–2223, 2009. [8](#)
- [24] A. Ben Abda, I. Ben Saad, and M. Hassine. On cauchy’s problem : I. a variational steklov-poincaré theory. *Applied Mathematical Modelling*, 37 :1–12, 2013. [9](#), [11](#), [12](#)
- [25] A. Ben Abda, M. Hassine, M. Jaoua, and M. Masmoudi. Topological sensitivity analysis for the location of small cavities in stokes flow. *SIAM Journal on Control and Optimization*, 48 :2871–2900, 2009. [20](#), [92](#), [96](#), [97](#), [98](#)
- [26] H. Ben Ameer, M. Burger, and B. Hackl. Level set methods for geometric inverse problems in linear elasticity. *Inverse Problems*, 20 :673–696, 2004. [20](#)
- [27] F. Ben Belgacem and H. El Fekih. On cauchy’s problem : I. a variational steklov-poincaré theory. *Inverse Problems*, 21 :1915–1936, 2005. [8](#)
- [28] L. Bourgeois. A mixed formulation of quasi-reversibility to solve the cauchy problem for laplace’s equation. *Inverse problems*, 21(3) :1087, 2005. [9](#), [26](#), [62](#)
- [29] L. Bourgeois and J. Dardé. A quasi-reversibility approach to solve the inverse obstacle problem. *Inverse Probl. Imaging*, 4(3) :351–377, 2010. [26](#)
- [30] L. Bourgeois and J. Dardé. The exterior approach to solve the inverse obstacle problem for the stokes system. *Inverse Problems and Imaging*, 8(1) :23–51, 2014. [27](#)
- [31] H. Brezis. *Functional Analysis, Sobolev Spaces and Partial Differential Equations*. Springer New York Dordrecht Heidelberg London, 2010. [111](#)

- [32] M. Bruhl, M. Hanke, and M. Pidcock. Crack detection using electrostatic measurements. *Mathematical Modelling and Numerical Analysis*, 35 :595–605, 2001. [8](#)
- [33] J. C ea. Conception optimale ou identification de formes, calcul rapide de la d riv e directionnelle de la fonction co ˆut. *ESAIM : Mathematical Modelling and Numerical Analysis*, 20 :371—402, 1986. [18](#)
- [34] F. Caubet. *D tection d’un objet immerg  dans un fluide*. PhD thesis, Universit  de Pau, 2012. [28](#), [33](#), [34](#), [73](#)
- [35] F. Caubet, C. Conca, and M. Godoy. On the detection of several obstacles in 2d stokes flow : Topological sensitivity and combination with shape derivatives. *Inverse Problems and Imaging*, 10 :327–367, 2016. [20](#), [27](#)
- [36] R. Chamekh, A. Habbal, M. Kallel, and N. Zemzemi. A nash game algorithm for the solution of coupled conductivity identification and data completion in cardiac electrophysiology. *Mathematical Modelling of Natural Phenomena*, 14 :Art. 201, 15 pp, 2019. [16](#), [26](#), [62](#)
- [37] Denise Chenais. Optimal design of midsurface of shells : differentiability proof and sensitivity computation. *Applied Mathematics and Optimization*, 16(1) :93–133, 1987. [37](#)
- [38] A. Cimetiere, F. Delvare, M. Jaoua, and F. Pons. Solution of the cauchy problem using iterative tikhonov regularization. *Inverse Problems*, 17 :553–570, 2001. [8](#), [26](#), [62](#)
- [39] S. Congreve and P. Houston. Discontinuous galerkin finite element approximation of quasilinear elliptic boundary value problems ii : strongly monotone quasineutronian flows. *IMA Journal of Numerical Analysis*, 33 :1386–1415, 2013. [21](#), [111](#)
- [40] P. Constantin and C. Foias. *Navier-stokes equations*. University of Chicago Press, 1988. [28](#), [67](#)
- [41] Xian-Bao Duan, Yi-Chen Ma, and Rui Zhang. Shape-topology optimization of stokes flow via variational level set method. *Applied Mathematics and Computation*, 202(1) :200–209, 2008. [36](#)
- [42] H. Egger and A. Leit ˆao. Efficient reconstruction methods for nonlinear elliptic cauchy problems with piecewise constant solutions. *Adv. Appl. Math. Mech.*, 1 :729–749, 2009. [21](#), [109](#)
- [43] I. Ekeland and R. Temam. *Analyse convexe et probl mes variationnels*. Bordas, 1974. [115](#)
- [44] A. El Badia and T. Ha-Duong. An inverse source problem in potential analysis. *Inverse Problem*, 16 :651–663, 2000. [62](#)
- [45] H.A. Eschenauer, V. Kobelev, and A. Schumacher. Bubble method for topology and shape optimization of structures. *Structural Optimization*, 8 :42–51, 1994. [68](#), [95](#)
- [46] C. Conca F. Caubet and M. Godoy. On the detection of several obstacles in 2d stokes flow : topological sensitivity and combination with shape derivatives. *Inverse Problems and Imaging*, 10 :327–367, 2016. [26](#)
- [47] C. Fabre and G. Lebeau. Unique continuation property of solutions of the stokes equation. *Communications in Partial Differential Equations*, 21 :573–596, 1996. [10](#), [30](#), [32](#), [33](#), [63](#), [116](#)

- [48] RS Falk and PB Monk. Logarithmic convexity for discrete harmonic functions and the approximation of the cauchy problem for poisson's equation. *Mathematics of computation*, 47(175) :135–149, 1986. [26](#), [62](#)
- [49] J. Ferchichi, M. Hassine, and H. Khenous. Detection of point-forces location using topological algorithm in stokes flows. *Applied Mathematics and Computation*, pages 7056–7074, 2013. [20](#), [62](#), [65](#), [67](#), [68](#)
- [50] P.C. Franzone and E. Magenes. On the inverse potential problem of electrocardiology. *Calcolo*, 16(4) :459–538, 1979. [8](#), [26](#), [62](#)
- [51] G. Galdi. *An introduction to the mathematical theory of the Navier-Stokes equations : Steady-state problems*. Springer Science & Business Media, 2011. [31](#)
- [52] S. Garreau, P. Guillaume, and M. Masmoudi. The topological asymptotic for pde systems : The elasticity case. *SIAM Journal on Control and Optimization*, 39 :1756–1778, 2001. [20](#), [96](#), [97](#)
- [53] A. Habbal. A topology nash game for tumoral antiangiogenesis. *Struct. Multi. Optim.*, 30 :404–412, 2005. [1](#), [14](#)
- [54] A. Habbal and P. E. Jabin. Two short presentations related to cancer modeling. *ARIMA Journal*, 10 :19–28, 2008. [x](#), [1](#), [14](#), [15](#)
- [55] A. Habbal and M. Kallel. Data completion problems solved as nash games. *Journal of Physics : Conference Series*, 386 :012004, 2012. [2](#), [9](#), [15](#), [109](#)
- [56] A. Habbal and M. Kallel. Neumann-dirichlet nash strategies for the solution of elliptic cauchy problems. *SIAM Journal on Control and Optimization*, 51 :4066–4083, 2013. [x](#), [2](#), [9](#), [15](#), [16](#), [17](#), [26](#), [27](#), [28](#), [29](#), [30](#), [39](#), [45](#), [62](#), [74](#), [92](#), [95](#), [109](#), [121](#)
- [57] A. Habbal, M. Kallel, and M. Ouni. Nash strategies for the inverse inclusion cauchy-stokes problem. *Inverse problems and imaging*, 13 :827–862, 2019. [21](#), [62](#), [75](#), [92](#), [95](#), [109](#), [110](#), [124](#), [125](#), [126](#), [133](#)
- [58] A. Habbal, J. Petersson, and M. Thellner. Multidisciplinary topology optimization solved as a nash game. *Internat. J. Numer. Methods Engrg.*, 61 :949–963, 2004. [1](#), [17](#)
- [59] J. Hadamard. *The cauchy problem and the linear hyperbolic partial differential equations*. Dover, New York, 1953. [2](#), [8](#), [10](#), [26](#), [61](#), [92](#), [109](#)
- [60] J. Haslinger and R. A. E. Makinen. *Introduction to shape optimization : Theory, approximation, and computation*. Society for Industrial and Applied Mathematics (SIAM), 2003. [18](#)
- [61] F. Hecht. New development in freefem++. *J. Numer. Math.*, 20(3-4) :251–265, 2012. [41](#), [77](#), [102](#), [128](#)
- [62] T. Johansson and D. Lesnic. Reconstruction of a stationary flow from incomplete boundary data using iterative methods. *European Journal of Applied Mathematics*, 17 :651–663, 2006. [9](#), [26](#)
- [63] T. Johansson and D. Lesnic. A variational conjugate gradient method for determining the fluid velocity of a slow viscous flow. *Appl. Anal.*, 85 :1327–1341, 2006. [9](#), [62](#)
- [64] T. Johansson and D. Lesnic. An iterative method for the reconstruction of a stationary flow. *Numerical Methods for Partial Differential Equations*, 23 :998–1017, 2007. [9](#)

- [65] M. Kallel, R. Aboulaich, A. Habbal, and M. Moakher. A nash-game approach to joint image restoration and segmentation. *Applied Mathematical Modelling*, 38 :3038–3053, 2014. [x](#), [14](#), [15](#), [16](#), [17](#)
- [66] M. Kallel, M. Moakher, and A. Theljani. The cauchy problem for a nonlinear elliptic equation : Nash-game approach and application to image inpainting. *Inverse Problems and Imaging*, 9 :853–874, 2015. [17](#), [21](#), [26](#), [110](#)
- [67] Seymour Katz and Craig F. Landefeld, editors. *On the Detection, Behaviour and Control of Inclusions in Liquid Metals*, pages 447–466. Springer US, Boston, MA., 1988. [25](#)
- [68] G.N Kawchuk, J. Fryer, J. L. Jaremko, H. Zeng, L. Rowe, and R. Thompson. Real-time visualization of joint cavitation. *PLoS one*, 10(4) :e0119470, 2015. [25](#)
- [69] A. Kirsch. An introduction to the mathematical theory of inverse problems. *Applied Mathematical Sciences*, 2011. [8](#)
- [70] R. V. Kohn and M. Vogelius. Relaxation of a variational method for impedance computed tomography. *Communications on Pure and Applied Mathematics*, 40(6) :745–777, 1987. [26](#)
- [71] V.A. Kozlov and V.G. Maz’ya. On iterative procedures for solving ill-posed boundary value problems that preserve differential equations. *Leningrad Mathematical Journal*, 1 :1207–1228, 1990. [9](#)
- [72] V.A. Kozlov, V.G. Maz’ya, and A.V. Fomin. An iterative method for solving the cauchy problems for elliptic equations. *Comput. Math. Phys.*, 31 :45–52, 1991. [9](#), [12](#), [26](#), [62](#), [109](#)
- [73] P. Kùgler and A. Leitão. An iterative method for solving the cauchy problems for elliptic equations. *Numer. Math.*, 96 :269–293, 2003. [21](#), [109](#)
- [74] R. Lattès and J. L. Lions. The method of quasi-reversibility : applications to partial differential equations. *New York, American Elsevier Pub. Co.*, 1969. [8](#)
- [75] Shu Li and T. Başar. Distributed algorithms for the computation of noncooperative equilibria. *Automatica*, 23(4) :523–533, 1987. [43](#)
- [76] Chi-Wen Lo, Sheng-Fu Chen, Chi-Pei Li, and Po-Chien Lu. Cavitation phenomena in mechanical heart valves : Studied by using a physical impinging rod system. *Annals of biomedical engineering*, 38(10) :3162–3172, 2010. [25](#)
- [77] R. Malladi, J. A Sethian, and B. C Vemuri. Shape modeling with front propagation : A level set approach. *IEEE transactions on pattern analysis and machine intelligence*, 17(2) :158–175, 1995. [35](#)
- [78] W. Mansouri, T. N. Baranger, H. Ben Ameer, and N. H. Tlatli. Identification of injection and extraction wells from overspecified boundary data. *Inverse Problems in Science and Engineering*, 25 :1091–1111, 2017. [62](#)
- [79] M. Masmoudi, J. Pommier, and B. Samet. The topological asymptotic expansion for the maxwell equations and some applications. *Inverse Problems*, 21 :547–564, 2005. [20](#), [96](#)
- [80] B. Messnarz, B. Tilg, R. Modre, G. Fischer, and F. Hanser. A new spatiotemporal regularization approach for reconstruction of cardiac transmembrane potential patterns. *IEEE Trans. Biomedical Engineering*, 51 :273–281, 2004. [8](#)
- [81] O. Morgenstern and J. Von Neumann. Theory of games and economic behavior. *Princeton University Press*, 1944. [13](#)



- [82] S. Osher and R. Fedkiw. Level set methods and dynamic implicit surfaces. *Applied mathematical sciences (Springer-Verlag New York Inc.)*, 2003. 17
- [83] S. Osher and A. Sethian. Fronts propagating with curvature-dependent speed : Algorithms based on hamilton-jacobi formulations. *Journal of computational physics*, 79 :12–49, 1988. 17
- [84] B. Rousselet. Note on the design differentiability of the static response of elastic structures. *Journal of Structural Mechanics*, 10(3) :353–358, 1982. 37
- [85] Andrieux S., Baranger T. N., and Ben Abda A. Data completion via the energy error functional. *Comptes Rendus Mécaniques*, 333 :171–177, 2005. 9
- [86] F. Santosa. A level-set approach for inverse problems involving obstacles. *ESAIM : Control, Optimisation and Calculus of Variations*, 1 :17–33, 1996. 35
- [87] F. Santosa and M. V. Klibanov. A computational quasi-reversibility method for cauchy problems for laplace’s equation. *SIAM Journal on Applied Mathematics*, 51 :1653–1675, 1991. 9
- [88] P. Saramito. Complex fluids : Modeling and algorithms. *Mathématiques et Applications*, 2016. 20
- [89] M. Seger, G. Fischer, R. Modre, B. Messnarz, F. Hanser, and B. Tilg. Lead field computation for the electrocardiographic inverse problem–finite elements. *Computer Methods and Programs in Biomedicine*, 77 :241–252, 2005. 8
- [90] J.A. Sethian. *Level Set Methods and Fast Marching Methods : Evolving Interfaces in Computational Geometry, Fluid Mechanics, Computer Vision and Materials Science*. Cambridge University Press, 1999. 125
- [91] J. Sokolowski and A. Zochowski. On the topological derivative in shape optimization. *SIAM Journal on Control and Optimization*, 37 :1251–1272, 1999. 68, 95
- [92] Younggon Son and K. B Migler. Cavitation of polyethylene during extrusion processing instabilities. *Journal of Polymer Science Part B : Polymer Physics*, 40(24) :2791–2799, 2002. 25
- [93] T. Stieger, H. Agha, M. Schoen, G Mazza, M., and A. Sengupta. Hydrodynamic cavitation in stokes flow of anisotropic fluids. *Nature communications*, 8 :15550, 2017. 25
- [94] M. Sussman, P. Smereka, and S. Osher. A level set approach for computing solutions to incompressible two-phase flow. *Journal of Computational physics*, 114(1) :146–159, 1994. 36
- [95] R. Temam. *Navier-Stokes equations : theory and numerical analysis*, volume 343. American Mathematical Soc., 2001. 28, 67
- [96] A. N. Tikhonov. Regularization of incorrectly posed problems. *Sov. Doklady*, 4 :1624–1627, 1963. 8
- [97] A. N. Tikhonov. Solution of incorrectly formulated problems and the regularization method. *Sov. Doklady*, 4 :1035–1038, 1963. 8
- [98] E.O. Velipasaoglo, H. Sun, F. Zhang, K.L. Berrier, and D.S. Khoury. A spatial regularization of electrocardiographic inverse problem and its application to endocardial mapping. *IEEE Trans. Biomedical Engineering*, 47 :327–337, 2000. 8
- [99] J. P. Zolésio. The material derivative (or speed) method for shape optimization. *Optimization of Distributed-Parameter Structures*, 2 :1089—1154, 1981. 18